Factors Affecting Waste Leachate Generation and Barrier Performance of Landfill Liners

TANG QIANG

ABSTRACT

This is a geo-environmental research about the factors affecting landfill leachate generation and the factors affecting barrier performance of landfill liners. The objectives of this dissertation are (1) to investigate the geometry effect on leachate generation and composition through laboratory-scale lysimeter test; (2) to study the factors affecting membrane behavior by laboratory-scale membrane test.

Decomposition of landfill waste is a long term process, which is always accompanied by the generation of landfill leachate. To reduce the research expense and duration, landfill environmental conditions were simulated inside laboratory-scale lysimeters and columns. The lysimeters were operated with various geometrical characteristics (e.g. height/width ratio and height) which can cause changes in physical and thermodynamic characteristics, resulting in different waste decomposition rates and leaching behavior. Considering all of above, in this study, the lysimeter test was conducted using six lysimeters to evaluate the geometrical effect on leachate generation and leaching behavior of Construction & Demolition waste residue. According to the lysimeter test results, increasing the width of the lysimeter can reduce the potential of side-edge-wall flow, and the filtration water can have a perfect flushing inside lysimeters with shorter lengths. Increasing the height merely results in an increase in upper loading, and causes denser micro-structure of waste and closer cohesion at the bottom of the lysimeters, which was not suitable for the leaching out of soluble constituents as well as heavy metals. Based on the Chemical Oxygen Demand (COD), Total Nitrogen (TN), Total Phosphorus (TP) and the emission behaviors of some inorganic ions, microbial activity can have significant effects on leaching behavior, which cannot be neglected when researching landfill waste. Relatively short lysimeters and lysimeters with low height/width ratio can provide more suitable conditions (density, upper loading, inter-particle cohesion, water content) for the motivation of microbial activity. The results from the experimental work will also help establish standardized and feasible designs for laboratory-scale lysimeter tests.

Compacted clay liners (CCL) are usually employed as bottom liners in waste containment facilities due to their affordability and excellent barrier performance against the migration of aqueous contaminants. It is rational to expect that the performance of these clay liners may be greatly enhanced if they exhibit a semipermeable membrane behavior, by which the liners can prevent the migration of contaminant, while without any restrict towards the passage of water. However, the observed membrane behavior has been too low to sufficiently prevent the migration of contaminants. According to previous research, bentonite has proved to improve membrane behavior effectively. Thus, in this study, bentonite is introduced to promote the barrier performance of clay towards contaminants and enhance its membrane properties. In addition, different factors were studied to evaluate their effect on membrane behavior, including bentonite content, compactness, thickness, potential Hydrogen of solution (pH), concentration and solute type. According to the results,

bentonite is an effective additive, and may greatly improve the membrane behavior of natural Fukakusa clay (FC). The membrane behavior increased as compactness increased. The thickness can also affect the membrane behavior, but very limited. pH can greatly affect the membrane behavior, especially in alkaline conditions. While the similarity of the membrane behavior under pH 4.0 and 7.0 suggested the existence of a very slight erosion effect of the acid solution. For different solute type, the membrane behavior follows the order that K, Na > Ca > Pb, Zn. Although the low membrane behavior of heavy metal ions, almost no diffusion occurred during the membrane test, which can be attributed to the adsorption. Additionally, the degrade effect of measured chemico-osmotic pressure can be regarded as the compression of the double layer. As the increase of bentonite content, compactness or pH value, soil particle size became bigger as well as closer cohesion based on scanning electron microscope analysis (SEM). And the further analysis was conducted to study the mechanism of the membrane behavior with the assistance of X-ray diffraction (XRD) and X-ray fluorescence (XRF) results. According to the results, the hydraulic conductivity of FC is 1.58×10^{-9} m/s, and as bentonite content increased, the hydraulic conductivity gradually decreased in response, which indicated that adding bentonite cannot only improve the membrane behavior, but also make natural FC suitable for use as a liner.

Based on the experiment results obtained from above membrane test, the numerical analysis work was conducted by using the solute transport equation proposed by previous research, which took into account of both advection and membrane behavior on solute transport. Four parameters $t_{0.001}$, $t_{0.02}$, $t_{0.5}$ and t_1 were utilized to describe the breakthrough curve of specimen, which represent the time period when the ratio of c_s/c_0 reached 0.001, 0.02, 0.5 and 1. $t_{0.02}$ and $t_{0.5}$ consider both the time spent and environmental impact, and can be regarded as balance criteria, while t_1 represent the time spent when the barrier has been completely breakdown, when the surrounding soil and groundwater environment has already been polluted. $t_{0.001}$ is the time cost when the contaminant started to breakdown, and it is occurred at very early stage and can be used for forewarning of the diffusion of contaminant. The barrier performance of liners was greatly improved when their membrane behavior was considered.

ACKONOWLEDGEMENTS

The author acknowledges the Ministry of Education, Culture, Sports, Science and Technology (MEXT), which providing me with a Ph.D. Japanese government scholarship to pursue my doctoral studies in Japan through Kyoto University‘s Environmental Management Leadership Program.

The author wishes to express his complete gratitude to his academic supervisor and main advisor of this research, Dr. Takeshi Katsumi, Professor of the Graduate School of Global Environmental Studies at Kyoto University, in virtue of his patience, motivation, invaluable guidance, constructive suggestions as well as his inestimable supports throughout this work at the Environmental Infrastructural Engineering Laboratory.

The author would like to extend his gratitude to Dr. Toru Inui, Associate Professor of the Graduate School of Global Environmental Studies at Kyoto University, for his creative advice, valuable support and for his comments on the manuscript of this research.

Special thanks to Prof. Takaoka Masaki, one of the reviewers of this doctor thesis. The author thanks to him for his invaluable guidance and constructive suggestions for the preparation of the author‘s doctor thesis.

The author gratefully thanks to Takai-sensei, Assistant Professor of the Graduate School of Global Environmental Studies at Kyoto University, for his invaluable support on the experimental work as well as his warmheartedly assistance in the aspects of Japanese culture, tradition and customs.

The author also would like to express his gratitude to Dr. Hermelinda Plata and Dr. Giancarlo Flores, for their encouragement and valuable suggestions and comments on the contents of this research.

Special thanks to Dr. Zhenze Li, Post Doctoral Fellow in University of Ottawa, Canada for his invaluable guidance, constructive suggestions in the experimental design and paper writing about this research.

The author also would like to thank Dr. Kazuto Endo and Dr. Kim, researcher of the National Institute for Environmental Studies (NIES), for their warmhearted assistance in the aspects of academia and daily life during the 4-month internship in NIES, Tsukuba. The author also would like to extend his thank to Mr. Sumio Miyoshi and Mr. Masahiko Kanou, general manager of Environmental Technology Division of Okumura Corporation, for their encouragement and valuable suggestions on this research during the 1-month internship there.

Special thanks go to Ms. Miho Yasumoto, the laboratory Assistant, Environmental Infrastructure Engineering Laboratory at Kyoto University, for all her help and support during his studying in Japan. The author is also grateful to all members at the Environmental Infrastructure Engineering Laboratory, Dr. Abedin, Mogami-san, Katayama-san, Kodama-san, Tua-san, Suwa-san, Giang-san, Sado-chan, Ikeda-san, Goto-san, Angelica-san, Lan-san, Harris-san, Uddin-san, Wang-san,

Bobea-san, Mae-san, Sano-san, Yano-san, Morita-san, Kihara-san, Oshima-san, Sumoto-san, Ogawa-san, Mo-san, Tamura-san, Kaori-san, Miura-san, Kimura-san, Yamane-san, who have the time stay in Japan not only an academic but a cultural journey.

The author also thanks to all his Chinese friends, Jianjian Li, Wei Liu, Heming Wang, etc., for supporting and sharing the most beautiful moments of life in Kyoto.

And last but not least, the author would like to send his gratitude to his family: his parents, his parents in law for their mental support and encouragement in the past three years as well as his loving wife, Junfang Sun, also Ph.D. Candidate in Kyoto University, for her being at his side all the way of three years abroad journey, showing her supporting and encouragement.

TABLE OF CONTENTS

LIST OF TABLES

LIST OF FIGURES

CHAPTER 1: INTRODUCTION

1.1 Background

Increasingly affluent lifestyles as well as continued industrial and commercial growth around the world has led to rapid increases in both municipal and industrial solid waste production (MSW and ISW), especially in developing countries. Fig. 1.1 presents the increase in the production of industrial solid waste in China (China Statistical Yearbook, 1991-2012).

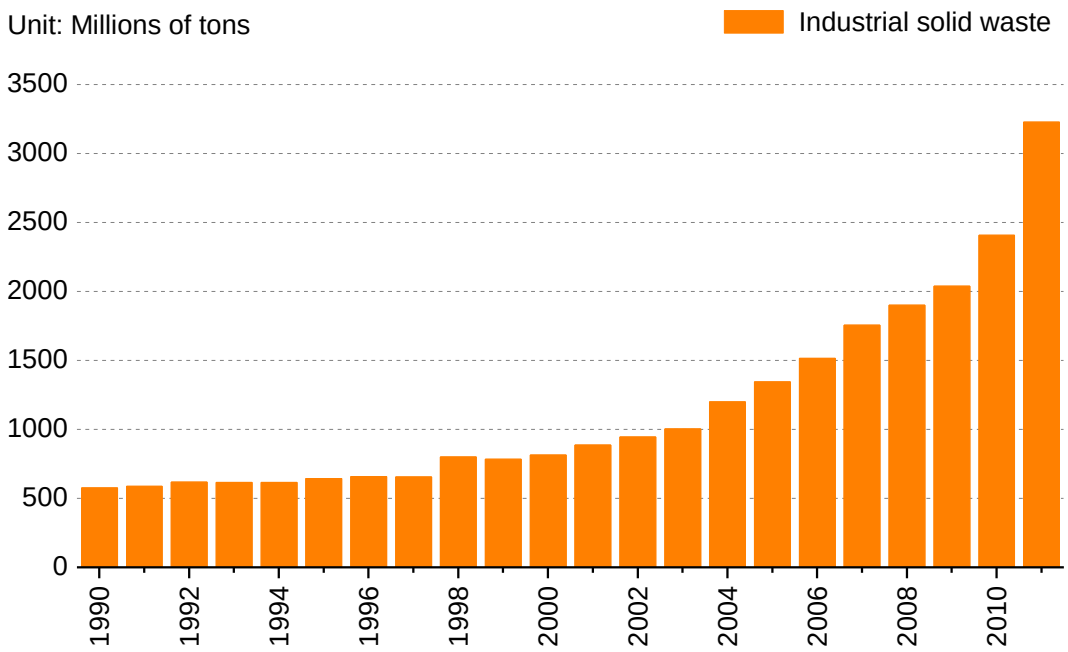

Fig. 1.1 Production of ISW in China (China Statistical Yearbook, 1991-2012)

Conventional treatment methods for ISW and MSW include reuse and recycling, composting, anaerobic digestion, incineration, and land disposal. Regardless of the method chosen, residue is produced; thus, a sanitary landfill for the ultimate disposal of solid waste is the most widely accepted method throughout the world (Westlake, 1995; Williams, 1998; Tanaka et al., 2005; Brunner and Fellner, 2007; USEPA, 2010; Laner et al., 2012). Besides its economic benefit, landfills minimize environmental impact and allow waste to decompose under controlled conditions until its eventual transformation into relatively inert, stabilized material (Renou, 2008). In the US, 54% of MSW was sent to landfills in 2008, compared to only 33% for recycling and composting (USEPA, 2009). In Australia, about 70% of MSW were sent directly to landfills without pre-treatment in 2002 (Productivity Commission, 2006). In China, 61.4% of MSW was treated through landfill method in 2011 (China Statistical Yearbook, 2012). Among the EU member states, 52% of waste production in

France was landfilled into regulated centers in 2002 (Renou et al., 2008). In 2008, 77%, 55%, and 51% of MSW generated were treated by landfilled in Greece, the UK, and Finland, respectively. According to El-Fadel (1997), up to 95% of the total MSW collected worldwide is disposed by landfills.

As shown in Fig. 1.2, sanitary landfills are engineered disposal facilities that use physical barriers to isolate solid waste from surroundings in order to minimize public health and environmental impacts (Allen, 2001; Tchobanoglous and Kreith, 2002). These barriers, including bottom liners and a cover layer, keep the waste body insulated for long periods of time. Nevertheless, water present in waste, origins from rainwater infiltration during and/or after the landfill process, and groundwater penetration provide favorable conditions for micro-organism development (Westlake, 1995). Through their own metabolic activities, micro-organisms degrade waste until their nutrient sources are depleted and the residues are no longer capable of supporting microbial growth, a process which is known as biological degradation; this generates landfill leachate (Zehnder, 1988; Palmisano and Barlaz, 1996; Zhang, 2002).

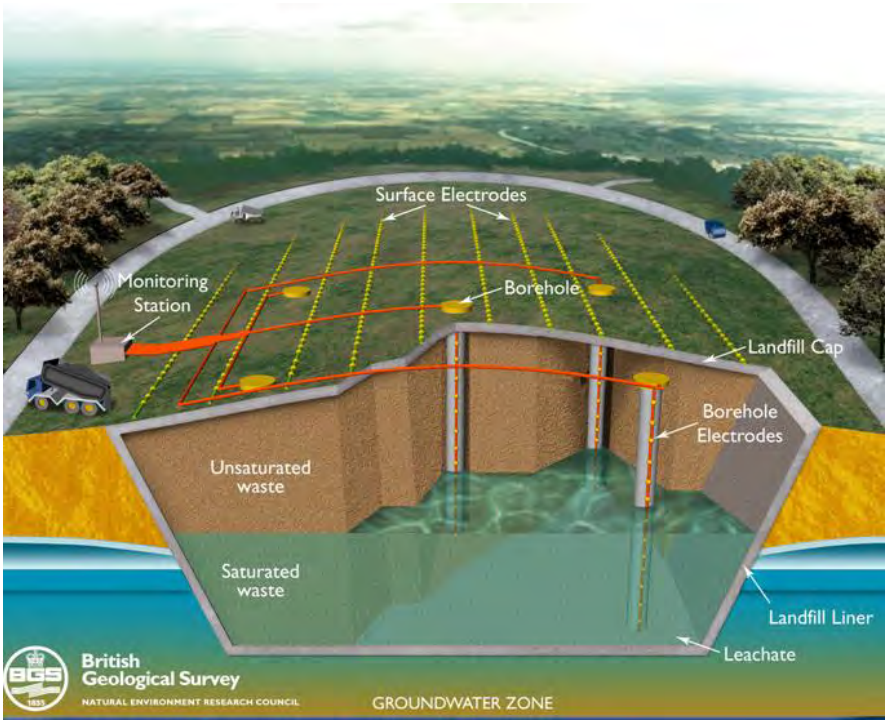

Fig. 1.2 Sanitary landfill

Landfill leachate is a water-based solution with four groups of pollutants: dissolved organic matter, inorganic components, heavy metals, and xenobiotic organic compounds (Christensen et al., 1994; Baun and Christensen, 2004). Unlike organic pollutants, heavy metals are not biodegradable; such pollution may last for two millennia (Hong et al., 1994). Heavy metals like zinc and lead tend to accumulate in biological systems and can result in severe environmental problems. Zinc (Zn) is an essential trace nutrient that is required by most living organisms for healthy growth and enzyme

function (Tang et al., 2012). However, it is toxic to plants and animals at elevated concentrations. Lead (Pb) is a common contaminant and even a little has the potential to cause chronic diseases and brain damage to human (Tang et al., 2009). Therefore, the maximum concentration limits for Zn(II) and Pb(II) in drinking water are strictly regulated. For example, Canadian Water Quality Guidelines (2004) and Indian Standards (1991) recommend that the concentration of Zn(II) in drinking water not exceed 5 mg/L, while the WHO (2006) recommends 3 ml/L as an upper limit for Zn(II) and 0.01 mg/L for Pb(II). The USEPA (2011) recommends concentrations of Zn(II) below 5 mg/L and of Pb(II) below 0.015 mg/L.

Thus, the high toxicity of landfill leachate has great potential for pollution of the surrounding environment, especially groundwater (Christensen et al., 2001). Surface water pollution caused by landfill leachate has also been observed, although relatively few cases have been described in the literature. According to Kjeldsen et al. (2002), the major potential effects of a leachate release to surface water are oxygen depletion in part of the surface water body, changes in the stream bottom fauna and flora, and ammonia toxicity. In order to prevent ecological environments from being polluted by the release of landfill leachate, two important issues should be taken into account:

1) Leachate generation
2) Containment capacity

Landfill leachate generation is a long-term process, ranging from several months to centuries depending on various factors, including soil properties, weathering conditions, waste composition, landfill operation, volume of infiltration water, landfill age, etc.(Wall and Zeiss, 1995; Townsend et al, 1996; Johannessen, 1999; Tchobanoglous and Kreith, 2002; Silva, 2004; Kulikowska and Klimiuk, 2008; Renou et al., 2008). To reduce research expenses and experiment duration, environmental conditions are usually simulated inside laboratory-scale lysimerters and columns. These lysimeters operate under various geometry characteristics (e.g. height/width ratio), which can change the physical and thermodynamic characteristics. According to Kim et al. (2010), the volume of reactors as well as the height/width ratio significantly vary, ranging from several liters to several cubic meters as shown in Fig. 1.3. Short- and long-term behaviors of pollutants based on different lysimeter volumes have been studied (Van der Sloot et al., 2001, Kylefors et al., 2003, Guyonnet et al., 2008). However, few studies have focused on the effects of the reactor‘s H/W ratio and height on the physical and thermodynamic characteristics. The H/W ratio and the height can easily influence external factors such as loading amount of substrate, internal temperature change, and water contents (Vicente-ferreira et al., 2007). Fig. 1.4 shows the effect of a reactor H/W ratio on leaching behavior and waste decomposition. Assuming two lysimeters of the same volume with different H/W ratios, the reactor with low H/W has less waste and more rainfall amount per unit volume than the lysimeter with high H/W. It might be possible for the lysimeter with low H/W to show a low settlement rate and high water flux, resulting in high water and air permeability and high liquid-to-solid (L/S) ratio of waste. Finally, the reactors might show different leaching behaviors and waste decomposition rates.

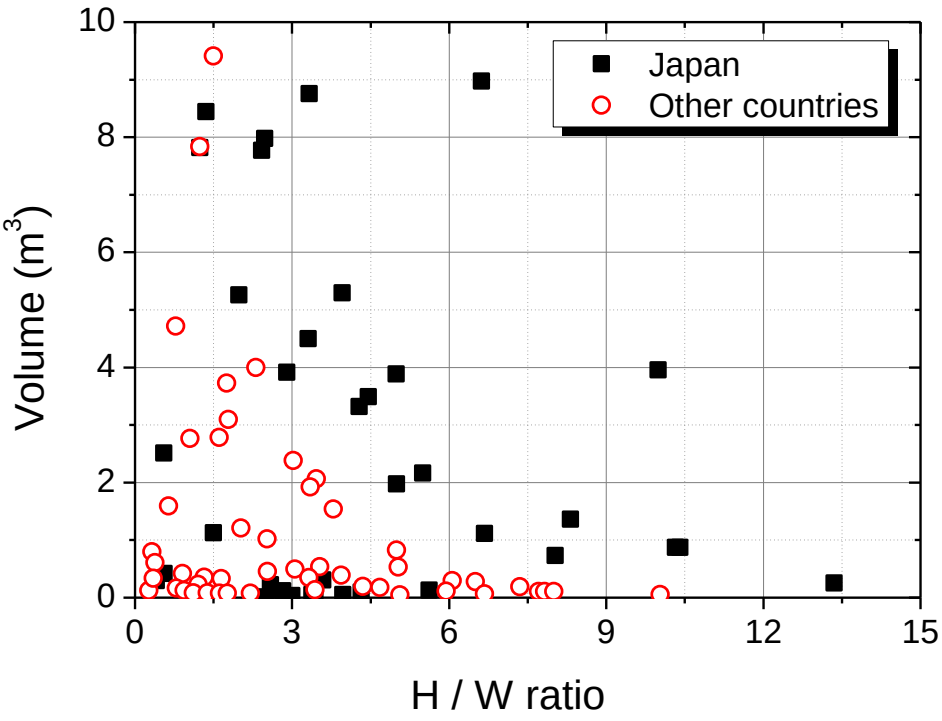

Fig. 1.3 Relationship volume with height/width ratio of lysimeters (Kim et al., 2011)

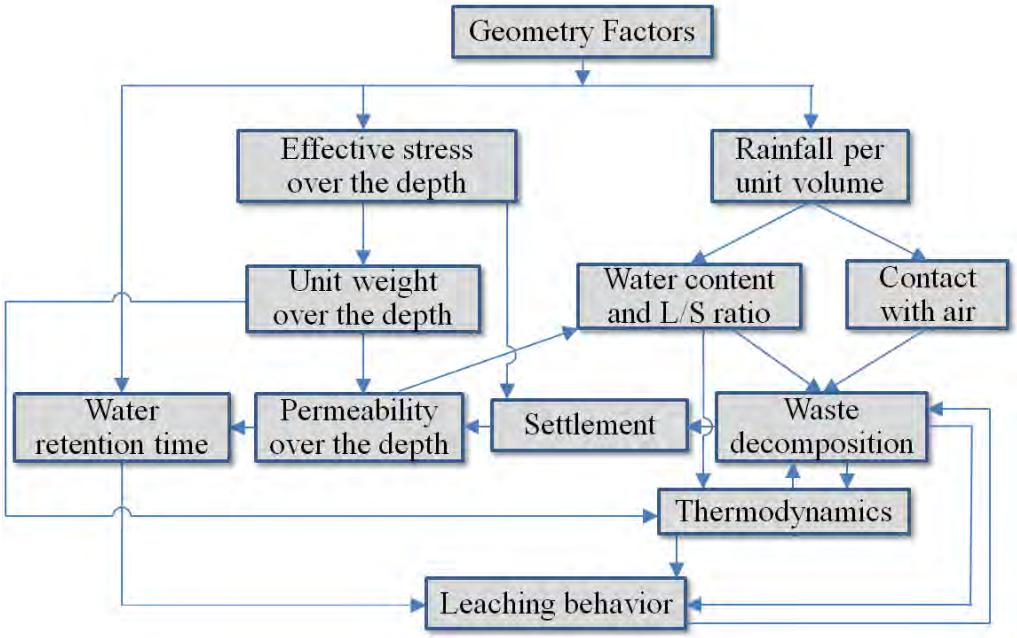

Fig. 1.4 The effect of geometry factors on leaching behavior and waste decomposition

Containment capacity mainly depends on the barrier performance of liner system, especially the

bottom liner system. Compacted clay liners (CCL) are usually employed as bottom liner systems in waste containment facilities due to their affordability and excellent barrier performance against the migration of aqueous contaminants (e.g., Boynton and Daniel, 1985; Shelley and Daniel, 1993; Chapuis, 2002). The CCL can greatly reduce leachate leakage but cannot eliminate it. Each engineered landfill is a closed system in the short term but an open one in geological terms (Zhang, 2002). The performance of these clay liners may be greatly enhanced if they exhibit semipermeable membrane behavior to prevent or restrict the migration of selected substances (Tuwiner, 1962; Mulder, 1991). In the case of a chemical solution, a semipermeable clay liner can inhibit the migration of solute molecules (Mitchell, 1993), allowing water to flow from a lower solute concentration (higher water activity) to a higher solute concentration (lower water activity) until equilibrium is reached (Olsen, 1969; Olsen, 1972; Greenberg et al., 1973; Manassero and Dominijanni, 2003; Shackelford and Lee, 2003; Henning et al., 2006).

Membrane behavior represents a potentially significant benefit that has not been considered in practical applications (Shackelford, 2013). It has been the subject of significant research over the past 15 years. Membrane behavior has been observed in several types of soils used as liners or barriers (e.g., Malusis and Shackelford, 2002a; Malusis and Shackelford, 2004; Yeo et al., 2005; Evans et al., 2008; Kang et al., 2010). However, the observed membrane behavior has been too low to sufficiently prevent the migration of contaminants. According to previous research, bentonite can improve membrane behavior effectively, and membrane behavior is likely to be significant only in clay barriers that contain high-swelling smectitie minerals such as sodium bentonite (Malusis and Shackelford, 2002b; Shackelford, 2013). Thus, combining the advantages of clay and bentonite, the latter is introduced to promote the barrier performance of clay towards contaminants and enhance its membrane properties (Malusis and Shackelford, 2002b; Yeo et al., 2005; Evans et al., 2008; Kang and Shackelford, 2010). Various factors influence membrane behavior, including clay mineralogy, solute concentration, and consolidation (Malusis and Shackelford, 2002; Van Impe, 2002; Kang and Shackelford, 2010; Kang and Shackelford, 2011). According to previous studies, bentonite can improve membrane properties. However, the bentonite content used in these studies significantly varied as shown in Table 1.1. Few studies (e.g. Shackelford, 2012) have evaluated the effect of bentonite content on membrane behavior.

Table 1.1 Bentonite content in membrane tests in references

Clay	Bentonite	Bentonite content (by dry weight)	References
NFC	Na-bentonite	0, 5%	Kang and Shackelford (2010)
CS	Na-bentonite	5%	Yeo et al. (2005)
Kaolin	Na-bentonite	20%	Van Impe (2002)
-	Na-bentonite	100%	Malusis and Shackelford (2002b)

* NFC, Nelson Farm Clay; CS, Clay-Sand mixture

Compacted clay liners used as bottom liners for landfills are exposed directly to leachate from the landfill, which contains very high concentrations of inorganic ions such as Na, K, Ca, and heavy metals. According to Baun and Christensen (2004), most landfill leachates contain up to 155 mg/L of Zn(II) and up to 1.5 mg/L of Pb(II). The pH of leachate varies from landfill to landfill, as shown in Table 1.2, due to factors such as waste composition, landfill age, and weather conditions. According to Christen et al. (2001), pH of the landfill leachate is usually acidic (4.5-7.5) during the acid phase at the early stage and then gradually increases to alkaline (7.5-9.0) during the methanogenic phase. Thus, to avoid pollution of the surrounding soil and groundwater environment, barriers must maintain excellent performance under both acid and alkaline conditions.

Table 1.2 Range of pH values for landfill leachates in various countries

Country	pH Range	Country	pH Range	Country	pH Range
U.S.	4.5 - 8.2	Greece	6.2 - 7.9	Japan	6.8 - 12.7
Canada	5.8 - 9.0	Denmark	4.5 - 8.6	China	6.8 - 9.1
UK	6.4 - 8.0	Netherlands	5.9 - 7.0	South Korea	7.3 - 8.6
France	7.0 - 8.4	Finland	7.1 - 7.6	Malaysia	7.5 - 9.4
Germany	4.5 - 9.0	Turkey	5.6 - 8.6	Brazil	8.2
Italy	8.0 - 8.4	Poland	~ 8.0		

* Data from Baun and Christensen (2004), Osako et al. (2004), and Renou et al. (2008).

Landfill leachate, especially when acidic, favors the solubilization of heavy metals, which can pose a severe threat to local ecosystems (Ritcey, 1989; Aubertin, 1996). Moreover, the thickness of the compacted clay liner differs depending on engineering and environmental requirements, and few researchers have evaluated the effect of compaction degree, which can be significant for soil cohesion, fabric, and pore-size distribution (Mitchell et al., 1965; Daniel and Benson, 1990; Prapaharan et al., 1991; Delage et al., 1996; Vanapalli et al., 1999; Watabe et al., 2000). Thus, compaction degree is expected to play an important role in the membrane behavior of clay.

1.2 Objectives and scope

The overall aim of this thesis is to evaluate the geometry effect on landfill leachate generation and the effect of different factors on the membrane behavior of compacted clay liner. The project highlights the importance of the geometry effect and the membrane behavior of the clay liner under different external conditions. These goals are stated as follows:

1) To investigate the geometry effect on leachate generation and composition through a laboratory-scale test with lysimeters of different size.

2) To study the membrane behavior change in a laboratory-scale test under different conditions,

including bentonite content, solute pH and concentration, compaction degree, and thickness, as well as different kinds of ions, such as Na, K, Ca and heavy metal ions.

1.3 Dissertation outline

This dissertation is comprised of six (6) chapters. The main points and the experimental approach of this study are listed in Fig 1.5. During the experimental work, a lysimeter test, a leaching test, and a membrane test were conducted and used to evaluate factors influencing landfill leachate generation and membrane behavior of the bottom compacted clay liner. The outline of this research is shown in Fig. 1.6 and summarized as follows:

1) Chapter 1 presents the background, objectives, and outline of this dissertation.
2) Chapter 2 includes a literature review of the general composition of landfill leachate, different factors affecting leachate generation, and two major bottom liners, geosynthetic clay liner (GCL) and compacted clay liner (CCL). Then, it presents an overview of membrane behavior, including the discovery of membrane behavior, measurement by laboratory-scale experiment, quantification, significant factors, as well as practical application.
3) Chapter 3 describes the effects of geometry on landfill leachate generation and composition based on the experimental results obtained from the lysimeter test, including height and height/width ratio. Leaching behavior is also studied by leaching test. Optimum values of height and height/width ratio of lysimeters are proposed based on the results and discussion.
4) Chapter 4 describes different factors of membrane behavior, including bentonite content, solute pH and concentration, compaction degree, thickness, and solute type. The major physical and chemical properties of the materials are measured through preliminary experiments, such as standard compaction test, and CEC value. A standard free swelling test is conducted to evaluate the materials‘ response under different test conditions, pH values, concentrations, and solute types. To further investigate the mechanism of membrane behavior, Scanning Electron Microscopy (SEM), X-Ray Fluorescence (XRF) and X-ray diffraction analysis (XRD) are performed.
5) Chapter 5 presents solute transport equations proposed by previous researchers that consider both advection and membrane behavior on solute transport. Based on these equations, a numerical analysis is presented. According to the results, the practical implications of this study are discussed.
6) Chapter 6 summarizes the experimental results and provides the conclusions of this study. Further research directions are suggested, including the improvement of current research and bio-geo-environmental engineering.

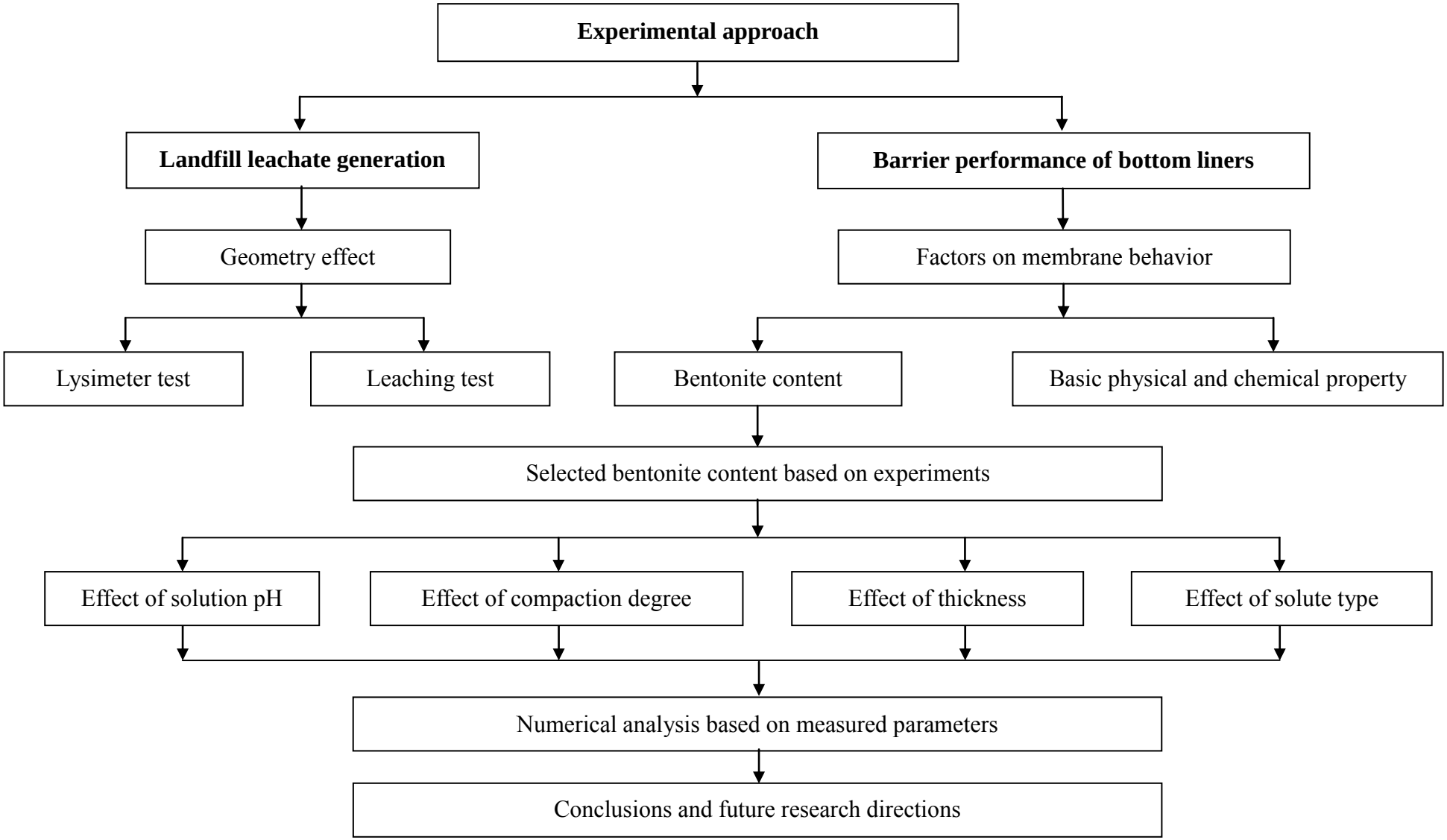

Fig. 1.5 Outline of experimental approach

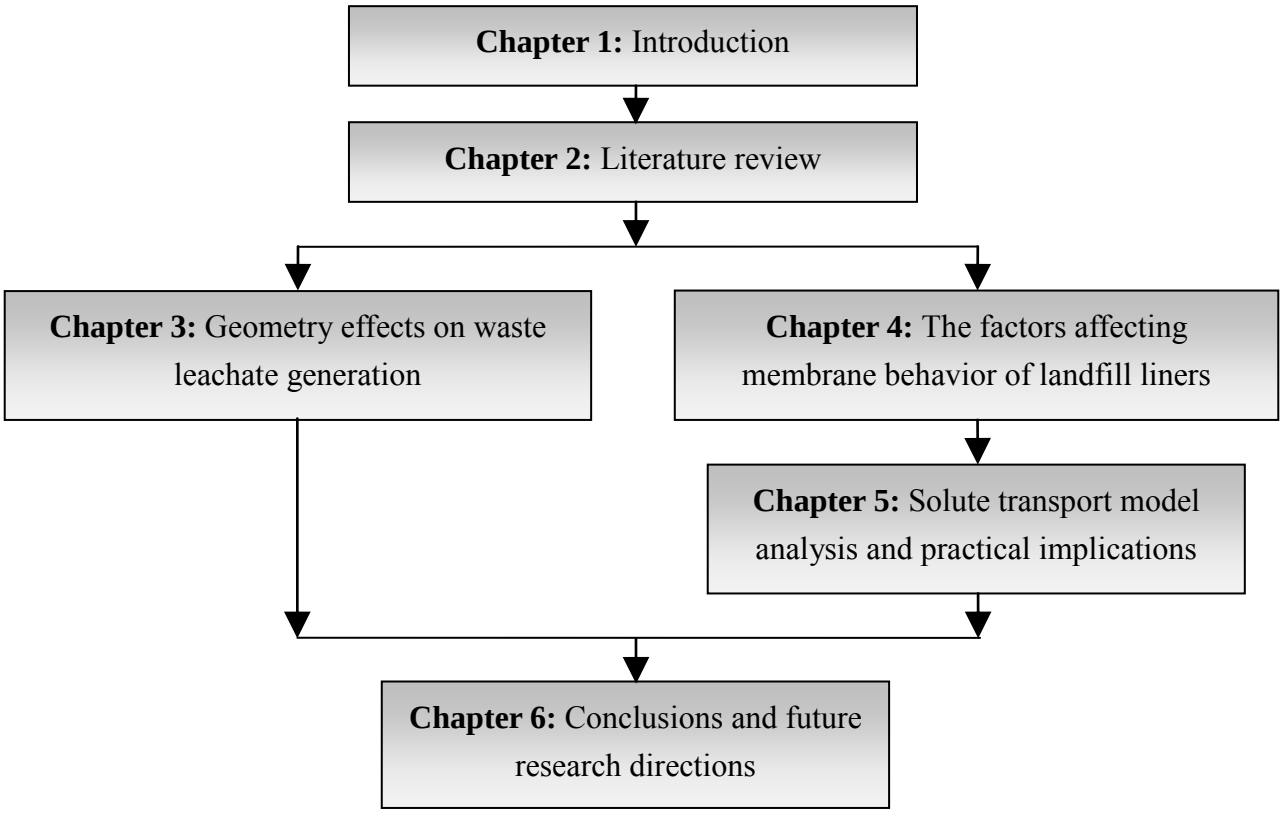

Fig. 1.6 Outline of dissertation

1.4 Originality

The lysimeter test, membrane test, and numerical analysis are conducted in Chapters 3, 4, and 5. The originality can be summarized as follows:

1) Lysimeters and columns have been widely applied to simulate landfills in the study of landfill leachate generation. Previous researchers have used different lysimeters, and many factors have shown significant effects, such as the existence of water, microorganisms, suitable temperature. However, the geometry effect has been neglected in these studies. In Chapter 3, a lysimeter test is conducted under different geometry factors to study the effect on landfill leachate generation and composition.
2) The membrane behavior of natural clay and clay mixtures has been previously observed. However, few studies have included the effects on membrane change. In the current research, a membrane test is conducted under different conditions (bentonite content, compaction degree, thickness of specimens, solution pH, and type).
3) Various methods are used to study membrane behavior in this study, including a pressure transducer to study chemico-osmotic pressure, an SEM image to observe the micro-structure of interparticle space, and XRD and XRF to analyze the mechanism of membrane behavior and the chemical reaction during the membrane test, respectively.

4) A new experimental apparatus was designed for this research which simplified operation and reduced expense. Using this apparutus, the actual chemico-osmotic pressures can be measured under different test conditions, which help to prove the reliability of this apparatus.
5) Besides the results obtained from the laboratory-scale membrane test, the membrane behavior is correlated to the service life of the bottom liners using the advection-diffusion model. Through the numerical analysis in Chapter 5, a relationship between the macro-scale service life of the bottom liner and the micro-scale phenomenon of membrane behavior is established.

CHAPTER 2: LITERATURE REVIEW

2.1 General remarks

Landfill has proven the most cost-effective method for solid waste disposal around the world, especially in developing countries. Nowadays, as waste generation increases significantly worldwide, more and more landfill sites are required. Nevertheless, no matter the location of the landfill site, it will cause a great potential to lead to the damage of surrounding environment and threaten to the health of human being. Therefore, research about landfill become a hot issue, and attract more and more attention in recent year.

However, landfill site is a very complicated issue, and causes many environmental challenges to geoenvironmental researchers. The research directions about landfill include risk assessment, landfill operation and management, barrier performance of landfill liners (cover liner and bottom liner system), the settlement process and stability of waste body, the generation of landfill emissions (landfill leachate and landfill gas), and relevant treatment technology towards them. This study covers on the generation of landfill leachate and the barrier performance of landfill bottom liners.

The generation of landfill leachate depends on lots of conditions, such as the existence of water, microorganism, suitable temperature etc. Thus a lot of factors can significantly affect the landfill leachate generation, including soil properties, weathering conditions, waste composition, landfill operation, volume of infiltration water and landfill age. Landfill leachate contains high concentration of contaminant, which is likely to cause the pollution to groundwater.

Thus bottom liners are always designed and applied to isolate the contaminant from surrounding soil. Hydraulic conductivity (k), diffusion coefficient (D) and retardation factor (R) are usually utilized to quantify the barrier performance of liners. In addition to them, in some cases, the liners can exhibit a membrane property like a semi-permeable membrane. Therefore, this membrane behavior, quantify with chemico-osmotic efficiency coefficient ω, provides a new perspective to evaluate the barrier performance of liners.

The purpose of this chapter is to briefly introduce (1) composition and generation of landfill leachate, (2) various factors affect landfill leachate generation and compostion, (3) bottom liner systems, including compacted clay liner (CCL) and geosynthetic clay liner (GCL) (4) Membrane behavior in liner system, including its observation and influence factors.

2.2 The usage of lysimeters and columns

Lysimeters and columns were widely utilized to simulate the landfill or other experimental conditions for researches in many fields since its raltive low expense, simple installation and operation etc.. For the research about the landfill, compared to field in site experiment, lysimeters are smaller, more self-contained and better monitored than landfills. Their small scale allows their

location in a laboratory, where it is convenient to perform extensive monitoring. In addition, their small size allows tests to be conducted in multiples that are simply not economically feasible with even pilot-scale landfills. As a result, they are often employed as the first step in investigating the implementation of a new concept in landfill management (Stessel and Murphy, 1992).

In Kim et al. (2011) research, lysimeters were used to study the long-term behavior and fate of metals in leachate from four simulated bioreactor landfills under both aerobic and anaerobic conditions. As shown in following Fig. 2.1, it was the schematic of the aerobic and anaerobic lysimeters used.

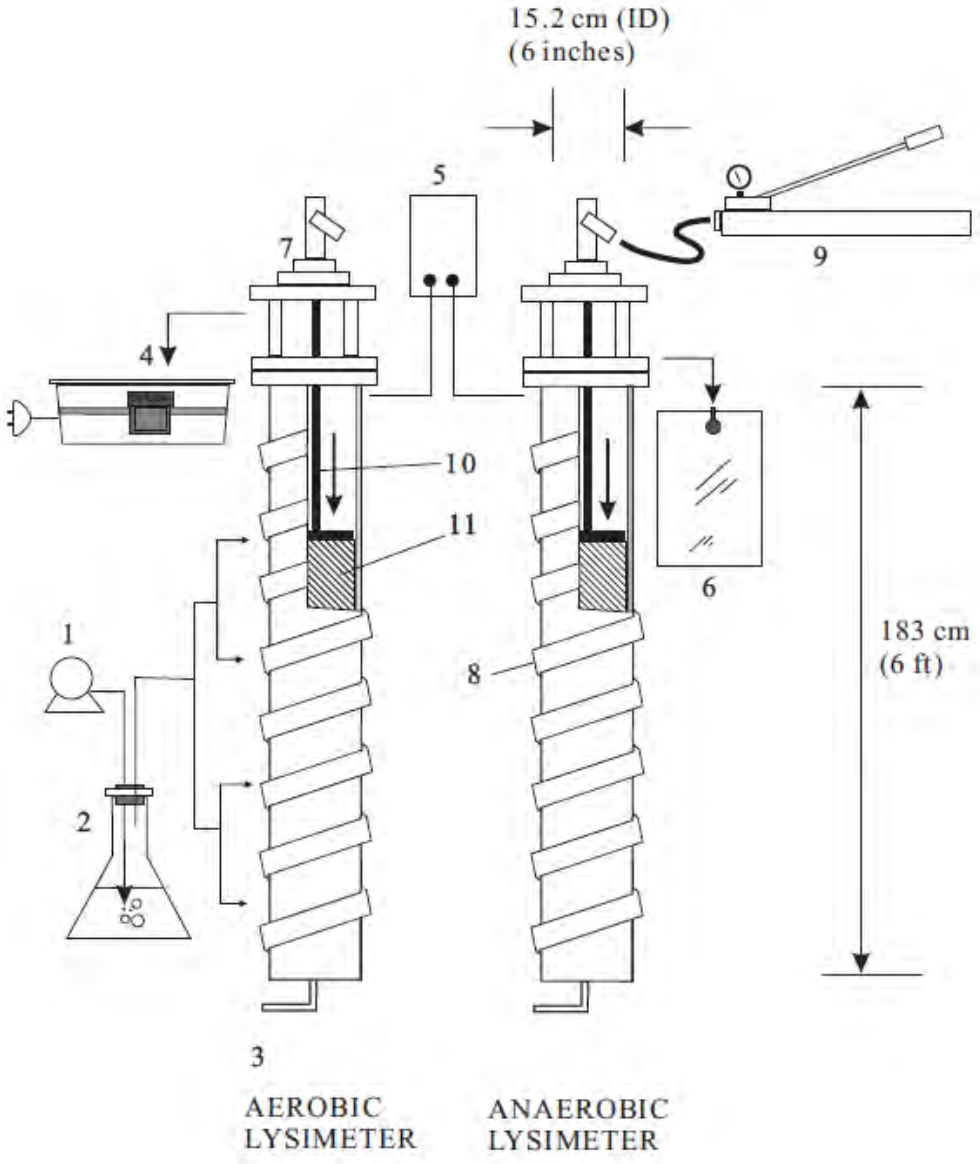

1. peristaltic pump; 2. air purging; 3. leachate collection port; 4. wet-tip gas totalizer; 5. temperature controller; 6. gas-sampling bag; 7. hydraulic cylinder; 8. heating tape; 9. hydraulic jack; 10. plunger; 11. fabricated wastes

Fig. 2.1 Schematic of the aerobic and anaerobic lysimeters used in Kim et al. (2011)

Each lysimeter consisted of a stainless steel column and carriage system. The 183-cm (6 ft) stainless steel body contained 5 front ports and 1 valve at the bottom for leachate collection. The front ports were used for air addition (in the case of the aerobic lysimeters). A small port located on the top flange was used for liquids addition. Perforations in the steel plate allowed added liquids to percolate into the waste. The amounts of gas produced from each lysimeter were monitored using a gas totalizer. The carriage system was designed to support a hydraulic pressurizing unit installed at the top of each lysimeter for the application of an external load to the fabricated waste. To maitain aerobic conditions, air was added and maintained at a rate between 70 and 120 mL/min (Kim et al., 2011).

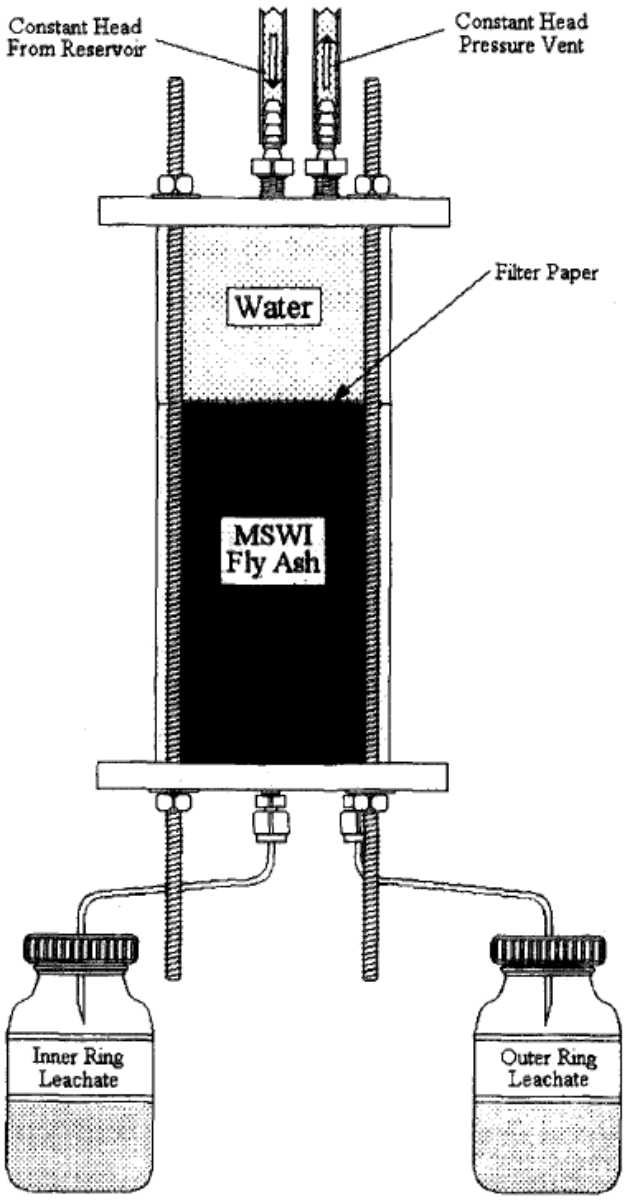

Fig. 2.2 Schematic drawing of column in Chichester and Landsberger (1996)

Chichester and Landsberger (1996) also used column for determination of the leaching dynamics of metals from municipal solid waste incinerator fly ash. The schematic drawing of column was as above Fig. 2.2. The cylinder wall, cylinder ring, top and bottom plate were made of cast acrylic plastic, while the 4 support rods and 8 nuts and washers were made of stainless steel. Besides above labortary-scale lysimeters, larger scale lysimeters and columns were also applied in labortary and field site experiments. As shown in the following Fig. 2.3, it is the larger lysimeters used in Henken-Mellies and Schweizer (2011). The properties of materials used in the lysimeter test were shown in Table 2.1.

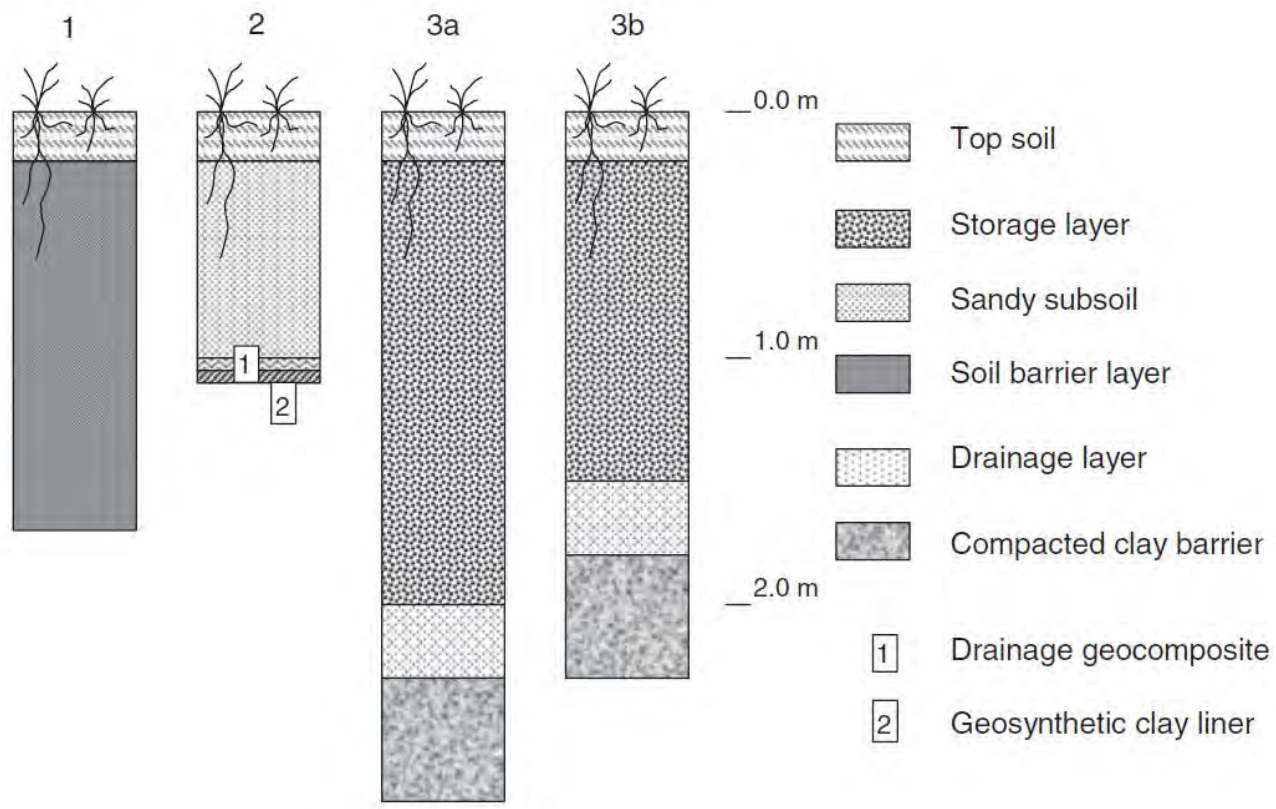

Fig. 2.3 Profiles of the lysimeter test field

The lysimeters in Fig. 2.3 is situated near the town of Aurach in Northern Bavaria, German, some 60 km south-west of the city of Nuremberg in a gently hilly region at an elevation of 500 m above sea level. The lysimeter test fields were erected on the slope of a municipal waste landfill, inclined at 14^{o}, exposed towards the south. Vegetation at the site is mainly grass and herbaceous plants.

Table 2.1 Properties of materials usd in Henken-Mellies and Schweizer, (2011)

Description of layer	Lysimeter 1: Simple soil barrier	Lysimeter 2: GCL	Lysimeter 3a/3b: CCL
Top soil	0.2 m loamy sand	0.2 m loamy sand	0.2 m loamy sand
Subsoil	1.5 m sandy loam; 6-14% clay(< 2μm) 16-24% silt 62-78% sand Compacted k: 10^{-7} to 10^{-10} m/s	0.8 m sand 4% clay 9% silt 87% sand Compacted k: 7 x 10^{-6} m/s	1.3/1.8 m sandy loam; 6-14% clay(< 2μm) 16-24% silt 62-78% sand Built with low compaction k: 10^{-6} to 10^{-7} m/s
Drainage layer	None	Drainage geocomposite	0.3 m gravel
Barrier layer	None	Ca-bentonite GCL permittivity: 8 x 10^{-9} m/s	0.5 m compacted clay layer Plastic limit: 20% Liquid limit: 41% k < 3 x 10^{-9} m/s

Rafizul et al. (2012) constructed three pilot scale landfill lysimeters in Bangladesh to evaluation the landfill emissions and leaching behavior of landfill leachate. As shown in the following Fig. 2.4, it was the schematic diagram of the lysimeter. The landfill lysimeter test facilities were set-up in the geo-environmental research station at the backyard of Civil Engineering Building, KUET, Bangladesh. Lysimeter was used to simulate the different landfill concept, operational condition and the total weight of MSW was deposited in each lysimeter around 2900 kg. The three landfill lysimeter, were constructed using the brick wall of 250 mm thick having outer and inner diameter of approximately 2.0 m and 1.48 m, respectively, with a total height of 3.35 m, resting on a 250 mm thick of reinforced cement concrete mat foundation at a depth of 760 mm below the existing ground surface. The landfill lysimeter was plastered both the inner and outer sides with two coatings of waterproofing agent to avoid leakages and corrosion due to acidic environment. Further, the anaerobic landfill lysimeters consists of LFG collection system above the MSW and leachate recirculation system below the MSW in landfill lysimeter. At the bottom of each landfill lysimeter, a cement concrete layer of 125 mm thick was provided then the landfill lysimeters were filled with stone chips (diameter 5–20 mm) and coarse sand (diameter 0.05–0.40 mm) to the height of 15 cmeach to ensure proper leachate drainage. At the base of each landfill lysimeter after placing the perforated leachate collection pipe, a geo-textile blanket having 0.60 m wide and 1.65 m length was placed to avoid rapid clogging by the sediments from landfill lysimeter. A leachate collection tank (3.68 x 1.56 x 1.64 m) accommodating four separate leachate discharge pipes in the temporary collection and storage containers, were constructed using 250 mm thick brick wall.

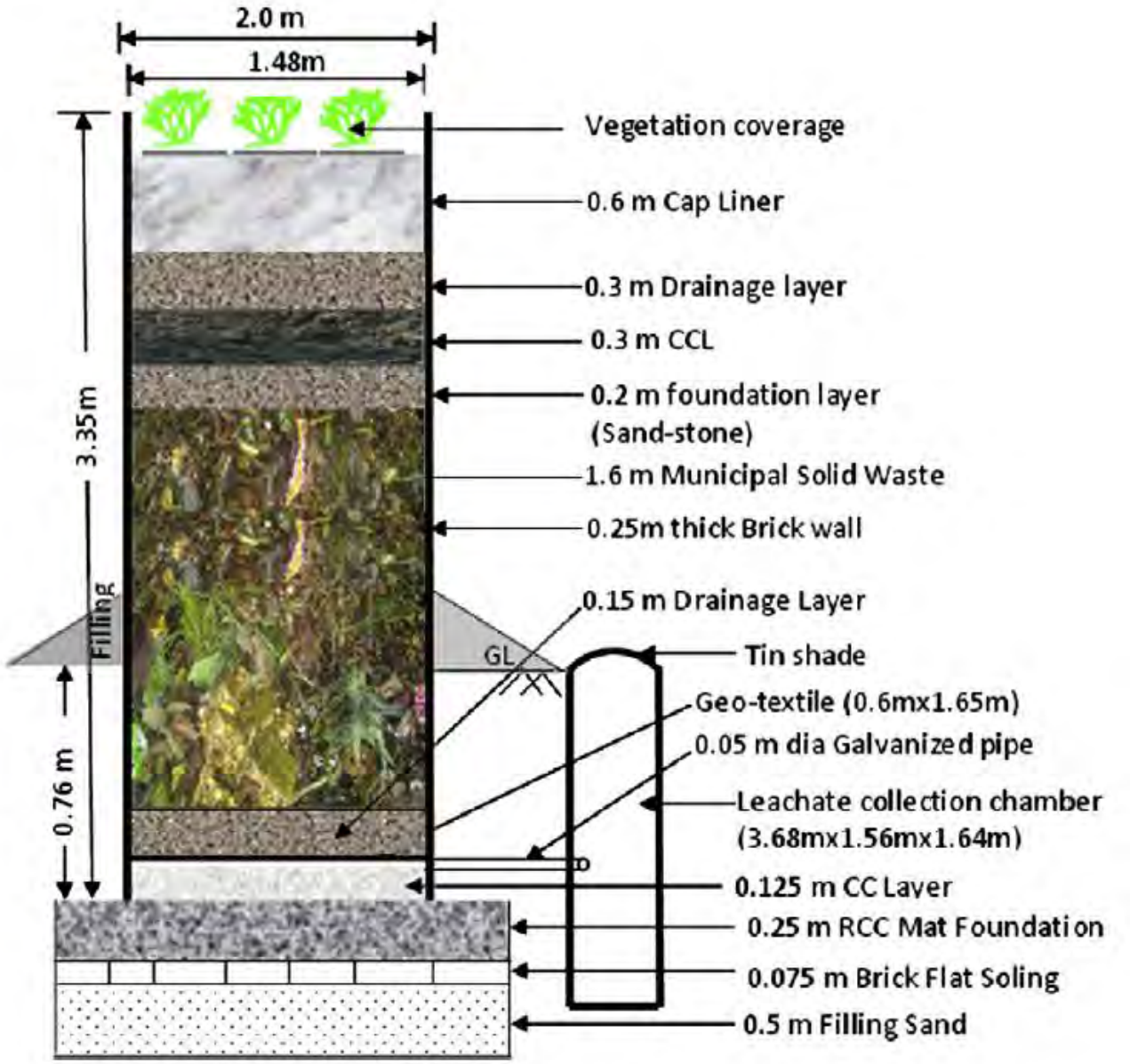

Fig. 1. Schematic diagram of reference cell.

Fig. 2.4 Schematic diagram of lysimeter in Rafizul et al. (2012)

According to all of above, the lysimeters and column used in previous literatures were usually of great difference on the factors, height and height / width ratio. Until now, very few researches were once concerned about this issue, although it can affect the leaching behavior and landfill leachate compositions. Consider all of above, one of the objectives of this research is to investigate the geometry effect on leachate generation, and the lysimeters with different sizes were designed for lysimeter test in Chapter 3.

2.3 Landfill leachate and influence factors

The infiltration of rain water, surface water into a landfill and water contained waste, coupled with physical, chemical and microbial processes, produces a kind of polluted liquor, landfill leachate (Christensen and Kjeldsen, 1989). Normally, landfill leachate consists of water that carries chemicals, metal contaminants and organic matter in the form of solution or suspension (Zhang, 2002).

According to Christensen et al. (2001), the contaminant contained in landfill leachate can be characterized and clarified into four groups.

1) Dissolved organic matter, expressed as chemical oxygen demand (COD) or total organic carbon (TOC), including CH_4, volatile fatty acids and more refractory compounds.

2) Inorganic macrocomponents: Ca, Mg, Na, K, NH_4^+, Fe, Mn, Cl, SO_4^{2-} and HCO_3^-

3) Heavy metals: Pb, Zn, Cd, Cr, Cu and Ni.

4) Xenobiotic organic compounds (XOCs) originating from household or industrial chemicals and present in relatively low concentrations (less than 1 mg/L).

In addition to above 4 groups of contaminant, some other compounds may be found in landfill leachate, e.g. B, As, Se, Ba, Li, Hg and Co. But compared to above contaminant from above 4 groups, they are found in very low concentrations and are only of secondary importance (Christensen et al., 2001).

The magnitude of particular parameters for leachate vary from site by site since a lot of influence factors, including soil properties, landfill age, weathering conditions, waste composition, landfill operation and volume of infiltration water. However, by taking an overview of the large amount of available previous literature, the author made a summary of the typical concentrations of common pollutant in leachate collected in leachate drainage systems of landfills in operation and in leachate-polluted groundwater collected below or within a few meters down-gradient of old unlined landfills from several countries or regions, and the results were presented in Table 2.2 (Johansen and Carlson, 1976; Ehrig, 1983, 1988; Chu et al., 1994; Clement and Thomas, 1995; Jørgensen and Kjeldsen, 1995; Robinson, 1995; Krug and Ham, 1997; Kjeldsen and Christophersen, 2001; Baun and Christensen, 2004).

Table 2.2 Typical concentrations of common pollutant in landfill leachate (Unit: mg/L)

	Germany	Denmark	USA	UK	Hong Kong	Netherlands	France
pH	4.5-9	4.5-8.6	4.5-8.2	6.4-8.0	7.2-8.4	5.9-7.0	7.8-8.4
COD	500-60000	16-2300	50-62000	< 10-33700	147-1670	110-9425	400-8000
TOC	NA	1-670	NA	2.8-5690	NA	30-1700	100-2700
Cl	100-5000	10-3200	10-6000	27-3410	140-1337	68-680	750-2185
NH_4	39-3860	0.05-910	NA	< 0.25-1560	84-2070	21-292	103-1247
SO_4	10-1750	0.5-820	NA	< 5-739	NA	10-100	< 5-506
Ca	10-2500	6-660	NA	60-1440	NA	99-400	15-246
Na	50-4000	7-1000	10-3700	12-3000	132-1190	34.8-462	519-2957
Mg	40-1150	3-430	NA	18-470	9-63	13-96	51-271
K	10-2500	1-1100	2.7-1480	NA	78-632	21.3-219	202-1612
Fe	3-2100	0.08-180	10-1100	0.1-664	1.14-5	11.5-234	0.3-10
Mn	0.03-65	0.01-20	NA	0.06-23.2	0.05-1.3	NA	NA
As	0.005-1.6	0.0005-0.13	NA	< 0.001-0.049	NA	NA	NA
Cd	0.0005-0.14	0.00002-0.030	0.001-0.130	< 0.01-0.03	< 0.01-0.02	0.0001-0.002	NA
Co	0.004-0.95	0.001-0.010	NA	NA	NA	0.004-0.033	NA
Cr	0.03-1.6	0.0005-1.3	0.05-1.05	<0.04-0.56	0.02-0.23	0.002-0.17	NA
Cu	0.004-1.4	0.0005-0.67	0.18-1.30	<0.02-0.16	0.01-0.13	0.008-0.085	NA
Hg	0.0002-0.05	0.00005-0.019	NA	<0.0001-0.001	NA	NA	NA
Ni	0.02-2.05	0.001-3.2	0.1-1.20	<0.03-0.33	0.04-0.18	0.005-0.12	NA
Pb	0.008-1.02	0.0005-1.5	<0.1-1.40	<0.04-0.28	0.03-0.12	0.001-0.015	NA
Zn	0.03-120	0.00005-7.2	5.3-155	<0.01-6.70	0.13-2.55	0.055-2.65	0.1-0.7

Johansen and Carlson (1976); Ehrig (1983); Ehrig (1988); Chu et al. (1994); Clement and Thomas (1995); Jørgensen and Kjeldsen (1995); Robinson (1995); Krug and Ham (1997); Kjeldsen and Christophersen (2001)

The generation of landfill leachate depends on lots of conditions, such as the existence of water, microorganism, suitable temperature etc. Thus a lot of factors can significantly affect the landfill leachate generation, including soil properties, landfill age, weathering conditions, waste composition, landfill operation and volume of infiltration water.

According to previous published literatures, the landfill leachate generation rates range from 15% to 55% of annual precipitation. Generally, landfill well-compacted cover produces only half the amount of leachate compared with that with loose cover, and an uncovered landfill produces almost 50% more leachate than one covered with soil and vegetation (Sarsby, 2000).

Trankler et al. (2005) reached the similar conclusions through laboratory experiment, in which 5 large-scale lysimers (3.5 m height with diameter of 1.4 m) were designed to simulate the sanitary landfill (SL1, SL2, SL3, OC and PL). SL1, SL2, SL3 and PL were constructed with different kinds of cover system, while OC was an open cell. All lysimeters were placed outside in Bangkok, Thailand. This was a long term experiment, which lasted for three years, thus experienced rainy season and dry season several times. Some of the test results were summarized as following Fig. 2.5.

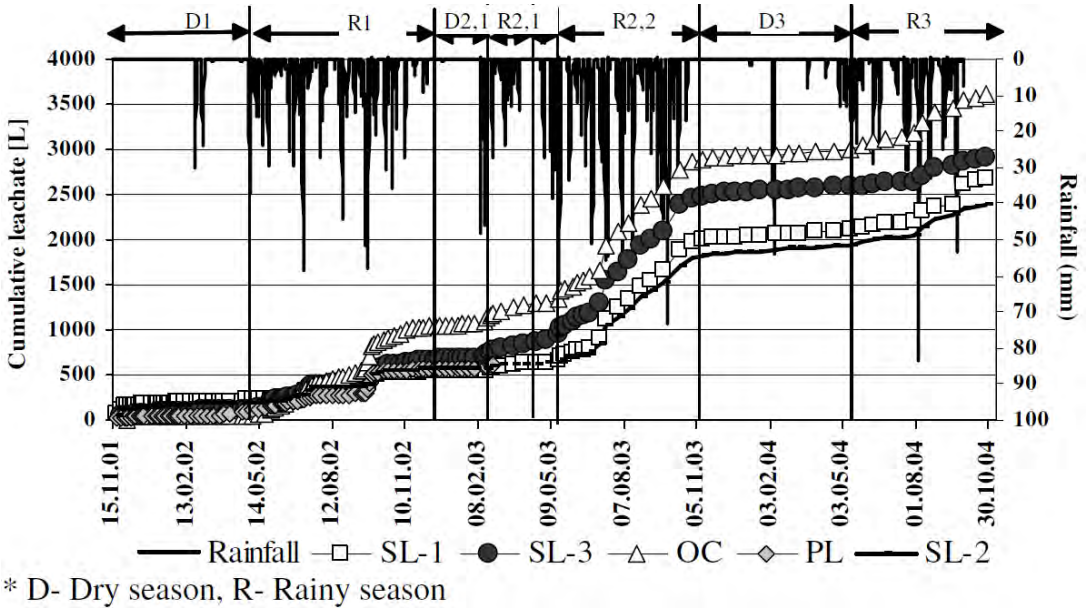

Fig. 2.5 Cumulative leachate production from lysimeters as function of rainfall

In Fig. 2.5, it presented the relationship between cumulative leachate productions from lysimeters with rainfall. The results over two subsequent dry and rainy seasons indicate that the open cell lysimeter showed the highest leachate generation throughout the rainy season compared to the other lysimeters with cover system. During the dry periods, the leachate flow in all lysimeters coming to a halt. These results exhibited a close relationship between landfill leachate generation amount with infiltration water origined from rainfall. Besides the leachate generation rate, the rainfall was also proved to have effect on the composition of leachate. As shown in the following Fig.

2.6 and Fig. 2.7, it was clear that after the heavy rainfall every time, the COD displayed a rapid decrease, which pH showed an increase tendency. The similar observations were also made under temperate climate by Khattabi et al. (2002) at Etueffont landfill, France. Such phenomenon can be attributed to the flushing effect or can be due to the enhancing of biological activities, which was stimulated by infiltration of rainfall, which resulted in the acceleration of decompose process.

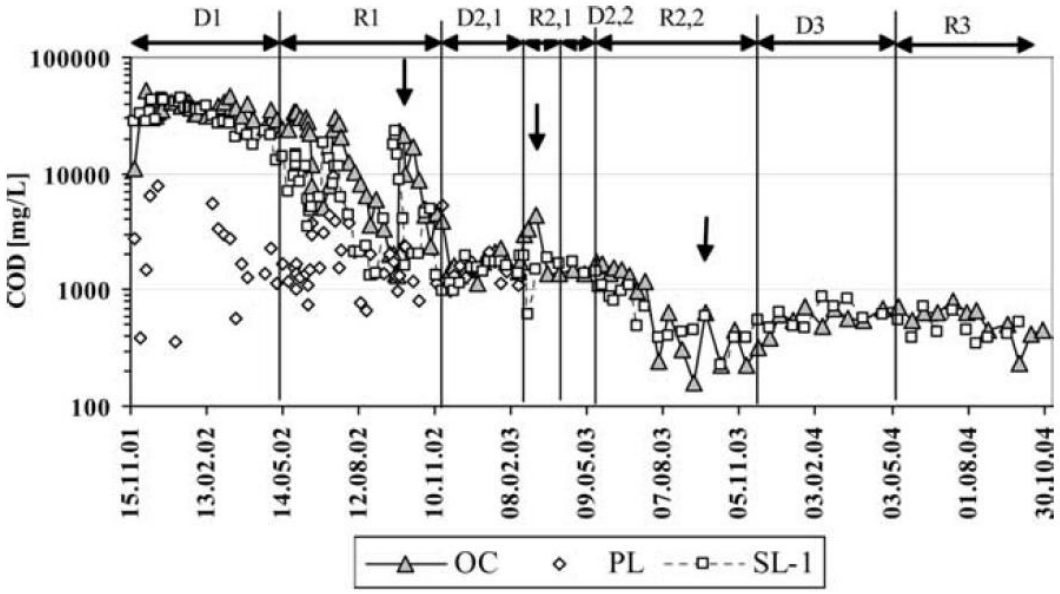

Fig. 2.6 Variable COD concentrations over the period of landfill operation

Therefore, in general current practice is to construct a cover system over a landfill as soon as the waste reaches the designed final grade, in order to minimize leachate production. However, there is a growing body of opinion in favor of delaying construction of the final cover. Hanashima and Furuichi (2000) thought much infiltration from rainfall can accelerate the process of decomposition or organic materials and settlement caused by biological activities (Hanashima and Furuichi, 2000; Trankler et al., 2005).

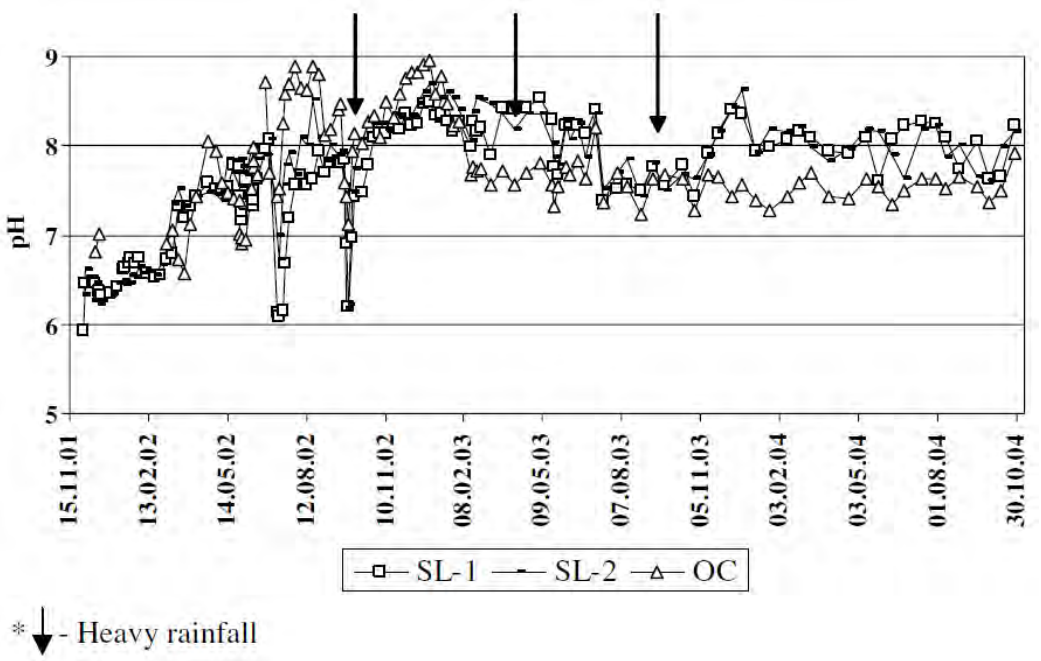

Fig. 2.7 pH variation in the lysimeters over the period of landfill operation

For the case of composition of landfill leachate, it was found to vary greatly depending on the age of the landfill (Baig et al., 1999). Usually the age of landfill can be defined by two decomposition phases: acid phase and methanogenic phase. For young landfills, containing large amounts of biodegradable organic matter, a rapid anaerobic fermentation takes place with the main products were volatile fatty acids (VFA) (Welander et al., 1997), and this early phase can be called acid phase. As a landfill matures, the methanogenic phase occurs. During this phase, methanogenic microorganisms develop in the waste, and the VFA are converted to landfill gas (CH_4, CO_2) (Renou et al., 2008). In addition, the organic fraction in the leachate becomes dominated by refractory (non-biodegradable) compounds such as humic substances (Chian and DeWalle, 1976). The reported values of composition of landfill leachate in Table 2.2, some concentrations of contaminants cover wide ranges, which can be mainly caused by the age of the individual landfills. Christen et al. (2001) made a summary by just dividing data from landfill sites according to their age or decomposition phase as shown in following Table 2.3, by which, the general behavior tendency can be observed and defined (Ehrig, 1983, 1988).

Table 2.3 Composition of landfill leachate at different decomposition phases (mg/L)

Parameter	Acid phase		Methanogenic phase		Average
	Average	Range	Average	Range	
pH	6.1	4.5-7.5	8	7.5-9	
Biological oxygen demand (BOD_5)	13000	4000-40000	180	20-550	
Chemical oxygen demand (COD)	22000	6000-60000	3000	500-4500	
BOD_5/COD (ratio)	0.58		0.06		
Sulfate (SO_4)	500	70-1750	80	10-420	
Calcium (Ca)	1200	10-2500	60	20-600	
Magnesium (Mg)	470	50-1150	180	40-350	
Iron (Fe)	780	20-2100	15	3-280	
Manganese (Mn)	25	0.3-65	0.7	0.03-45	
Ammonia-N (NH_4-N)					741
Chloride (Cl)					2120
Potassium (K)					1085
Sodium (Na)					1340
Total phosphorus (TP)					6
Cadmium (Cd)					0.005
Chromium (Cr)					0.28
Cobalt (Co)					0.05
Copper (Cu)					0.065
Lead (Pb)					0.09
Nickel (Ni)					0.17
Zinc (Zn)	5	0.1-120	0.6	0.03-4	

1) Acid phase: Landfill leachate generated during this stage is characterized by high concentrations of VFA, acidic pH value, high COD value and high BOD/COD ratio. The low pH values tend to solublize some heavy metals.

2) Methanoganic phase: Landfill leachate generated during this stage is characterized by almost neutral to alkaline pH values, low concentrations of some inorganic ions. As pH value rises, the heavy metals will have higher potential to be fixed.

In acid phase, as much as 95% of the organic content consisted of VFA and only 1.3% of the organic content consisted of high molecular weight compounds (MW > 1000) (Harsem, 1983). Compare to that, in methanogenic phase leachate, 32% of organic content consisted of high molecular weight compounds (Christen et al., 2001). According to the results based on one methanogenic-phase leachate obtained from Artiola-Fortuny and Fuller (1982), more than 60% of the organic content consisted of humic-like material (Artiola-Fortuny and Fuller, 1982).

The concentrations of some of the inorganic ions depend on the stabilization process in the landfill site. In Table 2.3, the concentrations of Ca, Mg, Fe and Mn in the methanogenic phase leachate are much lower than that in acid phase, which can be attributed to a higher pH (enhancing adsorption and precipitation) and lower content of dissolved organic content (dissolved organic content may complex the cations). SO_4 are also lower in methanorganic phase due to microbial reduction of SO_4^{2-} to S^{2-} (Christen et al., 2001). For Cl, Na and K, no obvious differences were observed, because only to a minor extent governed by adsorption, complexation and precipitation.

According to the age, the landfill site was classified into three types: recent, intermediate and old landfill (Chian and DeWalle, 1976). The recent landfill represent the operation period less than 5 years, 5-10 years responding to intermediate one, and landfill more than 10 years are defined as old. Table 2.4 presents the typical characteristics of leachate composition responding to these three types (Chian and DeWalle, 1976).

Table 2.4 Landfill leachate classification vs. age (Chian and DeWalle, 1976)

	Recent	Intermediate	Old
Age (years)	< 5	5-10	> 10
pH	6.5	6.5-7.5	> 7.5
COD(mg/L)	> 10000	4000-10000	< 4000
BOD_5/COD	> 0.3	0.1-0.3	< 0.1
Organic compounds	80% VFA	5-30% VFA + HFA*	HFA*
Heavy metals	Low-medium		Low
Biodegradability	Important	Medium	Low

*HFA: Humic and fulvic acids

2.4 Compacted clay liner system

According to international regulations, landfills must be constructed with containment systems with low hydraulic conductivity in order to avoid contamination of groundwater and soil. The containment system may comprise a combination of pollutant barriers and leachate collection or drainage layers. Bottom liners are the most important barriers used in solid waste disposal facilities, which can effectively cut off the leachate migration and prevent groundwater from being polluted. According to Sharma and Reddy (2004), the normal bottom liners can be classifies as natural clay liner, such as compacted clay liner (CCL), and synthetic liners which includes geosynthetic clay liner (GCL), geomembrane, geotextiles, geonets and geogrids. Since CCL is commonly accepted and applied around the world, the author will have a short introduction about them.

CCL are widely used in cover systems and bottom liners for landfills. CCL are liners that are made of natural clay material and directly compacted in field site. According to the Resource Conservation and Recovery Act (RCRA) Subtitle D program (40 CFR 258), the new municipal solid waste landfill units and lateral expansions must be constructed with a composite liner and leachate collection system. The composite liner must consist of an upper component of a flexible membrane liner and a lower component of a minimum 2-ft-thick compacted soil material with a hydraulic conductivity (k) value less than or equal to 1×10^{-9} m/s (Sharma and Reddy, 2004). The Wisconsin Department of Natural Resources (WDNR) who has monitored and operated over 80 clay lined municipal landfills since 1976, requires that their compacted clay liners have a minimum thickness of 1.5 m (Gordon et. al., 1990). In Japan, natural clay ≥ 5 m in thickness with hydraulic conductivity ≤ 10^{-7} m/s can be utilized as a liner according to the regulation for controlled landfill. Otherwise, it requires one of three following liner systems: (1) two geomembranes which sandwich a non-woven fabric or other cushin material, (2) a geomembrane underlain by an asphalt-concrete layer ≥ 5 cm in thickness with hydraulic conductivity ≤ 10^{-9} m/s, or (3) a geomembrane underlain by a clay liner ≥ 50 cm in thickness and having hydraulic conductivity ≤ 10^{-8} m/s (Kamon and Katsumi, 2001). It is argued that these requirements for controlled landfill in Japan are not enough from the engineering point view (Kamon, 1999). The usage of CCL as the bottom liners was accepted around the world, and the criterions or regulations were different country by country. According to large amount literature review, Manassero et al. (1997) and Kamon and Katsumi (2001) made a summary, based on that, representative bottom liner system for municipal solid waste landfills in some countries is shown as following Fig. 2.8.

The common characteristic of above CCL in different countries is the thickness, all which is higher than 0.6 m, ranged from 0.6 m to 5 m. Such high thickness can be attributed to its higher hydraulic conductivity compared to other synthetic liners, and higher thickness can provide substantial factor of safety towards contaminant migration.

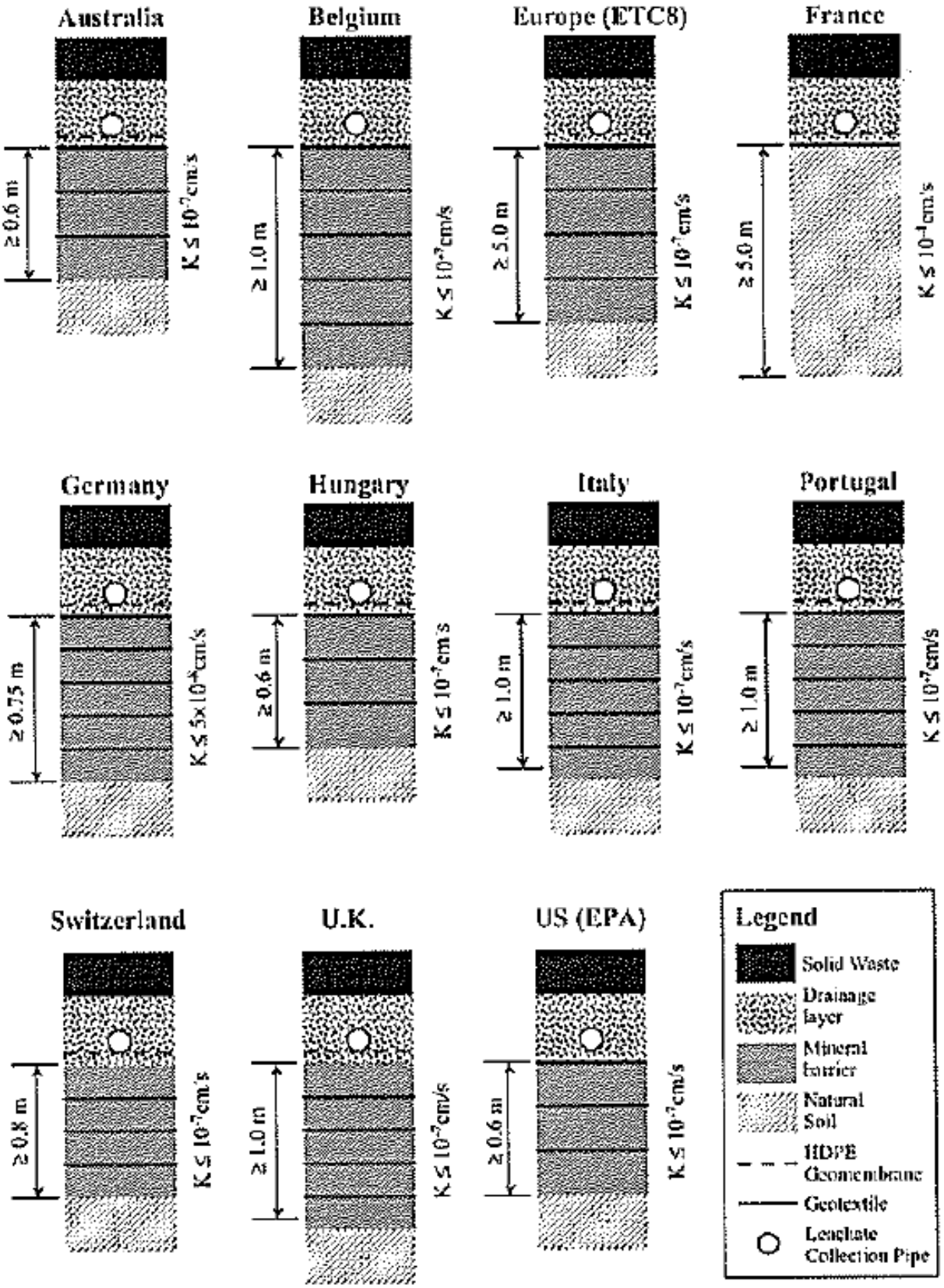

Fig. 2.8 The criterion for bottom liner system in some countries

2.5 Membrane behavior in compacted clay liner system

Membrane behavior in clays represents the ability of clays to exclude dissolved (aqueous misible) chemical species, or solutes, from entering the pores of the clays, thereby restricting the migration of the solutes through the clays (Shackelford, 2013). It is mainly attributed to two causes, i.e., size restriction and electrical repulsion from a diffuse-double layer (DDL) as shown in Fig. 2.9 (Van Impe, 2002).

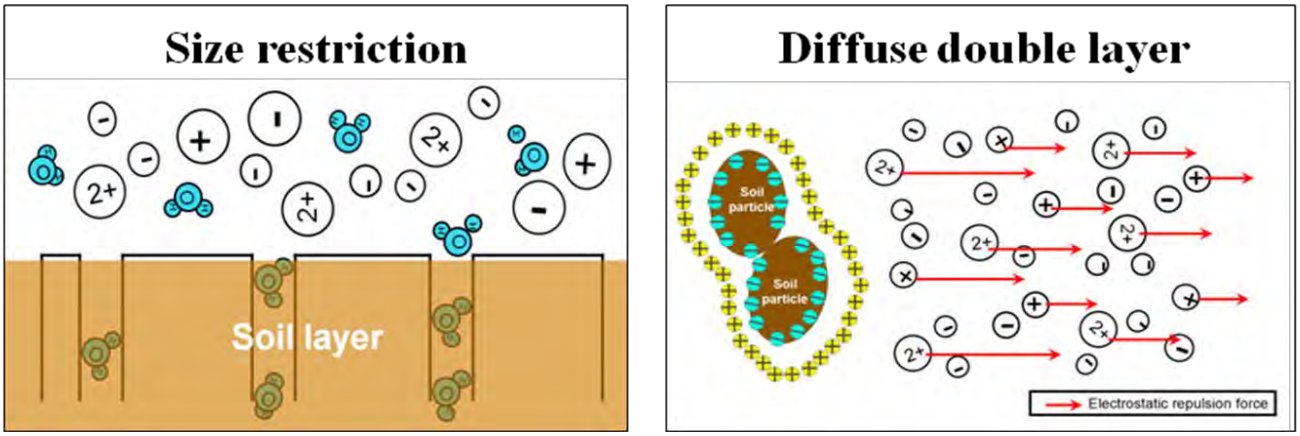

(a) (b)

Fig. 2.9 The mechanism of the membrane behavior, (a) Size restriction, (b) Diffuse double layer

Size restriction, which usually occurs in biological fields, is the process by which very large non-charged molecules, such as neutral organic compounds are blocked when the pore size is sufficiently small (Grathwohl, 1998). A DDL is composed of two components: a negative charge on the surface of the clay particles, and a distribution of counterions adjacent to the particle surface to counter balance the surface charge (Dominijanni and Manassero, 2012a). When the interparticle distance is on the same order as the pore size under an external load, the DDL overlap (Fritz and Marine, 1983; Fritz, 1986; Mitchell, 1993). In this case, anions cannot migrate through the pores due to the predominantly negative electrical potentials of the clay particle surface. To maintain electrical neutrality in solution, cations tend to remain with their co-ions, which restricts their movement (Hanshaw and Coplen, 1973; Marine and Fritz, 1981; Fritz and Marine, 1983; Fritz, 1986; Keijzer et al., 1997; Shackelford, 2011). Besides, for neutral (uncharged) solutes, they also may be restricted from migrating through clays if the solute exhibits polar charge character despite being neutral (e.g., carbon tetrachloride), or if the physical structure of the chemical molecule is simply too large to fit through the pores (Shackelford, 2013).

When a membrane can completely restrict the migration of solute, the membrane is ideal. In this case, only the solvent can cross an ideal semipermeable membrane regardless of the solute concentration gradient. In contrast, if both the solvent and solute can cross the membrane freely, then the membrane property dose not exist. Actually, the membrane behavior of natural materials falls in between these two extremes; a function of the solute can pass through the membrane and change the

concentration gradient. Over a sufficiently long period of time, diffusion of solute will gradually equalize the concentrations on both sides, decreasing the membrane behavior until it completely disappears (Malusis et al., 2003; Manassero and Dominijanni, 2003; Malusis and Shackelford, 2004).

Typically, the extent to which a soil acts as a membrane is quantified in terms of a reflection efficiency coefficient, σ, (Staverman, 1952; Katchalsky and Curran, 1965; Kemper and Rollins, 1966; Spiegler and Kedem, 1966; Olsen et al., 1990) or a chemico-osmotic efficiency coefficient (membrane efficiency coefficient), ω (Mitchell, 1993; Malusis et al., 2003; Malusis and Shackelford, 2004; Yeo et al., 2005; Evans et al., 2008; Kang and Shackelford, 2010; Shackelford, 2013). Because the σ symbol is usually designated as stress in engineering fields, ω is more commonly used to designate the degree of membrane behavior. The value of ω ranges from 0 representing no solute restrictions to 1 representing an "ideal" or "perfect" membrane that completely restricts the movement of solutes (i.e., $0 \leq \omega \leq 1$). In most cases involving the membrane behavior of clay, only a fraction of the pores are restrictive. Consequently, clay materials are usually referred to as "non-ideal" or "leaky" membranes (Kemper and Rollins, 1966; Olsen, 1969; Barbour and Fredlund, 1989; Mitchell, 1993; Keijzer et al., 1997).

Extensive researches have studied in this field. Mckelvey and Milne (1962) presented the experimental evidence of the salt filtering ability of compacted bentonite and shale material. This was also the first time that the membrane behavior was discovered in soil through experiment method. The chemico-osmotic efficiency of compacted sodium bentonite was measured towards NaCl and $CaCl_2$ solutions over a range of concentrations by Kemper and Rollins (1966), in which the concept of osmotic pressure was proposed by Kemper and Rollins (1966), and diffuse double layer theory was used to explain the mechanism of membrane behavior in soil for the first time. Kemper and Quirk (1972) reported the chemico-osmotic efficiency of several different kinds of clayed soil, including bentonite, illite, and kaolinite clays. According to the experiment conducted by Hanshaw and Coplen (1973), the compacted montmorillonite and illite systems behave under a wide range of conditions as ion-excluding or semipermeable membranes. And their results showed that the degree of salt filtering decreased with increasing solution concentration, which can be explained by the Teorell-Meyer-Siever theory.

In 2001, Malusis et al. (2001) proposed a new apparatus to measure chemico-osmotic efficiency coefficients of soil through lab-scale experiment, in which the actual chemico-osmotic pressure can be measured by the pressure transducer connected to both surface of specimen. The chemico-osmotic testing cell consisted of an acrylic cylinder (7.1-cm diameter), top piston, and base pedestal, as shown in Fig. 2.10.

As shown in above Fig. 2.10, the top piston was used to control the vertical stress or void ratio of the soil specimen and can be locked in place to prevent soil expansion. The top piston and base pedestal were equipped with ports that enable circulation of separate electrolyte solutions through porous stones at the specimen boundaries to establish and maintain a constant concentration difference across the specimen. Additional ports were installed in the top piston and base pedestal to

allow for measurement of differential pressure across the specimen.

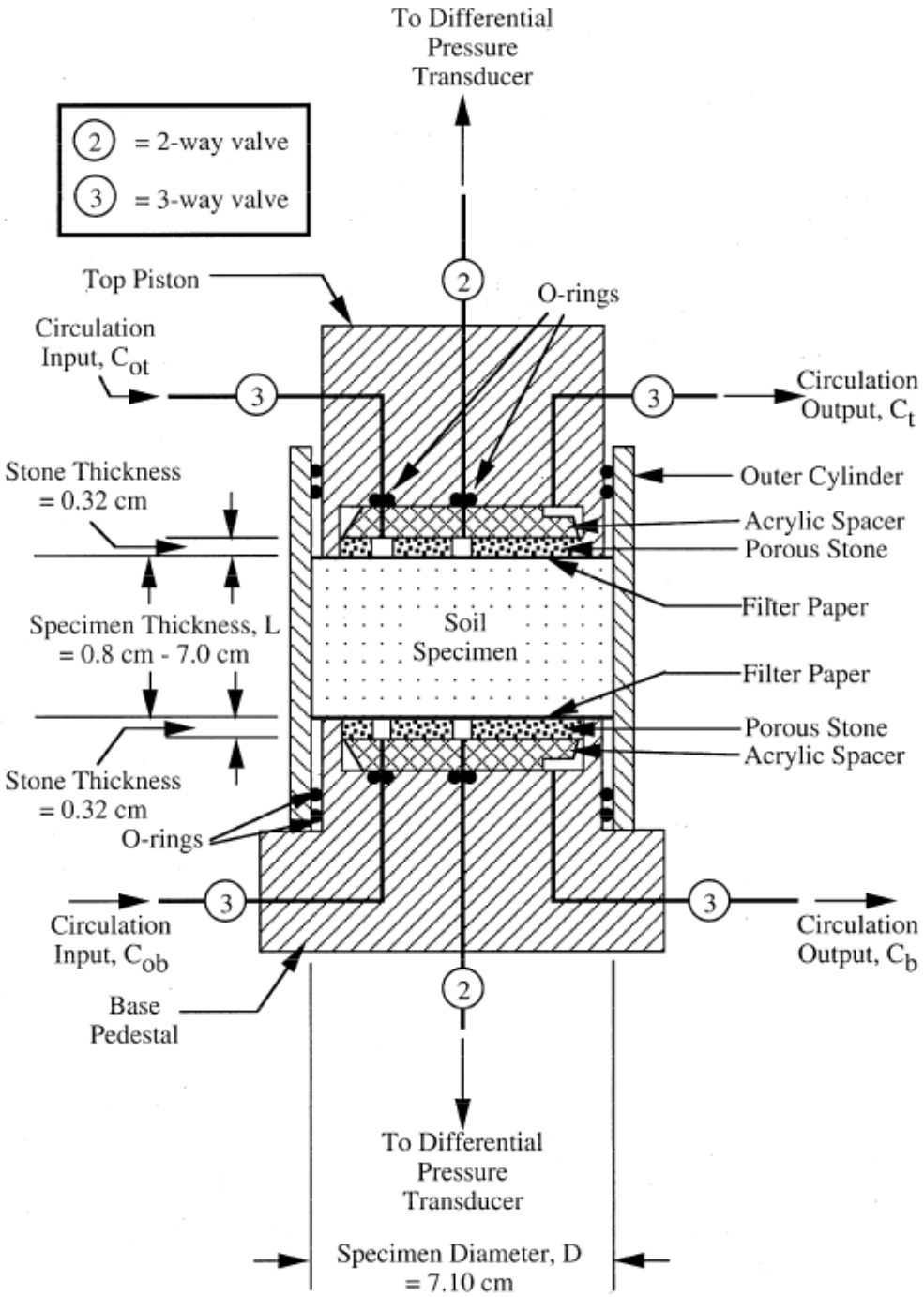

Fig. 2.10 The schematic of test apparatus in Malusis et al. (2001)

With above test apparatus, Malusis and Shackelford (2002b) measured the chemico-osmotic efficiency coefficient of GCL sodium bentonite towards KCl under different concentration and porosity conditions. Manassero and Dominijanni (2003) proposed a model to describe the osmosis effect on solute migration within fine-grained porous media as shown in following Eq. (2.1) and

(2.2).

$$J_v = \frac{k}{V_w \gamma}[\nabla(-P) - \omega RT\nabla(-c_s)] \tag{2.1}$$

$$J_s = (1-\omega)\{\frac{c_s k}{\gamma}[\nabla(-P) - \omega RT\nabla(-c_s)] + n\tau D_0 \nabla(-c_s)\} \tag{2.2}$$

Where J_v is the molar flow of the solvent and J_s is the solute flow rate; k is the hydraulic conductivity of the porous medium, V_w is the partial molar volume of the solvent (the volume occupied by a mole of the solvent in the solution), γ is the unit weight of the solution (equal to the unit weight of the solvent for practical purposes), P represents the hydraulic pressure, ω is chemico-osmotic efficiency coefficient which reflect the membrane behavior, R is the universal gas constant, T is the absolute temperature, c_s is the molar concentration of the solute; n is the effective or connected porosity of the soil skeleton, which represented by the interconnected voids related to the motion of pore fluids. D_0 is the diffusivity in free solution and τ is a tortuosity factor given by the squared ratio of the straight-line macro-scopic distance between two points along a solute molecule migration path, to the actual length of the same solute molecule migration path (Porter et al., 1960).

Considered the assumed rigid skeleton for the porous medium, incompressible solvent and the continuity of solvent flux, as well as the mass balance for the solute (Freeze and Cherry, 1979), the general differential equations that describe the evolution in space and time of the solute concentration and solution pressure can be obtained as follows (Manassero and Dominijanni, 2003),

$$\omega RT\frac{\partial^2 c_s}{\partial x^2} - \frac{\partial^2 P}{\partial x^2} = 0 \tag{2.3}$$

$$R_d\frac{\partial c_s}{\partial t} = (1-\omega)\{[\tau D_0 - \frac{k\omega RT}{\gamma n}c_s]\frac{\partial^2 c_s}{\partial x^2} - \frac{k}{\gamma n}\frac{\partial}{\partial x}(-\frac{\partial P}{\partial x}c_s) - \omega\frac{kRT}{\gamma n}(\frac{\partial c_s}{\partial x})^2\} \tag{2.4}$$

Through this model, the membrane behavior was the first taken into account in the solute transportation model together with advective and diffusion. This model was then tested using some previous results to verify its consistency in terms of the physical means. Based on this model, Manassero and Dominijanni (2003) also made a calculation of the breakthough curve of contaminant towards barrier under different membrane properties, and the result was shown in the following Fig. 2.11.

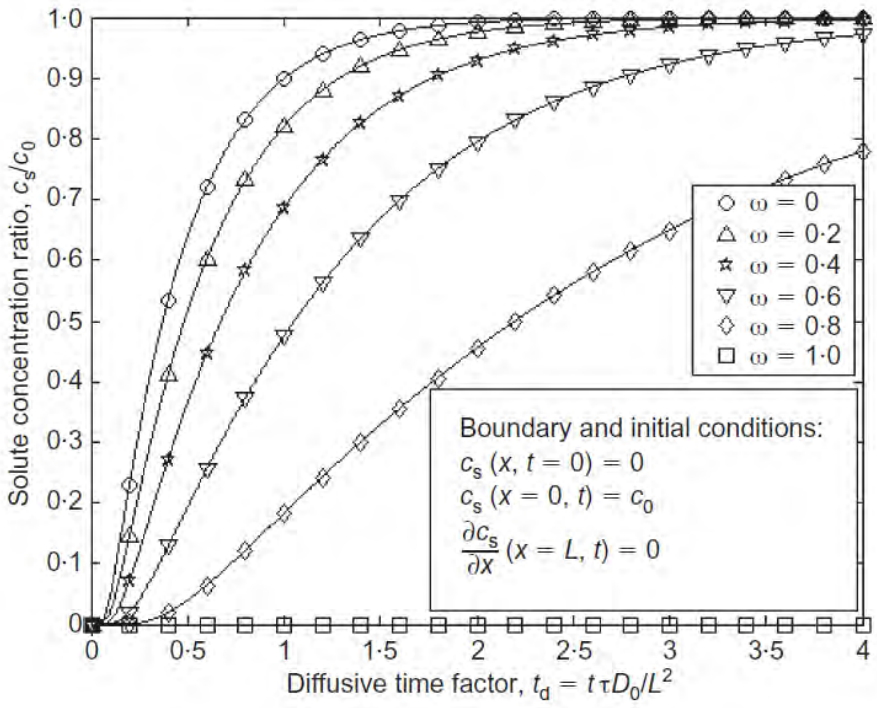

Fig. 2.11 Breakthrough curves under different membrane properties based on Manassero and Dominijanni (2003)

Not only Laboratory-scale experiment, the membrane behavior was also observed in cutoff walls in practice reported by Henning et al. (2006) and Evans et al. (2008). In 2009, some improvements on the membrane test apparatus were proposed by Kang and Shackelford (2009), in which the flexible-wall cell was used instead of original rigid wall. With such test apparatus, Kang and Shackelford (2010) measure the chemico-osmotic efficiency coefficient of Nelson Farm Clay and bentonite amended clay under different KCl concentration. As shown in above Fig. 2.12, the results proved that bentonite was effective to enhance the membrane property of normal clay. Also with the same test apparatus and through the laboratory-scale experiment, Kang and Shackelford (2011) proved the consolidation process have the positive effect on membrane behavior.

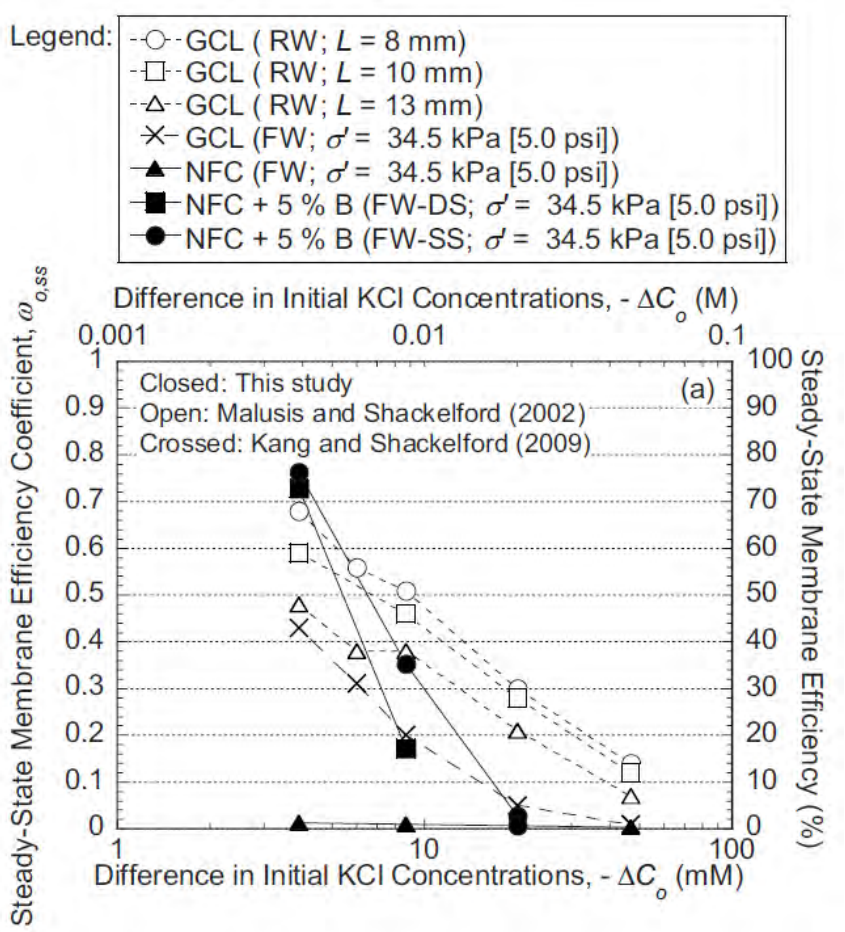

Fig. 2.12 The membrane test results in Kang and Shackelford (2010)

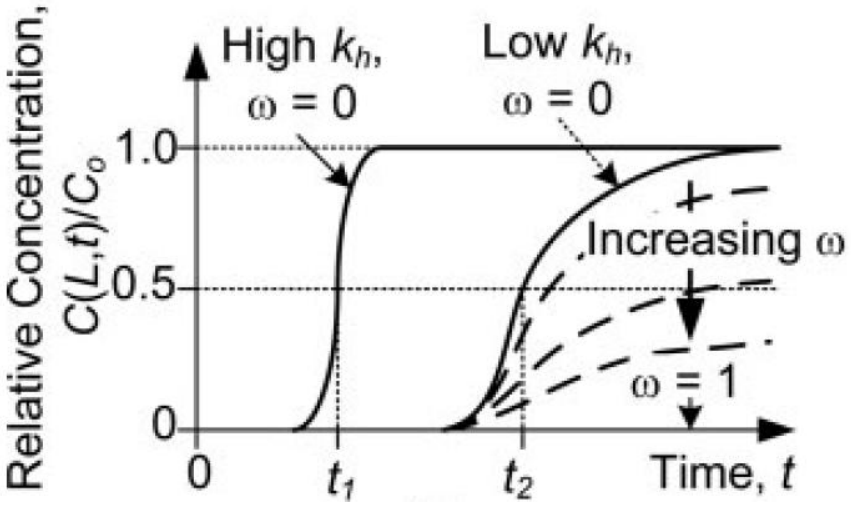

Fig. 2.13 Breakthrough curve for the barrier (ω = membrane efficiency coefficient, k_h = hydraulic conductivity)

Shackelford (2013) gave a clear explanation and proposed the theory about the scope of the application of the membrane for the first time. For the barrier with a relatively high hydraulic

conductivity, the breakthrough curve reflects advective (hydraulic) dominated transport conditions with some solute dispersion due to mechanical processes (e.g., variations in pore water velocity through the barrier), while the membrane behavior has no obvious effect, as shown in Fig. 2.13.

However, as the hydraulic conductivity of the barrier is reduced, solute transport through the barrier becomes increasingly dominated by diffusion, resulting in an overall greater degree of solute dispersion and an increase in the time required to achieve breakthrough as shown in above Fig. 2.13. This increase in containment time is the primary reason for using clays with low hydraulic conductivity as engineered containment barriers. Furthermore, if the low-k_h barrier also exhibits semipermeable membrane behavior (i.e., $0 < \omega \leq 1$), then solute restriction will reduce the maximum possible value of C(L, t) at steady-state transport relative to the case where $\omega = 0$, such that C(L, t)/$C_0 \rightarrow 0$ as $\omega \rightarrow 1$. Thus, as illustrated schematically in Fig. 2.13, the primary reason for considering engineered clay containment barriers with membrane behavior is that the containment function of the barrier can be improved significantly if the barrier exhibits membrane behavior (Shackelford, 2013).

Shackelford (2013) also pointed out that although no direct correlation between hydraulic conductivity and ω has been found, there is a general expectation that ω will be greater than zero only in the case where k_h of a soil is low, primarily because small pore sizes are required for both low k_h and $\omega > 0$. This is the reason why membrane behavior generally is relevant only in the case of clays. Furthermore, for the pore sizes to be sufficiently small to restrict the migration of dissolved chemical species, the clay particle sizes must be relatively small, which is a reason why membrane behavior generally is substantially greater in bentonites with smaller particle sizes relative to other clays, such as kaolin (Shackelford et al., 2003).

Consider above, the bentonite can improve the membrane property, however, very few studies have evaluated the effect of bentonite content on the membrane behavior (Shackelford, 2012). Considering compacted clay liners that are used as bottom liners for landfills will be exposed directly to the leachate from the landfill, which contains very high concentration of inorganic ions such as Na, K, Ca and heavy metals as well as different pH conditions at different phase. For compacted clay liner itself, the thickness and the compaction degree differed one by one, which depends on the engineering case and environmental requirement. Thus, one objective of this study is to evaluate the factors affecting membrane behavior, including bentonite content, compaction degree, thickness, solution pH, concentration and solute type. Based on experiment results, the mechanisms of the membrane performance change were discussed with assistance of XRD patterns, free swelling results and SEM images.

CHAPTER 3: GEOMETRY EFFECT ON WASTE LEACHATE GENERATION

3.1 General remarks

For landfill leachate generation, it is a long term process, ranging from several months to centuries, which varies one by one depending on a lot of factors, including soil properties, weathering conditions, waste composition, landfill operation, volume of infiltration water, landfill age etc.. The lysimeters are usually simulated the waste body by many researchers. Nevertheless, the effect of geometry characteristics were ignored usually, and those lysimeters were operated under various geometry factor (height/width ratio and height), which can cause the change in physical and thermodynamic characteristics. However, there are few studies focusing on the effect of reactor‘s height and H/W ratio on the physical and thermodynamic characteristics, while H/W ratio can easily have an influence on the external factors and resulted in the different leaching behavior and waste decomposition rate.

Considering all of above, in this study, the lysimeter with different geometry factor was simulated the real landfill waste body, and the lysimeter test was conducted. According to the test results, the author had a further discussion about the geometry effect (height and height/width ratio) of landfill leachate generation and composition. Leaching behavior was also studied by leaching test to obtain the basic information of the material. Based on the lysimeter test and the discussion, the author also proposed optimum values of height and height/width ratio of lysimeter at the last part of this chapter.

3.2 Materials and methods

3.2.1 Construction and demolition waste

Solid waste tends to increase with the improvement of life style and development of the economy. It is usually classified into three types; industrial solid waste (ISW), municipal solid waste (MSW) and hazardous waste. Construction and demolition wastes (C&D waste) are a major portion of industrial solid wastes of most countries. In Hong Kong, the amount of C&D waste generated per year was about four to five times that of municipal solid waste (Poon, 2007). Table 3.1 displays the C&D waste production of some countries in recent years.

C&D waste includes materials generated from residential and commercial buildings, and from road construction as shown in Fig. 3.1 (Cosper et al., 1993). Utilization is a preferred management option for C&D waste, however, inherent pollutants may affect its potential for reuse and might have an environmental impact. Since the majority of C&D waste includes concrete, sand and gravel, it is

generally regarded as inert waste, without putrescible materials such as those found in municipal solid waste (MSW)(e.g., food waste), and is sometimes disposed of in unlined landfills directly (Bianchini et al., 2005; Rao et al., 2007; Jambeck et al., 2008). In 27 states of the U.S., the landfill sites for C&D waste disposal are not required to have a liner (Clark et al., 2006; Jambeck et al., 2006).

Table 3.1 C&D Waste production in some countries

Country	latest year available	C&D Waste collected (1000 tones)	References
Finland	1995	About 8,000	(EEA, 2002)
Germany	1996	219,921	(EEA, 2002)
U.S.A.	1996	49,640,000	(Nunes et al., 2007)
Australia	1996	About 25,500	(EEA, 2002)
Netherlands	1996	About 13,500	(EEA, 2002)
Italy	1997	About 20,500	(EEA, 2002)
Spain	1999	About 21,000	(EEA, 2002)
England	2002	772	(Environment Agency, 2002)
Japan	2004	79,055	(Ministry of the Environment, 2010)
Denmark	2005	3,785	(DEPA, 2005)
France	2007	17,000	(Roussat et al., 2008)

Fig. 3.1 C&D Waste

However, research has shown that C&D waste does go through active processes of microbial activity that affect both leachate and gas concentrations (Jang and Townsend, 2003). In addition, a small fraction of C&D waste contains chemicals that are hazardous to human health and the environment, for example, heavy metals and organic matters (Fatta et al., 2003). These components are less relevant, because they are usually considered to be immobilized in the product. However, under certain conditions, such as soil acidification and microbial activity, they can be extracted (Burnes et al., 2000; Voegelin et al., 2003; Kalbe et al., 2008). Although these hazardous wastes only represent a very small mass fraction of total C&D waste, they are a principal risk to the environment. In addition, separation of these hazardous wastes at the source requires a significant deconstruction effort by the demolition operator (Roussat et al., 2008). Thus, the economical and actual condition of the leaching behavior of C&D waste in landfills requires further research.

In Japan, almost 20% of the industrial wastes are generated from the construction sector. Although several C&D wastes such as concrete, asphalt and wood have been recycled or reused at very high rates, as for mixed C&D waste, one third was disposed of into landfills due to the difficulty of recycling. In Japan, mixed C&D wastes are sent to sorting facilities to increase recycling rate and decrease final disposal rate. About 33% recovery can be achieved by the sorting, but 59% of the total is still landfilled, and it contains fine residue. The fine residue contains high content of gypsum and organic matter which can generate a toxic gas, hydrogen sulfide (H_2S) in anaerobic condition (Montero, 2011). Thus, the leaching potential of sulfate and organic matter from the fine residue should be estimated.

For the laboratory scale column and lysimeter tests, the size of the particle of filled waste is an important parameter, because it strongly affects the leaching behavior of contaminants and the decomposition rate of landfill waste (Matsufuji et al., 2007). The particle size of waste samples sometimes needs to be uniformalized by shredding them so that representative data can be obtained from all reactors, lessening the effects of difference in waste particle size. For this reason, in this study, C&D waste residues with a particle size less than 5 mm were used. C&D waste residue used in this study was collected from a intermediate treatment facility located in Ibaraki Prefecture, where mixed C&D waste was crushed and recyclable matter recovered by manual separation, sieving, crushing, magnetic separation, and air classification. Fig. 3.2 shows photographs of the C&D waste utilized in this study.

To understand the physical properties of C&D waste residues, bulk density, particle density (Pycnometer method, JIS A 1202), moisture content (raw sample at 105°C for 24 h, JIS A 1203), combustible content (dried sample at 600°C for 3 h), and particle size distribution (dried sample: sieve mesh sizes were 0.053, 0.075, 0.106, 0.250, 0.425, 0.850, 2 mm, JIS A 1204) were measured.

(a) (b)

Fig. 3.2 (a)(b) C&D Waste used in this study

3.2.2 Experimental apparatus

The lysimeter utilized in this study was made from PVC pipe with a wall thickness of 2 cm. The schematic diagram of the lysimeter is shown in Fig. 3.3. A water supply tank was fitted to the top of the lysimeter, to simulate rainfall. Tap water was supplied by a peristaltic pump (MP-1000, EYELA, Japan) after impurities and chloride ions were removed by an activated carbon filter, and was distributed equally by installing needles in a circle on the bottom of the water tank. Landfill gas was collected in a gas bag (AAK-1, GL Sciences, Japan) connected to a gas sampling tube which was installed through the water tank as shown in Fig. 3.3. A glass bead layer, 3 cm in thickness (Diameter, 10 mm) was placed on the surface of the landfill waste to avoid preferential flows and to distribute the water evenly. A 10 cm thick layer was also placed at the bottom of the waste layer to drain the leachate. A 5 cm thick layer of glass beads with a smaller diameter of 5 mm was placed on top of the bottom glass bead layer, to prevent C&D waste loss during the test, as shown in Fig. 3.3. An online temperature sensor was placed at the specific height of each lysimeter to monitor the internal temperature, which was reported by a data logger (GL200A, Graphtec, Japan). Another gas sampling tube was also installed into each lysimeter to monitor the vertical distribution of landfill gas concentration. Glass wool was installed at the bottom of the lysimeters to avoid clogging of the leachate collection pipe. The leachate collection pipe was connected a bottle to collect the generated leachate from the C&D waste during the lysimeter test.

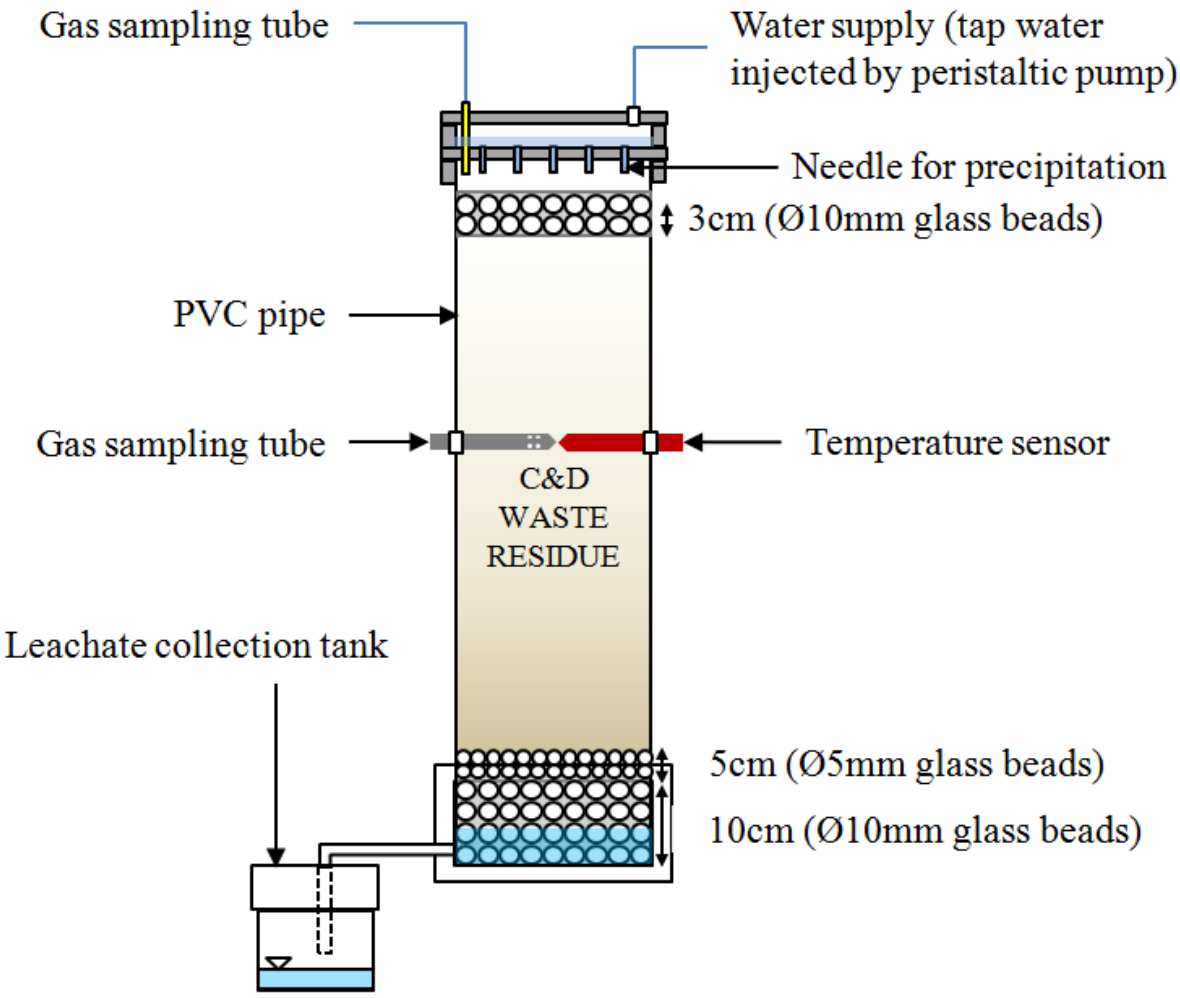

Fig. 3.3 Schematic diagram of the lysimeter

3.2.3 Experimental procedure

3.2.3.1 Leaching test

The Leaching test is carried out to extract minerals from a solid by dissolving them in a liquid, either in nature or through an industrial process. As mentioned in previous section, the C&D waste particles were separated into eight groups by sieve mesh based on particle size; < 53 μm, 53-75 μm, 75-106 μm, 106-250 μm, 250-425 μm, 425-850 μm, 850 μm-2 mm and > 2 mm. Since the particle size might affect the leaching behavior, batch leaching tests were conducted on each particle size group. The leaching test followed the Japanese standard leaching test protocol (JLT-13), and the procedures and experimental set-up are listed in Table 3.2. The liquid to solid (L/S) ratio in the leaching test to determine leaching potential of inorganic ion constituents (Na, Cl, K, SO_4 and Ca) was 10 as shown in Fig. 3.4. The liquid to solid (L/S) ratio of 10 used in this study was also recommended by many other researchers since it is considered to be the optimal ratio to dissolve most of the soluble content of the samples (Crannell et al., 2000; Sakai et al., 2000; Kalbe et al.,

2008). The samples were shaken for 6 hours at a rotation speed of 200 rpm by shaker (NR-150, Taitec, Japan). The influence of reaction kinetics cannot be measured exactly within 6 hours, thus, the continued leaching of contaminants into the environment was not addressed. However, for leaching tests with a contact time of 6 hours, equilibrium conditions were assumed to have been reached. The filtrates were obtained using 0.45 μm filter papers with assistance of a pump and were analyzed for pH value and electrical conductivity (EC) with a portable EC/pH meter (F-55, HORIBA, Japan). The concentrations of selected inorganic cations and anions in the filtrates were measured by ion chromatography (IC-2001, Tosoh, Japan) and Inductively Coupled Plasma (ICP-MAS).

Table 3.2 Experimental set-up of leaching test

L/S ratio	10, mass/mass (dry matter)
Sample mass	70 g
leachant	De-ionized water
Agitation step	6 hours, 200 rpm, 25 ± 2 ^{o}C
Filtration step	Vacuum-pressure filtration equipment, 0.45 μm filter papers and porous stone
Parameters for measurement	EC, pH, concentrations of cations and anions

(a) (b)

Fig. 3.4 Leaching test with liquid-solid ratio of 10

3.2.3.2 Column test

In order to study the effect of geometry on leachate generation and composition, six lysimeters were designed with various geometrical characteristics. Based on the influential factors, the six lysimeters can be divided into two groups as shown in Fig. 3.5. The first group, including R1, R2, R3 and R4, was used to estimate the effect of lysimeter height on leaching behavior, in which the

diameters of all four lysimeters are constant, while the height was increased from 0.35 m to 2.1 m. The second group, including R2, R5 and R6, was used to estimate the effect of lysimeter width and height / width ratio (H/W), in which the lysimeter volumes were constant, but the H/W ratio increased from 0.5 to 3.5.

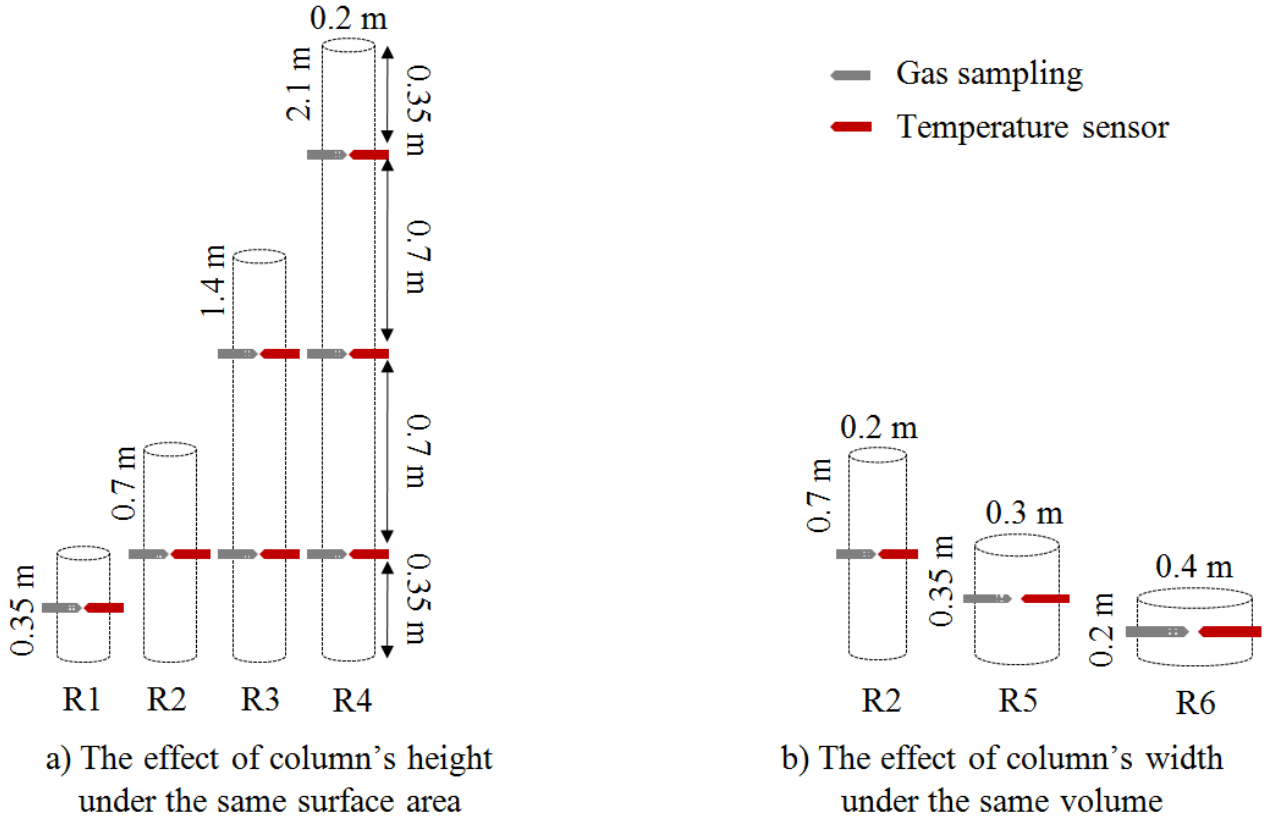

a) The effect of column's height under the same surface area

b) The effect of column's width under the same volume

Fig. 3.5 Two groups of lysimeters

The geometrical factors of the lysimeters, as well as the amount of C&D waste used are listed in Table 3.3. During the lysimeter test, all lysimeters were filled with C&D waste residue at a dry density of 1100 kg/m^3. The lysimeter test was run at a controlled temperature of around 25 ºC. Water was injected into every lysimeter from the water tank every day to simulate rainfall at about 0.13-0.32 mL/s. According to statistics from WEPA, Japanese annual mean precipitation is 1700 mm (WEPA, 2011). When the evapotranspiration rate, surface flow and run off in other forms are considered, only around 40% of the total precipitation actually filtrates the cover soil (Kim et al., 2011). Thus, based on the assumption of 680 mm of water injection every year the volumes of injected water every day can be calculated and listed in Table 3.3. Such rainfall water, together with the generated CO_2 from landfill decomposition which will dissolve in the water, can establish mild acidic conditions. This carbonic acid water simulated natural rainfall. During the operation of lysimeter test, leachate generation was collected and weighted from the leachate collection tank several times per week, and then nitrogen purging was conducted to evacuate oxygen content from

the tank by injecting nitrogen gas directly into the tank. After the purging, the tank was sealed and connected to a leachate collection valve. The leachate samples were measured for temperature, pH, electrical conductivity (EC), inorganic ion concentrations (Na, Cl, K, SO_4 and Ca) and heavy metals (Ba, Cu, Fe, Mg, Mo, Ni and Sr) to estimate leaching behavior. The photograph of the six lysimeters is shown in Fig. 3.6.

Table 3.3 Characteristics and operating parameters of each lysimeters

Lysimeter parameter	Unit	R1[a]	R3[a]	R4[a]	R2[a,b]	R5[b]	R6[b]
Type of solid waste		Construction and demolition waste residues					
Landfill type		Anaerobic					
Filling density	g/cm^3	1.1					
Operation period	days	121	121	121	150	121	121
Length	mm	350	1400	2100	700	300	200
Diameter	mm	Ø200	Ø200	Ø200	Ø200	Ø300	Ø400
Cross section area	m^2	0.03	0.03	0.03	0.03	0.07	0.13
Volume	L	11	44	65.9	22	21.2	25.1
H/W ratio		1.8	7.0	10.5	3.5	1.0	0.5
Total mass of waste	kg- wet	12.1	48.4	72.5	24.2	23.3	27.6
Daily water injection	mL	58.53	58.53	58.53	58.53	131.69	234.11

[a] belongs to the group 1 which has the same diameter (Ø200mm).

[b] belongs to the group 2 which has almost the same volume and the different H/W ratio.

Fig. 3.6 The photograph of the six lysimeters used in this study

3.3 Results and discussions

3.3.1 Basic physical and chemical properties of the material

Table 3.4 shows the initial characteristics of C&D waste residue. Average moisture and combustible content are 17.7 % and 9.3 %, respectively, which are lower than the values of municipal solid waste in Japan. Bulk density, particle density and water permeability are 0.967 and 2.46 g/cm^3, and 3.2 × 10^{-3} cm/s, respectively, and these values are similar to those of sand and ash. Particle size distribution of C&D waste residue is shown in Fig. 3.7, and the sand fraction (> 0.075 mm) is almost 90%, while the silt fraction (0.005-0.075 mm) and clay fraction (< 0.005 mm) are only about 6.5% and 3.5% respectively. The coefficient of uniformity and the coefficient of curvature were calculated using following equations

$$C_u = D_{60} / D_{10} \tag{3.1}$$

$$C_c = \frac{{D_{30}}^2}{D_{60} \times D_{10}} \tag{3.2}$$

where C_u represents the coefficient of uniformity, and D_{60} and D_{10} represent the grain diameters of 60% and 10% passing, C_c represents the coefficient of curvature and D_{30} represents a grain diameter of 30% passing. D_{60}, D_{30} and D_{10} were all obtained based on observations from the particle size distribution curve shown in Fig. 3.7.

Table 3.4 Initial characteristics of the C&D waste residue used in this study

Characteristics	Unit	Value
Moisture content	%	17.7
Combustible content	%	9.3
Ash content	%	72.9
Bulk density	g/cm^3	0.967
Particle density	g/cm^3	2.46
Water permeability	cm/s	3.20 × 10^{-3}
Grain size distribution		
Sand fraction (> 0.075 mm)	%	90
Silt fraction (0.005-0.075 mm)	%	6.5
Clay fraction (< 0.005 mm)	%	3.5
Coefficient of uniformity		5
Coefficient of curvature		12.5

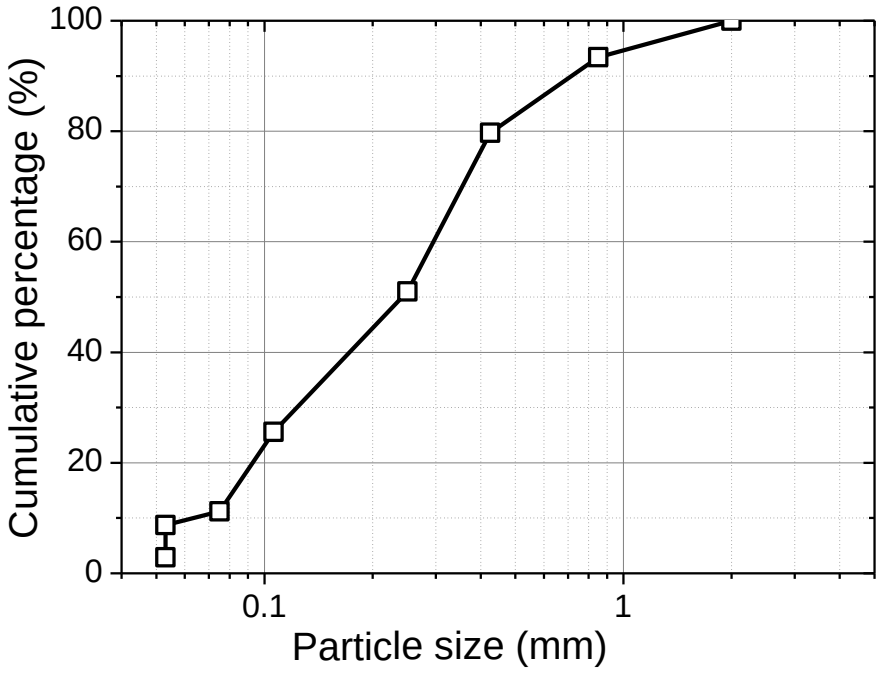

Fig. 3.7 Particle size distributions for C&D waste residue

Figure 3.8 shows the water retention curve for C&D waste residue. A water retention test was conducted to measure field capacities at different depths. Field capacity is the amount of water content held in soil after excess water has drained away and the rate of downward movement has materially decreased. Field capacity reflected the C&D waste water content in natural conditions. The experiment was conducted as per the following procedures.

18 columns of 5 cm length were used, first, filled with C&D Waste residues and combined one by one. After constructing a column of 90 cm in length, this was put into a tank and tap water was injected into the tank from the bottom. This water injection continued until the column was saturated, and air was removed. After 15 hours, the water was removed from the port at the bottom of the tank. Then after a drying process at 105 ^{o}C, the mass of the waste samples was measured and the water retention curve was calculated. A water retention curve is usually used to predict the material water storage, field capacity and material aggregate stability. From the data the field capacity of C&D waste in this research was around 30%.

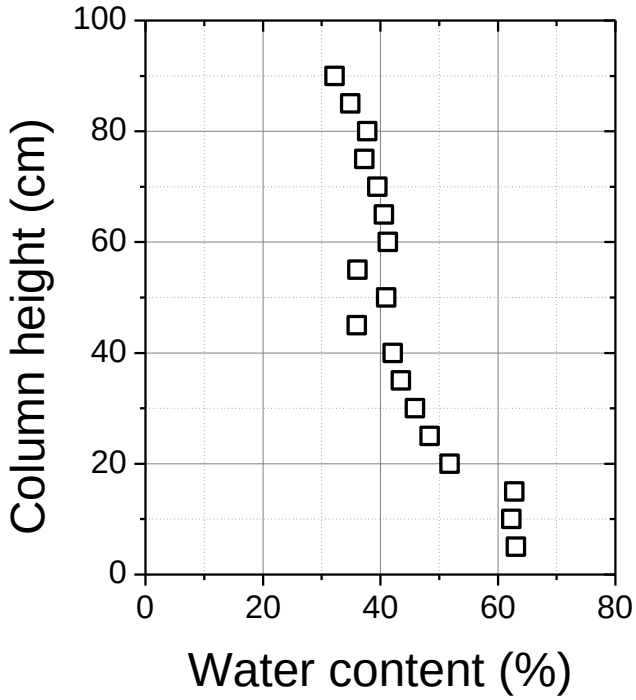

Fig. 3.8 Water retention curve for C&D waste residue

3.3.2 Leaching test results

The particle density and combustible content of the materials were measured according to particle size group. To estimate leaching potential of the residue, a leaching test was conducted at a L/S ratio of 10 for 6 hours, then the mixture was passed through filter paper, and the supernatant was stored for further measurement. The results are summarised in Table 3.5. The results of the leaching tests, including EC, pH, and the concentration of Ca, Na, K, SO_4 and Cl of the different particle size groups are shown in Fig. 3.9 and Fig. 3.10.

The filtrates showed strong alkalinity with pH ranging from 11.7 to 12.2, and electrical conductivity (EC) ranging from 0.313 to 0.494 S/m, as shown in Fig. 3.9. The samples exhibited high pH values in the leaching tests, which can be attributed to the high content of CaO in C&D waste, originating from cement or other construction materials (Kalbe et al., 2008). It is also apparent that both pH and EC values in the small particles were higher than those in the large particles, especially for EC. Such decline in EC value as function of particle size can be attributed to the soluble content of the particles, since in most cases, soluble content exists in the form of powder or very small particles in nature.

Table 3.5 Physical and leaching property according to particle size group

Particle size	Unit	< 53 μm	53-75 μm	75-106 μm	106-250 μm	250-425 μm	425-850 μm	0.85-2 mm	> 2 mm
Particle density	g/cm^3	-	2.57	2.49	2.47	2.58	2.44	-	-
Combustile content	%	12.12	12.37	12.49	7.66	6.09	7.36	11.51	21.15
Leaching behavior									
pH		12.2	12.2	12.0	11.7	11.7	11.9	11.8	11.7
EC	S/m	0.494	0.455	0.383	0.313	0.314	0.332	0.332	0.325
Ca^{2+}	mg/L	903.53	820.71	741.65	658.82	632.47	677.65	651.29	677.65
Na^{+}	mg/L	86.418	77.7	75.759	61.958	54.088	64.853	78.724	61.253
K^{+}	mg/L	35.029	36.194	37.641	36.265	33.477	29.276	30.442	19.747
SO_4^{2-}	mg/L	1434.4	1374.1	1453.2	1475.8	1494.6	1509.6	1475.8	1520.9
Cl^{-}	mg/L	25.994	22.077	20.136	14.524	11.736	14.877	15.477	12.689

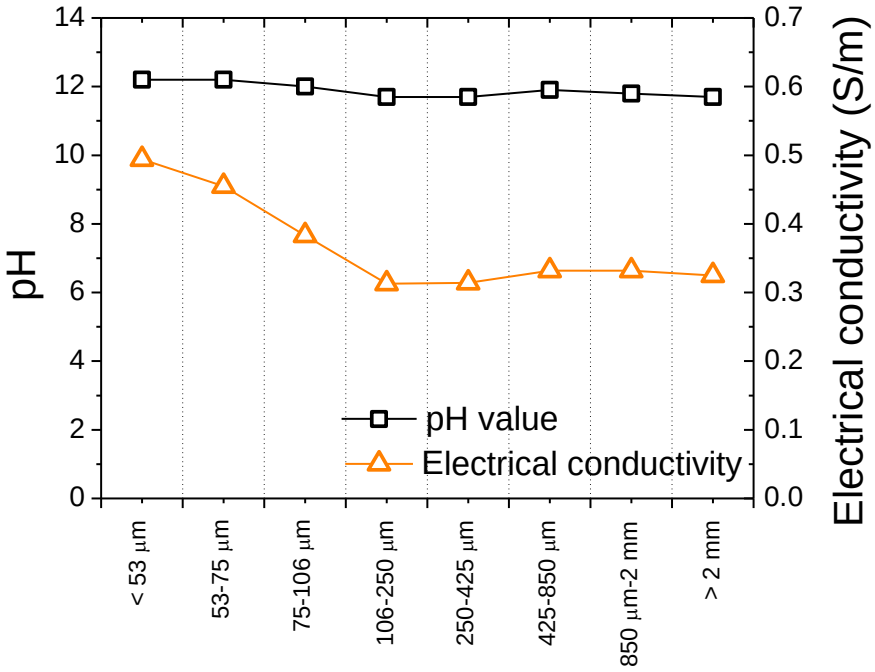

Fig. 3.9 Leaching characteristics of pH and EC from the C&D waste residue

Leaching potential of inorganic ions (Na, Cl, K, SO_4 and Ca) by particle size is shown in Fig. 3.10. Overall, most particles showed similar levels of ion concentration regardless of the particle size, although the values of Na^{+} varied, with relatively high levels in particles < 0.053 mm, almost 1.8 times higher than that of the 250-425 μm fraction. In addition, most of the inorganic ions, such as Na, Ca, K and Cl, exhibited a similar tendency of pH and EC, as shown in Fig. 3.10, which decreased as

particle size increased. The exception is SO_4, which showed a slight increase as the particle size increased. Such a phenomenon can be attributed to the particle size of sulphate, which might be a little bigger than the others.

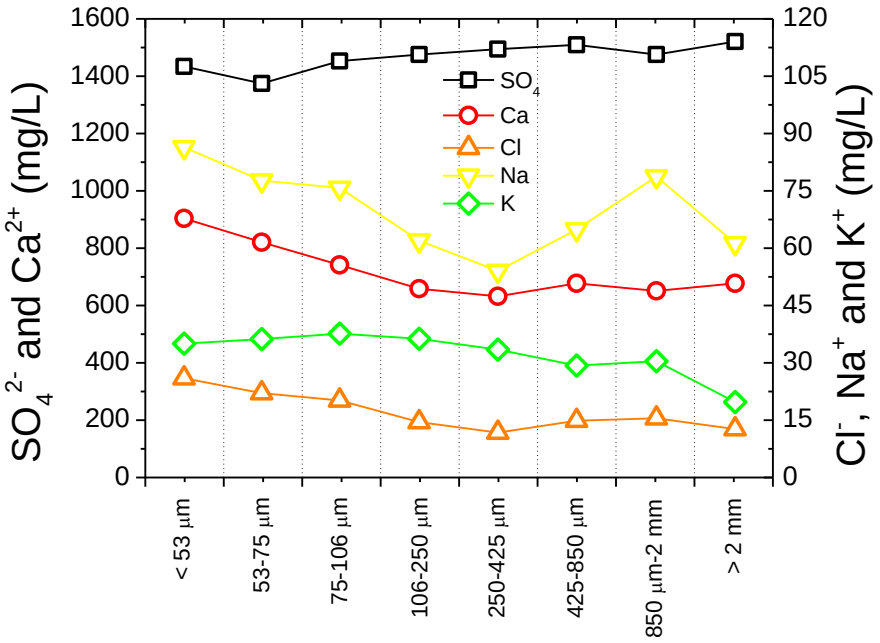

Fig. 3.10 Leaching characteristics of inorganic ions from the C&D waste residue

3.3.3 Column test results

Figures 3.11 and 3.12 compare the change in pH and electrical conductivity (EC) with L/S ratio which is defined as collected leachate related to dry substance of waste included in each lysimeter (mass/mass). Differed from acid pH values of landfill leachate during the acid phase in previous literature, very strong alkaline, pHs, ranging from 11 to 12 were observed in all lysimeters, as shown in Fig. 3.11 (Ehrig, 1983, 1988; Christensen et al., 2001; Baun and Christensen, 2004). Such a high pH value can be attributed to the high CaO content contained in C&D waste. The pH values displayed during the lysimeter test all reached peak values, followed by a decreasing trend. This trend is likely to also be related to CaO content, since CaO in the C&D waste can react with CO_2, and form $CaCO_3$. This ageing process leads to lower pH values in the leaching tests with water (Kalbe et al., 2008). Since the instability of C&D waste is mainly due to CaO, a 3-month storage period is required in Germany prior to utilization (Van Gerven et al., 2005). The initial pH in this study was slightly higher in R5 and R6 (11.5-12.2) than the others, while the value from R2 appears to fluctuate occasionally around 0.2-0.3 L/S ratio. The pH value of R1 experienced a sharp decline of 0.3-0.45 L/S ratio. In addition, for R1 and R5, which have same height but different widths, the

change in pH values differed significantly; a gradual drop in R5 and a great decrease in R1.

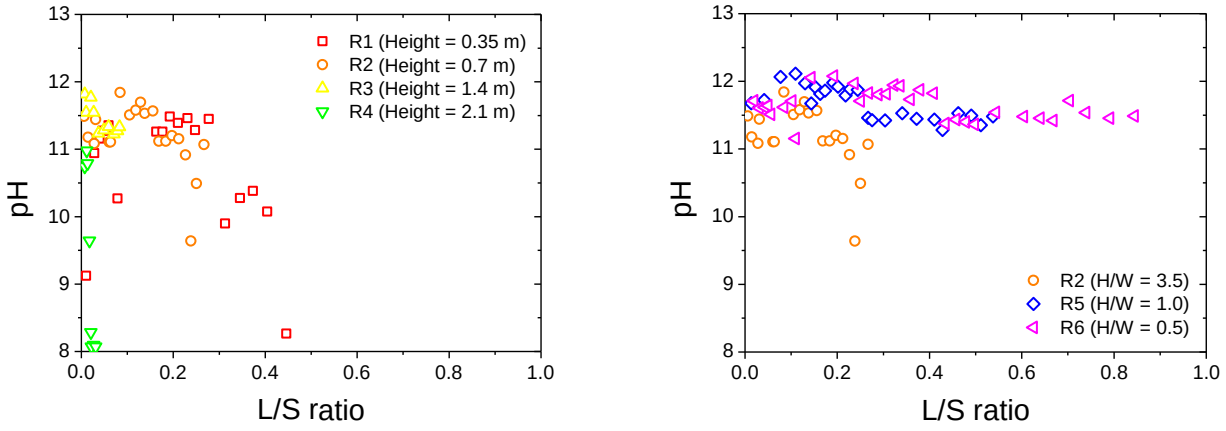

(1) (2)

Fig. 3.11 pH values from lysimeter tests as a function of L/S ratio

It was also apparent that EC reached a peak around 0.05-0.1 L/S ratio and then had a subsequent decline, as shown in Fig. 3.12. However, the rates of the decrease differed between the groups. When the L/S ratio was 0.3, the EC values of R1 and R2 decreased by 34.6 and 36.7 % from their maximum values in the initial phase, while R5 and R6 showed only a 29.2 and 18.2% decrease, respectively. It should be mentioned that the decrease rate of R1 was a little faster than that of R5.

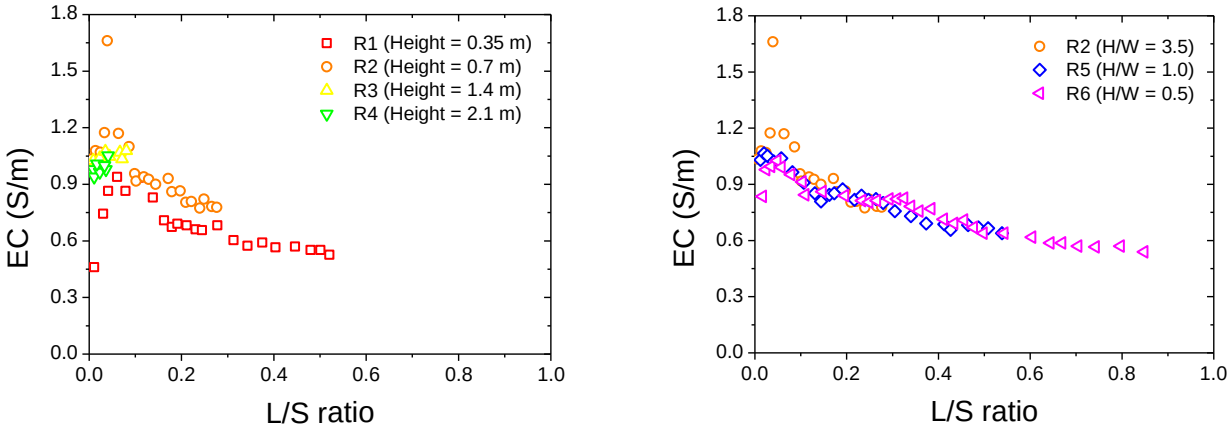

(1) (2)

Fig. 3.12 EC values from lysimeter tests as a function of L/S ratio

The soluble constituent (Cl, Na, K, Ca) concentrations of inorganic ions which are not-reactive (or are poorly reactive), are shown in Fig. 3.13 as a function of L/S ratio. All values decreased with

increasing L/S ratio regardless of the lysimeters, which suggests that soluble constituents are dissolved and then gradually diluted by water added through rainfall. As shown in Fig. 3.13(1c)(2c), Cl concentrations decreased sharply by more than 50 % compared to the peak values which are at least 30-50 times higher than the value of the batch leaching test (around 14.7 mg/L) in R1, R2, R5 and R6. Cl concentrations in R3 and R4 also decreased as L/S ratio increased, although this change was limited. Ca concentrations also decreased significantly, as shown in Fig. 3.13(1b)(2b), and reached a level below that of the batch leaching test (around 762 mg/L) for R1 and R2. Concentrations of Na and K in R1 also showed the largest decrease in value, as shown in Fig. 3.13(1a) and Fig. 3.13(1d), while R3 and R4 had a little increase, however, since very limited leachate was collected from these lysimeters, it was difficult to predict their pattern of change.

Although the concentrations of inorganic ions in all lysimeters displayed a similar decreased as a function of L/S ratio, some slight differences in leaching behavior among lysimeters can be observed, based on the decrease rate. Specifically, the concentrations of Ca, Na and K showed a larger decrease in R1 and R2 compared to R5 and R6 with increasing L/S ratio. In addition, the concentrations of the four ions from R1 display a greater decrease than R5, shown in Fig. 3.13, and such a difference was also observed in the changes in EC and pH value, in Fig. 3.11 and Fig. 3.12. The lysimeters differ in diameter, as shown in Fig. 3.5 (group one: R1 and R2, and group two: R5 and R6). A lysimeter with a short width (R1 and R2) maybe can easily create a preferential flow and sidewall flow inside the waste layer. For this reason, only some waste in those flows can be washed out, which can also explain the sharp decrease in soluble constituent concentrations in the leachate of R1 and R2. In particular for R1 and R2, the pH values were fluctuated significantly between L/S ratios of 0.1 and 0.4 as well as EC values. This fluctuation could be also considered as the evidence of those flows. On the other hand, R5 and R6, which have a greater width (0.3 m and 0.4 m) and low H/W ratio (1.0 and 0.5), showed a gradual decrease in all parameters without observable fluctuations. Based on the above observations, it is rational to estimate that the lysimeter‘s width or H/W ratio has an influence on the leaching behavior of soluble constituents. Therefore, the proper width and H/W ratio of a reactor should be fully considered in a laboratory scale test.

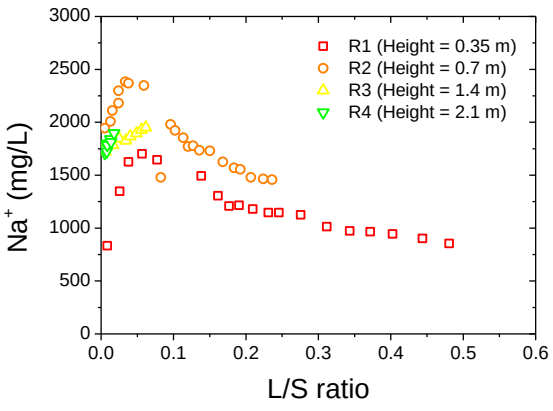

(1a)

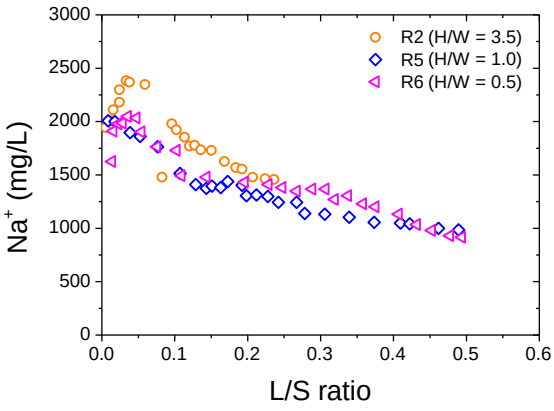

(2a)

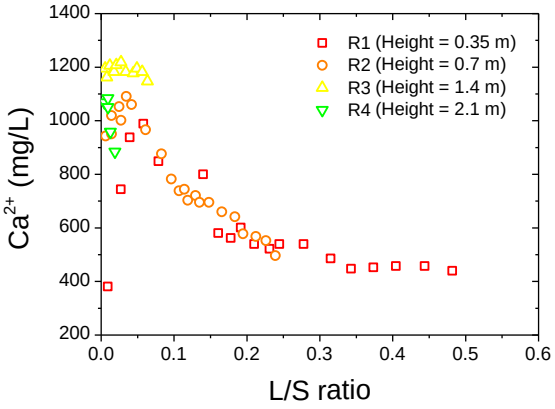

(1b)

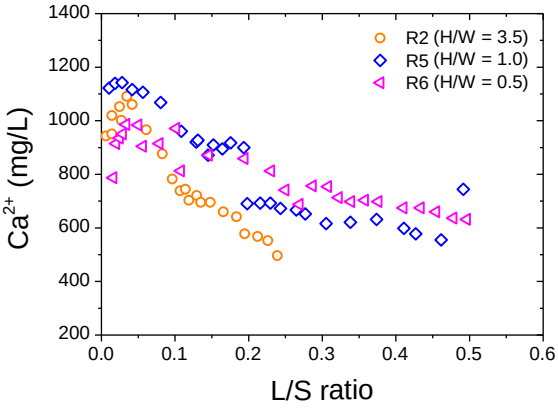

(2b)

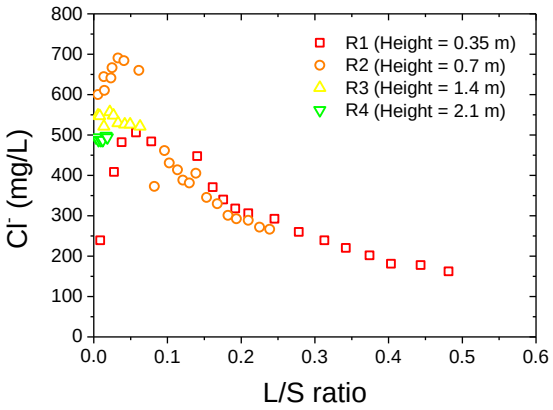

(1c)

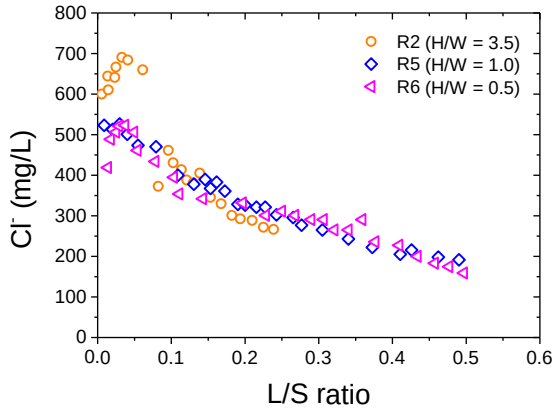

(2c)

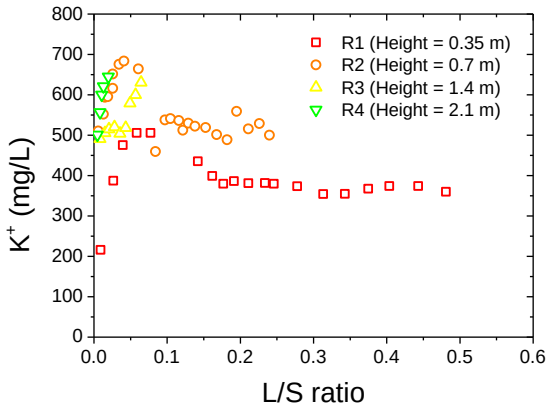

(1d)

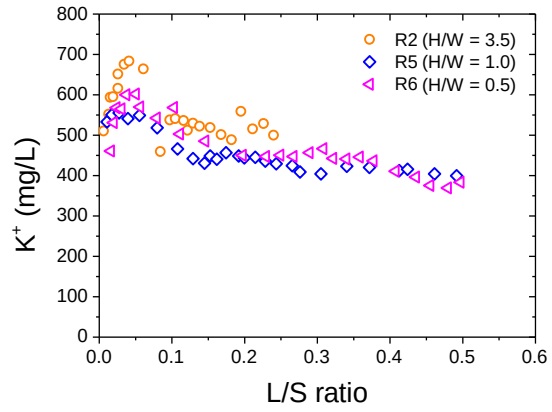

(2d)

Fig. 3.13 The inorganic ions from lysimeter tests as a function of L/S ratio

The height of a lysimeter is also a critical factor for the estimation of leaching behavior. Based on the results obtained from the lysimeter test, it was apparent that excluding Ca, the highest value of soluble constituent concentrations was found in R2, and not R3 or R4, which have the greater height.

It is suggested that soluble constituents such as Cl, Na and K can reach their equilibrium concentrations while water is passing through the lysimeter of 0.7 m in height. It also suggested that for the lysimeters with a length lower than 0.7 m, the percolation rainfall water can effectively wash out everywhere within the lysimeters, or the waste below 0.7 m will be submerged completely in the leachate. In addition, although the height of R1 and R5 are equal (0.35 m), R1 showed larger decreases in ion concentrations under the same L/S ratio conditions. This indicates that even if the height of a reactor is less than 0.7 m, as long as the width of the reactor is wide enough (more than 0.3 m which is the width of R5) the effect of the reactor‘s height on the leaching behavior can be minimized. When the soluble constituents concentrations from R2, R5 and R6 in the second group are compared, it is apparent that even for the same volume, the waste with a low H/W ratio displays a slower decrease in leachate concentration, which can effectively weaken the effect of side-wall flow or preference flow, and under relatively low H/W ratio lysimeters, the waste can be washed out completely. A comparison of the concentration of inorganic ions in R1 and R2, shows that although they had the same diameter, their leaching behaviors were a little different. For the concentrations of all four ions, as shown in Fig. 13(1a)(1b)(1c)(1d), R1 decreased by a greater degree and more quickly than R2. Such a difference can be attributed to the height of these lysimeters, and since the R2 was longer than R1, it is rational to expect that the particles of C&D waste at the bottom must bear a greater upper loading, which resulted in more inter-particle cohesion. To some extent, relatively dense microstructures restricted the decomposition rate by micro-organisms.

Figures 3.14 and 3.15 compare the concentrations of reactive constituents (SO_4 and NH_4). The values of NH_4 varied between the lysimeters, but the general trends are the same in that the values decreased gradually after reaching their peaks: R1 showed the largest decrease, as shown in Fig. 3.15(1). Values of SO_4 were a little different in that they increased gradually with increasing L/S ratio in all lysimeters. In general, SO_4 concentration in leachate is decreased under anaerobic conditions by sulphate reducing bacteria. It is reported that SO_4 in a semi-aerobic lysimeter decreased significantly, but gradually from 2000 mg/L to 200-300 mg/L over 20 years, while SO_4 in an anaerobic lysimeter decreased quickly to 20 mg/L over 10 years (Yanase et al., 2009). In addition, the leaching ability of sulfate from incinerator ash decreased with increasing pH value in a solvent (Miyawaki et al., 1995). However, in this study, SO_4 values are increasing gradually despite the anaerobic conditions. A similar increase in SO_4 concentration was observed in a leaching experiment using a 375 ton heap of municipal solid waste bottom ash (Freyssinet et al., 2002). The progressive increase in SO_4 with time is related primarily to changes in Ca concentration in the leachate. High concentrations of Ca released mainly by the dissolution of non-sulphated species (e.g. portlandite [$Ca(OH)_2$] and Ca silicates) can reduce gypsum solubility which contain the majority of sulphur. Therefore, more sulphate is able to be released from gypsum with the decrease in Ca concentration in the leachate. This may be the reason that SO_4 increased with increasing L/S ratio. Guyonnet et al. (2008) also observed the same pattern of leaching behavior in a large lysimeter and indoor cell test, and reported that the increase in SO_4 over time was caused by the late release of neoformed sulphates

that have time to accumulate (Ca-sulphates but also neoformed ettringite). These may be the reasons that SO_4 increased with increasing L/S ratio.

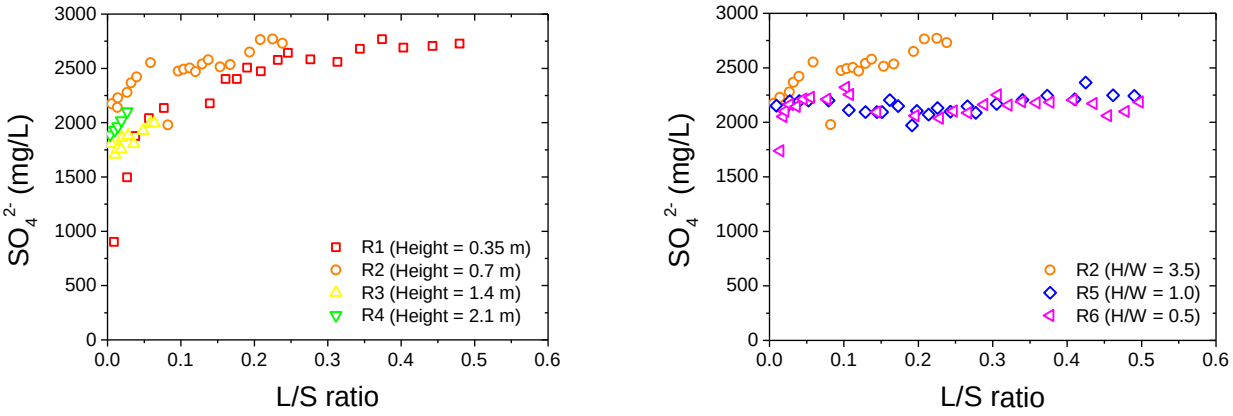

(1) (2)

Fig. 3.14 SO_4 from lysimeter tests as a function of L/S ratio

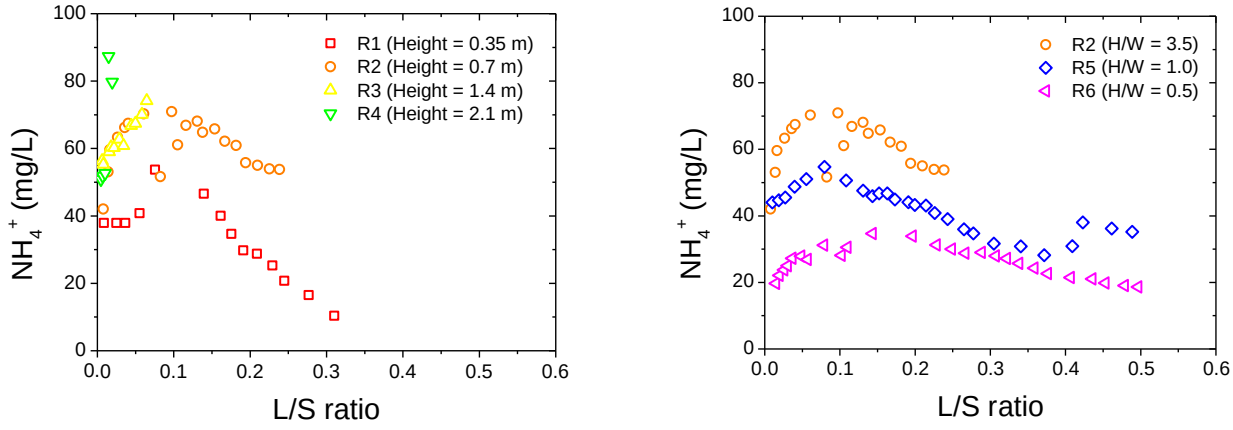

(1) (2)

Fig. 3.15 NH_4 from lysimeter tests as a function of L/S ratio

Figure 3.16 shows the concentrations of the heavy metals Ba, Cu, Fe, Mg, Mo, Ni and Sr from the lysimeter tests as a function of L/S ratio. Although C&D waste is regarded as inert, under special conditions such as microbial activity or relatively low pH conditions, large amounts of inherent heavy metals can be leached out. As shown in Fig. 3.16, the concentrations of leached out heavy metals were much higher compared to those from normal landfill leachate, especially for Cu and Ni (Johansen and Carlson, 1976; Chu et al., 1994; Clement and Thomas, 1995; Jørgensen and Kjeldsen, 1995; Robinson, 1995; Krug and Ham, 1997; Kjeldsen and Christophersen, 2001). Although the physical characteristics of C&D waste residue, such as particle density and hydraulic conductivity,

closely resembled those of sandy soil or ash, the chemical characteristics were totally different. For sandy soil or ash, which are abundant in the composition of clay mineral, possess excellent adsorption capacity towards heavy metals, while for C&D waste residue, the adsorption towards heavy metals was very limited even under extremely alkaline conditions, as shown in Fig. 3.11 (Tang et al., 2009, 2010). Such a phenomenon can be attributed to three factors; first, C&D waste has a lack of clay minerals in its composition, such as feldspar, mica, quartz and silicate salts. which contribute greatly to heavy metal adsorption capacity (Tang et al., 2012); second, heavy metal ions exist in the form of aquatic free ions since microbial activity can affect the overall environment inside the lysimeter, and this results in the extraction of the heavy metals (Jambeck et al., 2006); third, most heavy metals exhibit parabolic concentration curves as a function of the pH value due to their amphoteric character (Dijkstra et al., 2006; Kalbe et al., 2008). For example, Cu is soluble at low pH values as a Cu^{2+} or $CuCl^{+}$ ion, and as a hydroxy-complex at higher pH values ($Cu(OH)_2(aq)$, $Cu(OH)_4^{2-}$). In addition, in the presence of complexing ligands such as Cl^- or CO_3^{2-}, other complexes are possible (Dijkstra et al., 2006; Kalbe et al., 2008). Thus considering the pH conditions inside most of the lysimeters in the present study (R3, R4, R5 and R6) which were higher than 11.0, it was rational to expect the heavy metals were soluble and leached out, as shown in Fig. 3.16.

In addition, two types of change were observed in the concentration of heavy metals. The first type was a gradual decrease directly as the L/S ratio increased, observed for metals such as Ba, Cu and Mg (see Fig. 3.16(1a)(2a), Fig. 3.16(1b)(2b) and Fig. 3.16(1d)(2d)), while the other was an increase and followed by a gradual decrease or stable value, seen in metals such as Fe, Ni, Sr, and Mo (see Fig. 3.16 (1c)(2c) and Fig. 3.16(1e)(2e)(1f)(2f)(1g)(2g)). The direct decrease as a function of L/S ratio, can be attributed to the dilute effect from the continuous wash due to the percolation of rainfall water. From the pH conditions shown in Fig. 3.11, it is also suggested that the amphoteric character of heavy metals contributed to the decrease in leached out concentrations, since pH values decreased as L/S ratio increased, resulting in more heavy metal ions transitioning to chemical precipitation from instead of free ions. In Fig. 3.16 (1c)(2c) and Fig. 3.16(1e)(2e)(1f)(2f)(1g)(2g), it is interesting to see that the concentrations of leached out heavy metals reached peak values around an L/S ratio of 0.1, and similar peaks around this L/S ratio of 0.1 were also observed in EC change, as shown in Fig. 3.12. It suggested that around this L/S ratio value, the water content inside the lysimeters was optimal. Such an environment was suitable for the waste decomposition by micro-organism, and resulted in more leached out inherent heavy metal ions, which can help to explain the increase that is followed by a graduate decrease or kept stable as a function of L/S ratio for Fe, Ni, Sr, and Mo. As the continuous water filtration and microbial activity were restricted to some extent, the concentration of heavy metals gradually decreased.

The leaching behavior of certain lysimeters also differed significantly. The concentrations of Ba, Cu and Sr in R1 and R2, which had relatively low widths and high H/W ratios, decreased significantly faster than from R3, R4, R5 and R6, which also proved the previous judgement that the preferential and side edge-wall flow occurred, as shown in Fig. 3.16 (1a)(2a) (1b)(2b) and (1g)(2g).

It was also apparent that the concentrations of heavy metals from R1 changed much more quickly than R2, as shown in Fig. 3.16, and this can be attributed to the denser C&D waste residue and closer micro-structure especially at the bottom of R2, which restrict the leaching. In Fig. 3.16, it was interesting to find that the highest concentration appeared in R2, not the longest lysimeter, R4, which can be attributed to the complete washing out in R2 as mentioned previously.

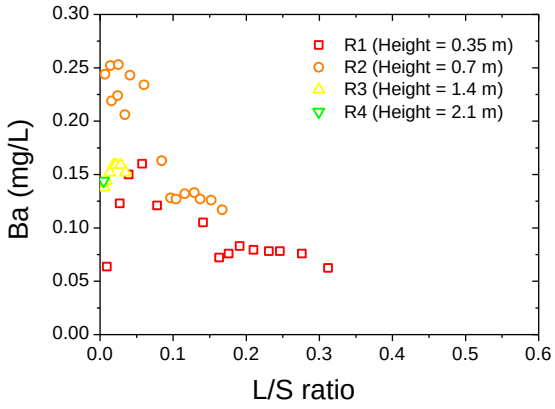

(1a)

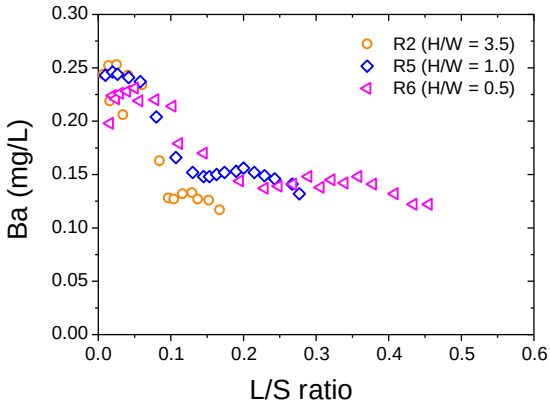

(2a)

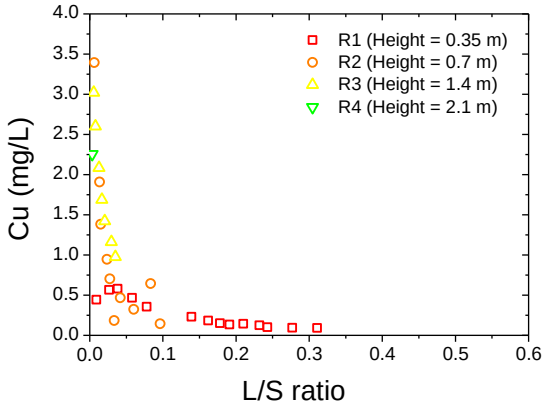

(1b)

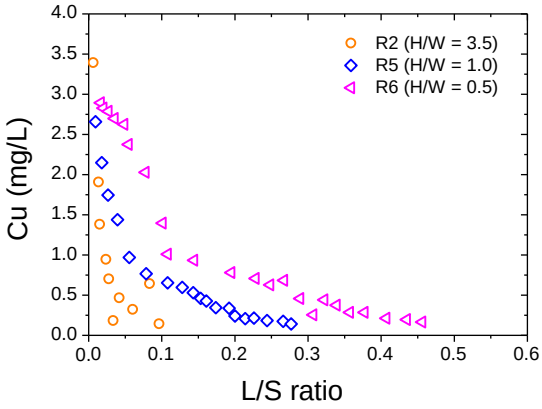

(2b)

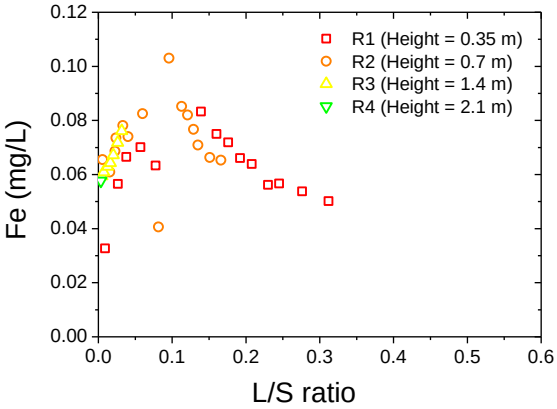

(1c)

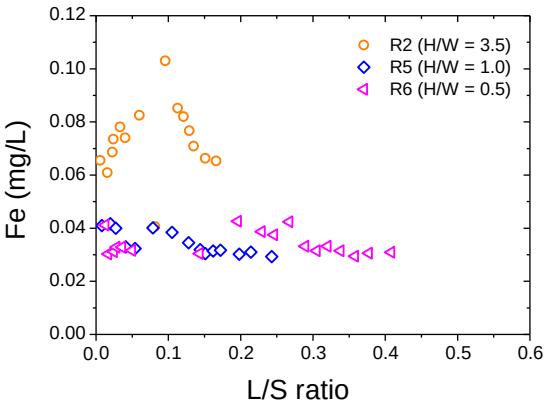

(2c)

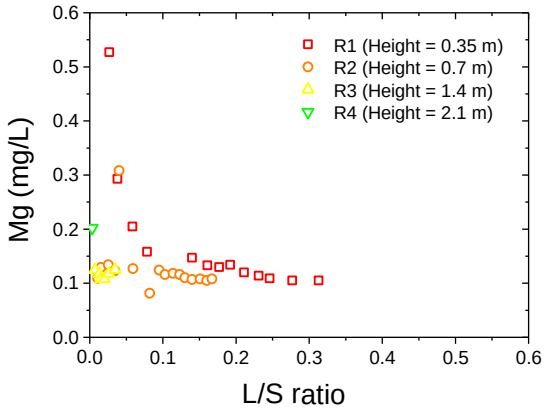

(1d)

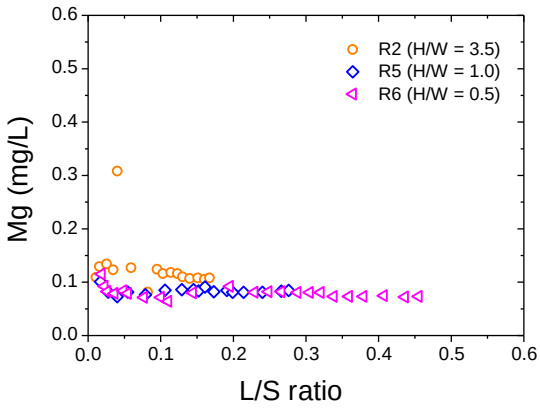

(2d)

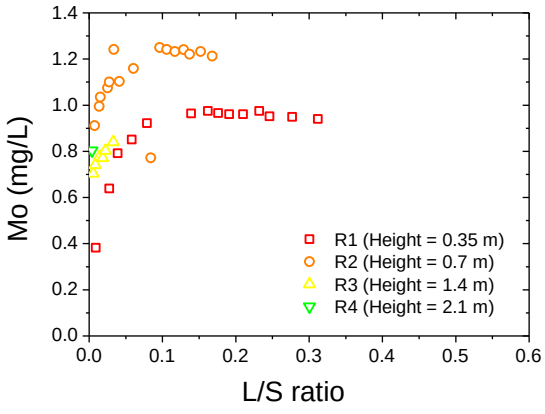

(1e)

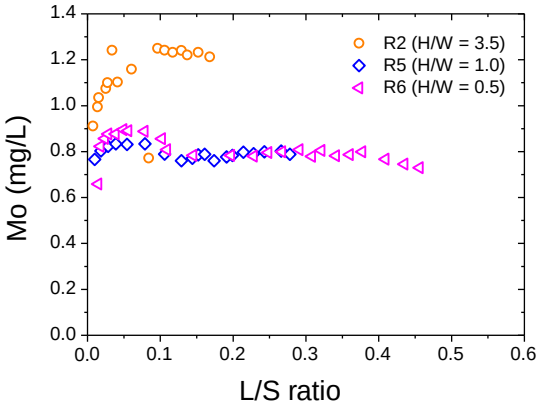

(2e)

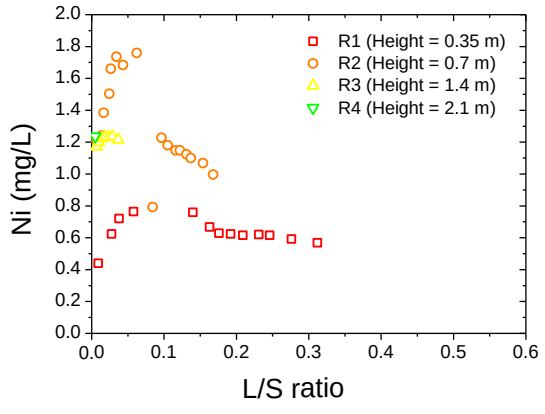

(1f)

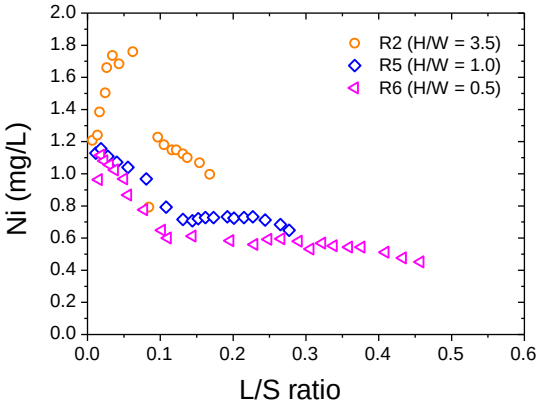

(2f)

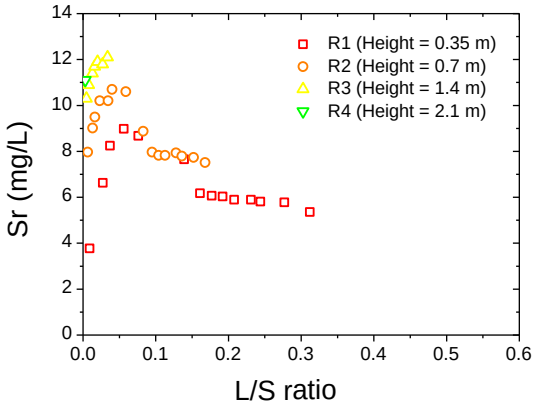

(1g)

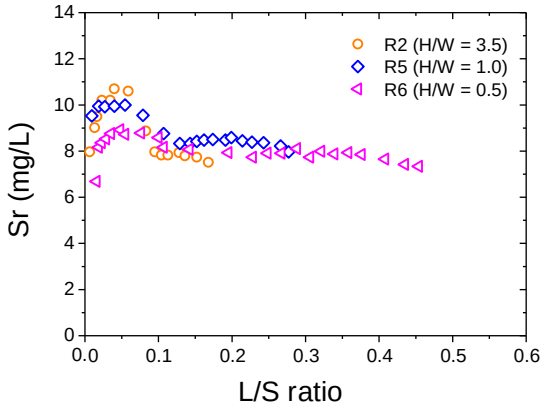

(2g)

Fig. 3.16 Heavy metals from lysimter tests as a function of L/S ratio

Figure 3.17 shows the COD from lysimeter tests as a function of L/S ratio. It was apparent that the initial COD values ranged from 7000 to 15000 mg/L, which indicated that the landfill waste can be classified in acid phase. In this phase, the COD values ranged between 6000 and 60000 mg/L (Christensen et al., 2001). Compared with the COD values in this study, greater COD values were reported by other researchers (Trankler et al., 2005; Castrillón et al., 2010; Salati et al., 2013). Such a difference in COD values can be attributed to landfill design and age, waste composition, temperature and precipitation conditions (Christensen et al., 2001). According to the standard B of Environmental Quality Regulations 1979 in Malaysia and Guidance for the Treatment of Landfill Leachate proposed by Environment Agency in UK, the effluent COD of landfill leachate should be less than 100 mg/L (Trankler et al., 2005; Environment Agency, 2007). The Ministry of Environment in Republic of Korea also proposed the regulation criteria towards COD, no more than 400 mg/L (Ahn et al., 2002). According to above regulations, the COD values in current study are considerably high. Therefore, further treatment is required to be carried out before discharge of leachate, or liners system should be designed and applied to cut off the migration of leachate to surrounding environment.

The general tendency of COD is decreased as L/S ratio, and can be explained as dilution effect due to the rainwater percolation (Monteiro et al., 2002; Trankler et al., 2005). The COD values in R1, R2 and R6 experienced an increase tendency first and followed by a gradual decline; while for R3, R4 and R5, the COD decreased gradually along the L/S ratio. According to Kostova (2006), before acid phase, some landfill sites would experience a transition phase, which is characterized as an increase in COD values, and this might to help demonstrate the increase tendency in R1, R2 and R6. Around L/S ratio of 0.2-0.4, COD values of leachate from most lysimeters decreased to lower than 4500 mg/L, which indicated landfill transferred into the methanogenic phase (COD, 500-4500 mg/L) (Christensen et al., 2001). The time spent on transfer from the acid phase to the methanogenic phase in this study were much shorter compared to previous studies, and one reason might to that the full

scale landfills generate leachate composed of various ages and this cannot be simulated in lysimeters (Trankler et al., 2005). As shown in Fig. 3.17 (1), the general tendency was decrease as L/S ratio, however, the decrease rates were different. Within the experimental durations, the COD from R1 and R2 with relative low heights, decreased more than that from R3 and R4 with longer heights. In Fig. 3.17 (2), although the decrease tendency were similar, some conclusions can be obtained based on the COD decrease rate, R2 (from ~14500 to ~4500 mg/L, 69%), R5 (from ~11000 to ~3000 mg/L, 73%) and R6 (from ~9000 to 1500 mg/L, 83%). It was obvious that for the same volume, the lysimeter with low H/W ratio can result in greater decease in COD values within same durations. Since the COD value reflect the amount of the organic contaminant, which is abundant in elements such as C, N, P, S, which was the basic nutrient for micro-orgamism and can be fixed during the leaching process, and to some extent, the change of COD partially reflected the microbial activity. Thus, from the results shown in Fig. 17(2), the lower H/W ratio can promote the microbial activity and result in the better performance of micro-organism in degradation of organic contaminant.

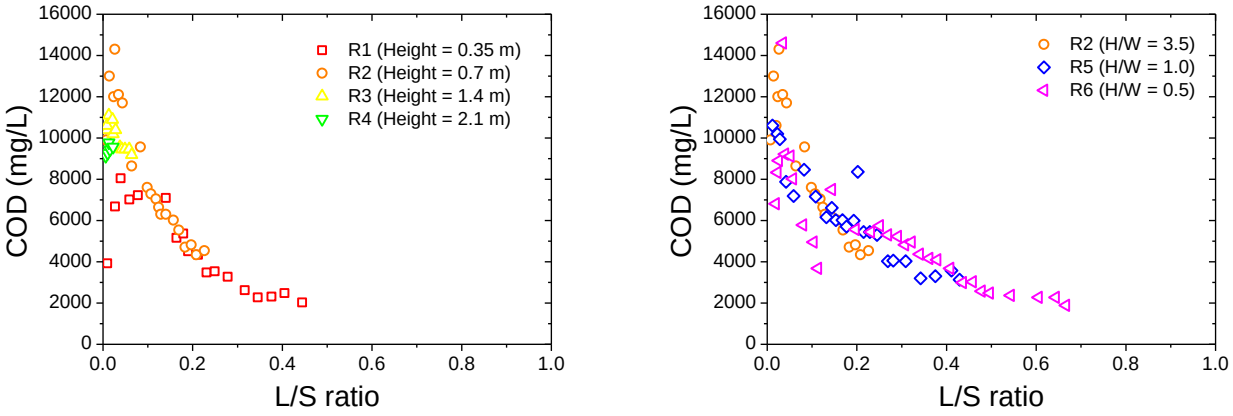

(1) (2)

Fig. 3.17 COD from lysimter tests as a function of L/S ratio

Figures 3.18 and 3.19 show the TN and TP from lysimeter test as function of L/S ratio. The TN mainly originated from ammonia-N (NH_3-N), nitrate-N (NO_3^--N) and nitrite-N (NO_2^--N). While for TP, it is usually predominantly present in the form of phosphates, with a minor fraction of organic phosphate mainly in proteins. The initial TN values from lysimeters ranged between 125 and 275 mg/L, while initial TP values ranged between 2.5 and 7 mg/L, both of that were a little lower compared to that from MSW leachate (Aziz et al., 2010). This phenomenon can be attributed to the composition of waste, for MSW landfill, domestic such as food waste is the major part, which is abundant in N and P; while for C&D waste, the major part is limestone, calcite, gypsum etc. Nevertheless, compared to the quality criteria of drinking water proposed by USEPA (2013), TN and TP were extremely high. Typically, the existence of high levels of TN and TP in landfill leachate over a long period of time is one of the most critical problem (Bashir et al., 2010).The high concentrations

of TN and TP, as essential nutrient, lead to motivated algal growth, accelerated eutrophication, promoted dissolved oxygen depletion and increased toxicity of living organisms in water bodies (Aziz et al., 2010). As shown in Fig. 3.18 (1) and Fig. 3.19 (1), the highest decrease rate of TN and TP appeared in R1, the shortest lysimeter (TN, 91%; TP, 62%). In Fig. 3.18 (2) and Fig. 3.19 (2), for the lysimeters with same volume, the lysimeter R6 with lowest H/W ratio exhibited highest decrease rate in TN and TP (TN, 92%; TP, 73%). Both nitrogen and phosphorus are important composition of protein, which is the essential nutrient for micro-organism. Thus, compared to other inorganic ions, nitrogen and phosphorus are more likely to be fixed by micro-organisms and promote the microbial activity (Cervantes et al., 2006). Considering above, the results in Fig. 3.18 and Fig. 3.19 suggested that the lysimeter with shorter height and low H/W ratio is more suitable for microbial activity, and to some extent, can accelerate the decomposition rate.

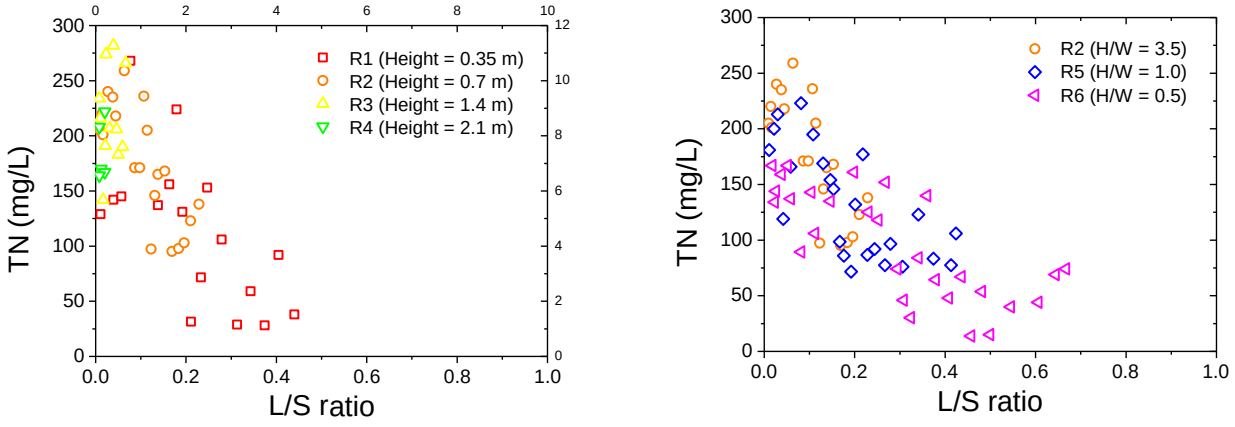

(1) (2)

Fig. 3.18 TN from lysimter tests as a function of L/S ratio

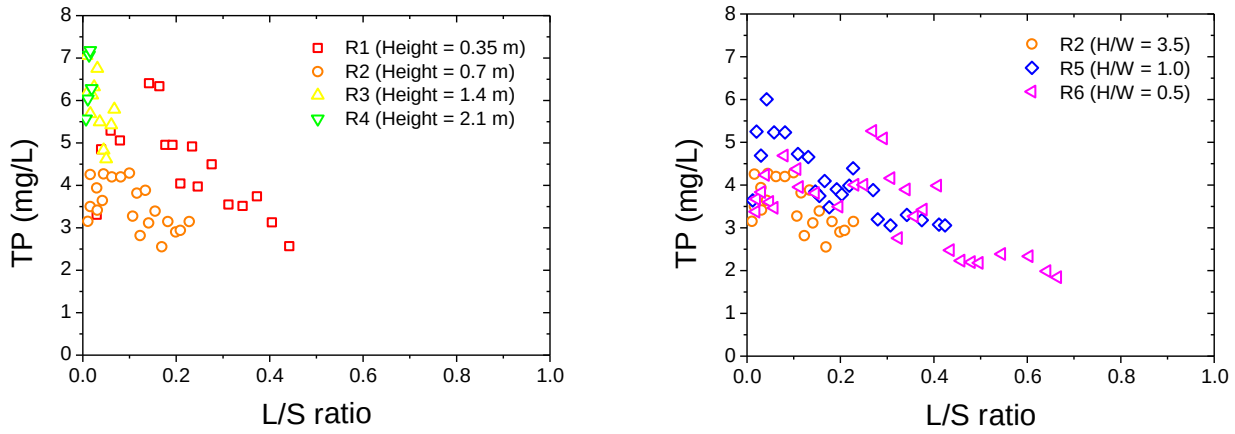

(1) (2)

Fig. 3.19 TP from lysimter tests as a function of L/S ratio

In order to further analyze the mechanism of leaching behavior in every lysimeter, based on the results shown in Fig. 3.13, Fig. 3.14 and Fig. 3.15, together with the volume and mass of leachate collected each time, the emission behavior of inorganic ions as a function of L/S ratio were obtained, as shown in Fig. 3.20. As the L/S ratio increased, the emission of SO_4^{2-} increased, as shown in Fig. 3. 20(1f)(2f), due to the promoted microbial activity, by which the sulfate salts originating from the gypsum in C&D waste were continually decomposed. In this figure, the emission from R1 was a little higher than others, which suggested that the microbial activity in R1 was greater. This conclusion was also supported by the NH_4^+ emission behavior. As shown in Fig. 3.20 (1e), the amount of NH_4^+ emission from R1 first increased, then gradually became stable, and the final emission amount was obviously lower than the others. Even with an L/S ratio of 0.25, the emission of NH_4^+ stopped, which indicated the greatest amount of microbial activity, since NH_4^+ can be fixed by micro-organisms, because ammonium salt is basic and provides excellent nutrient for their propagation. These findings can also help to explain the great decrease in NH_4^+ from R1 in Fig. 3.15. In Fig. 3.20(1e)(2e) the amount of NH_4^+ emission followed the order R1&R6 < R5 < R2 < R3&R4), which clearly indicated that lower height, or looser micro-structure inside the waste leads to more motivated microbial activity. Therefore, it was also helpful to demonstrate the phenomenon that emissions from R6 were higher than R5, since in R6, more C&D waste was decomposed and transited to the form of salts, then leached out, as shown in Fig. 3.20 (2a)-(2c). From Fig. 3.20 (1b)-(1d), it can be seen that the amount of emission from R2 was highest, which can be attributed to both relatively motivated microbial activity and complete washing out.

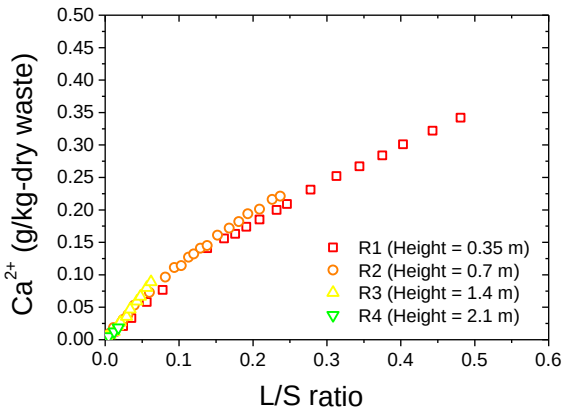

(1a)

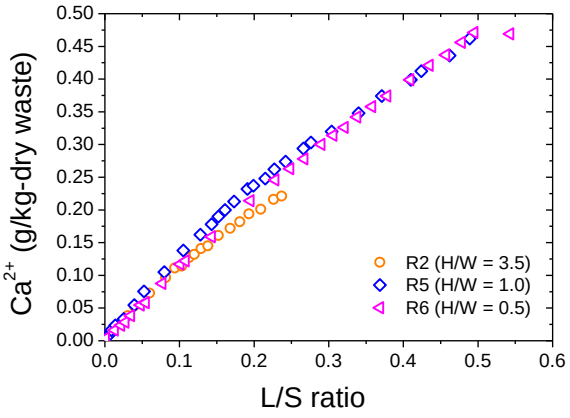

(2a)

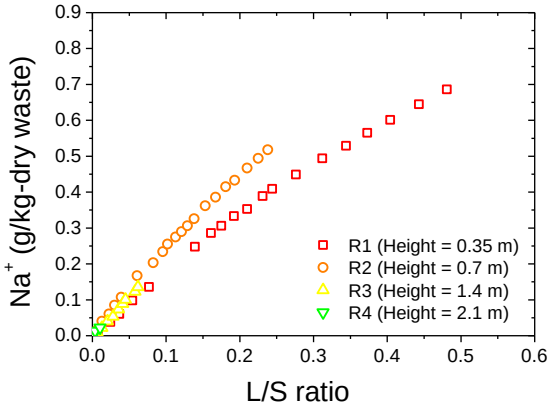

(1b)

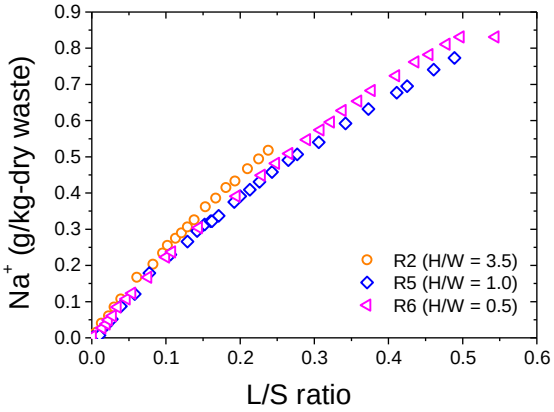

(2b)

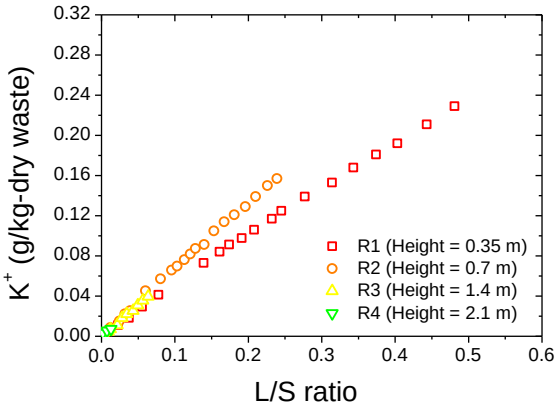

(1c)

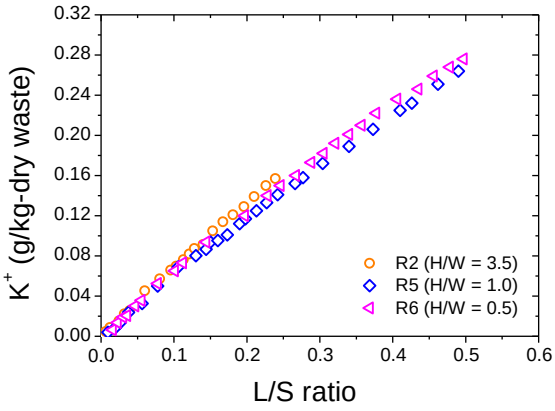

(2c)

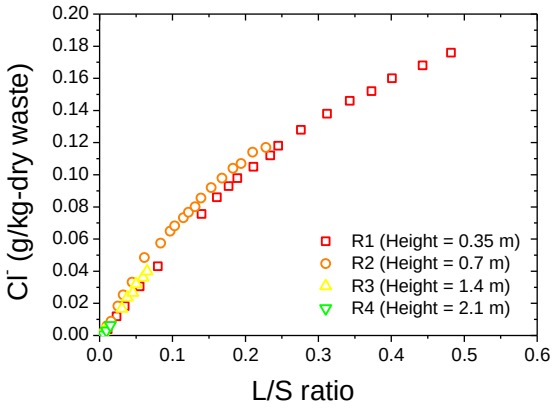

(1d)

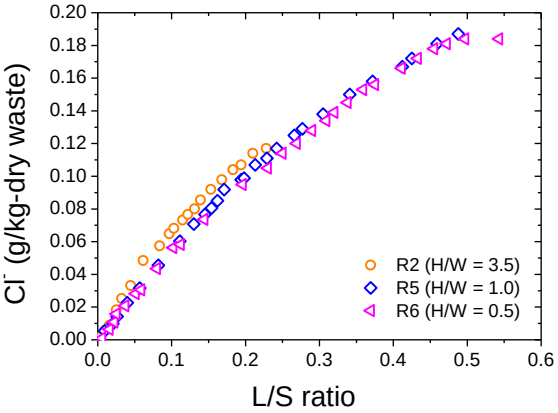

(2d)

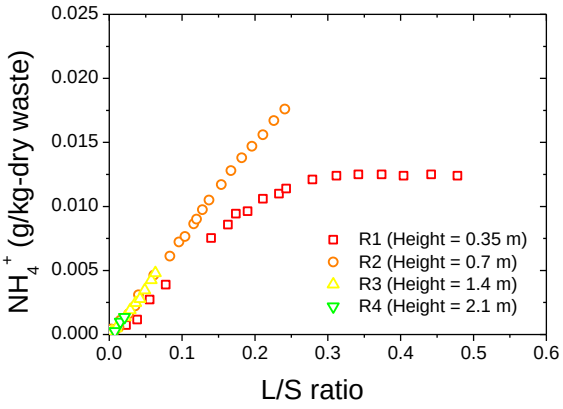

(1e)

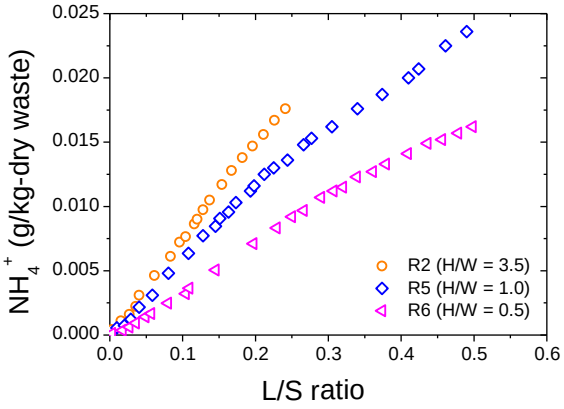

(2e)

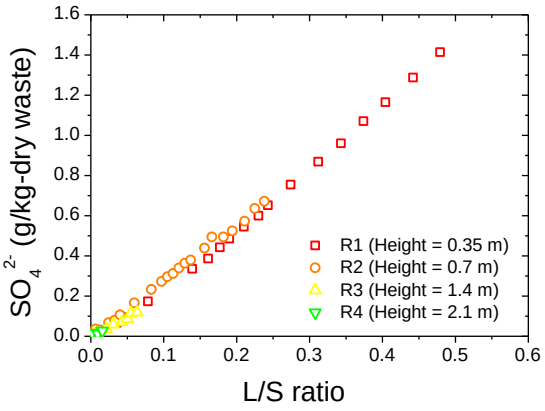

(1f)

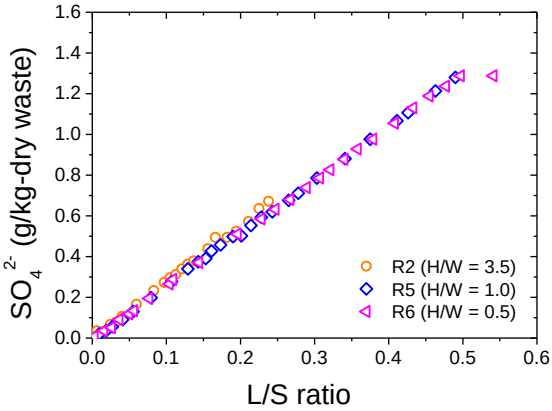

(2f)

Fig. 3.20 Emission behaviors of inorganic ions as a function of L/S ratio

As shown in Fig. 3.5, gas sample tubes and temperature sensors were installed in every lysimeter and, according to the original experimental design, the landfill gas would be extracted by pump, and the temperature inside the C&D waste in lysimeter would be monitored and reported automatically by data logger. However, since the laboratory for lysimeter test is located in Tsukuba, Ibaraki Prefecture, and the Tohoku earthquake and tsunami occurred during the lysimeter test (March 11th, 2011), the power supply of the laboratory was disrupted for almost one month. Thus, the gas and the temperature data were not obtained, and are not discussed in this study.

3.4 Summary

In this study, lysimeter tests were conducted in six lysimeters to estimate the effect of height and H/W ratio on leachate generation and leaching behavior of C&D waste residue. The C&D waste was collected from an intermediate treatment facility located in Ibaraki Prefecture. To avoid the effect of

particle size on test results, the C&D waste selected in this study had particles of < 5 mm.

The physical characteristics of C&D waste residue, such as particle density and hydraulic conductivity, closely resembled those of sand and ash. According to the leaching test results, the concentrations of each inorganic ion showed similar levels regardless of the particle size of the residue. The C&D waste showed strong alkalinity with pHs in the range of 11.7 to 12.2, and EC values in the small particles were found to be higher than those in the large particles. Such a decrease of pH and EC value as a function of particle size can be attributed to particle size of soluble content, since in most cases, soluble content exists in the form of powder or very small particle in nature.

In the lysimeter tests, the soluble constituent (Cl, Na, K, Ca) concentrations decreased with increasing L/S ratio. There were two types of decreasing shape; First is the relatively sharp decrease in concentrations of non-reactive constituents, shown in R1 and R2 which have a short width; second is the gradual decrease shown in R5 and R6. It is likely that it is caused by the preferential and sidewall flows which can easily occur in lysimeters with high H/W ratios. The highest concentrations of inorganic constituent always appeared in R2, rather than the longer R3 and R4, which suggests that the filtration water can completely wash the inside of the lysimeters which have a height lower than 0.7 m. The concentration of salt leached out in R2 was lower than that from R1, which can also be attributed the height of the lysimeter; as the height of lysimeter increased, the waste particles at the bottom must bear a greater upper loading, resulting in the lower leaching behavior. The leaching behavior of heavy metal ions (Ba, Cu, Fe, Mg, Mo, Ni and Sr) clearly prove that although C&D waste is regarded as inert, under certain conditions (lower pH and microbial activity), the inherent heavy metals might be leached out, as their concentrations are higher than normal MSW leachate.

According to the results of COD, TN and TP, the values were a little lower compared to the leachate from MSW landfill due to several factors such as the composition of the waste. The general tendency of COD, TP and TN is decreased as L/S ratio, and can be explained as dilution effect due to the rainwater percolation. Nevertheless, for certain lysimeter, the decrease rate was different, the lysimeter with short height or low H/W ratio displayed more reduction. Since the COD value reflect the amount of the organic contaminant, which is abundant in elements such as C, N, P, S, which was the important composition of protein and the essential nutrient for micro-orgamism and can be fixed during the leaching process, and to some extent, the change of COD, TN and TP partially reflected the microbial activity. The conclusion can be arrived that the lysimeter with lower H/W ratio or shorter height can promote the microbial activity and result in the better performance of micro-organism in degradation of organic contaminant.

Based on the emission behavior of some soluble constituents, the microbial activity can have a significant effect on leaching behavior, the amount of SO_4^{2-} emission increased with L/S ratio, due to the active microbial activity, by which the sulfate salts originating from the gypsum in C&D waste were continually decomposed. Thus, the decomposition by microbial activity inside C&D waste has great effect on the leaching behavior, and should not be neglected in the research. The amount of NH_4^+ emission followed the order R1& R6 < R5 < R2 < R3& R4, which clearly indicated that

shorter height, low H/W ratio or looser micro-structure inside the waste can provide more suitable conditions (density, upper loading, inter-particle cohesion, water content) and led to more active microbial activity.

CHAPTER 4: FACTORS AFFECTING MEMBRANE BEHAVIOR OF CLAY LINERS

4.1 General remarks

Containment capacity of sanitary landfill or other hazardous waste containment infrastructure mainly depends on the barrier performance of liner system, especially bottom liner system. To some extent, liner system is the most important part to prevent the migration of contaminants, and take the significant responsibility to preserve the surrounding environment and humans‘ health. It is rational to expect that the performance of these clay liners can be greatly enhanced if they exhibit a semipermeable membrane behavior, by which the liners can prevent or restrict the migration of selected substances such as contaminants while allowing the passage of water molecules like a perfect semipermeable membrane.

According to previous researches, membrane behavior has been observed in several types of soils used as liners or barriers, including natural soil and sodium bentonite. The observed membrane behavior in natural clay has been too low to sufficiently prevent the migration of contaminants. For sodium bentonite, it has been observed to have very excellent membrane property. However, very few studies have been done about the factors on membrane behavior. Since the liner applied in practice will be exposed to leachate or other contaminant contained solutions, and the physical characteristics of liner such as compactness are also differed one by one. All of above made the research about the membrane behavior of liners very urgent and necessary.

Thus, considering combining the advantages of clay and bentonite, bentonite is introduced to make the composite material to promote the barrier performance of natural clay towards contaminants and enhance its membrane properties. Laboratory-scale test will be conducted, and different test conditions will be used to study the factors on membrane behavior, including sodium bentonite content, solute pH and concentration, compactness and thickness as well as different kinds of ions. Based on the membrane test results, the mechanism will be also discussed with assistance of SEM, XRD, XRF and photographs.

4.2 Materials and methods

4.2.1 Soils

4.2.1.1 Fukakusa clay and bentonite

Two types of soils were evaluated: a locally available natural clay and a kind of bentonite. The local natural clay is known as Fukakusa clay (FC) since its abundant deposit and well distributed around the Fukakusa area in Kyoto, Japan. Fukakusa clay, as a kind of local clay, are widely used in

civil engineering and environmental infrastructures in local or surrounding areas.

Bentonite is a well-known member of the clay family for fine grained swelling types of clay. It contains high content of swelling clay minerals (smectites). The most common two types of bentonite are calcium bentonite and sodium bentonite, where sodium has the greater ability to swell and consequently gives better sealing i.e. lower hydraulic conductivity (Mitchell, 1976; Lundgren, 1981; Sällfors and Öberg-Högsta, 2002). However, the sodium bentonite is only available in large quantities in Wyoming and Horth Dakota in the U.S. The transportation costs of moving bentonite from these locations to worldwide are relatively high. An alternative is to transform calcium bentonite into sodium bentonite, since calcium bentonite has been found in large deposits, and much more available around the world (Di Emidio, 2010). The peptizing process is a common method for replacement of calcium ions by using sodium hydroxide to treat the calcium bentonite (Sällfors and Öberg-Högsta, 2002). The powered sodium bentonite utilized in this study is a commercial one, referred to a ―super clay", and is originally from Wyoming, U. S. (purchased from Hojun Co. Ltd.). Sodium bentonite is widely used as a soil mixture additive and in slurry walls.

4.2.1.2 Basic physical and chemical properties of two kinds of soil

Table 4.1 presents the physical properties of Fukakusa clay and sodium bentonite. The soil particle density is 2.717 and 2.635 g/cm^3 and the natural water content is 3.7% and 6.5% for Fukakusa clay and bentonite. The pH of Fukakusa clay is 3.0, a little different with other clay, which were usually exhibited alkaline nature, and the mechanism will be discussed in the section 4.4. The Free swell index of Fukakusa clay was only 3 mL/2g-solid, which represent almost no swelling property. The particle size distribution curve of Fukakusa clay is shown in Fig. 4.1.

Table 4.1 Physical properties of Fukakusa clay and bentonite

Property	Units	Standard	Values	
			Fukakusa clay	Bentonite
Soil particle density	g/cm^3	JIS A 1202	2.717	2.635
Natural water content	%	JIS A 1203	3.7	6.5
pH	--	ASTM D 4972-01	3.0	9.7
Swell index	mL/2g-solid	ASTM D 5890-06	3.0	23.0
Plastic limit	%	JIS A 1205	14	47.3
Liquid limit	%	JIS A 1205	53	540
Grain size distribution		JIS A 1204		
Sand fraction (> 0.075 mm)	%		30.1	
Silt fraction (0.005-0.075 mm)	%		53.7	
Clay fraction (< 0.005 mm)	%		16.2	
Uniformity coefficient	--		29.1	
Coefficient of curvature	--		2.2	

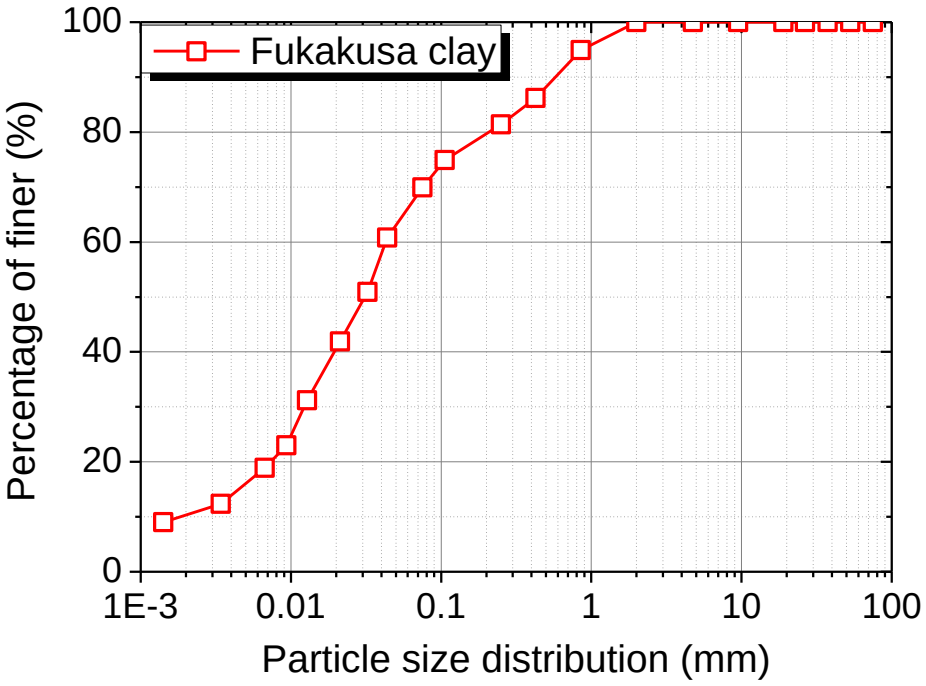

Fig. 4.1 Particle size distribution of Fukakusa clay

Table 4.2 presents the chemical properties of Fukakusa clay and sodium bentonite. For Fukakusa clay, the main exchangeable metal was identified as Ca^{2+} (10.5 meq/100g), and small amount of Mg^{2+}, Na^{+} and K^{+} (3.8, 0.6 and 2.2 meq/100g). For the bentonite, the dominant exchangeable metal was identified as Na^{+} (43.7 meq/100g), then Ca^{2+} (22.1 meq/100g), Mg^{2+} (13.8 meq/100g), and only small amount of and K^{+} was detected. The sum of exchangeable metals is a little higher than CEC (cation exchange capacity), which can be ascribed to the presence of carbonate in the soils and part of the measured cations might therefore originated from the carbonates and not from the exchange complex of the soil particles (Heister, 2005).

Table 4.2 Chemical properties of Fukakusa clay and bentonite

Property	Units	Standard	Values	
			Fukakusa clay	Bentonite
Cation exchange capacity	meq/100g	JGS 0261-2009	14.9	56.1
Exchangeable metals	meq/100g	ASTM D7503-10		
Ca			10.5	22.1
Mg			3.8	13.8
Na			0.6	43.7
K			2.2	1.8
Sum			17.1	81.3
Soluble salts	mg/kg	ASTM D7503-10		
Ca			1578	664
Mg			798	1210
Na			578	7423
K			108	195
Chemical composition	%	JIS M 8853		
SiO_2			49.3	66.1
Fe_2O_3			20.4	21.6
Al_2O_3			13.6	4.2
CaO			2.2	3.8
K_2O			6.9	1.7
TiO_2			2.4	0.8
ZrO_2			0.2	0.2
SrO			0.1	0.2
MnO			0.2	0.2

Figure 4.2 shows the XRD patterns of both Fukakusa clay and bentonite (RAD-2B, Rigaku Corporation, Japan). In the case of bentonite, it was abundant in Montmorillonite as can be observed by the characteristic peaks that appeared at $2\theta = 7.02^o$, 19.78^o, 26.60^o, 29.84^o, 34.86^o and 36.14^o. In the case of the Fukakusa clay, and based on the characteristic peaks appeared at $2\theta = 20.94^o$, 26.62^o, 36.62^o, 39.54^o, 40.32^o, 42.56^o and 45.86^o, it is clear the main mineral composition was quarts. Montmorillonite was not observed in Fukakusa clay, which can help to explain its low swelling property as listed in Table 2. Feldspars, illite and albite were observed in both Fukakusa clay and bentonite. The weak characteristic peak at $2\theta = 12.43^o$ indicates that the Fukakusa clay contained very limited Mica composition.

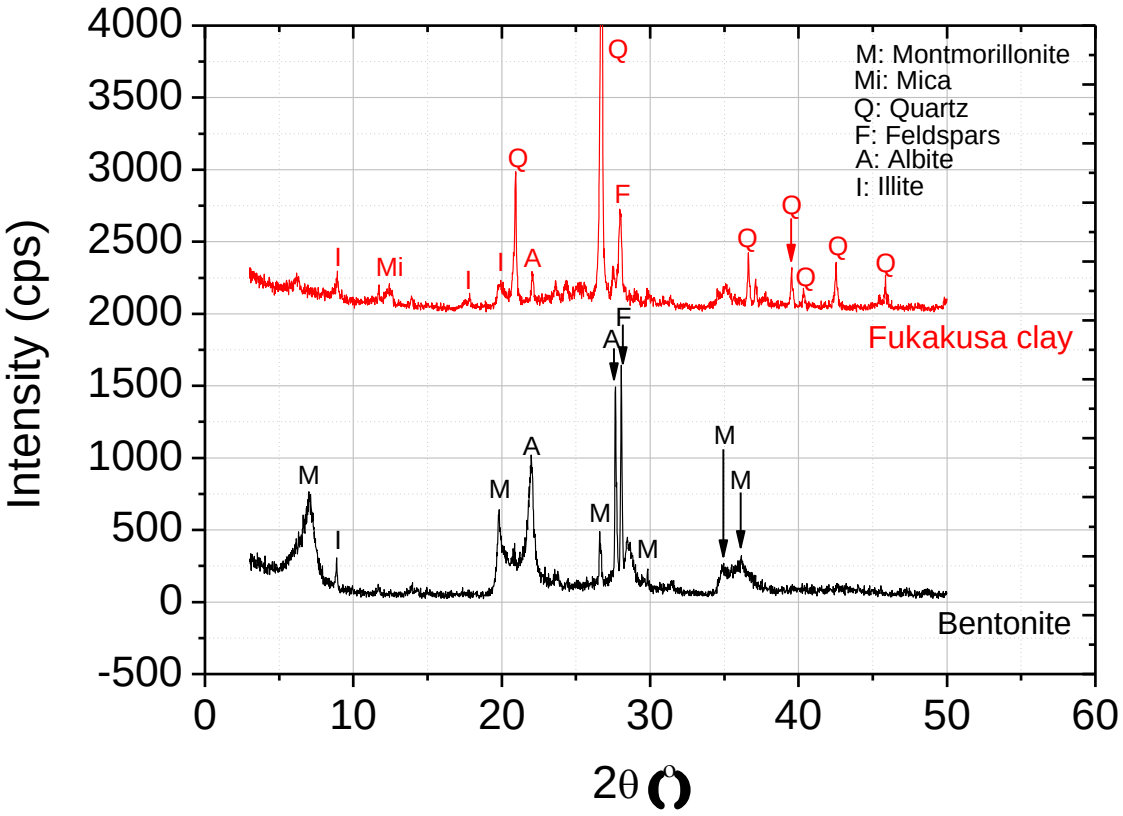

Fig. 4.2 XRD patterns of Fukakusa clay and bentonite

4.2.2 Solutions

De-ionized water (DIW) and solutions containing various concentrations of KCl, NaCl, $CaCl_2$, $ZnCl_2$ and $Pb(NO_3)_2$ were used in this study. The DIW was prepared from tap water by using a water distillation apparatus (RFD240NA, Advantec, Japan). Potassium chloride (Guaranteed reagent, Nacalai Tesque, Inc., Japan), sodium chloride, calcium chloride, zinc chloride and lead nitrate (Guaranteed reagent, Wako Ltd., Japan) are dissolved in DIW to prepare a standard KCl solution, then diluted to target concentrations of 0.5, 1, 5, 10, and 50 mM. Thirty-five percent HCl and 1 M KOH standard solution (guaranteed reagent, Nacalai Tesque, Inc., Japan) were diluted and used to regulate pH. The pH and electrical conductivity (EC) of the electrolyte solutions were measured by a pH/ion/cond.-meter (F-55, Horiba, Japan), and the results are shown in Table 4.3.

To avoid the effect from other ions, prior to the membrane tests, all the specimens were flushed by permeation with DIW to remove soluble salts. As shown in Table 4.2, the dominant cations of the exchangeable complex in Fukakusa clay and bentonite were Ca^{2+} and Na^{+}. For Ca^{2+} in Fukakusa clay, the ion exchange reaction can be neglected since its relative low atomic weight compared to K (Mitchell and Soga, 2005). For the case of Na^{+}, it was hard to quantify the ion exchange with K.

However, considering the very low amount of bentonite, it was rational to assume that after flushing, the EC of the circulation outflow from the specimen boundaries during the tests was due solely to KCl. Additionally, the correlation between EC and KCl concentration was linear over the concentration range in this study. Accordingly, to simplify the measurements, the KCl concentrations of the circulation outflow during the test were calculated based on the measured EC values in accordance with the calibration line shown in Fig. 4.3.

Table 4.3 Measured chemical properties of the solutions

Liquid	Concentration		pH	EC (mS/m) @18 °C
	(mM)	(mg/L)		
De-ionized water	0	0	6.8	0.1
KCl solutions	0.5	38	6.87	7.14
	1	75	6.95	14.06
	5	380	6.43	68.3
	10	750	6.3	126.7
	50	3800	6.56	642
NaCl solutions	0.5	29	6.7	5.69
	1	58	6.7	11.14
	5	290	6.6	57.1
	10	580	6.6	102
	50	2900	6.5	492
$CaCl_2$ solutions	0.5	56	6.8	12.68
	1	111	6.8	21.4
	5	555	6.6	106
	10	1110	6.7	184
	50	5550	6.6	886
$ZnCl_2$ solutions	0.5	68	6.3	10
	1	136	6.5	19.7
	5	680	6.5	92.8
	10	1360	6.3	184
	50	6800	6.1	867
$Pb(NO_3)_2$ solutions	0.5	166	6.2	13.92
	1	331	5.8	26.7
	5	1655	5.7	117
	10	3310	5.7	199
	50	16550	5.3	863

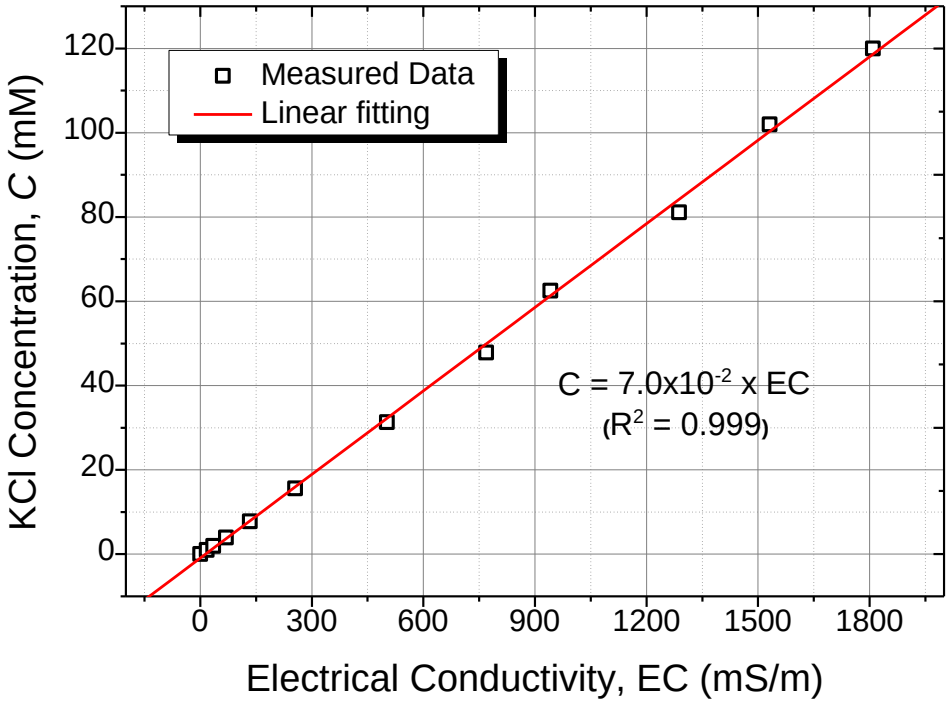

Fig. 4.3 Linear relationship between EC and KCl concentration

To validate this assumption, Malusis and Shackelford (2002b) compared the KCl concentration from the outflow based on the EC calculation to direct measurements. The results indicated an excellent agreement between the calculated KCl and measured Cl^- concentrations, while the change in the K^+ concentration slightly lagged behind that of Cl^-. Thus, using the EC values to estimate KCl concentrations should be accurate, i.e., in the case of sufficiently flushed specimens.

4.2.3 Test apparatus

For laboratory scale membrane tests, two types of cells are common: flexible-wall cells (Kang and Shackelford, 2009; 2011) and rigid-wall cells (Malusis et al., 2001; Malusis and Shackelford, 2002a; Malusis et al., 2003). Considering the boundary condition, the test cells can be classified by two groups, closed system and opern system (Shackelford, 2013). Due to simplicity and economic considerations as presented by Daniel et al. (1985), this study employed only rigid-wall cells and open boundary system.

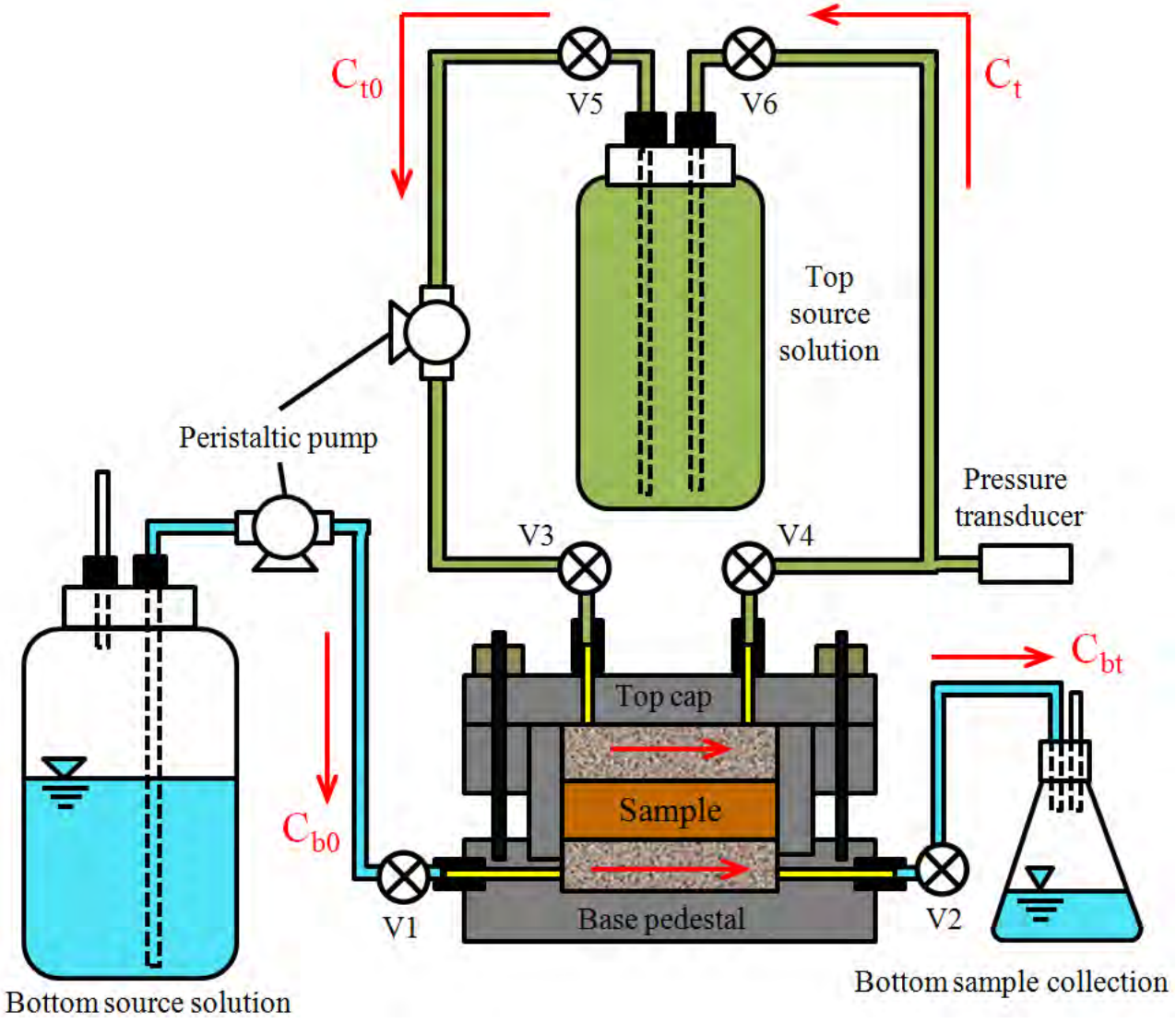

Fig. 4.4 Schematic diagram of the testing apparatus

Figures 4.4 and 4.5 schematically depicts the testing apparatus which resembles the system proposed by Malusis et al. (2001). The specimen was placed into a rigid acrylic cylinder with the top cap and base pedestal locked in place to prevent soil from expanding and to maintain the specimen initial thickness. Both the top and bottom surfaces were covered by porous stones and filter papers to prevent the porous stones from clogging by soil particles, while the inside cylinder edge was covered with vaseline to prevent wall-edge flow. Ports were equipped at both the top cap and base pedestals. When Valve 3, 4, 5 and 6 are open, the ports are at the top cap allowed a circulation loop of electrolyte solution through the porous stones, whereas when Valve 1 and 2 are open, the port at the base pedestal allows the bottom surface of the specimen to be flushed. The electrolyte solutions on both sides of the specimen were circulated continuously through the porous stones by cassette peristaltic pumps (SMP-23AS, As One, Japan), which simulated a constant-concentration boundary condition at the top and a perfect flushing boundary at the bottom (Malusis et al., 2001; Malusis and

Shackelford, 2004). Thereby, a constant concentration difference across the specimen was established and maintained.

During membrane testing, Valves 3, 4, 5 and 6 were kept open at the top. A solution of constant concentration from the top source solution bottle was infused through the porous stones, and traveled back to top source solution bottle. This configuration comprised a closed circulation loop, such that at the top surface boundary, the circulation inflow and outflow volumes were equal to prevent a solution flux through the specimen. The pressure transducer (PTI-S-JC300-22AQ-T, Swagelok, German), with power supplied by a regulated DC power supply (LX018-2A, Takasago, Japan), was installed at the top to measure and record the pressure inside the top circulation loop with the assistance of data acquisition system (Data logger) (NR-1000, Keyence, Japan). To avoid the elevation head differences between the transducer and the top, center of the specimen, and between the vent in the bottom circulation outflow and the bottom, center of the specimen, the transducer and top center of the specimen were designed at the same height. For the case of vent of bottom circulation outflow, it was at the bottom of the sample collection conical flask, which was placed on the top of specimen as shown in the image in Fig. 4.5. Moreover, to minimize stress loss, half-rigid acrylic bottles, connectors, valves and tubes were used for assembling the circulation loop. For the bottom, Valves 1 and 2 were kept open, and DIW was flushed at the bottom to provide outflow for sample collection.

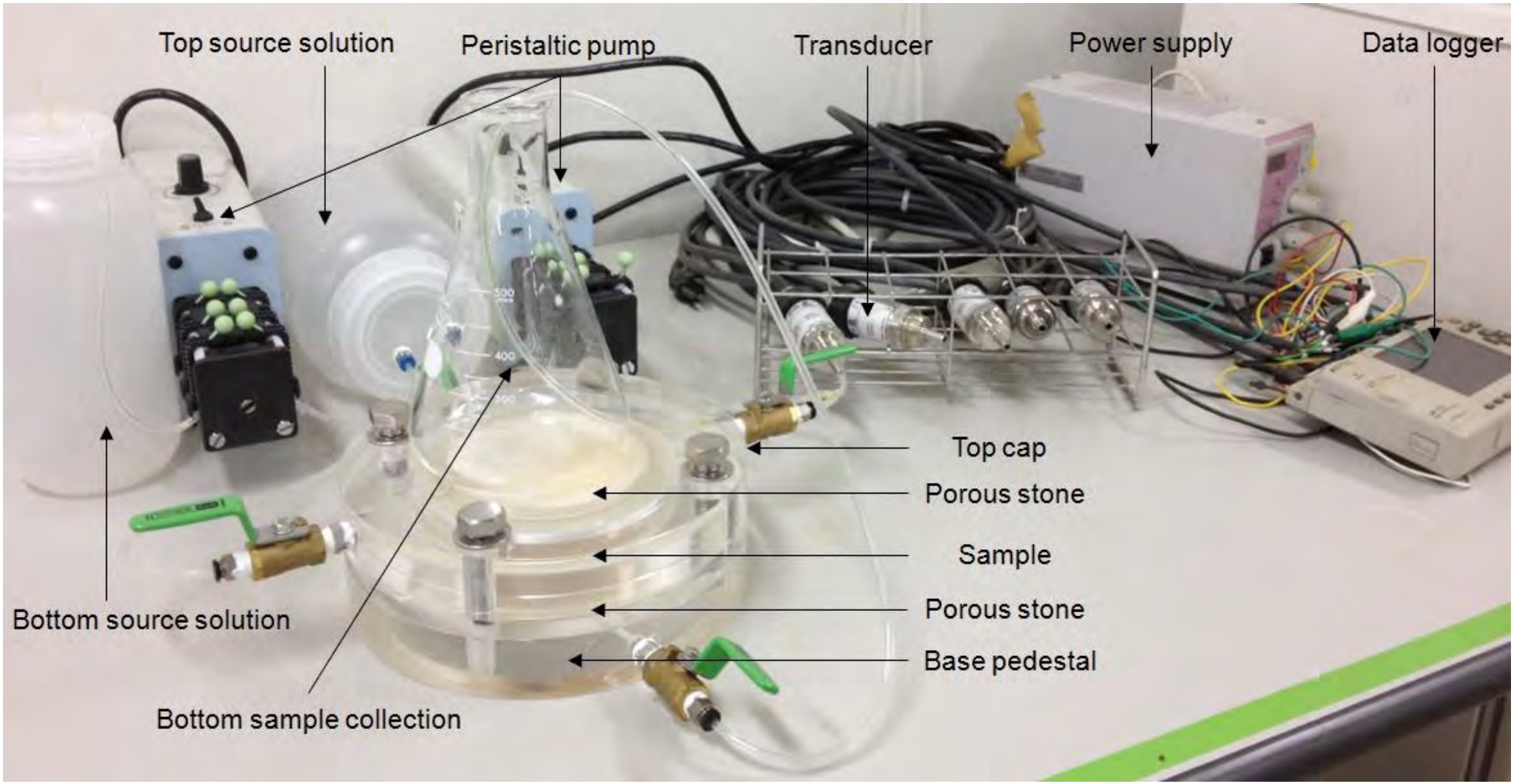

Fig. 4.5 Photograph of the testing apparatus

4.2.4 Membrane test program

Table 4.4 presents the total membrane test program. As shown in this table, the whole membrane tests required totally 16 specimens, which can be divided into 5 groups based on the factor on membrane behavior.

Group 1, Group 2 and Group 3 take into account of the effect of physical characteristics on membrane behavior. As the cost of bentonite is high, in most cases, the research was focus on the minimum percentage of gentonite necessary to fulfill the given requirements. Thus Group 1 contained 5 specimens, in which the bentonite content ranged from 0 to 20%. This group is designed to study the optimum bentonite content to improve the membrane behavior of natural clay. Group 2 contained two specimens with compactness 80% and 90% to study the effect of compactness on membrane behavior, since in practice, the compactness of bottom liners are a little difficult to reach 100%. Group 3 included 3 specimens with different thickness ranged from 5 cm to 9 cm.

Group 4 and Group 5 were used to study the membrane behavior under leachate with different conditions. Group 4 contained two specimens and the solution with different pH (4.0 and 11.0) were used in the membrane test. Group 5 had four specimens, and during the test, different types of solutes were used, including heavy metals. It has to be mentioned that during the membrane test on every specimen, solutes with different concentrations were utilized to study the effect of concentrations. According to the membrane test results obtained from membrane test towards Group 1, bentonite content 5% is the optimum, thus from Group 2 to Group 5, bentonite content was fixed at 5%.

Table 4.4 The total membrane test program

Group	No.	Specimens' conditions			Contaminant			
		Bentonite content	Thickness	Compactness	Type	Valence	pH	Concentration (mM)
1	1	0%	3 cm	Standard	KCl	1+	About 7.0	0.5, 1, 5, 10 and 50
	2	5%	3 cm	Standard	KCl	1+	About 7.0	0.5, 1, 5, 10 and 50
	3	10%	3 cm	Standard	KCl	1+	About 7.0	0.5, 1, 5, 10 and 50
	4	15%	3 cm	Standard	KCl	1+	About 7.0	0.5, 1, 5, 10 and 50
	5	20%	3 cm	Standard	KCl	1+	About 7.0	0.5, 1, 5, 10 and 50
2	6	5%	3 cm	90%	KCl	1+	About 7.0	0.5, 1, 5, 10 and 50
	7	5%	3 cm	80%	KCl	1+	About 7.0	0.5, 1, 5, 10 and 50
3	8	5%	5 cm	Standard	KCl	1+	About 7.0	0.5, 1, 5, 10 and 50
	9	5%	7 cm	Standard	KCl	1+	About 7.0	0.5, 1, 5, 10 and 50
	10	5%	9 cm	Standard	KCl	1+	About 7.0	0.5, 1, 5, 10 and 50
4	11	5%	3 cm	Standard	KCl	1+	About 4.0	1, 5, 10 and 50
	12	5%	3 cm	Standard	KCl	1+	About 11.0	1, 5, 10 and 50
5	13	5%	3 cm	Standard	$CaCl_2$	2+	About 7.0	0.5, 1, 5, 10 and 50
	14	5%	3 cm	Standard	NaCl	1+	About 7.0	0.5, 1, 5, 10 and 50
	15	5%	3 cm	Standard	$PbCl_2$	2+	About 7.0	0.5, 1, 5, 10 and 50
	16	5%	3 cm	Standard	$ZnCl_2$	2+	About 7.0	0.5, 1, 5, 10 and 50

4.2.5 Specimen assembly and preparation

Both Fukakusa clay and bentonite were dried under 105 ^{o}C for at least 24 hours by using constant temperature oven (DNE600, Yamato, Japan). Then the FC was mixed with bentonite at several different content (0, 5%, 10%, 15%, and 20%) on a total dry weight basis (e.g., 5% bentonite content = 5 g dry bentonite per 100 g of FC-bentonite mixture). As shown in Table 4.4, for Group 1 which contained five specimens to study the effect of bentonite content, the bentonite content ranged from 0 to 20%, while the other 4 groups the bentonite content was fixed at 5%. Then, water was added to the soil mixture by a mixing machine (KM-800, Kenmix, Japan) to achieve the optimum water content shown in Table 4.5. The optimum water content was based on preliminary standard compaction tests following JIS A 1210. To ensure that water was well distributed without evaporation, each sample was covered with a polyethylene membrane and allowed to stand for 12 h after blending. After that, the specimens were started to prepare following three stages: assembly, saturation and flushing.

Table 4.5 Results of the standard compaction tests

Soils	Standard compaction test (JIS A 1210)	
	Maximum dry density	Optimum water content
Fukakusa clay (FC)	1.51 g/cm^3	23.0%
FC + 5% bentonite	1.42 g/cm^3	23.2%
FC + 10% bentonite	1.48 g/cm^3	24.0%
FC + 15% bentonite	1.46 g/cm^3	24.8%
FC + 20% bentonite	1.43 g/cm^3	25.6%

First, each specimen was compacted to reach maximum dry density directly in a cell column with an inner diameter of 100 mm and height of 30 mm. For the specimens in Group 3 as shown in Table 4.4, special cell column with height of 50 mm, 70 mm and 90 mm were designed and used. Compared to the molds used in standard compaction tests (JIS A 1210), this study employed thinner specimens to reduce the duration of the membrane tests (Shackelford et al., 2003; Kang and Shackelford, 2010). Wider diameters were used compared to standard hydraulic conductivity tests (ASTM D 5084) to minimize side-wall flow (Kim et al., 2011).

Second, all the specimens were submerged in DIW inside a vacuum chamber connected to a pump (LMP100, Welch, Japan). Because the specimens contained bentonite, which has its own swelling properties, each specimen was mounted between two porous stones and filter papers and clamped by three vices to prevent expansion while reaching saturation. Since in Group 1, the specimen contain bentonite content 20%, 15% and 10%, to ensure sufficient saturation, the saturation process lasted three days under a vacuum with a pressure of about −85 kPa, and for the case of specimens in other groups, the saturation process lasted for only one day.

After saturation step, each specimen was assembled with a top cap and base pedestal. Then, specimens were permeated with DIW for flushing. To accelerate the flushing stage, an average of four meters‘ constant water head was applied with the hydraulic gradient around 135. Despite the high hydraulic gradient during flushing, the flushing stage still took about 60-70 days for most of specimens, and almost 160 days for specimens in Group 3. Following previous research, the flushing stage in this study terminated when the EC of the outflow was less than 3.6 mS/m (50% of the EC of the lowest KCl concentration used in this study) (Kang and Shackelford, 2009, 2011). The primary purpose of flushing was to remove soluble salts from the specimens in order to enhance the potential of the membrane behavior (Malusis et al., 2001; Malusis and Shackelford, 2002a, b; Kang and Shackelford, 2009, 2011). During the flushing stage, the outflow volume, duration, and hydraulic gradient were recorded for use in the hydraulic conductivity calculation following Darcy‘s law. For every specimen with certain bentonite content in Group 1, parallel specimen was prepared under duplicate test condition. After the saturation process, the specimen was used for the membrane test, while its parallel specimen was for the measurement and calculation of initial saturation degree. The saturation degree of specimens in Group 2, 3, 4 and 5 were calculated based on measurement of the dry and saturated specimens after the membrane test.

4.2.6 Membrane test procedures

To establish a steady baseline pressure difference across a specimen, DIW was circulated first over both the top and bottom boundaries of the specimens at a constant circulation rate (about 205 mL/d) for six days prior to introducing different concentration solutions.

Each membrane test consisted of five individual circulation stages. In each stage, one of the five electrolyte solutions with solute concentrations of 0.5, 1, 5, 10 and 50 mM was infused sequentially into the top porous stone of the specimen, while flushing the bottom surface with DIW. Each stage of the test was conducted until a stable chemico-osmotic pressure difference across the specimen was observed.

The outflow from the bottom circulation was sampled for EC measurement. For the five specimens in Group 1, the concentration of KCl due to the diffusion during membrane test was estimated based on the EC values in accordance to the correlation curve shown in Fig. 4.3. However, for the top surface, which had a closed circulation loop, the samples were only collected and measured for EC at the beginning and end of every stage, as a check on the boundary conditions. With the concentration at top and bottom boundary, the theoretical chemico-osmotic pressure can be calculated.

After the saturation process of specimen, the circulation loop system was full of water without air inside. Since both water molecules and soil particles were incompressible, the pressure can be transferred through the soil and water media inside the system. The transducer was installed at the top circulation to measure the chemico-osmotic pressure difference indirectly as shown in Fig. 4.4.

After six days of DIW circulation process, there was no concentration gradient across the specimen, thus theoretically, the pressure at both top and bottom side were same, equal to the atmospheric pressure. However, because of some unknown factors, minor pressure differences were measured between the top and the bottom circulation loop which was the baseline pressure referred before. After introducing electrolyte solutions, with the concentration difference as well as the existence of membrane behavior, the pressure of the top circulation loop changed and caused to establish new pressure equilibrium. The sum of the osmotic pressure and atmospheric pressure was equal to the pressure measured by the transducer. Hence, the chemico-osmotic pressure $\Delta P'$ firstly can be approximately calculated as follows:

$$\Delta P' = P_{transducer} - P_{atmosphere} \tag{4.1}$$

$P_{transducer}$ represented the pressure measured by the transducer at the top circulation loop; $P_{atmosphere}$ was the local atmospheric pressure. To eliminate the unknown factor which leaded to the minor pressure difference, the actual chemico-osmotic pressure, ΔP, can be written as follows:

$$\Delta P = \Delta P' - P_{baseline} \tag{4.2}$$

Where $P_{baseline}$ represented the measured baseline pressure during the first six days. To prevent variations in the conditional parameters during the tests, the membrane tests were carried out in a room with control temperature. The temperature during the membrane test was measured and reported by a Thermo Recorder (TR-72Ui, T&D, Japan), and the results were shown as following Table 4.6.

Table 4.6 Temperature range and average value during membrane test

Group	Temperature range (^{o}C)	Average value (^{o}C)
1	16.8 - 18.8	17.8
2	21.0 - 23.0	22.0
3	21.0 - 23.0	22.0
4	21.0 - 23.0	22.0
5	21.0 - 23.0	18.0

4.2.7 Calculation of chemico-osmotic efficiency coefficient

The membrane test aimed to maintain a steady-state concentration gradient across the specimen while preventing hydraulic flow inside the specimen. Consequently, a chemico-osmotic pressure developed and was directly related to the value of ω. Throughout the membrane tests, the thickness

and volume of the remained constant, and the amount of infused circulation liquid was equal to the amount of the outflow circulated. Therefore, the source solution and DIW were not allowed to enter or exit the specimens during the test. Moreover, because an electrical current was not applied across the specimen and the non-conductive acrylic cell prevented short-circuiting inside the specimen. ω was defined as (Katchalsky and Curran, 1965; Groenevelt and Elrick, 1976; Van et al., 1996; Malusis et al., 2001; Malusis and Shackelford, 2002b):

$$\omega = \frac{\Delta P}{\Delta \pi} \tag{4.3}$$

Where ΔP is the actual chemico-osmotic pressure difference across the specimen due to membrane behavior, and $\Delta \pi$ is the theoretical maximum chemico-osmotic pressure across an ideal semipermeable membrane subjected to an applied concentration difference (Olsen et al., 1990). As defined by Eq. (4.3), ω represents the ratio of the actual to the theoretical maximum chemico-osmotic pressure difference across the specimen, and indicates how close a membrane is to an ideal semipermeable membrane.

The actual ΔP was measured by a transducer, as shown in Fig. 4.4 and indicated by Eq. (4.1) and (4.2). $\Delta \pi$ for a single salt system can be approximated using the van't Hoff equation based on the solution concentration difference across a specimen as (Katchalsky and Curran, 1965; Metten, 1966; Tinoco et al., 1995):

$$\Delta \pi = vRT\Delta C \tag{4.4}$$

Where v is the number of ions in one salt molecule (e.g., $v = 2$ for a 1:1 electrolyte solution (e.g. NaCl, KCl), whereas $v = 3$ for a 2:1 electrolyte solution (e.g., $CaCl_2$)), R is the universal gas constant (8.314 J/mol·K), T represents the absolute temperature of the membrane testing system in K, and ΔC is the concentration difference across the specimen. For NaCl and KCl solutions used in this study, Eq. (4.4) can be rewritten as (Malusis and Shackelford, 2002b):

$$\Delta \pi = 2RT(C_t - C_b) \tag{4.5}$$

While for the case of $CaCl_2$, $PbCl_2$ and $ZnCl_2$, Eq. (4.4) can be rewritten as:

$$\Delta \pi = 3RT(C_t - C_b) \tag{4.6}$$

The van't Hoff expression is based on the assumption that the electrolyte solutions are ideal and

dilute. Hence, it provides only approximate values of the chemico-osmotic pressure difference. Fritz (1986) noted that the error associated with the van't Hoff expression is low (< 5%) for 1:1 electrolytes with concentrations < 1 M (Malusis et al., 2001; Malusis and Shackelford, 2002b).

In this study, the source solution was circulated at the top surface to provide an upper boundary concentration of $C_{t0} > 0$, while the bottom surface was flushed with DIW to provide a bottom boundary concentration of $C_{b0} = 0$. Thus, the chemico-osmotic efficiency coefficient, ω_0, can be expressed as follows (Malusis and Shackelford, 2002b):

$$\omega_0 = \left.\frac{\Delta P}{\Delta \pi}\right|_0 = \frac{\Delta P}{\Delta \pi_0} = \frac{\Delta P}{vRT\Delta C_0} = \frac{\Delta P}{vRT(C_{t0} - C_{b0})} = \frac{\Delta P}{vRTC_{t0}} \tag{4.7}$$

$\Delta\pi_0$ exists under a perfect flushing boundary condition when the circulation rate is sufficiently large so that the boundary solute concentrations caused by diffusion are negligible. However, in practice, the circulation rate is insufficient, and changes in the boundary concentrations due to diffusion may result in a time-dependent reduction of $\Delta\pi$ (Malusis et al., 2001). In terms of the average solute concentration, the average chemico-osmotic efficiency coefficient, ω_{ave}, is given as follows (Kang and Shackelford, 2009):

$$\omega_{ave} = \left.\frac{\Delta P}{\Delta \pi}\right|_{ave} = \frac{\Delta P}{\Delta \pi_{ave}} = \frac{\Delta P}{vRT\Delta C_{ave}} = \frac{\Delta P}{vRT(C_{t,ave} - C_{b,ave})} \tag{4.8}$$

Where $C_{t,\,ave}$ and $C_{b,ave}$ are the average solute concentrations across the top and bottom of the specimen boundaries, respectively, and are defined as follows (Malusis et al., 2001; Kang and Shackelford, 2011):

$$C_{t,ave} = \frac{C_{t0} + C_t}{2}; \quad C_{b,ave} = \frac{C_{b0} + C_b}{2} = \frac{C_b}{2} \tag{4.9}$$

Because $C_{t,\,ave} < C_{t0}$ and $C_{b,ave} > C_{b0}$, the initial chemico-osmotic pressure difference, $\Delta\pi_0$, is slightly greater than the average chemico-osmotic pressure difference, $\Delta\pi_{ave}$. Consequently for the same measured osmotic pressure ΔP, ω_0 will be less than ω_{ave} in accordance with Eq. (4.7) and (4.8) (Malusis et al., 2001; Kang and Shackelford, 2011).

4.3 Results

4.3.1 Specimen flushing

Figure 4.6 presents the EC of the outflow during the flushing stage for all five group specimens. The general trends were same that EC of the outflow for all specimens decreased as the flushing

stage due to continual permeation with DIW and the eventual reduction in the dissolved salt content. However, there was still a little difference among the specimens. It is obvious to find that for specimens in Group 1, as the bentonite content increased, the initial effluent EC increased. In addition, it can be found that for the same material (FC + 5% bentonite in Group 1, Group 4 and Group 5) flushed in different group, the initial EC values were significantly different. Such difference can be attributed to the solute loss during the saturation process, for specimens in Group 1, the saturation process lasted for 3 days to make sure completely saturate, while in Group 4, and 5, the saturation process lasted for only 1 day. Thus, it is rational to explain the much lower initial EC in Group 1 compared to the same material used in Group 4 and Group 5. Most of the specimens were flushed by about 60 days except specimens in Group 3, in which the flushing stage lasted for about 160 days.

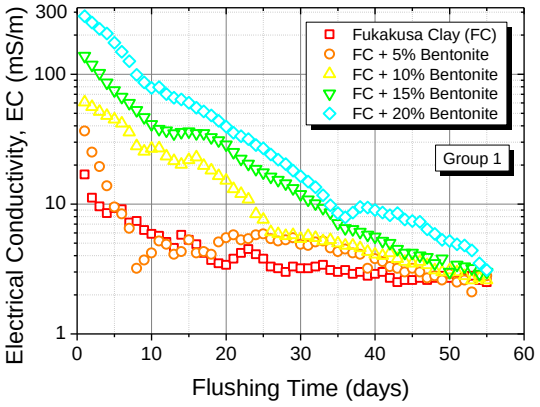

(a)

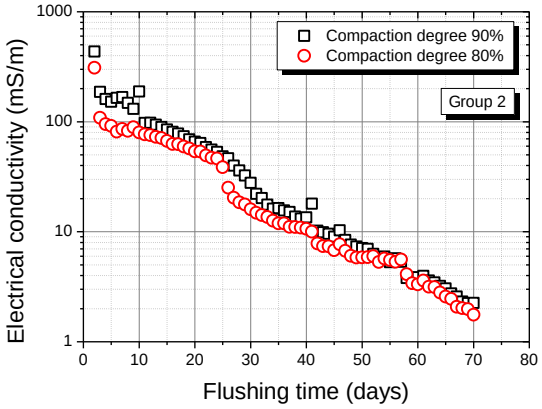

(b)

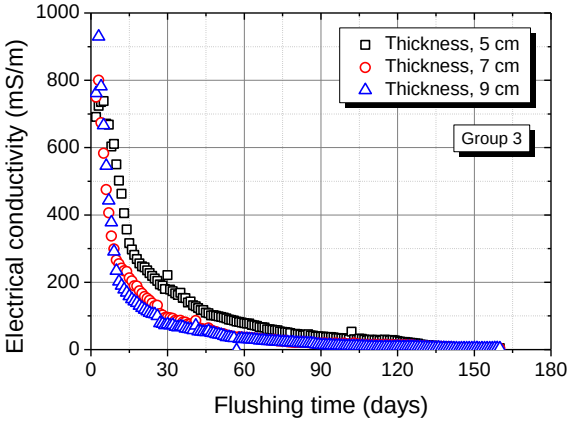

(c)

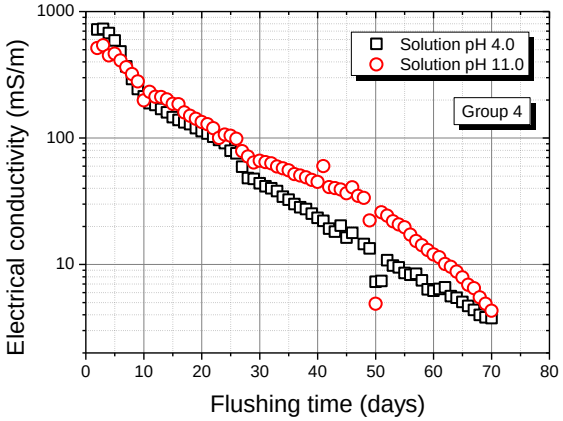

(d)

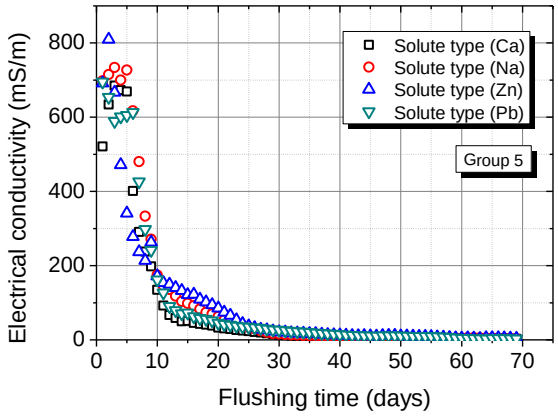

(e)

Fig. 4.6 EC values for the specimens during the flushing stage: (a) Group 1, (b) Group 2, (c) Group 3, (d) Group 4, (e) Group 5.

Figure 4.7(a)-(e) presents the hydraulic conductivities of all the specimens measured during the flushing stage. For a certain specimen, it is apparent that in most specimens, the hydraulic conductivity slightly decreased with time, and such phenomenon were especially apparent in Group 1, Group 3 and Group 5 as shown in following Fig. 4.7(a), Fig. 4.7(c) and Fig. 4.7(e). This time dependent decrease might to be attributed to the concentration of leaching flow. With the flushing stage going, the leached out soluble salts became less, which resulted in the increase of the thickness of DDL and the decrease of concentration of the outflow in response. And according to the results observed by Shackelford et al., (2000), lower concentration result in lower hydraulic conductivity.

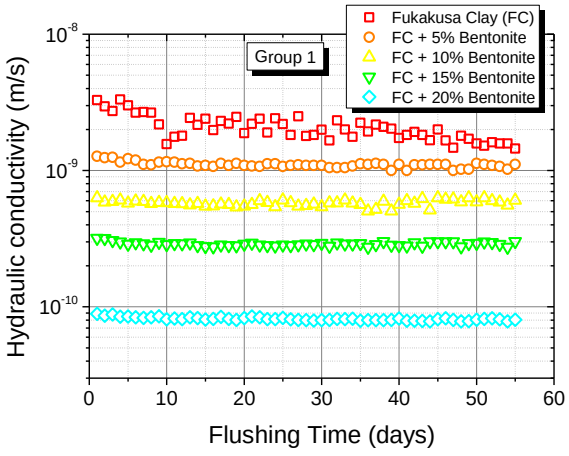

(a)

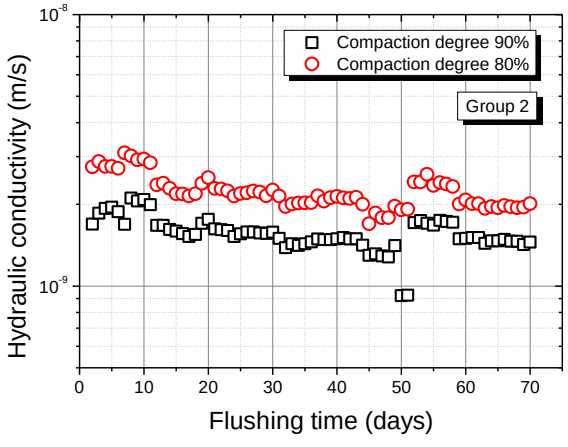

(b)

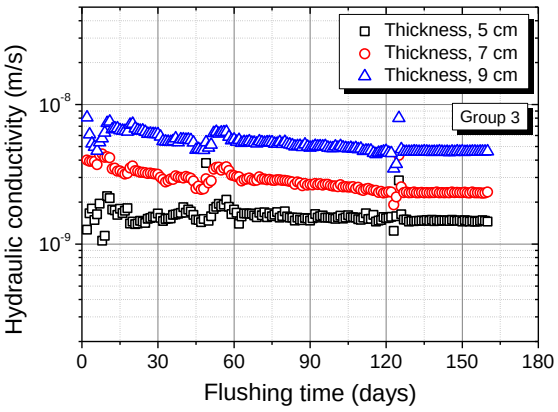

(c)

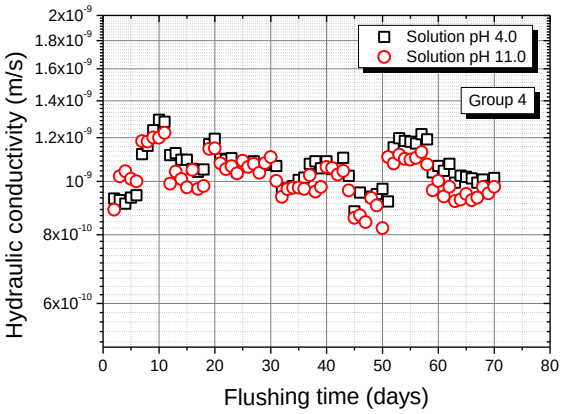

(d)

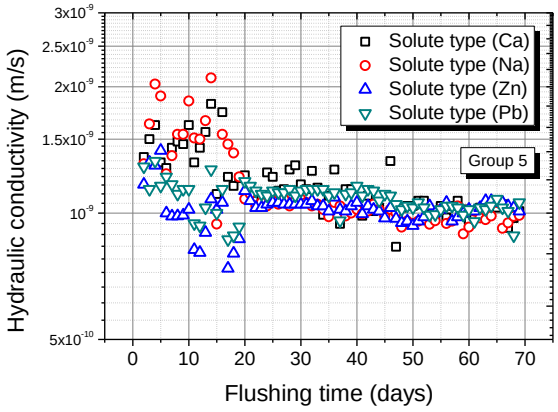

(e)

Fig. 4.7 Hydraulic conductivities for the specimens during the flushing stage: (a) Group 1, (b) Group 2, (c) Group 3, (d) Group 4, (e) Group 5.

From Fig. 4.7 (a), it can be seen the hydraulic conductivity of FC at the end of flushing stage is 1.58×10^{-9} m/s, several times higher than that of Nelson Farm Clay (1.5×10^{-10} m/s) reported by Kang and Shackelford (2010), and this difference can be attributed to the micro-structure and composition of the soils. The hydraulic conductivity for FC is greater than the common upper limit for landfill liners of 1.0×10^{-9} m/s, which indicate that it is not suitable to use as landfill liner directly (Katsumi et al., 2008a; Kamon and Katsumi, 2001). However, as the bentonite content increased, the hydraulic conductivity decreased as shown in Fig. 4.8, which plots hydraulic conductivities at the end of flushing stage (y-axis) versus bentonite content (x-axis). As bentonite content increased to 5, 10, 15 and 20%, the hydraulic conductivity decreased to 1.07×10^{-9} m/s for FC plus 5% bentonite, 6.04×10^{-10} m/s for FC plus 10% bentonite, 2.74×10^{-10} m/s for FC plus 15% bentonite, and 8.23×10^{-11} m/s for FC plus 20% bentonite. The introduction of bentonite also made natural Fukakusa clay suitable for use as a liner. Based on the results by Shackelford et al. (2000), as

bentonite content increase, the swelling nature will cause to decrease or block the effective void for permeation, which can lead to the decrease of hydraulic conductivity (Shackelford et al., 2000).

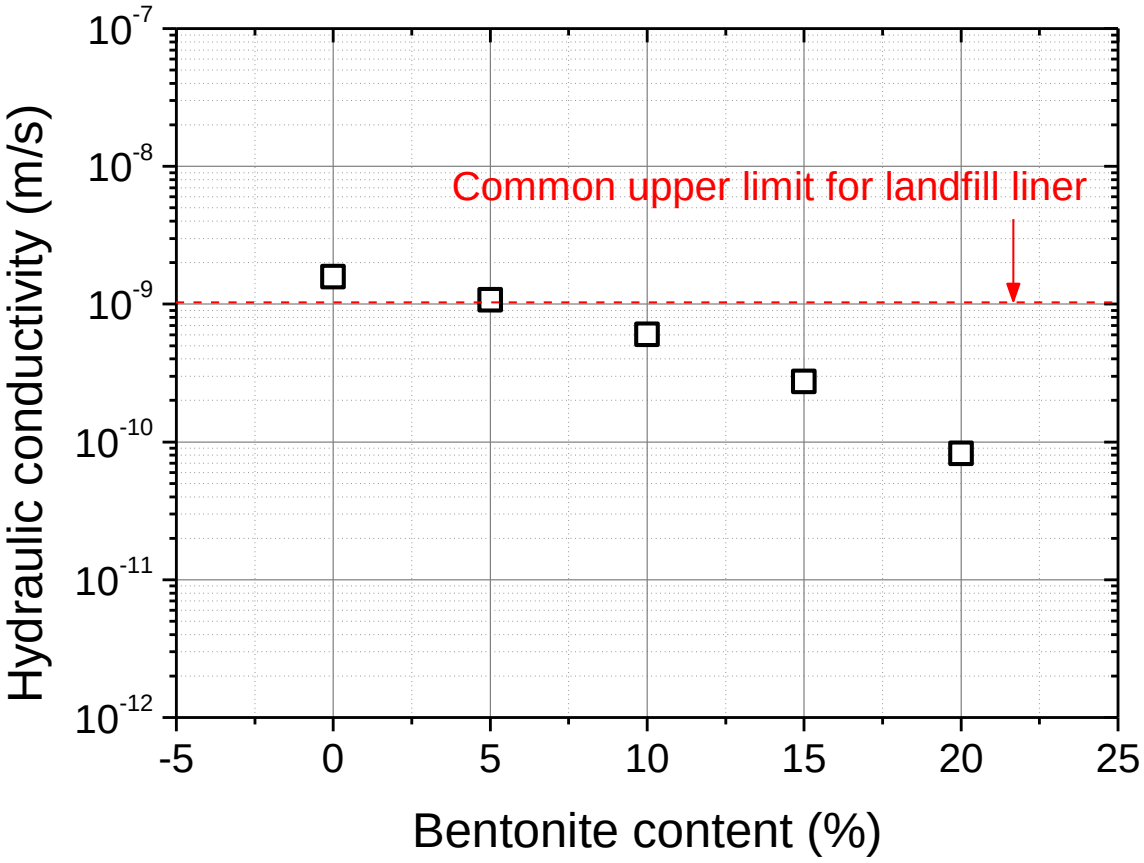

Fig. 4.8 Hydraulic conductivity change as function of bentonite content

Figure 4.9 shows the pH of the outflows during the flushing stages for specimens in Group 2, Group 3, Group 4 and Group 5. Based on the results of the flushing, it was evident that a time period of two months more would be required to bring the pH of the outflow pH much closer to 7.0 for specimens in all groups. To reduce the total duration of the membrane tests, the flushing stage was discontinued after the pH of the outflow from the two specimens increased to about 6.0-6.5.

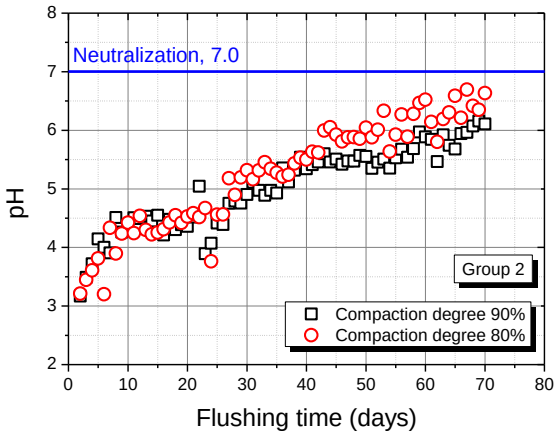

(a)

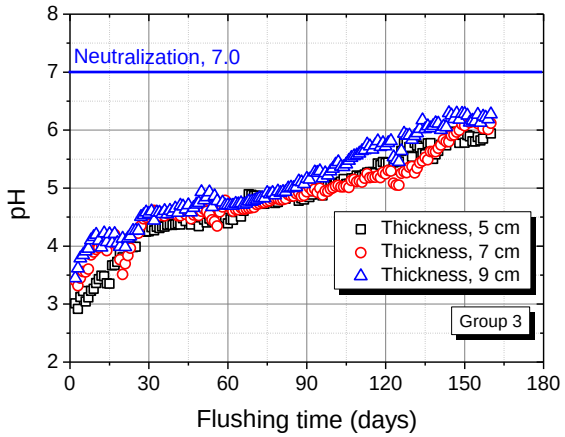

(b)

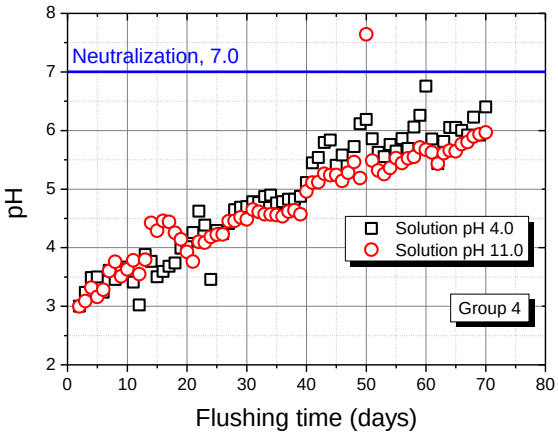

(c)

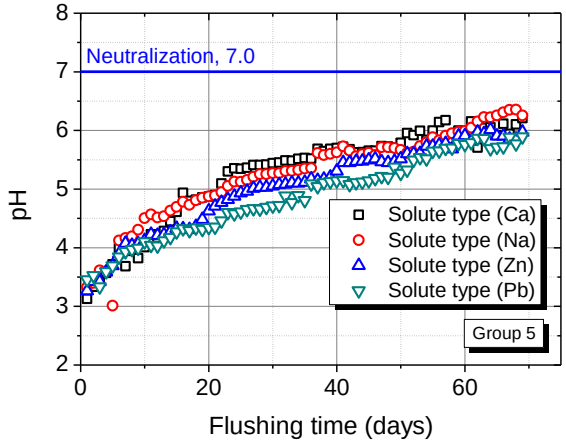

(d)

Fig. 4.9 pH for the specimens during the flushing stage: (a) Group 2, (b) Group 3, (c) Group 4, (d) Group 5.

Based on above Fig. 4.6, Fig. 4.7 and Fig. 4.9, the electrical conductivity (EC), hydraulic conductivity (k) and pH of the outflow before and after the flushing stage was summarized in following Table 4.7.

Table 4.7 Electrical conductivity (EC), hydraulic conductivities (k) and pH before and after the flushing

Group	No.	Specimens' conditions			Flushing stage start			Flushing stage terminate		
		Bentonite content	Thickness (cm)	Compactness	EC (mS/m)	pH	k (m/s)	EC (mS/m)	pH	k (m/s)
1	1	0%	3	Standard	16.9		3.28×10^{-9}	2.5		1.58×10^{-9}
	2	5%	3	Standard	36.5		1.27×10^{-9}	2.8		1.07×10^{-9}
	3	10%	3	Standard	61		6.3×10^{-10}	2.6		6.04×10^{-10}
	4	15%	3	Standard	138		3.19×10^{-10}	3		2.74×10^{-10}
	5	20%	3	Standard	280		8.9×10^{-11}	3.1		8.23×10^{-11}
2	6	5%	3	90%	435	3.2	1.69×10^{-9}	2.25	6.1	1.49×10^{-9}
	7	5%	3	80%	310	3.2	2.75×10^{-9}	1.76	6.6	2.01×10^{-9}
3	8	5%	5	Standard	738	2.9	1.27×10^{-9}	4.1	6	1.45×10^{-9}
	9	5%	7	Standard	800	3.3	3.99×10^{-9}	3.8	6.2	2.33×10^{-9}
	10	5%	9	Standard	930	3.4	8.08×10^{-9}	3.6	6.3	4.60×10^{-9}
4	11	5%	3	Standard	720	3	9.30×10^{-10}	3.76	6.4	1.01×10^{-9}
	12	5%	3	Standard	514	3	8.88×10^{-10}	4.3	6	0.98×10^{-9}
5	13	5%	3	Standard	685	3.1	1.36×10^{-9}	2.5	6.2	1.01×10^{-9}
	14	5%	3	Standard	734	3.3	1.37×10^{-9}	2.9	6.4	0.95×10^{-9}
	15	5%	3	Standard	810	3.1	1.17×10^{-9}	3.5	6	0.98×10^{-9}
	16	5%	3	Standard	695	3.5	1.29×10^{-9}	2.8	5.9	0.99×10^{-9}

4.3.2 Boundary concentration during the membrane tests

4.3.2.1 Effect of bentonite content

Figure 4.10 presents the boundary KCl solute concentrations calculated according to the calibration (Fig. 4.3). The tests consisted of five stages where the KCl concentrations for the source solutions circulated through the top increased from 0.5 mM to 50 mM. The KCl concentration of outflow at the top (C_t) decreased slightly compare to source solution at the beginning of every stage (C_{t0}) ($C_t < C_{t0}$) in most cases, while that of the bottom circulating effluent eventually increased over time ($C_b > C_{b0}$) (Malusis and Shackelford, 2002b; Kang and Shackelford, 2010). These observations were consistent with the solute loss from the source solutions due to KCl diffusion or adsorption by soil minerals inside the specimens (Tang et al., 2009; Tang et al., 2010; Li et al., 2010; Tang et al., 2012).

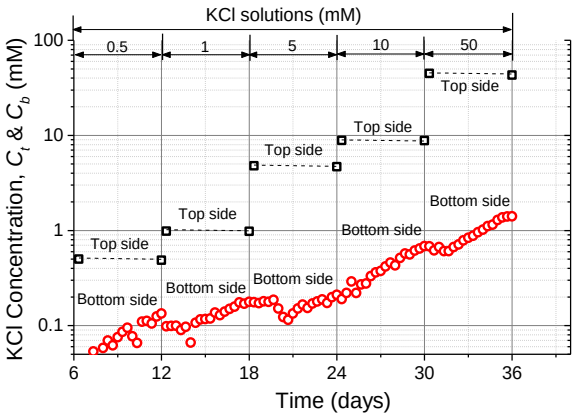

(a)

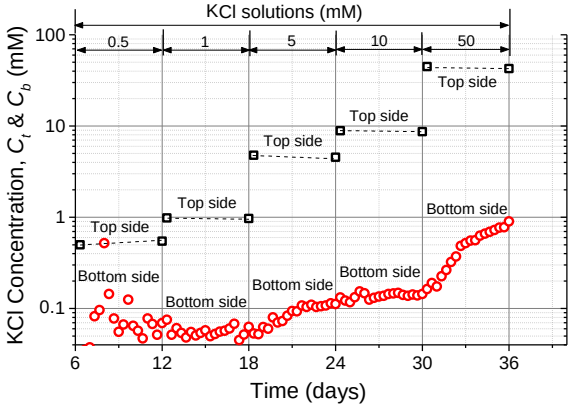

(b)

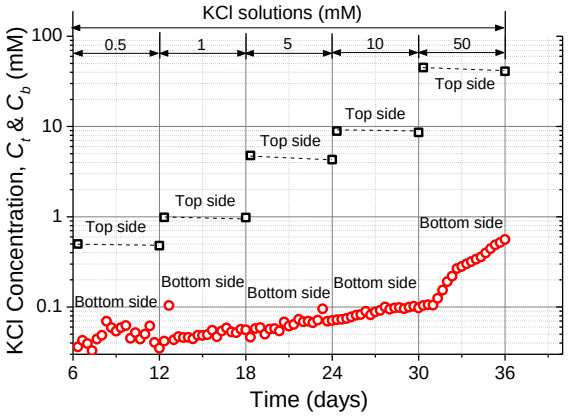

(c)

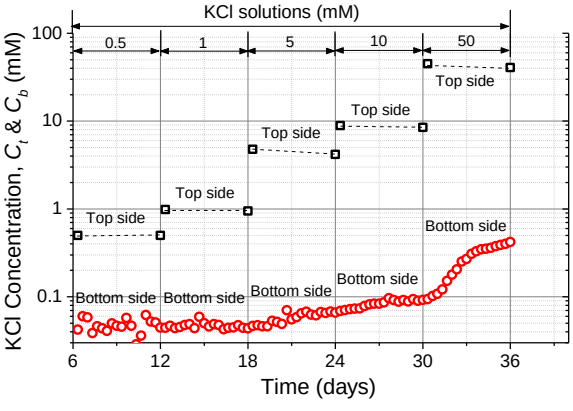

(d)

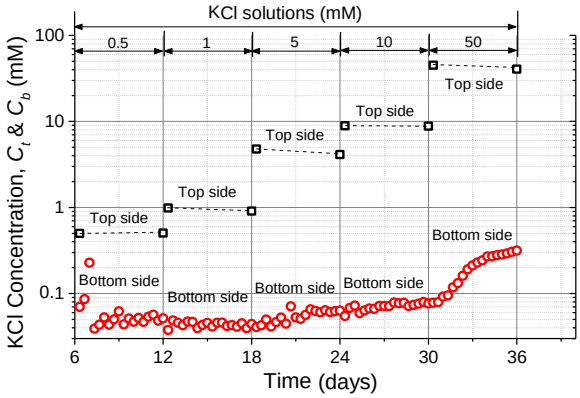

(e)

Fig. 4.10 KCl concentration at boundaries during the membrane tests (a) FC; (b) FC plus 5% bentonite; (c) FC plus 10% bentonite; (d) FC plus 15% bentonite; (e) FC plus 20% bentonite

4.3.2.2 Effect of compactness

Figure 4.11 shows the boundary KCl concentrations for the specimens under different compaction degree. The KCl concentration of the source solution at the top decreased slightly compare to the beginning of every stage ($C_t < C_{t0}$), while that of the bottom circulating effluent eventually increased over time ($C_b > C_{b0}$). The continuous diffusion from the top side across the specimens leaded to the increase of concentration at bottom side. For top side, the solute loss can also be attributed to adsorption or ion-exchange reaction between free ions and soil minerals (Tang et al., 2010; Tang et al., 2012). Although the concentration at the bottom side was still increasing within 6 days, it can be neglected compared to that at top side by magnitude order, and already possible for calculating a stable concentration difference.

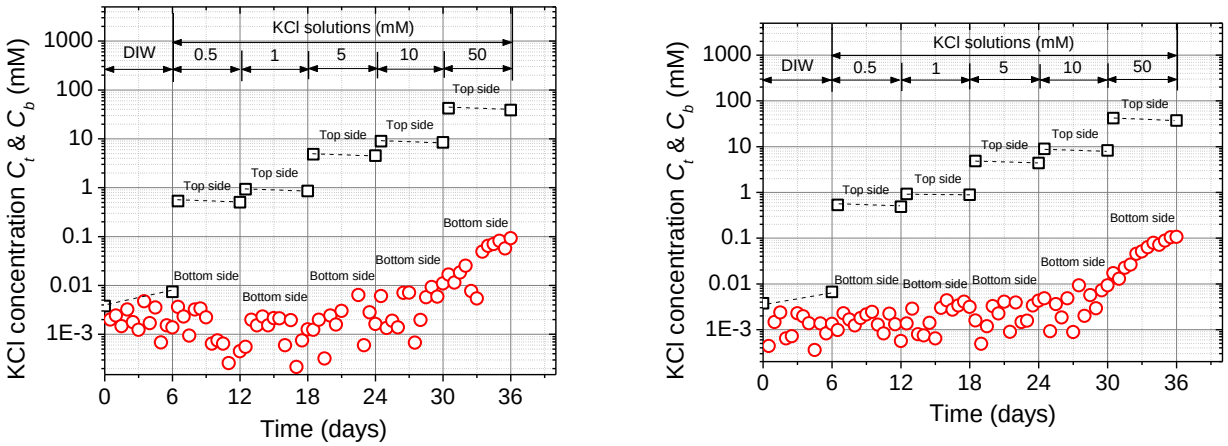

(a) (b)

Fig. 4.11 Boundary KCl concentrations during membrane test: (a) 90%, (b) 80%

The boundary pH values during membrane test are shown in Fig. 4.12(a)(b). pH values of source solution at top side decreased after every stage, which display the acidification trend since the acidic nature of Fukakusa clay. While for pH at the bottom side, although the specimens have been flushed before membrane test, some acidic materials distributed deeply in pores began to leach out with diffusion process, especially when concentration difference was higher than 10 mM.

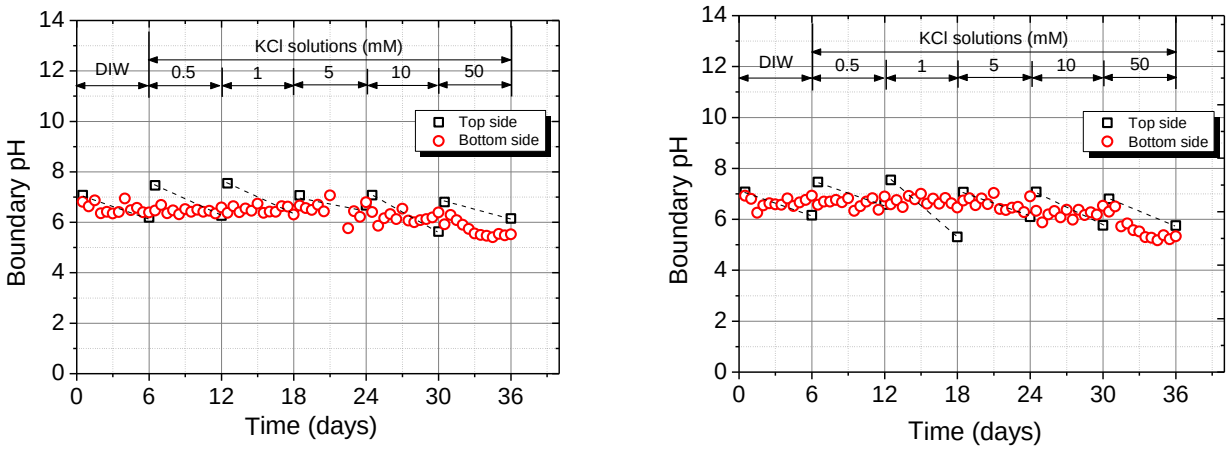

(a) (b)

Fig. 4.12 Boundary pH values during membrane test: (a) 90%, (b) 80%

4.3.2.3 Effect of specimen‘s thickness

Figure 4.13 shows the boundary KCl concentrations for the specimens with different thickness. The KCl concentration of the source solution at the top decreased slightly compare to the beginning of every stage ($C_t < C_{t0}$), while that of the bottom circulating effluent eventually increased over time ($C_b > C_{b0}$). The continuous diffusion from the top side across the specimens leaded to the increase of concentration at bottom side. Compared to the specimens in other groups, less diffusion phenomenon can be observable except the specimen with thickness of 5 cm at highest concentration in Fig. 4.13 (a), and such phenomenon can be attributed to the length of permeable paths.

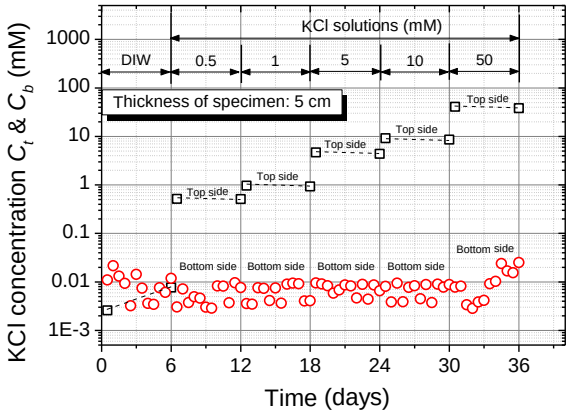

(a)

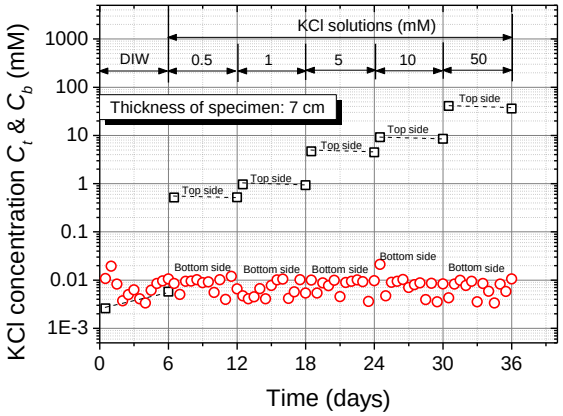

(b)

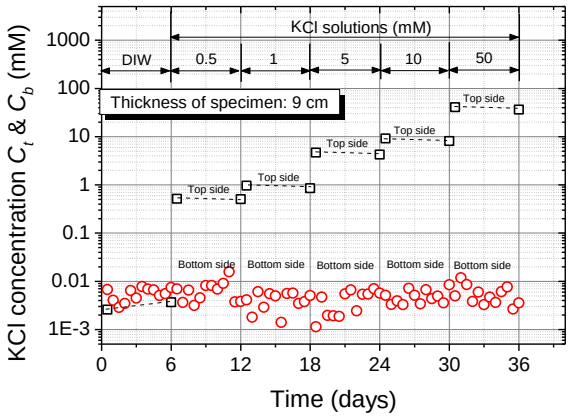

(c)

Fig. 4.13 Boundary KCl concentrations during membrane test: (a) 5 cm, (b) 7 cm, (c) 9 cm

The boundary pH values during membrane test are shown in Fig. 4.14(a)-(c). pH values of source solution at top side decreased after every stage, which display the acidification trend since the acidic nature of Fukakusa clay. While for pH at the bottom side, although the specimens have been flushed before membrane test, some acidic materials distributed deeply in pores began to leach out with diffusion process, especially when concentration difference was higher than 10 mM, such pH decrease was especially for specimen with thickness of 5 cm.

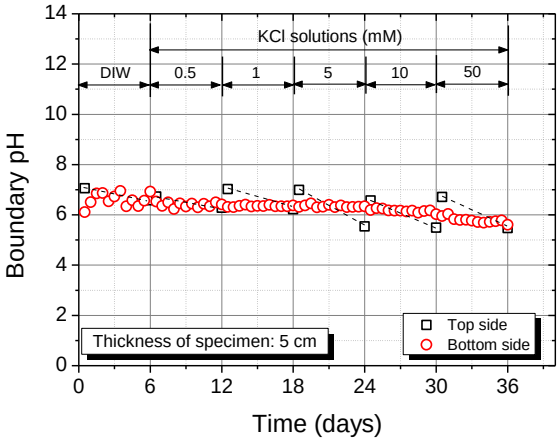

(a)

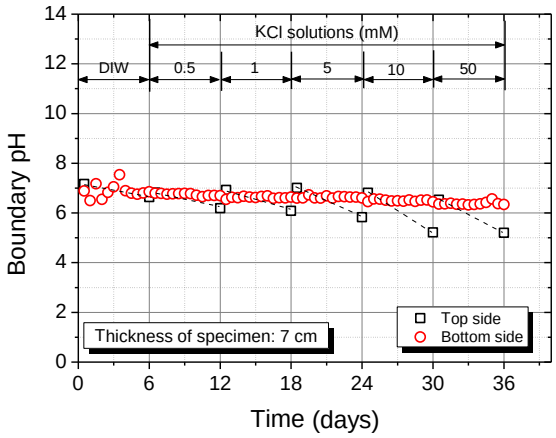

(b)

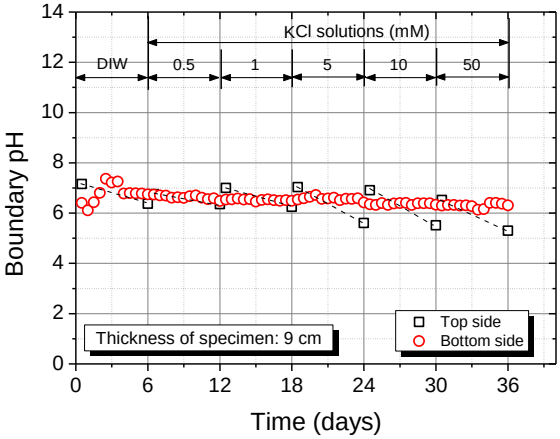

(c)

Fig. 4.14 Boundary pH values during membrane test: (a) 5 cm, (b) 7 cm, (c) 9 cm

4.3.2.4 Effect of solute pH

Figure 4.15 shows the boundary concentrations of KCl under different solution pH. The tests consisted of five stages in which the KCl concentrations for the top circulation were increased from 1 mM to 50 mM. The KCl concentration of the source solution at the top decreased slightly compared to its concentration at the beginning of each stage ($C_t < C_{t0}$), while the concentration of the bottom circulating effluent eventually increased over time ($C_b > C_{b0}$). The decrease in concentration at the top can be attributed to both diffusion and adsorption, considering that, at the pH range of on 5.0 - 7.0, it was possible for ion exchange and complex adsorption to occur (Tang et al., 2009; Li et al., 2010). The continuous diffusion led to the increase of the concentration at the bottom. Although the concentration at the bottom was still increasing after six days, the increases can be neglected compared to the concentrations at the top, which were three orders of magnitude greater, so it was

already possible to obtain a stable concentration difference.

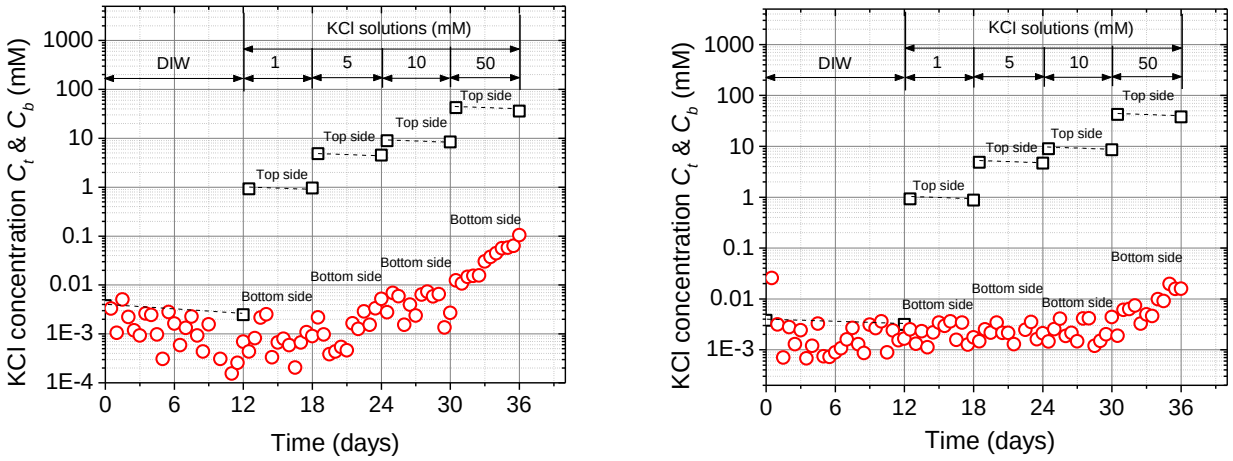

(a) (b)

Fig. 4.15 Boundary concentrations of KCl during the membrane tests: (a) Solution with a pH of 4.0, (b) Solution with a pH of 11.0.

The pH values of the solutions at the boundary during the membrane tests are shown in Fig. 4.16 (a) and (b). At the acidic condition (pH = 4.0), the pH of the outflow showed a trend of acidification when the concentration was increased to 5 mM, as shown in Fig. 4.16(a). In contrast, at the alkaline condition (pH = 11.0), the pH of the outflow maintained stable even after the concentration reached 50 mM, as shown in Fig. 4.16(b). Both of the source solutions at the top resisted any change in their pH values.

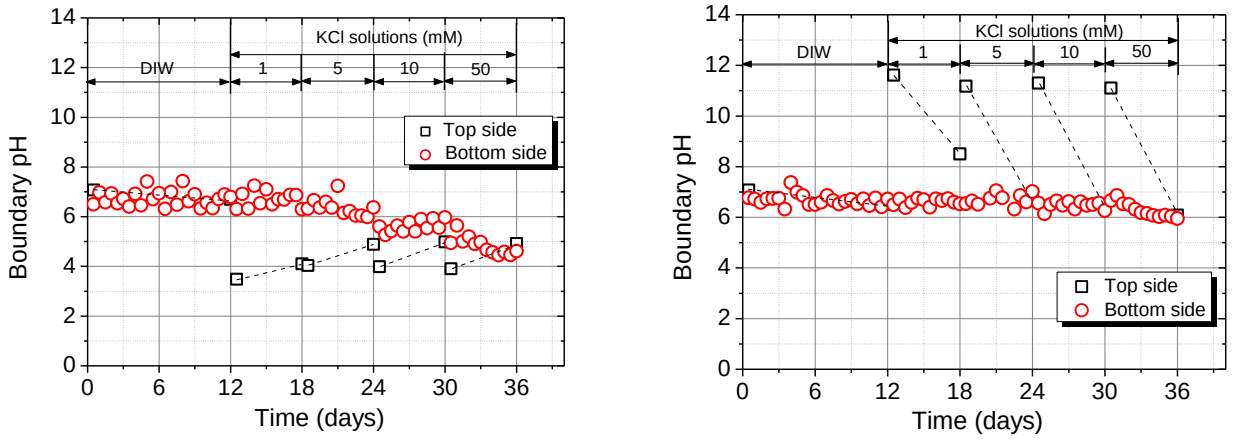

(a) (b)

Fig. 4.16 pH values at the boundary during the membrane tests: (a) Solution with a pH of 4.0, (b) Solution with a pH of 11.0

4.3.2.5 Effect of solute type

Figure 4.17 shows the top and bottom boundary concentrations for different kinds of solute during the membrane test. The tests consisted of five stages where four kinds of solution ($CaCl_2$, NaCl, $ZnCl_2$ and $Pb(NO_3)_2$) were utilized in each specimens, while concentrations for the top circulation increased from 0.5 mM to 50 mM. It was apparent that Ca and Na concentration inside the top circulation slightly decreased at the end of almost every stage ($C_t < C_{t0}$). Compared with Ca and Na, it was apparent that Zn(II) and Pb(II) concentration inside the top circulation decreased greatly ($C_t < C_{t0}$), especially at the first two stage in which the concentration of solute almost decreased to 0. The decrease of concentration at top side can be attributed to diffusion and adsorption (Tang et al., 2009; Tang et al., 2012). At the first two stages, almost all Zn(II) and Pb(II) were absorbed by the soil at the top surface of the specimens, and the soil at the top surface reached the adsorption capacity as continually increased the solute concentration. The concentration of Zn(II) and Pb(II) still decreased at relative high concentration can be attributed to that more heavy metal ions diffused to the deeper places. For the case of concentration at the bottom boundary, Ca concentration increased from concentration difference increased to 1 mM, compared to that, Na ion concentration until concentration difference increased to 50 mM. However, for Zn(II) and Pb(II), at the bottom side, the concentration kept stable ($C_t \approx C_{t0}$). Such phenomenon appeared because the Zn(II) and Pb(II) were absorbed by surrounding soil minerals when transport across the specimens.

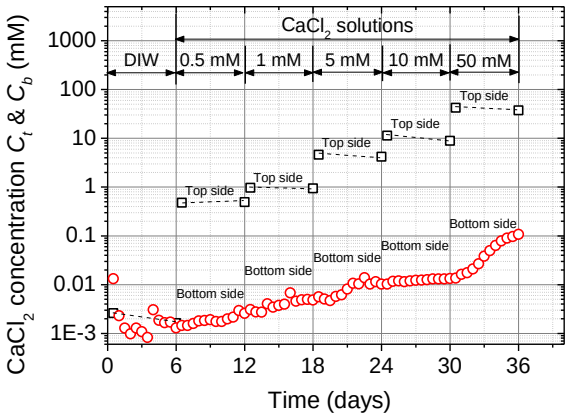

(a)

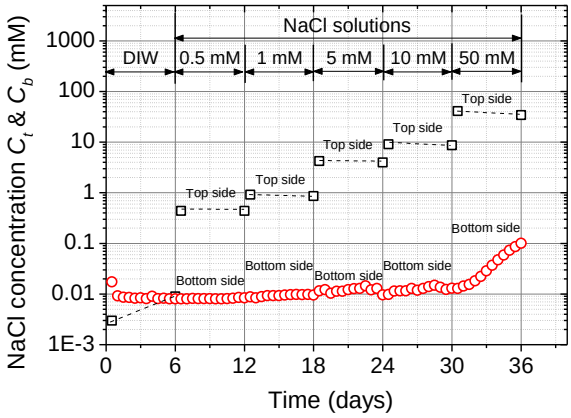

(b)

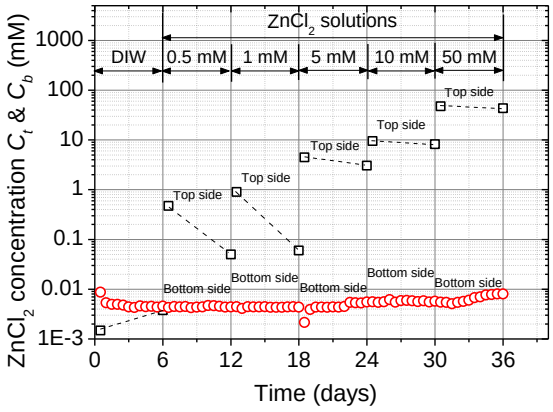

(c)

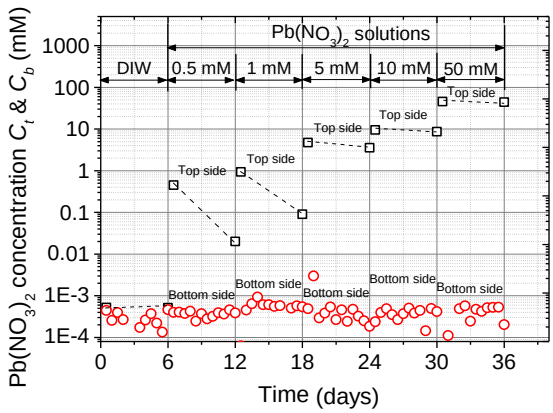

(d)

Fig. 4.17 Boundary concentrations during membrane test: (a) $CaCl_2$, (b) NaCl, (c) $ZnCl_2$, (d) $Pb(NO_3)_2$

Figure 4.18 presents the boundary pH values under different solution during membrane test. The pH values at top side decreased after almost every stage, and some acidic salts origin from the ion-exchange adsorption or leached out from specimen since the diffusion process resulted in the decrease of pH values. For the case of pH at bottom side, the decrease trends can be observed at the beginning from concentration difference higher than 5 mM. The phenomenon was attributed to the leaching out of acidic substance origin from diffusion and ion-exchange adsorption.

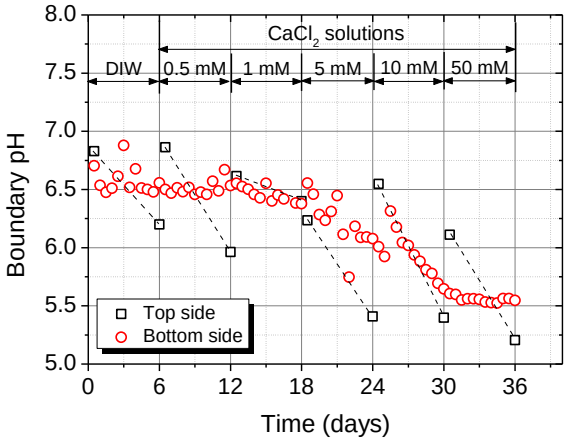

(a)

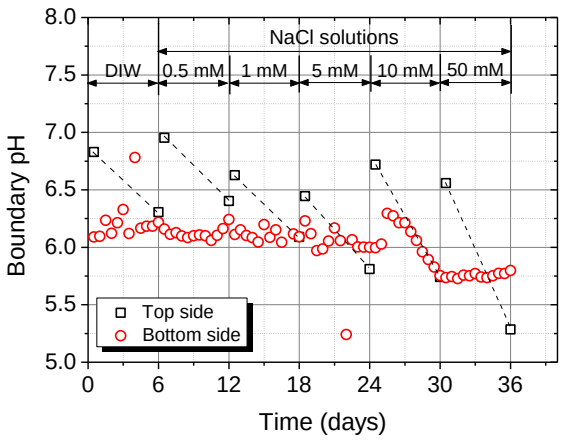

(b)

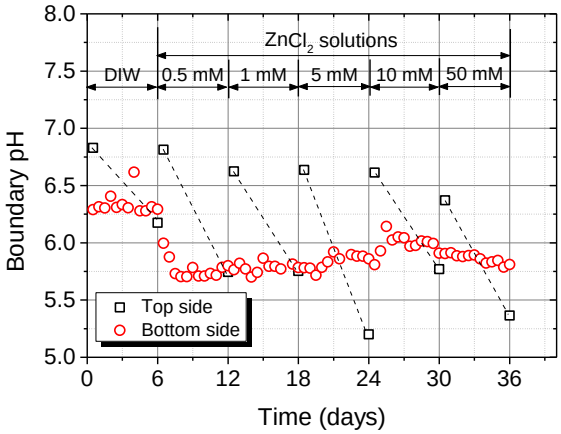

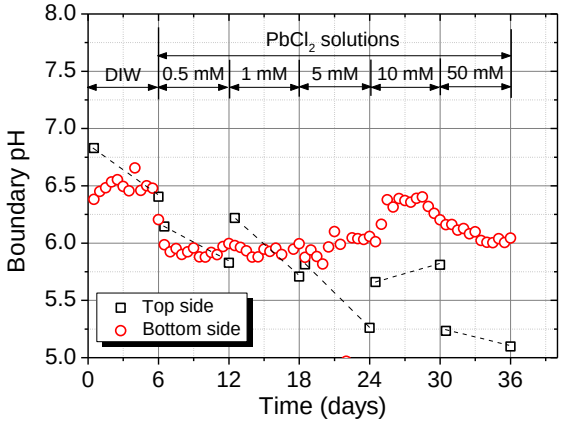

(c) (d)

Fig. 4.18 Boundary pH values during membrane test: (a) $CaCl_2$, (b) NaCl, (c) $ZnCl_2$, (d) $Pb(NO_3)_2$

4.3.3 Chemico-osmotic pressure

4.3.3.1 Effect of bentonite content

The actual values of ΔP calculated according to Eq. (4.1) and (4.2) are shown in Fig. 4.19. DIW was circulated at both top and bottom sides of the specimens ($C_t = C_b = 0$) during the first six days, and the baseline chemico-osmotic pressures ranged from 0.76 kPa to 1.70 kPa. This baseline pressure might be due to the pressure loss inside the porous stone or remaining soluble salts of the specimens were leached out inside the top circulation loop ($C_t > 0$), while the bottom boundaries were flushed ($C_b = 0$), therefore resulted to a slight concentration difference across the specimens. However, both negative effects can be eliminated duration the calculation as shown in Eq (4.2). The similar phenomenon was also observed by Malusis and Shackelford (2002b), but it was attributed to slight differences in the hydraulic resistance of the porous stones at the opposite ends of the specimens. Shackelford (2013) attributed that to (1) the existence of remnant or residual salts or other chemical species stored within the porous stone, (2) slightly different circulation rates between the top and bottom, (3) slightly different hydraulic properties of the porous disks.

From the figures, it is apparent that the introduction of KCl solution resulted in an immediate and rapid increase in the chemico-osmotic pressure. However, the incremental change decreased as the concentration difference increased. Except for FC where the concentration difference increased from 0.5 mM to 1 mM, ΔP of all the specimens decreased slightly. The time required for the chemico-osmotic pressure to equilibrate increased with increasing KCl concentration: less than one day for 0.5 mM solution, about two or three days for the 1 mM solution, and about four or five days for the 50 mM solution. Although some measures was taken to eliminate the negative effect of elevation head difference mentioned in Section 4.2.3, about 1 cm elevation head difference still existed between the vent of bottom circulation outflow and the top, center of the specimen as a result

from the thickness of porous stone and top cap. This negative effect will attenuate as concentration increased, and compared to the chemico-osmotic pressure, the 1 cm elevation head difference here can be neglected.

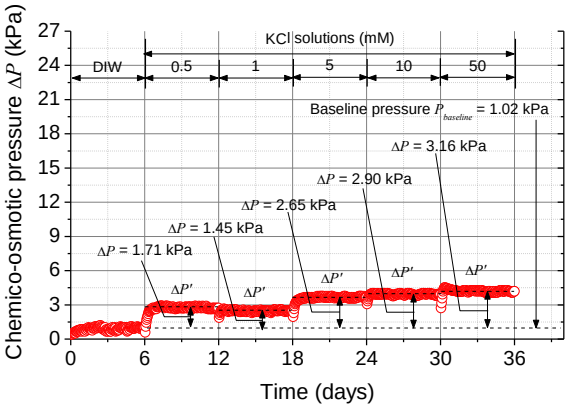

(a)

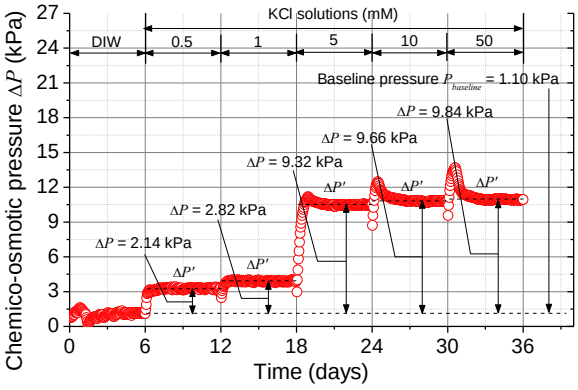

(b)

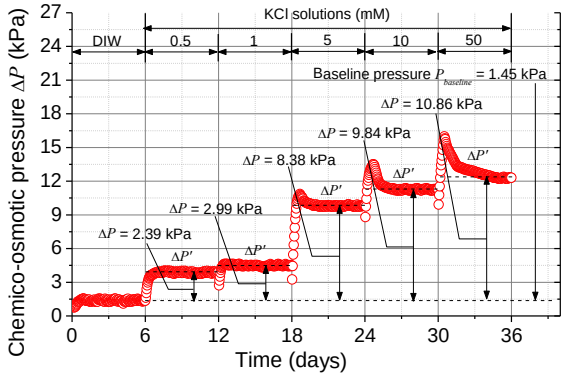

(c)

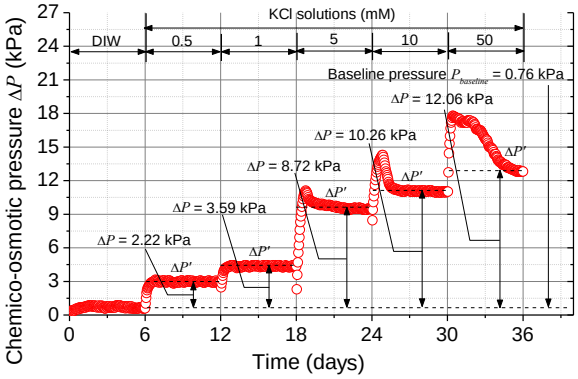

(d)

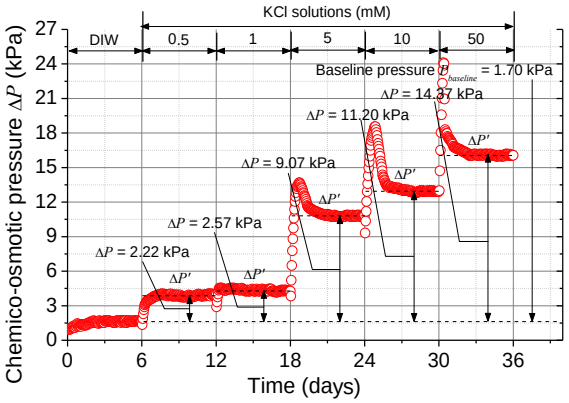

(e)

Fig. 4.19 Measured chemico-osmotic pressure across the specimens (a) FC; (b) FC plus 5% bentonite; (c) FC plus 10% bentonite; (d) FC plus 15% bentonite; (e) FC plus 20% bentonite

4.3.3.2 Effect of compactness

Figure 4.20 shows the actual values of ΔP of the two specimens (compactness 90% and 80%). DIW was circulated at both top and bottom sides of the specimens during the first six days to obtain the baseline pressure 1.10 kPa and 1.36 kPa. From the figures, it is apparent that the introduction of KCl solution resulted in an immediate increase in the chemico-osmotic pressure. However, the incremental change decreased as the concentration difference increased, e.g. when the concentration difference had a five times‘ increase from 1 mM to 5 mM, ΔP increased from 2.57 kPa to 8.21 kPa for case of compactness 90% with increasing percent 220% and from 2.48 kPa to 6.59 kPa for that of compactness 80% with increasing percent 170%; Compare to that, when concentration difference had a five times‘ increase from 10 mM to 50 mM, the increase of ΔP were very limit.

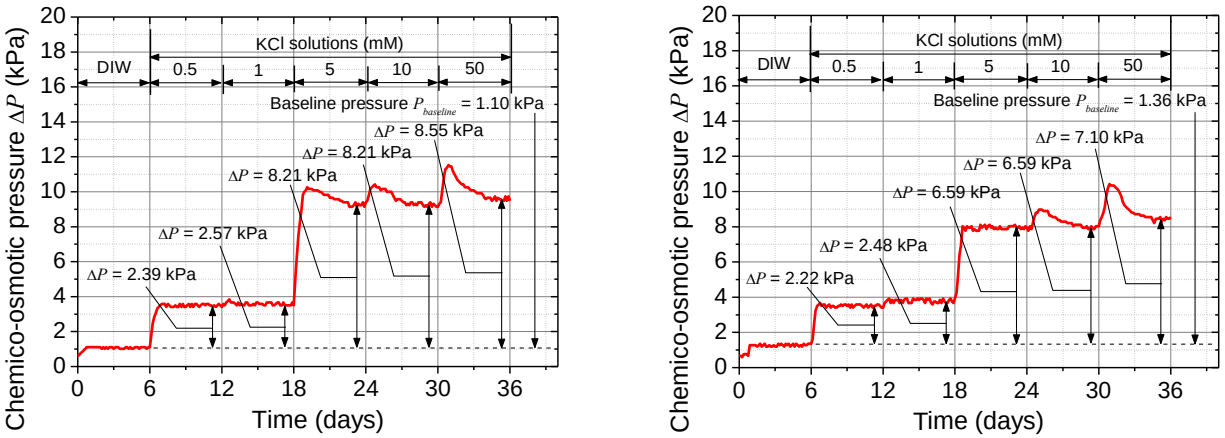

(a) (b)

Fig. 4.20 Measured chemico-osmotic pressure across the specimens: (a) 90%, (b) 80%

4.3.3.3 Effect of specimen‘s thickness

Figure 4.21 shows the actual values of ΔP of the three specimens with thickness of 5 cm, 7 cm and 9 cm. DIW was circulated at both top and bottom sides of the specimens during the first six days to obtain the baseline pressure 0.85, 1.27 kPa and 1.23 kPa. From the figures, it is apparent that the introduction of KCl solution resulted in an immediate increase in the chemico-osmotic pressure. Such increase was especially obvious when concentration increased from 1 mM to 5 mM, and as the concentration increased continually, the concentraton increase became less and even decrease such as under concentration of 50 mM in Fig. 4.21 (b) and (c).

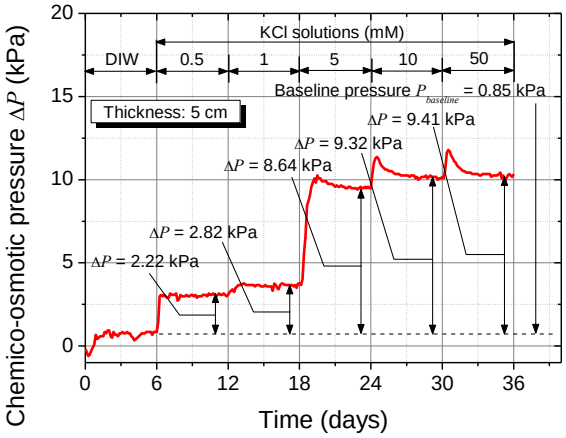

(a)

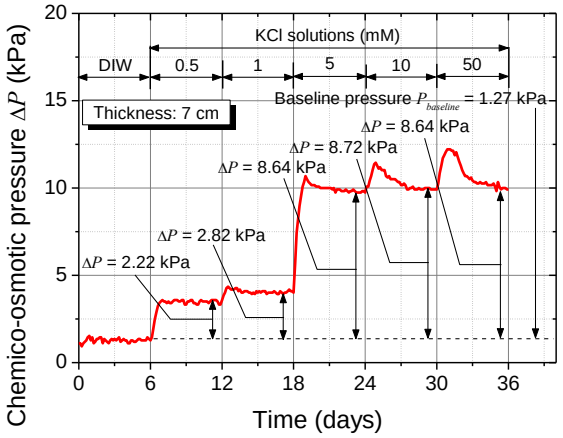

(b)

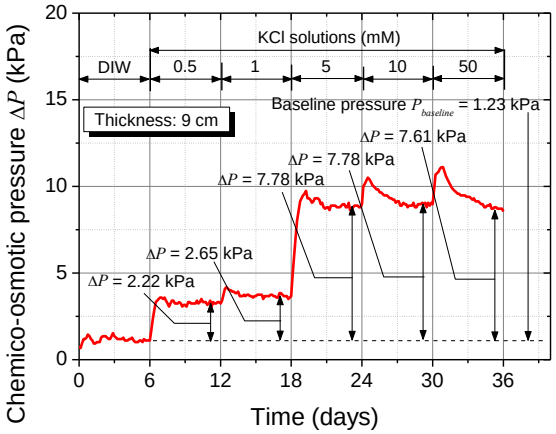

(c)

Fig. 4.21 Measured chemico-osmotic pressure across the specimens: (a) 5 cm, (b) 7 cm, (c) 9 cm

4.3.3.4 Effect of solute pH

Figure 4.22 shows the actual values of ΔP for the two specimens under solution with different pH. DIW was circulated at both the top and bottom of the specimens ($C_t = C_b = 0$) during the first 12 days to obtain the baseline pressures of 0.85 kPa and 1.45 kPa. From the figures, it is apparent that the introduction of KCl solution resulted in an immediate and rapid increase in the chemico-osmotic pressure. However, the incremental change decreased as the concentration difference increased. When the concentration difference increased from 1 mM to 5 mM, ΔP increased from 2.91 kPa to 8.30 kPa for the case of pH around 4.0 with increasing percent 185%, but ΔP increased from 3.25 kPa to 11.63 kPa for the case of pH around 11.0 with increasing percent 260%. In comparison, ΔP increased 7.2% and 98% in cases of pH 4.0 and pH 11.0, respectively as the concentration of KCl increased from 5 to 50 mM. The time required for the behavior of the membrane to equilibrate

depended on the concentration of KCl, and this time was about two to three days for 1 and 5 mM solution, and it was about three to four days for the 10 mM and 50 mM solutions.

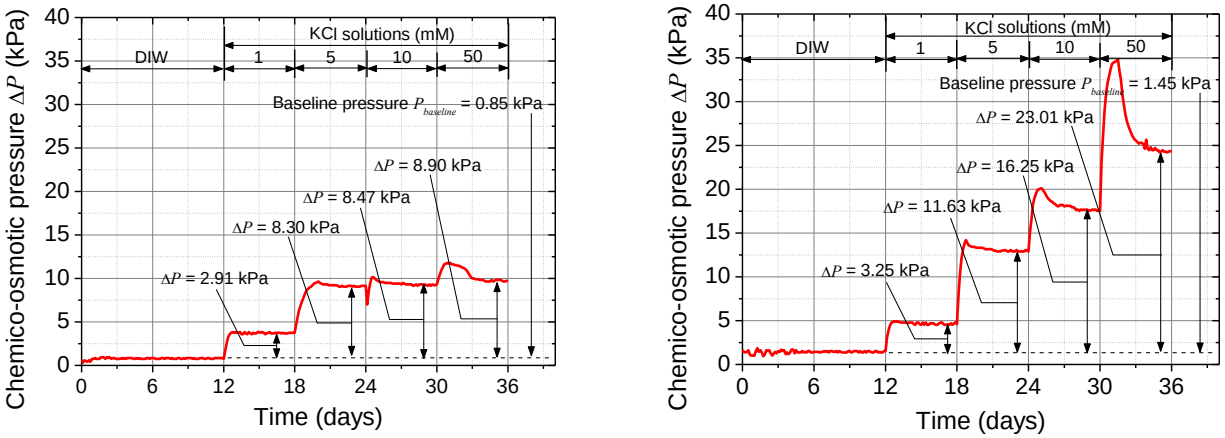

(a) (b)

Fig. 4.22 Measured chemico-osmotic pressure across the specimens: (a) Solution with a pH of 4.0, (b) Solution with a pH of 11.0

4.3.3.5 Effect of solute type

Figure 4.23 shows the actual values of ΔP of the four specimens under four different kinds of solutions (Ca, Na, Zn and Pb). DIW was circulated at both top and bottom sides of the specimens ($C_t = C_b = 0$) during the first 6 days to obtain the baseline pressure 0.42 kPa, 0.76 kPa, 0.93 kPa and 0.59 kPa. The baseline pressures were also observed by Tang et al. (2013a, 2013b, 2014) and Malusis and Shackelford (2002). Tang et al. (2013a) ascribed it to the leaching out of the remaining soluble salts in specimens, while it was due to slight differences in the hydraulic resistance of the porous stones at the opposite ends of the specimens by Malusis and Shackelford (2002).

From the Fig. 4.23 (a) and (b), it is apparent that the change of chemico-osmotic pressure under $CaCl_2$ and NaCl were significantly different . For the case of $CaCl_2$, when concentration difference increased from 0 to 0.5 mM, then from 0.5 to 1 mM, the introduction of electrolyte resulted in an immediate and rapid increase in the chemico-osmotic pressure. However, as the continuous increase of concentration difference to 5 mM, 10 and 50 mM, the chemico-osmotic pressure had a slight decrease. For the case of NaCl, the chemico-osmotic pressure has a rapid increase immediately when introducing electrolyte at the beginning of every stage. The distinctive change of chemico-osmotic pressure appeared under Zn(II) and Pb(II) concentration of 0.5 mM and 1 mM as shown in Fig. 4.23 (c) and (d), in which the chemico-osmotic pressure increased greatly to the peak, then followed by the decrease until reached or closed to the baseline pressure value. Consider the pH condition, such phenomenon can be attributed to the adsorption process, by which the heavy metal ions were absorbed and resulted in the decrease of concentration difference (Tang et al. 2010). Therefore, the

chemico-osmotic pressure decreased until baseline pressure value since all heavy metal ions were absorbed and concentration difference decreased to zero. After the soil at the top surface of specimen reached the maximum adsorption capacity, the stable chemico-osmotic pressure can be observed at concentration of 5 and 10 mM. For the Pb(II) at concentration of 50 mM, the chemico-osmotic pressure was still decreasing, which might to be due to the adsorption inside the specimen since the solute diffused into the deeper place at relative high concentration.

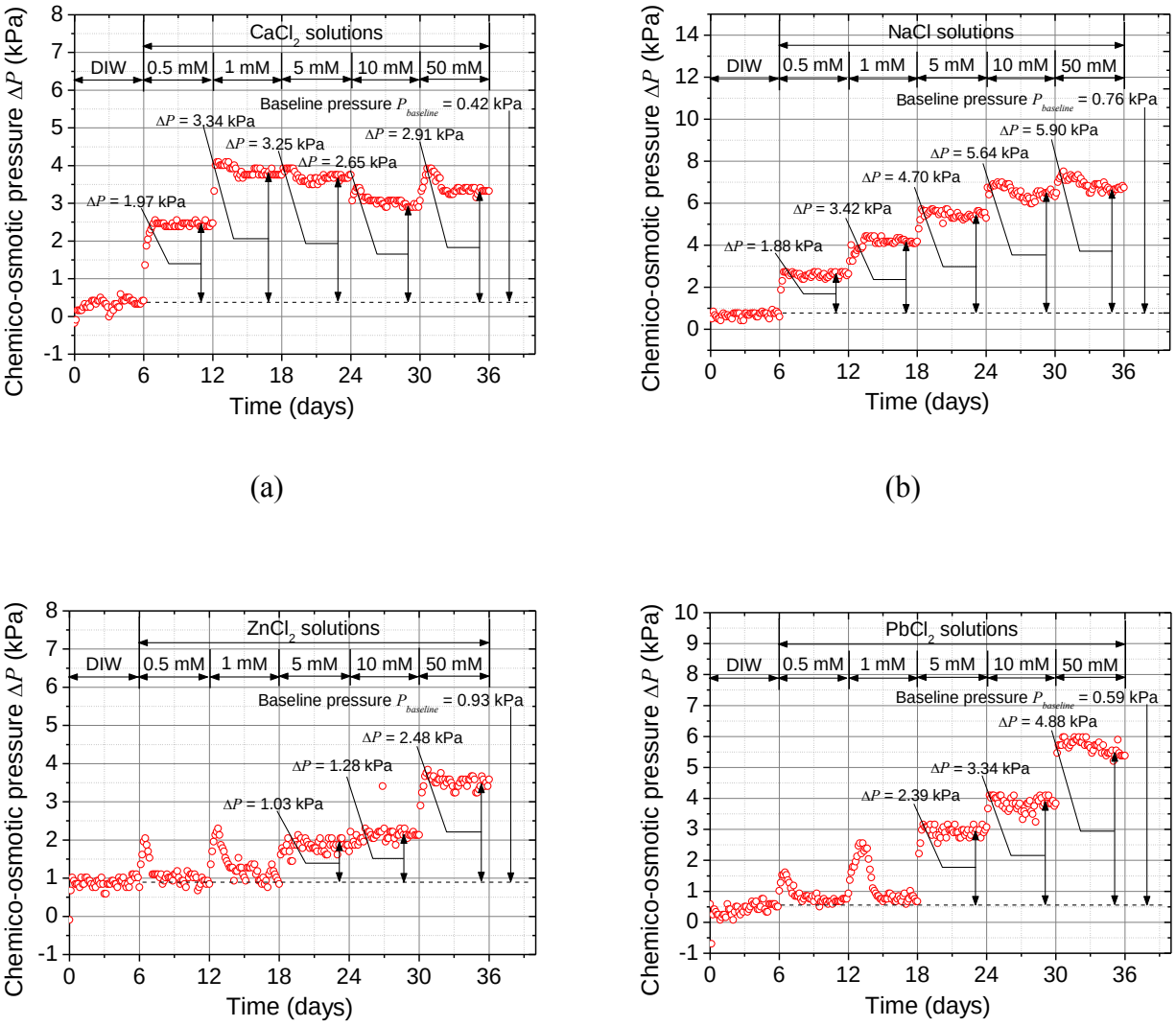

Fig. 4.23 Measured chemico-osmotic pressure across the specimens: (a) $CaCl_2$, (b) $NaCl_2$, (c) $ZnCl_2$, (d) $Pb(NO_3)_2$

Considering the fluctuation of the chemico-osmotic pressure under 0.5 and 1 mM for Zn(II) and Pb(II) solution, and the extremely low boundary concentrations after the adsorption at the corresponding stages shown in previous Fig. 4.17 (c)(d) which reduced by almost 90%, it is very

difficult to caculate accurate average chemico-osmotic efficiency coefficients. To make the results more reliable and easily compared, the average chemico-osmotic efficiency coefficients at the 0.5 and 1 mM for Pb(II) and Zn(II) solutions were calculated follow the Eq. (4.7), which used to calculate the initial chemico-osmotic efficiency coefficient.

4.4 Discussions

Figure 4.24 shows a comparison of the boundary solute concentrations at the bottom for specimens with different bentonite content during the membrane tests. It was obvious that the KCl concentration at the bottom side for specimen of Fukakusa clay started to increase from concentration difference increased to 1 mM, while for bentonite amended clay, it increased until concentration difference reached to 50 mM. Among four bentonite amended clay specimens, it was also apparent that the higher bentonite content was contained, the faster occurred in the KCl diffusion.

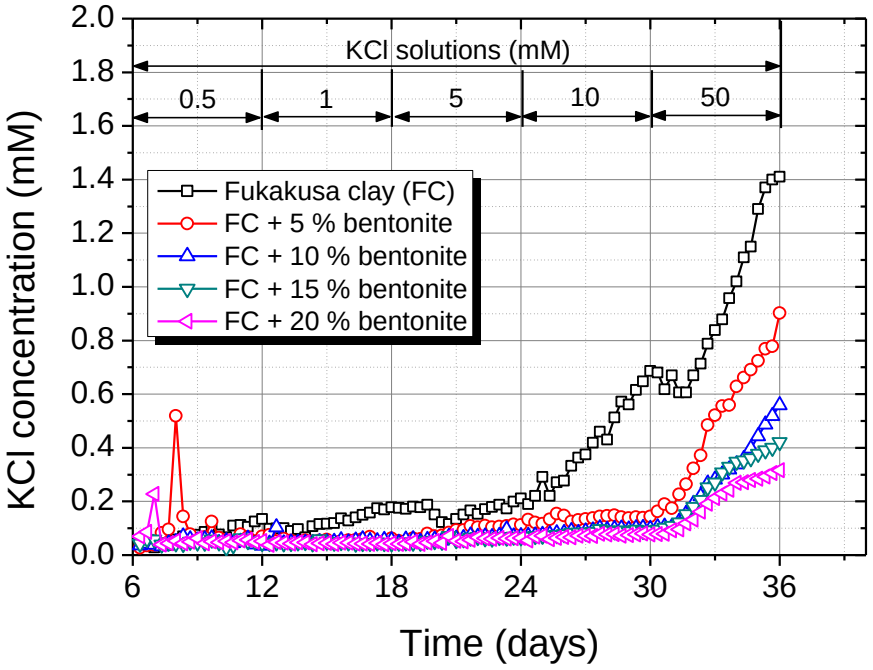

Fig. 4.24 Compare of the boundary concentration of the outflows at the bottom for specimens with different compactness

Figure 4.25 shows the boundary pH at bottom side during membrane test for specimens with different bentonite content. The pH of the outflow at the bottom side almost kept the same pace with KCl concentration as shown in Fig. 4.24. For Fukakusa clay, when KCl diffusion can be observed

from concentration difference of 5 mM, the pH started to decreased. For the case of bentonite amended clay, the pH decreased when concentration difference reached to 50 mM, by which the diffusion also started at that moment.

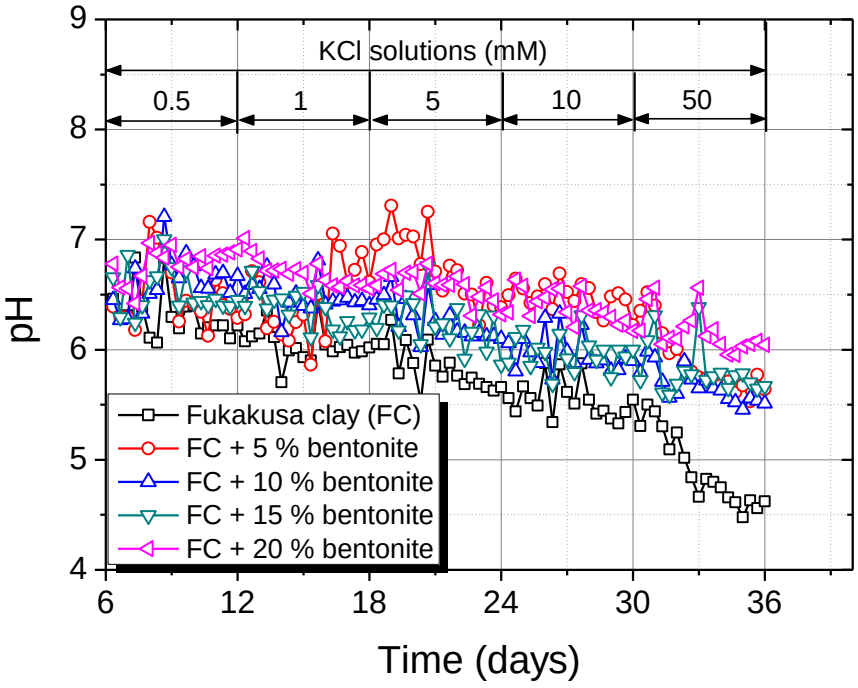

Fig. 4.25 Compare of the boundary pH of the outflows at the bottom for specimens with different compactness

The compare of boundary concentrations at bottom side for specimens with different compactness during membrane test were displayed in Fig. 4.26. The outflow EC kept stable under concentration 0.5 and 1 mM, and started to increase from concentration increased to 5 mM as shown in Fig. 4.26 (a). For KCl concentration of the outflow, it kept stable until the concentration difference increased to 50 mM. The change of KCl concentration was lagged behind by outflow EC, which can be attributed to two causes, ion-exchange and the remaining salts distribute deeply in the pore. The diffusion of KCl leaded to the enlargement of pore, thus more remaining soluble salts were leached out. And as the diffusion continues, some free K ions were fixed by the soil minerals through ion exchange reaction or through the form of complex which occurred ahead of the passage of KCl (Tang et al., 2009; Li et al., 2010). And it was apparent that as the compactness increase, both EC and KCl concentration of outflow decrease, which indicated the diffusion can be restricted through compaction method.

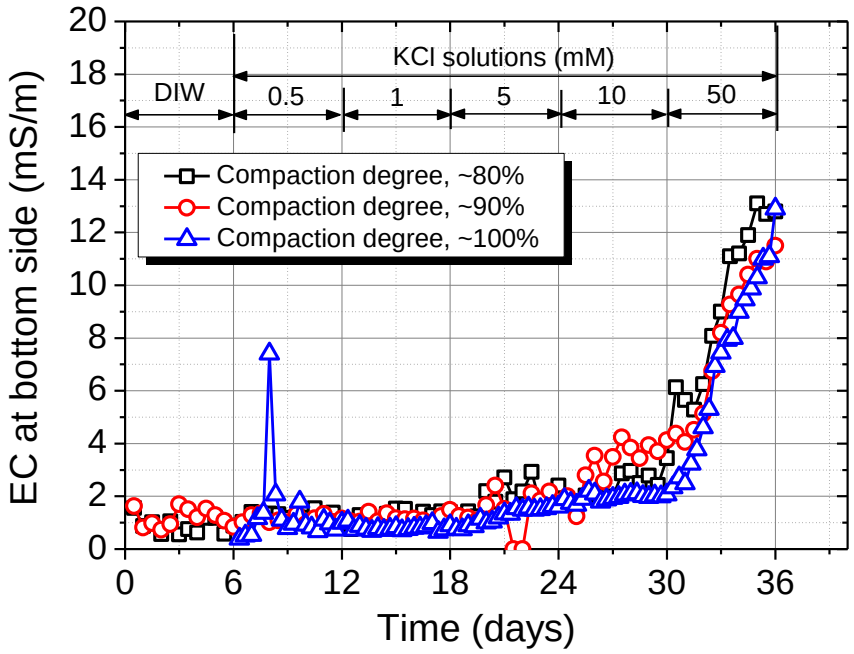

(a)

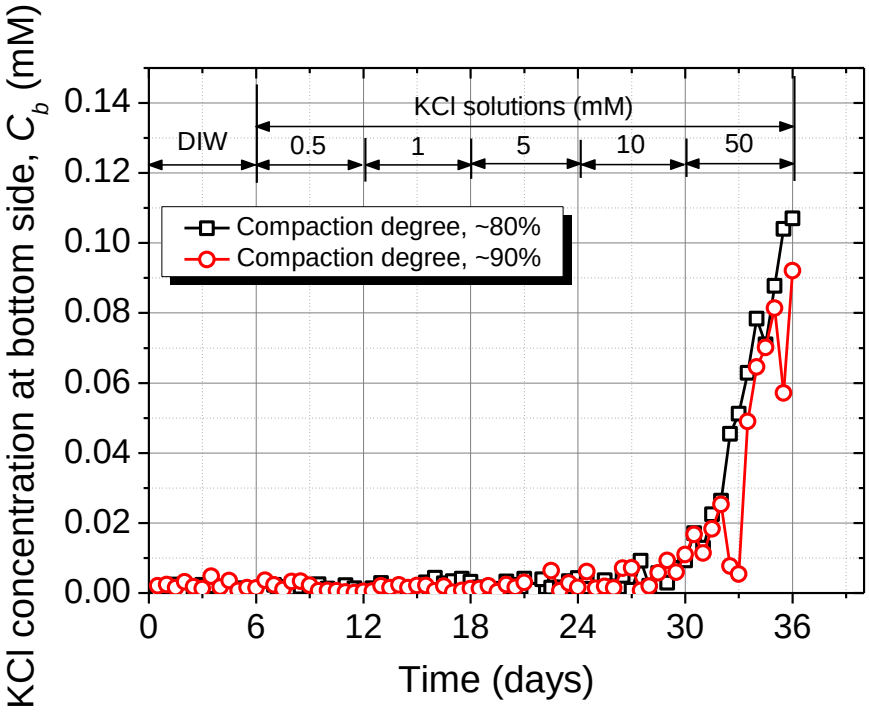

(b)

Fig. 4.26 Compare of boundary condition of outflow at bottom side for specimens with different compactness: (a) Outflow EC, (b) KCl concentration of outflow

Figure 4.27 shows the boundary pH at bottom side for specimens with different compactness during membrane test. The pH kept stable until the concentration difference reached 50 mM, which almost as the same pace as diffusion. And this phenomenon can also proved above judgment that as the diffusion continued, some soluble salts as well as acidic substance were leached out, which resulted in the decrease of pH values. And as compactness increased, the pH decreased less.

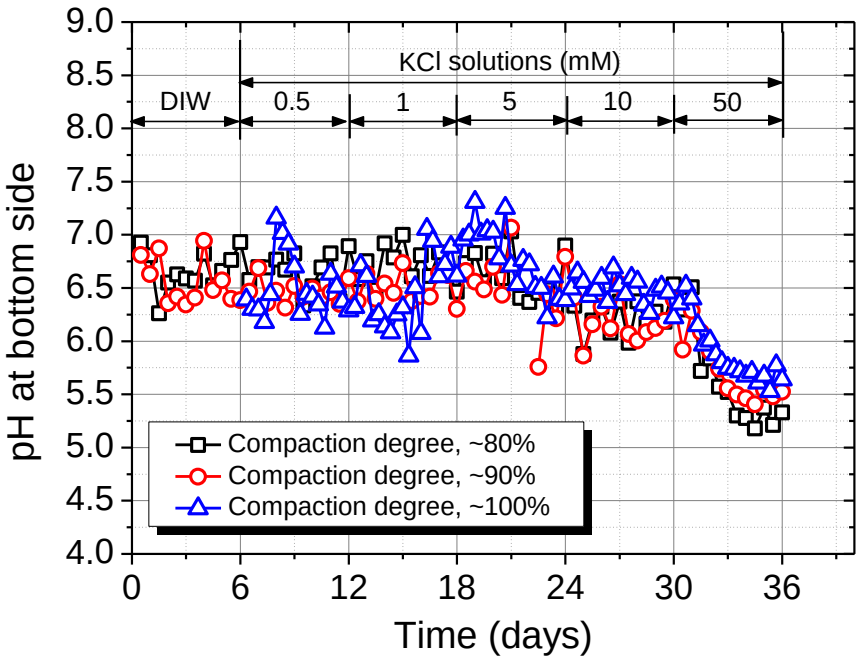

Fig. 4.27 Boundary pH at bottom for specimens with different compactness

The compare of boundary concentrations at bottom side for specimens with different thickness during membrane test were displayed in Fig. 4.28. From Fig. 4.28(a), the EC of the outflow for specimens 7 cm and 9 cm kept stable, the similar tendency of KCl concentration also appeared as shown in Fig. 4.28(b). For the case of specimen with thickness of 5 cm, both EC and KCl concentration of the outflow at the bottom started until concentration difference reached 50 mM, while KCl change was a little lag behind by the EC.

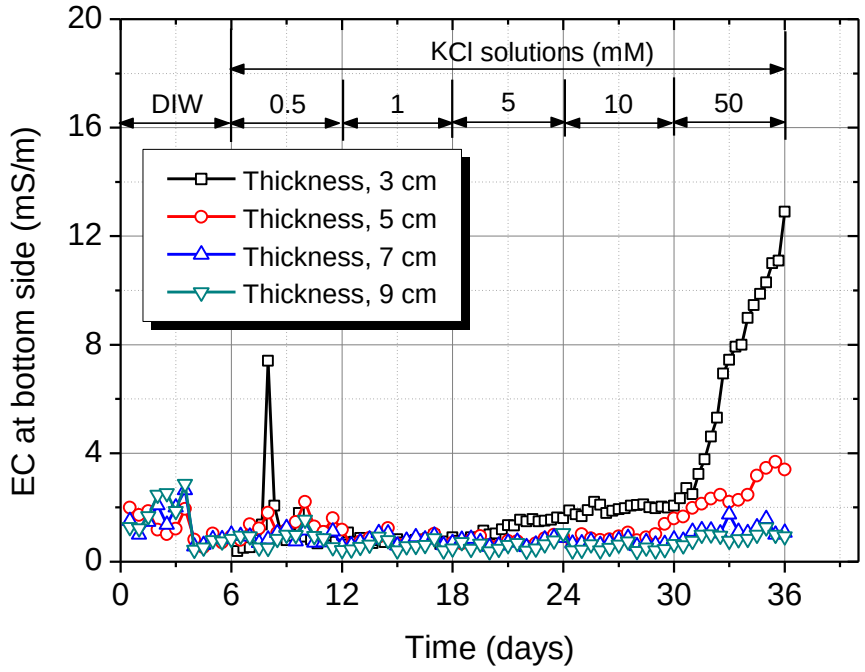

(a)

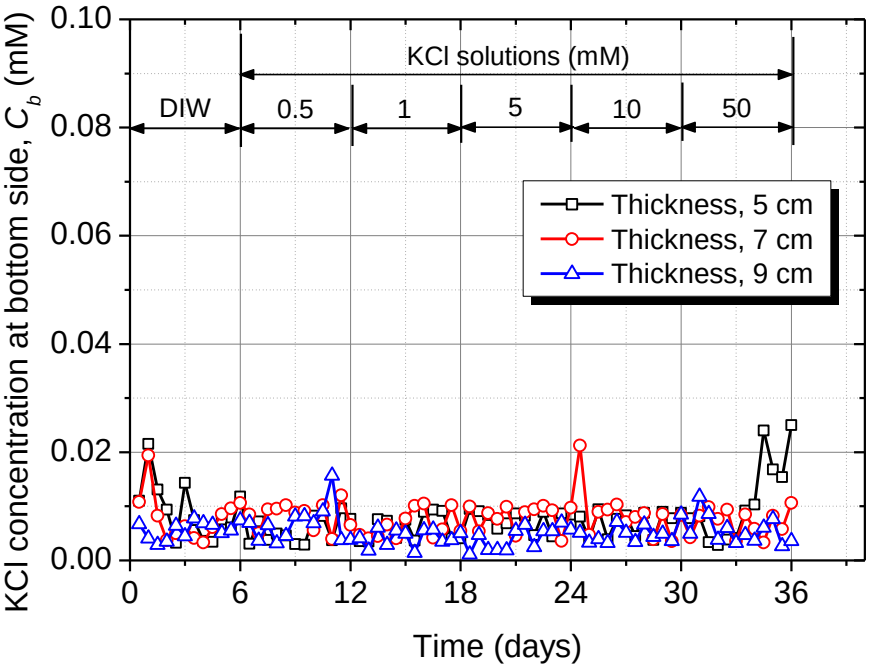

(b)

Fig. 4.28 Compare of boundary condition at bottom side for specimens with different thickness: (a) Outflow EC, (b) KCl concentration of outflow

Figure 4.29 shows the boundary pH at bottom side for specimens with different thickness during membrane test. The pH change kept same pace as diffusion that started to decrease when concentration difference increased to 50 mM for specimen with 5 cm, while pH kept stable for specimens with thickness of 7 cm and 9 cm. And this phenomenon can also proved above judgment that as the diffusion continued, some soluble salts as well as acidic substance were leached out, which resulted in the decrease of pH values.

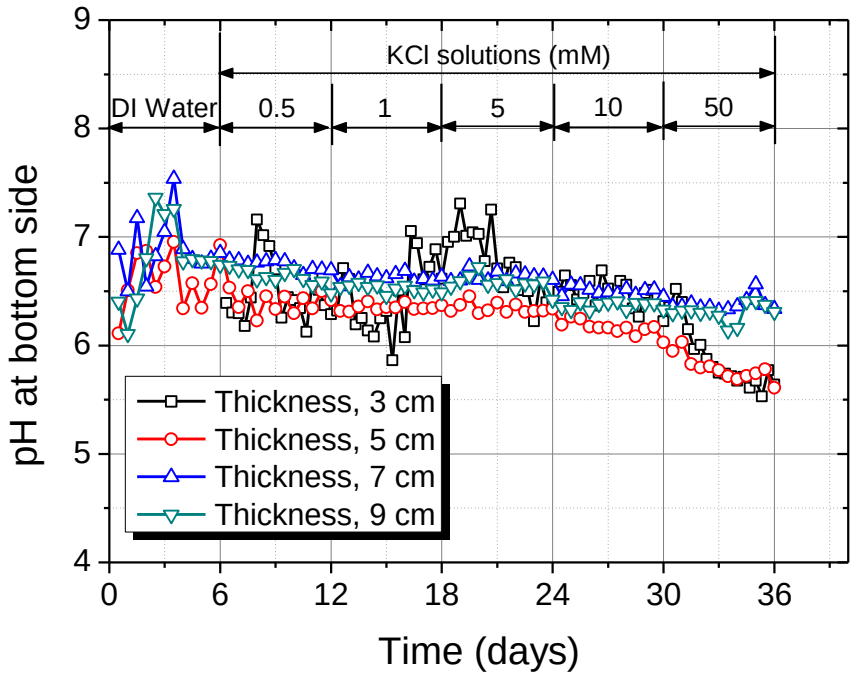

Fig. 4.29 Compare of pH at bottom for specimens with different thickness

Figure 4.30(a) and (b) compare the EC contributed by KCl and the total salts at the bottom during the membrane tests under solution with different pH values. The black curve represents the EC of the total salts, which was measured directly by an EC meter, the red curve is the EC contributed by KCl, while was calculated based on ICP measurements and the linear relationship between EC and concentration (Tang et al., 2013a). Before KCl penetrated across the specimens ($C <$ 10 mM), KCl was a minor part of total salts that had been leached out, i.e., only 1% or 2%; however, after the KCl penetrated the specimens when the concentration was greater than 10 mM, its proportion increased sharply and finally reached about 10%. Compared to the concentration at the top side, the change at the bottom can be neglected when calculate the concentration difference. However, to make the results more accurate and reliable, in the following test, the boundary solute concentration were measured directly by using ICP-MAS (ICPS-8000, Shimadzu, Japan).

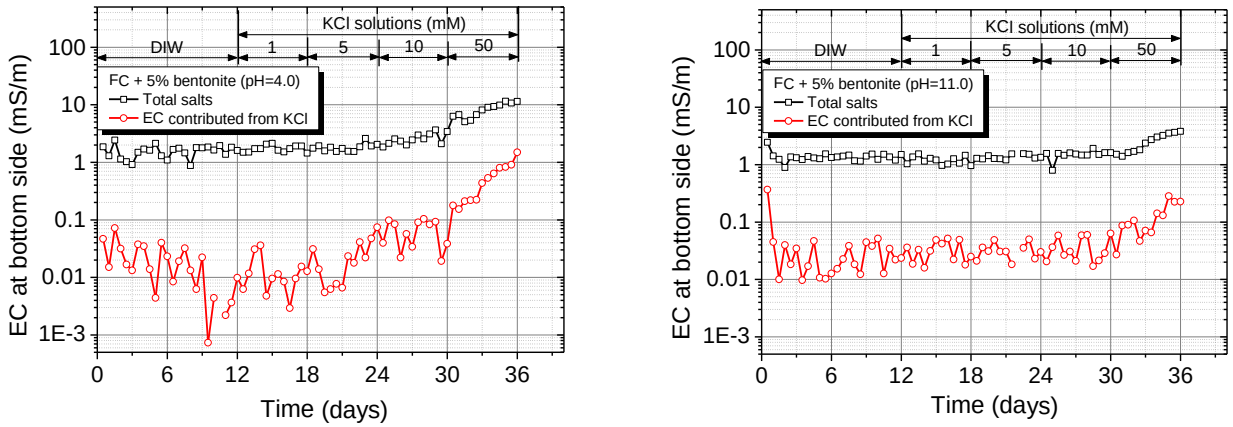

(a) (b)

Fig. 4.30 EC of KCl and total salts in the outflow at the bottom for (a) Solution with a pH of 4.0, (b) Solution with a pH of 11.0

Figure 4.31(a) and (b) show a comparison of the boundary concentrations at the bottom during the membrane tests under solution with different pH values. When the pH of the solution was 4.0, the salt content that remained in specimens began to dissolve when the concentration reached 5 mM, as indicated in Fig. 4.31(a), and Fig. 4.31(b) shows that the penetration of KCl occurred even after the concentration was increased to 50 mM. Thus, it was indicated that, under acid conditions, at concentrations between 5 mM and 50 mM, only the salt content that remained began to leach out at the bottom, since the solute cannot transfer across the specimens. This phenomenon was due to the ion exchange adsorption, by which most K ions were fixed by minerals in the soil (Tang et al., 2010; Tang et al., 2012). In contrast, when the pH of the solution was 11.0, the concentrations of both EC and KCl began to increase after the concentration reached 50 mM. According to the changes in EC shown in Fig. 4.31 (a), the changes in the outflows for both the pH = 4.0 and pH = 7.0 cases exhibited great similarity, showing almost the same increase rate and the same equilibrium value, which proved the very slight erosion effect of the acid solution on the specimens. In addition, it was easy to determine that, when the pH of the source solution increased, less solute diffused, suggesting that the performance of Fukakusa clay-bentonite as a barrier was much better in alkaline conditions than in acidic conditions.

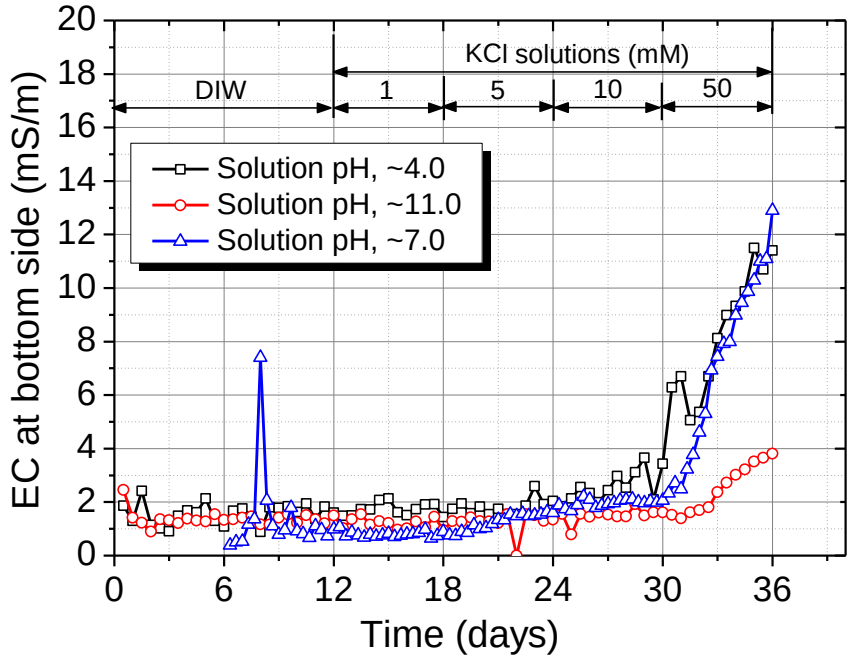

(a)

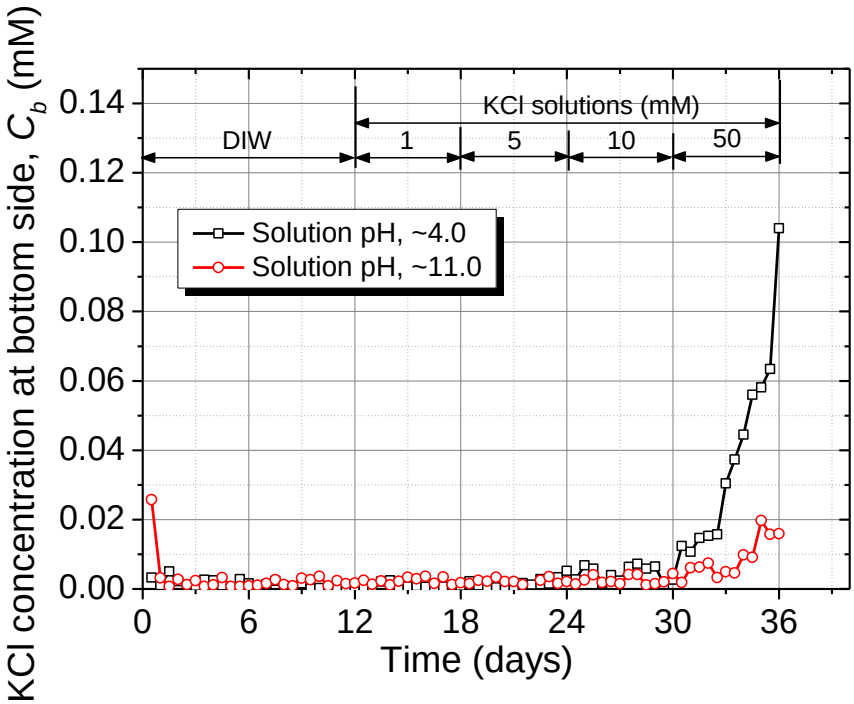

(b)

Fig. 4.31 Comparison of the boundary condition of the outflows at the bottom for specimens with different solution pH: (a) EC of the outflow and (b) KCl concentration of outflow

Figure 4.32 shows the boundary pH at bottom side under solution with different pH values during membrane test. All three specimens displayed excellent buffer capacity, and can resist the pH change under relative low concentration. As the concentration increased to higher than 5 mM, the buffer capacity appeared to diverse. Under pH 11.0, it still remains strong as before, while in pH 4.0 and 7.0‘s case, the buffer capacity were weaken to great extent. Compare Fig. 4.32 with Fig. 4.31, it can be found that buffer capacity change and kept the same step as solute diffusion, maybe the diffusion process accelerate this acidification rate.

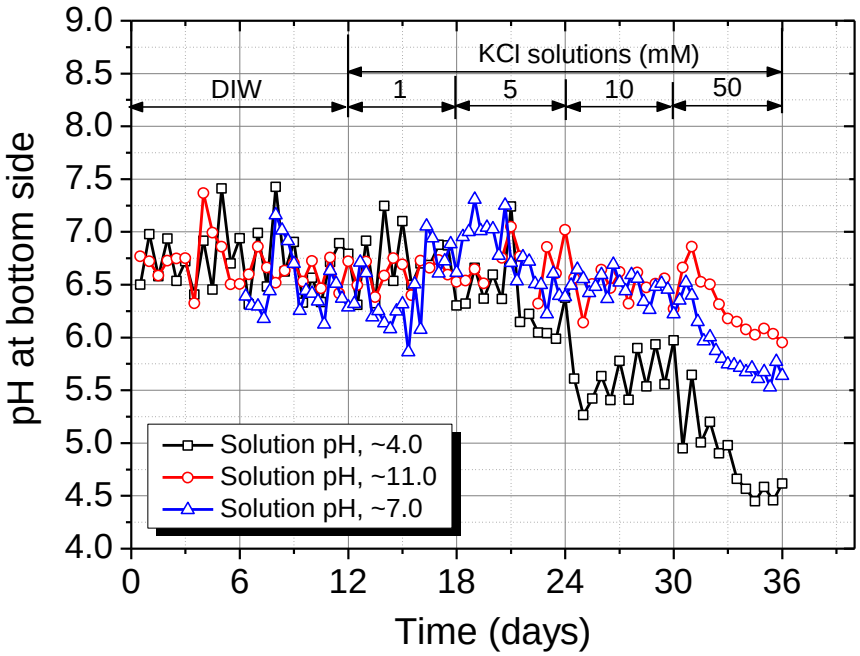

Fig. 4.32 Comparison of the boundary pH of the outflow at the bottom

The compare of boundary concentrations at bottom side for specimens with different solution during membrane test were displayed in Fig. 4.33(a) and (b). From Fig. 4.33 (a), the EC of outflow for K, Ca and Na increased when concentration higher than 5 mM. In Fig. 4.33(b), it was clear that the concentration of Ca and Na of the outflow at the bottom side exhibited similar trend that the solute concentration kept stable and started to increased until the concentration difference increased to 50 mM. Compare to solute concentration of the outflow, the EC increased almost 12 days earlier, which can be attributed to the ion-exchange adsorption and some soluble salts were generated. While for heavy metal ions, it was clear that the concentration of Pb(II) of the outflow at the bottom side keep stable, no apparent increase can be observed during the membrane test. It also indicated Pb(II) cannot transport across the specimens. However, for the case of Zn(II), when concentration difference reached 50 mM, the diffused Zn(II) across the specimen was observed. And the EC of outflow for both Zn(II) and Pb(II) increased when concentration difference increased to 50 mM as shown in Fig. 4.33(a). Compare to the stable concentration of Zn(II) and Pb(II) at outflow, the

increase of EC can be attributed to the ion-exchange adsorption and some soluble salts were generated. And the EC of outflow for Zn(II) was a little higher than Pb(II), which resulted from the diffusion of some Zn(II).

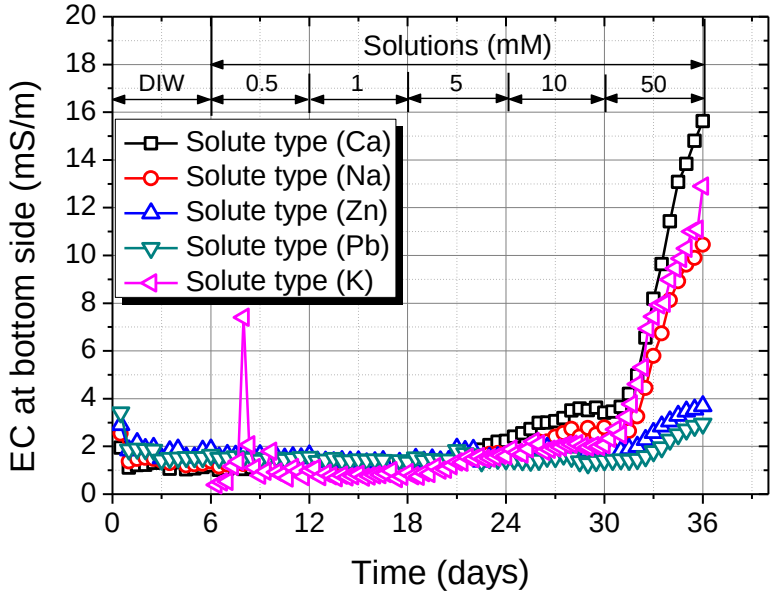

(a)

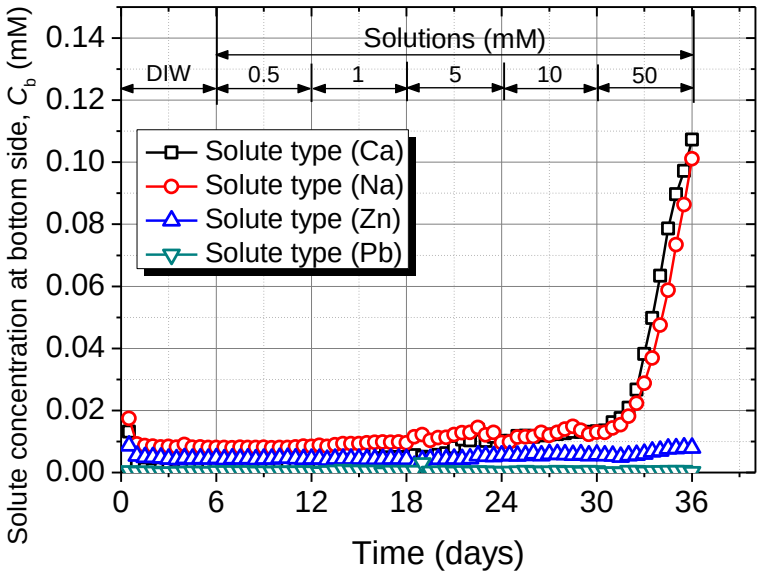

(b)

Fig. 4.33 Compare of boundary condition at bottom side for specimens with different solution: (a) Outflow EC, (b) Solute concentration of outflow

Figure 4.34 shows the boundary pH at bottom side for specimens under different solutions

during membrane test. For Ca and Na ions, the pH of outflow started to decrease from concentration difference reached 50 mM, while for heavy metal ions, there was no observable change occurred during the membrane test. Such same pace of change with diffusion as shown in Fig. 4.33(b) can also proved above judgment again that some soluble salts as well as acidic substance were leached out as the diffusion continued, which resulted in the decrease of pH values.

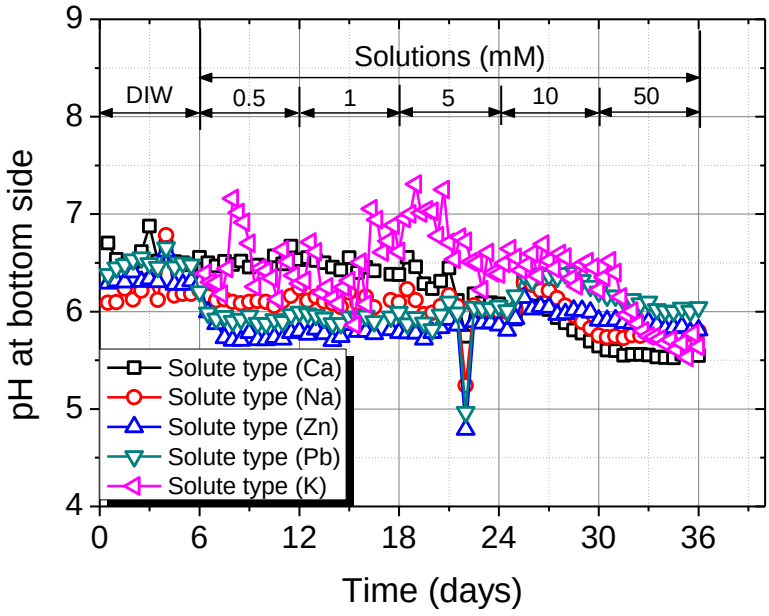

Fig. 4.34 Compare of pH at bottom side for specimens with different solutions

Table 4.8, 4.9, 4.10, 4.11 and 4.12 list the values of ω for all specimens in the five groups. The ω_{ave} listed in these tables were calculated using Eq. (4.8). As previously noted, because the solute diffuses from the source solution into the specimen through top boundary and dissolved salts from the specimen to DIW are flushed from bottom boundary, the values of ω_{ave} tend to be slightly larger than ω_0. It has to be mentioned when the KCl concentration C_{t0} is sufficiently low (C_{t0}= 0.5 mM), the values of ω_{ave} for the bentonite amended FC composite materials exceed 1 (1.03, 1.12, 1.01, and 1.04) as shown in Table 4.8, which can be ascribed to the calculated concentration difference. During the membrane test, the measured EC value at the bottom boundary was contributed from not only KCl but also other leached out salts, which cause the calculated bottom boundary concentration (C_b) increase a little. Thus the theoretical osmotic pressure decreased in response ($\Delta\pi = vRT\Delta C$), since the concentration difference decreased ($\Delta C = C_t - C_b$), which leaded to the ω_{ave} a litter higher. And such experimental deviation became ignorable, as concentration increase. However, under such conditions (C_{t0}= 0.5 mM), FC plus 5%, 10%, 15%, or 20% bentonite can be regarded as an ideal permeable membrane in which only water can pass. This finding is consistent with the diffusion trend for the KCl concentration at the specimen bottom boundary shown in Fig. 4.10. Additionally, the difference between the values of ω_{ave} and ω_0 tend to become smaller as the concentration increased.

Table 4.8 Summary of the membrane test results for specimens with different bentonite content

No.	Physical property			Experimental condition				Test results				
	D (mm)	T (mm)	k (m/s)	BC	S (%)	C_{t0} (mM)	ΔC_{ave} (mM)	ΔP (kPa)	$\Delta\pi$ (kPa)	$\Delta\pi_{ave}$ (kPa)	ω_0	ω_{ave}
1	100	30	1.58×10^{-9}	0	97.4	0.5	0.42	1.71	2.42	2.02	0.71	0.85
						1	0.86	1.45	4.84	4.17	0.3	0.35
						5	4.60	2.65	24.19	22.24	0.11	0.12
						10	8.44	2.91	48.39	40.81	0.06	0.07
						50	43.11	3.16	241.94	208.44	0.01	0.02
2	100	30	1.07×10^{-9}	5%	98	0.5	0.43	2.14	2.42	2.08	0.88	1.03
						1	0.92	2.82	4.84	4.45	0.58	0.63
						5	4.57	9.32	24.19	22.11	0.39	0.42
						10	8.63	9.66	48.39	41.74	0.2	0.23
						50	43.28	9.84	241.94	209.28	0.04	0.05
3	100	30	6.04×10^{-10}	10%	96.1	0.5	0.44	2.39	2.42	2.13	0.99	1.12
						1	0.93	2.99	4.84	4.5	0.62	0.66
						5	4.48	8.38	24.19	21.67	0.35	0.39
						10	8.64	9.84	48.39	41.79	0.2	0.24
						50	42.61	10.86	241.94	206.04	0.04	0.05

Table 4.8 Summary of the membrane test results for specimens with different bentonite content (conti.)

No.	Physical property			Experimental condition				Test results				
	D (mm)	T (mm)	k (m/s)	BC	S (%)	C_{t0} (mM)	ΔC_{ave} (mM)	ΔP (kPa)	$\Delta\pi$ (kPa)	$\Delta\pi_{ave}$ (kPa)	ω_0	ω_{ave}
4	100	30	2.74×10^{-10}	15%	96.2	0.5	0.45	2.22	2.42	2.19	0.92	1.01
						1	0.93	3.59	4.84	4.51	0.74	0.8
						5	4.42	8.72	24.19	21.36	0.36	0.41
						10	8.59	10.26	48.39	41.54	0.21	0.25
						50	42.60	12.06	241.94	206	0.05	0.06
5	100	30	8.23×10^{-11}	20%	93.8	0.5	0.44	2.22	2.42	2.13	0.92	1.04
						1	0.90	2.57	4.84	4.37	0.53	0.59
						5	4.39	9.07	24.19	21.24	0.37	0.43
						10	8.77	11.20	48.39	42.39	0.23	0.26
						50	42.53	14.37	241.94	205.63	0.06	0.07

D = Specimen diameter; T = Specimen thickness; k = Hydraulic conductivities; BC = Bentonite content; S = Saturation degree; C_{t0} = Initial upper boundary concentration; ΔC_{ave} = Average concentration difference across specimen; ΔP = Measured actual chemico-osmotic pressure; $\Delta\pi$ = Theoretical chemico-osmotic pressure; $\Delta\pi_{ave}$ = Average theoretical chemico-osmotic pressure; ω_0 = Chemico-osmotic efficiency coefficient; ω_{ave} = Average chemico-osmotic efficiency coefficient

Table 4.9 Summary of the membrane test results for specimens with different compactness

No.	Experiment condition							Membrane test results					
	D (mm)	T (mm)	BC (%)	Compactness (%)	S (%)	k (m/s)	C_{t0} (mM)	ΔC_{ave} (mM)	ΔP (kPa)	$\Delta\pi$ (kPa)	$\Delta\pi_{ave}$ (kPa)	ω_0	ω_{ave}
1	100	30	5	~ 80	98.9	2.01×10^{-9}	0.5	0.51	2.22	2.45	2.49	0.91	0.89
							1	0.90	2.48	4.91	4.43	0.51	0.56
							5	4.61	6.59	24.53	22.6	0.27	0.29
							10	8.58	6.59	49.05	42.08	0.13	0.16
							50	39.54	7.1	245.26	193.96	0.03	0.04
2	100	30	5	~ 90	98.6	1.49×10^{-9}	0.5	0.52	2.39	2.45	2.54	0.98	0.94
							1	0.89	2.57	4.91	4.35	0.52	0.59
							5	4.67	8.21	24.53	22.92	0.33	0.36
							10	8.67	8.21	49.05	42.52	0.17	0.19
							50	40.34	8.55	245.26	197.87	0.03	0.04
3	100	30	5	~ 100	98.4	1.07×10^{-9}	0.5	0.42	2.14	2.42	2.08	0.88	1.03
							1	0.91	2.82	4.84	4.45	0.58	0.63
							5	4.51	9.32	24.19	22.11	0.39	0.42
							10	8.51	9.66	48.39	41.74	0.2	0.23
							50	42.66	9.84	241.94	209.28	0.04	0.05

D = Diameter of specimens; T = Thickness of specimens; BC = Bentonite content; S = Saturation degree; k = hydraulic conductivities; C_{t0} = Initial upper boundary concentration; ΔC_{ave} = Average concentration difference across specimen; ΔP = Measured chemico-osmotic pressure; $\Delta\pi$ = theoretical chemico-osmotic pressure; $\Delta\pi_{ave}$ = Average theoretical chemico-osmotic pressure; ω_0 = Chemico-osmotic efficiency coefficient; ω_{ave} = Average chemico-osmotic efficiency coefficient

Table 4.10 Summary of the membrane test results for specimens with different thickness

	Experiment conditions						Membrane test results				
	D(cm)	T(cm)	Dry density(g/cm^3)	S(%)	k(m/s)	C_{t0}(mM)	ΔP(kPa)	$\Delta\pi$(kPa)	$\Delta\pi_{ave}$(kPa)	ω_0	ω_{ave}
1	10	3	1.503	98.4	1.07×10^{-9}	0.5	2.14	2.42	2.08	0.88	1.03
						1	2.82	4.84	4.45	0.58	0.63
						5	9.32	24.19	22.11	0.39	0.42
						10	9.66	48.39	41.74	0.2	0.23
						50	9.84	241.94	209.28	0.04	0.05
2	10	5	1.486	99.3	1.45×10^{-9}	0.5	2.22	2.42	2.48	0.91	0.9
						1	2.82	4.84	4.6	0.58	0.61
						5	8.64	24.19	22.22	0.35	0.39
						10	9.32	48.39	43.41	0.19	0.21
						50	9.41	241.94	193.27	0.04	0.05
3	10	7	1.449	98.6	2.33×10^{-9}	0.5	2.22	2.42	2.45	0.91	0.91
						1	2.82	4.84	4.64	0.58	0.61
						5	8.64	24.19	22.37	0.35	0.39
						10	8.72	48.39	43.17	0.18	0.2
						50	8.64	241.94	188.36	0.04	0.05
4	10	9	1.4	96.6	4.60×10^{-9}	0.5	2.22	2.42	2.47	0.91	0.9
						1	2.65	4.84	4.46	0.54	0.59
						5	7.78	24.19	21.88	0.32	0.36
						10	7.78	48.39	42.23	0.16	0.18
						50	7.61	241.94	189.34	0.03	0.04

Table 4.11 Summary of the membrane test results for specimens under solutions with different pH

No.	Physical properties			Experiment conditions					Membrane test results				
	D(mm)	T(mm)	k(m/s)	BC	Compactness	S(%)	solution pH	C_{t0}(mM)	ΔP(kPa)	$\Delta\pi$(kPa)	$\Delta\pi_{ave}$(kPa)	ω_0	ω_{ave}
1	100	30	1.07×10^{-9}	5%	~ 100%	98.4	~7.0	0.5	2.14	2.42	2.08	0.88	1.03
								1	2.82	4.84	4.45	0.58	0.63
								5	9.32	24.19	22.11	0.39	0.42
								10	9.66	48.39	41.74	0.2	0.23
								50	9.84	241.94	209.28	0.04	0.05
2	100	30	1.01×10^{-9}	5%	~ 100%	96	~4.0	1	2.91	4.91	4.63	0.59	0.63
								5	8.3	24.53	22.98	0.34	0.36
								10	8.47	49.05	42.35	0.17	0.2
								50	8.9	245.26	191.27	0.04	0.05
3	100	30	0.98×10^{-9}	5%	~ 100%	97.8	~11.0	1	3.25	4.91	4.41	0.66	0.74
								5	11.63	24.53	23.33	0.47	0.5
								10	16.25	49.05	42.79	0.33	0.38
								50	23	245.26	196.22	0.09	0.12

D = Diameter of specimens; T = Thickness of specimens; k = hydraulic conductivities; BC = Bentonite content; S = Saturation degree; C_{t0} = Initial upper boundary concentration; ΔP = Measured osmotic pressure; $\Delta\pi$ = theoretical chemico-osmotic pressure; $\Delta\pi_{ave}$ = Average theoretical chemico-osmotic pressure; ω_0 = Chemico-osmotic efficiency coefficient; ω_{ave} = Average chemico-osmotic efficiency coefficient

Table 4.12 Summary of the membrane test results for specimens with different solutions

	Experiment conditions						Membrane test results				
	D(cm)	T(cm)	S(%)	k(m/s)	Solute type	C_{t0}(mM)	ΔP(kPa)	$\Delta\pi$(kPa)	$\Delta\pi_{ave}$(kPa)	ω_0	ω_{ave}
1	10	3	99.5	1.01×10^{-9}	Ca	0.5	1.97	3.60	3.50	0.55	0.56
						1	3.34	7.21	6.84	0.46	0.49
						5	3.25	36.04	31.58	0.09	0.10
						10	2.65	72.08	64.13	0.04	0.04
						50	2.91	360.41	286.55	0.01	0.01
2	10	3	93.8	0.95×10^{-9}	Na	0.5	1.88	2.40	2.07	0.78	0.91
						1	3.42	4.81	4.23	0.71	0.81
						5	4.70	24.03	19.54	0.20	0.24
						10	5.64	48.05	42.70	0.12	0.13
						50	5.90	240.27	180.64	0.02	0.03
3	10	3	97.7	0.98×10^{-9}	Zn	0.5		3.60		0.33	
						1		7.21		0.19	
						5	1.03	36.04	27.01	0.03	0.04
						10	1.28	72.08	63.75	0.02	0.02
						50	2.48	360.41	327.56	0.01	0.01
4	10	3	95.7	0.99×10^{-9}	Pb	0.5		3.60		0.28	
						1		7.21		0.27	
						5	2.39	36.04	29.69	0.07	0.08
						10	3.34	72.08	65.34	0.05	0.05
						50	4.88	360.41	322.93	0.01	0.02

Based on above Table 4.8, 4.9, 4.10 and Table 4.11, Chemico-osmotic efficiency coefficient was plotted as functions of time period and concentration difference as shown in following Fig. 4.35, Fig. 4.36, Fig. 4.37 and Fig. 4.38. As shown in Fig. 4.35, the chemico-osmotic efficiency coefficients ω_0 decreases as the KCl concentration increases, besides, it also displayed time dependent decrease, which was also observed by Malusis and Shackelford (2002b). However, the rate of decrease varies by specimen. For example, ω_0 for FC decreases from 0.71 to 0.30 as C_{t0} increases from 0.5 mM to 1 mM, and then further decreases to 0.11 as C_{t0} increases to 5 mM, but this further decrease is negligible. In contrast, as C_{t0} increases for bentonite amended FC, ω_0 decreases gradually, and remains above 0.20 when C_{t0} is 10 mM. The results indicate that membrane behavior of natural FC can be neglected unless amended with bentonite (Kang and Shackelford, 2010).

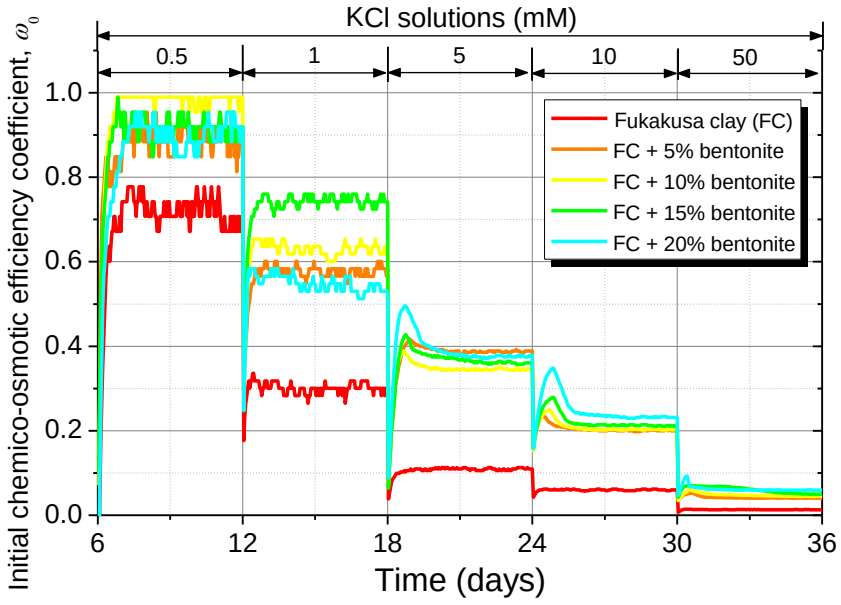

Fig. 4.35 Chemico-osmotic efficiency coefficient as a function of time for Group 1

Figure 4.36 plots ω_{ave} as functions of time and concentration difference. It was obvious that ω_{ave} increased as compactness increased, e.g., the ω_{ave} of specimen with compaction degree 100% was almost 30% higher than that with compaction degree 80% under concentration difference of 5, 10 and 50 mM. Although difference existed among the three specimens, the general trend was same that ω_{ave} decreased as concentration increased, which was also observed in above Fig. 4.35.

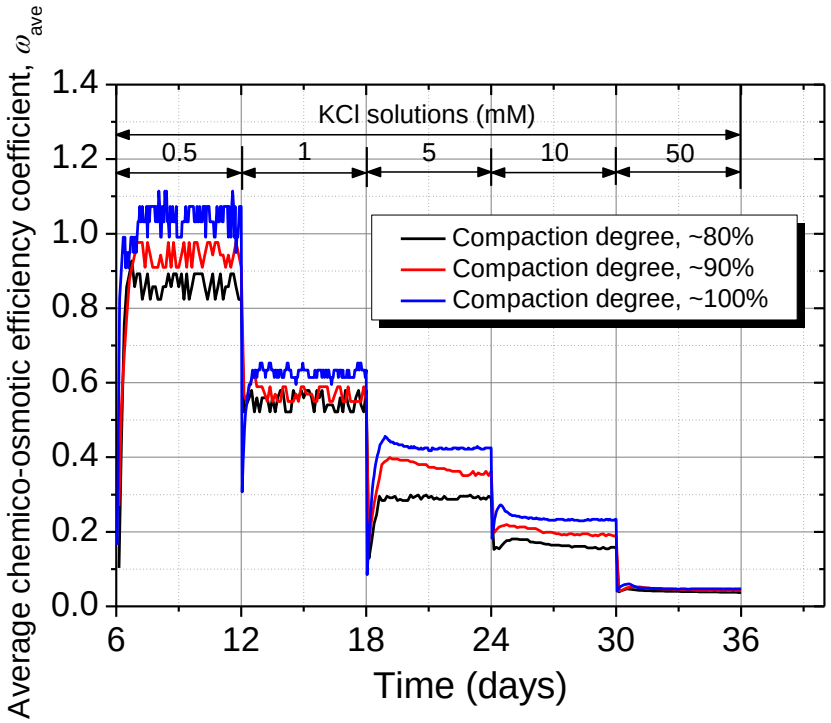

Fig. 4.36 Chemico-osmotic efficiency coefficient ω_{ave} as function of time for Group 2

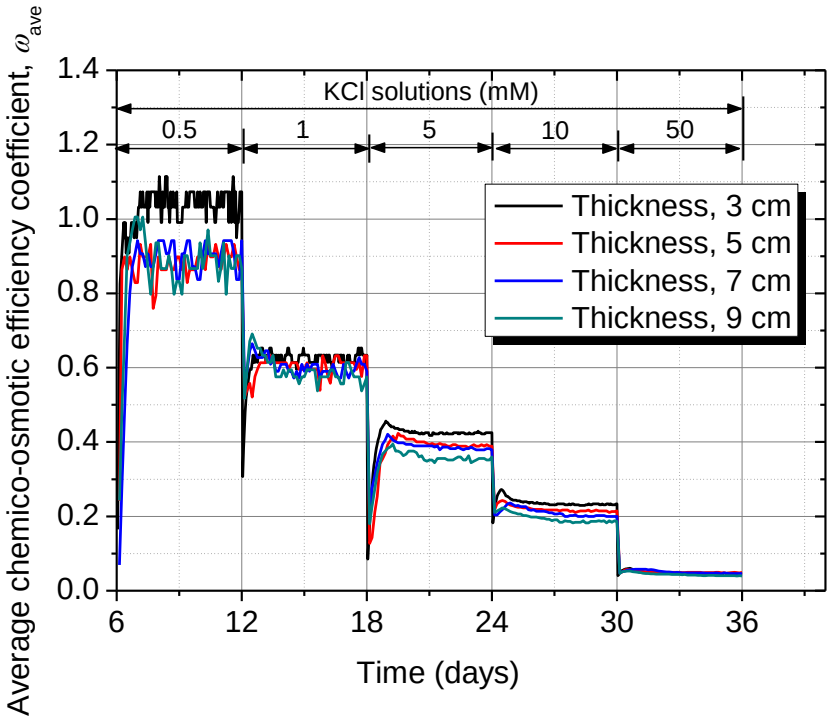

Fig. 4.37 Chemico-osmotic efficiency coefficient ω_{ave} as function of time for Group 3

Figure 4.37 plots ω_{ave} as functions of time and concentration difference for specimens with different thickness ranged from 3 cm to 9 cm. The general trend was same that ω_{ave} decreased as concentration increased no matter the thickness of specimen. However, under certain concentration, it was obvious that ω_{ave} increased as the thickness decreased, and especially under concentration of 0.5, 5 and 10 mM.

Figure 4.38 shows ω_{ave} as a function of time and as a function of concentration difference. Although the general trend was the same, i.e., ω_{ave} decreased as concentration increased, the rate of decrease rate varied. For example, as concentration increased from 1 mM to 10 mM for the solution with a pH of 4, ω_{ave} decreased from 0.63 to 0.2 (68.3%), whereas, for the solution with a pH of 11.0, ω_{ave} decreased from 0.74 to 0.38 (48.6%). When concentration increased to 50 mM, the membrane behaviors can be neglected ($\omega_{ave} < 0.05$) for pH values of 4.0 and 7.0, but, when pH is 11.0, ω_{ave} can still be as high as 0.12. Thus, while the performances of the membranes improved as the pH of the increased, especiall in the improvements in alkaline condition.

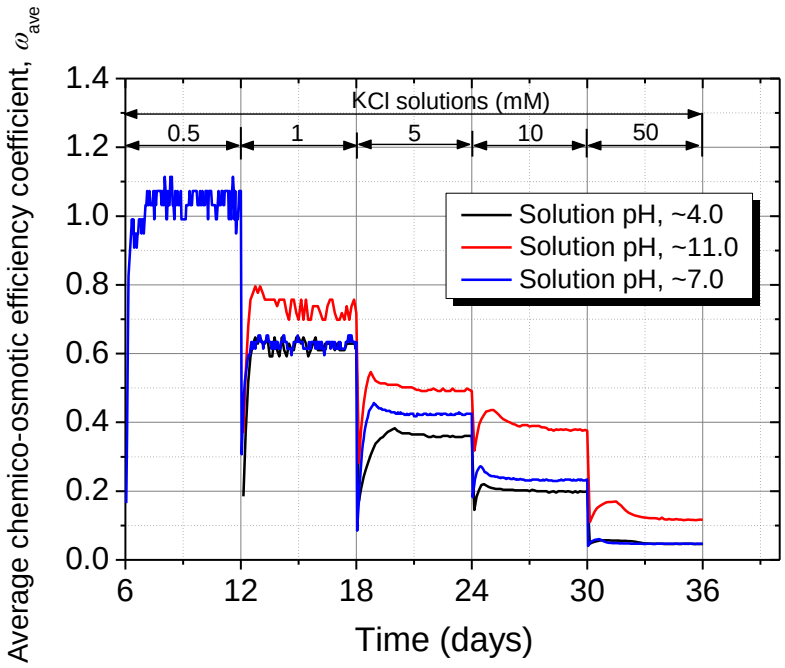

Fig. 4.38 Chemico-osmotic efficiency coefficient as a function of time for Group 4

The values of ω_{ave} in this study are compared to those reported in the literature for Nelson Farm Clay (NFC) and sodium bentonite subjected to the same KCl solutions presented by Kang & Shackelford (2010) and Malusis & Shackelford (2002b) in Fig. 4.39(a)-(e). The relative positions of the lines indicate that the membrane behaviors are following the order; bentonite > clay-bentonite mixture > natural clay (Nelson Farm Clay and FC) as shown in Fig. 4.39(a). Although the differences in membrane behaviors reported in Fig. 4.39 are likely due to multiple reasons, two factors are readily apparent: the DDL and inter-particle pores.

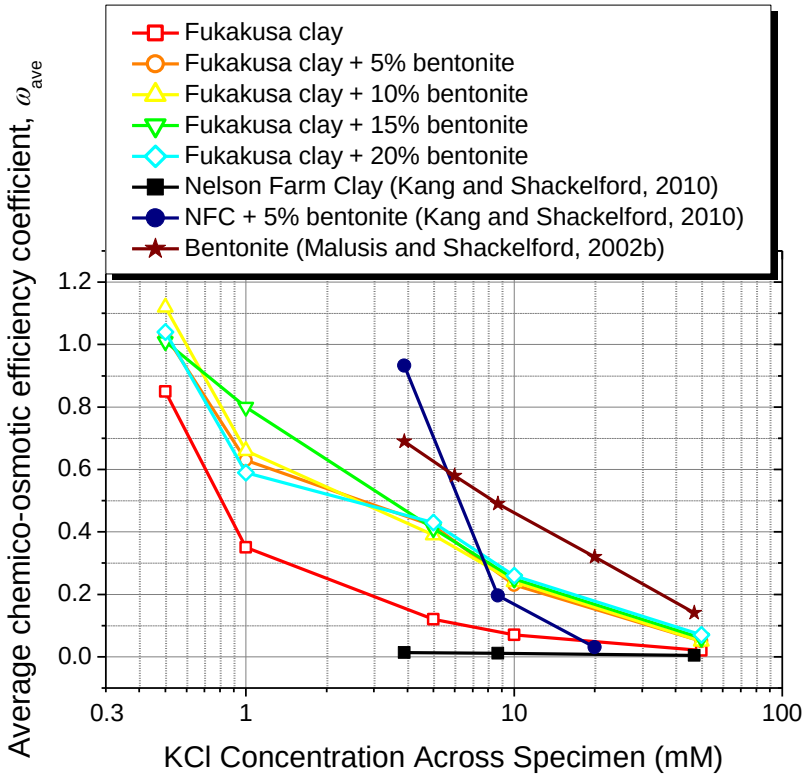
Fukakusa clay
Fukakusa clay + 5% bentonite
Fukakusa clay + 10% bentonite
Fukakusa clay + 15% bentonite
Fukakusa clay + 20% bentonite
Nelson Farm Clay (Kang and Shackelford, 2010)
NFC + 5% bentonite (Kang and Shackelford, 2010)
Bentonite (Malusis and Shackelford, 2002b)
Average chemico-osmotic efficiency coefficient, ω_{ave}
1.2
1.0
0.8
0.6
0.4
0.2
0.0
0.3
1
10
100
KCl Concentration Across Specimen (mM)

(a)

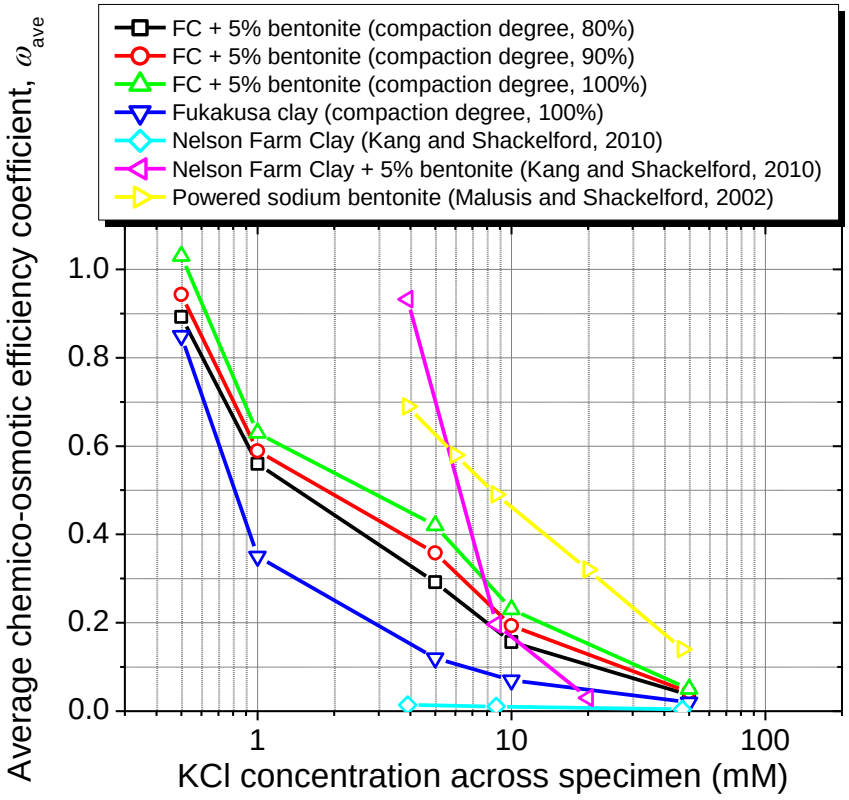
FC + 5% bentonite (compaction degree, 80%)
FC + 5% bentonite (compaction degree, 90%)
FC + 5% bentonite (compaction degree, 100%)
Fukakusa clay (compaction degree, 100%)
Nelson Farm Clay (Kang and Shackelford, 2010)
Nelson Farm Clay + 5% bentonite (Kang and Shackelford, 2010)
Powered sodium bentonite (Malusis and Shackelford, 2002)
Average chemico-osmotic efficiency coefficient, ω_{ave}
1.0
0.8
0.6
0.4
0.2
0.0
1
10
100
KCl concentration across specimen (mM)

(b)

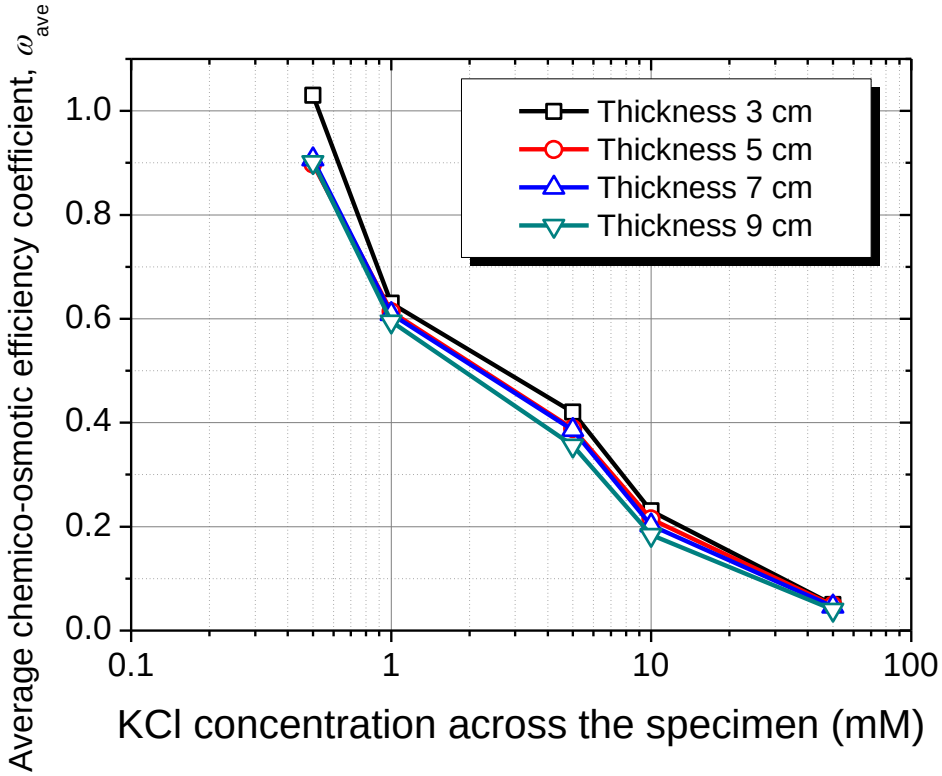
Average chemico-osmotic efficiency coefficient, ω_{ave}
1.0
0.8
0.6
0.4
0.2
0.0
0.1
1
10
100
KCl concentration across the specimen (mM)
Thickness 3 cm
Thickness 5 cm
Thickness 7 cm
Thickness 9 cm

(c)

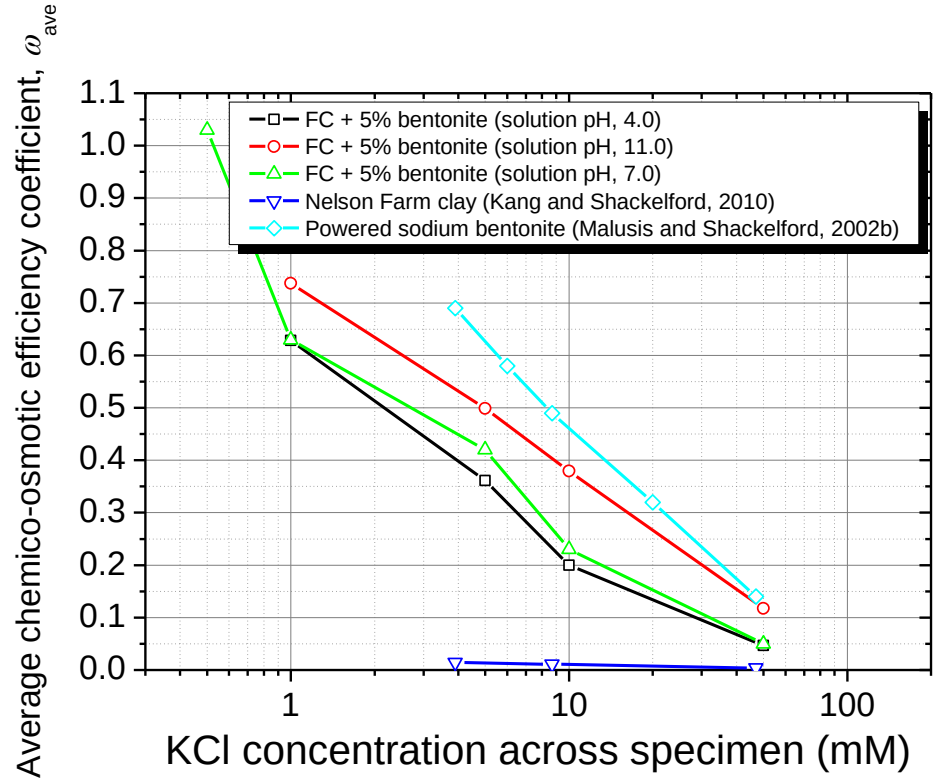
Average chemico-osmotic efficiency coefficient, ω_{ave}
1.1
1.0
0.9
0.8
0.7
0.6
0.5
0.4
0.3
0.2
0.1
0.0
1
10
100
KCl concentration across specimen (mM)
FC + 5% bentonite (solution pH, 4.0)
FC + 5% bentonite (solution pH, 11.0)
FC + 5% bentonite (solution pH, 7.0)
Nelson Farm clay (Kang and Shackelford, 2010)
Powered sodium bentonite (Malusis and Shackelford, 2002b)

(d)

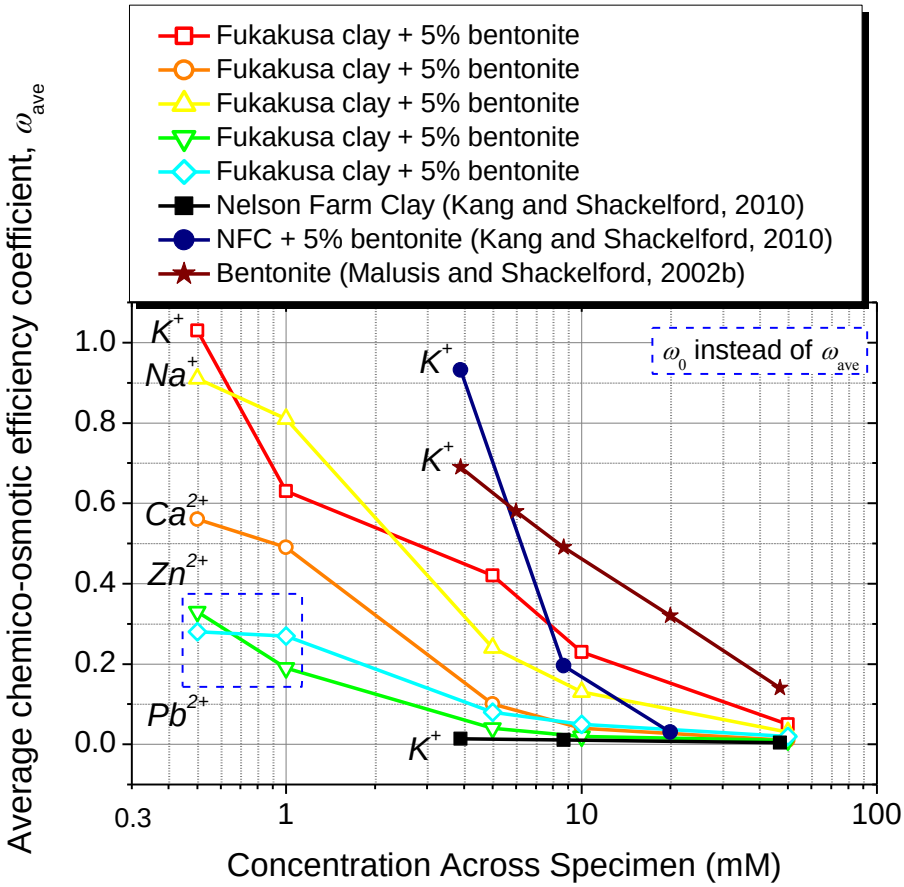

(e)

Fig. 4.39 Chemico-osmotic efficiency coefficient, ω_{ave}, as function of concentration: (a) Bentonite content, (b) Compactness, (c) Specimen thickness, (d) Solution pH, (e) Different solutes

The DDL is a special characteristic of clay, and is particularly evident in bentonite, which possesses extremely active surface charges (Van Impe, 2002). The migration of solute molecules is restricted due to the static electro-repulsion caused by the existence of the DDL around the clay particles (Fritz and Marine, 1983; Fritz, 1986; Keijzer et al., 1997). Therefore, the membrane behavior partially depends on the bentonite content, which determines the thickness and activities of the DDL (Shackelford, 2012). For example, in Fig. 4.39(a), when C_{t0} is relative low (0.5 mM), the ω_0 values of the four specimens with bentonite contents ranging from 5% to 20% are similar. When C_{t0} is 1 mM, ω_0 follows the order of FC plus 15% bentonite > FC plus 10% bentonite > FC plus 5% bentonite > FC plus 20% bentonite. However, when C_{t0} is 5 mM, the membrane behavior of FC plus 5% bentonite displays the highest, and the order is FC plus 5% bentonite > FC plus 20% bentonite > FC plus 15% bentonite > FC plus 10% bentonite. As the KCl concentration C_{t0} is continuously increased to 10 mM and 50 mM, the membrane behavior decreases in proportion to the decrease of the bentonite content (FC plus 20% bentonite > FC plus 15% bentonite > FC plus 10% bentonite >

FC plus 5% bentonite). This work reveals that for the same solute concentration, ω increases as the bentonite content increases: FC < bentonite amended FC materials < bentonite.

Although the values of the ω differ between specimens with varying bentonite content, the general trend is the same. For example, ω decreases as the solute concentration difference across the specimen increases as shown in Fig. 4.39(a)-(e), which is consistent with Kang & Shackelford (2009, 2010, 2011). It is hypothesized that none of the specimens will exhibit a membrane behavior when the solute concentration difference exceeds 100 mM. The decreasing trends of ω as the solute concentration increased are consistent with the Gouy-Chapman theory (DDL theory). Based on the Gouy-Chapman theory, the thickness of the DDL decreases as the solute concentration increases (Mitchell, 1993; Malusis and Shackelford, 2002b).

Figure 4.39(a) presents membrane test results of two kinds of clay-5% bentonite materials, one is FC plus 5% bentonite tested in this study, the other is Nelson Farm Clay (NFC) plus 5% bentonite from previous research (Kang and Shackelford, 2010). Although bentonite content is same (5%), their membrane behaviors are totally different. At lower concentration, the membrane behavior of NFC + 5% bentonite is higher than that of FC + 5% bentonite, and this can be attributed to the excellent barrier performance of NFC, which hydraulic conductivity (1.5×10^{-10} m/s) is much lower compare to FC (1.58×10^{-9} m/s). However, as concentration increases, the membrane behavior of NFC + 5% bentonite become lower than that of FC + 5% bentonite, and it can be regarded as the contribution of FC, which membrane behavior is higher as shown in Fig. 4.39(a).

Yaroshchuk (1995) provided an explanation to the correlation between membrane behavior and the DDL. According to Yaroshchuk (1995), the properties of macroscopic liquid inside the porous medium are determined by the mechanisms caused by interaction between the solid skeleton and the liquid components at the microscopic scale, such as the effect of the DDL (Yaroshchuk, 1995; Dominijanni and Manassero, 2012a). And the state variables of electrolyte solution are discontinuous between the bulk and the pore solution, which phenomenon is called partition effect (Yaroshchuk, 1995; Dominijanni and Manassero, 2012a). The partition effect suggests the inter-particle pore is independent system, and the migration of solute inside is dominated by micro-mechanism, including the effect from the DDL (Yaroshchuk, 1995; Dominijanni and Manassero, 2012a, 2012b). According to Mitchell (1993), the hydration of bentonite during swelling process involves four basic interaction mechanisms: (i) hydrogen bonding, (ii) dipole-charged surface attraction, (iii) van der Waals attraction, and (iv) hydration of exchangeable cations. For bentonite, hydration of exchangeable cations is most important, which occurs as the positively charged ions attract water dipoles, which form a hydration shell surrounding the cation (Di Emidio 2010). Because the cations are restrained by the layer charge field, their water of hydration shell is restrained as well. Secondary layers of water can H-bond with the primary layer of hydration water, forming multiple hydration shells. Beyond two or three layers, the water of these shells behaves as bulk water (Di Emidio 2010). However, such layers adsorbed by bentonite are particularly sensitive to changes in the composition of the pore fluid that influence the thickness significantly. The electrolyte with high concentration

causes the adsorbed layer to collapse, which results in the increase of interlayer space, finally leaded to the decrease of chemico-osmotic efficiency coefficient as concentration increase (Mesri and Olson 1971).

Bentonite is a kind of mineral which consist of tetrahedral and octahedral layers stacked in a 1:1 or 2:1 arrangement, and has many hydration sites since the crystal lattice (Katsumi et al., 2007; Yong et al., 2010; Dominijanni and Manassero, 2012a). According to Katsumi et al. (2007), during the hydration process, some of the water molecules are fixed and occupied the interlayer space and cause the swelling of bentonite particle, thus the pore space for solute transport was also decreased. However, when the solution concentration increases, more hydration sites are occupied by cations, which resulted in a stronger attraction force. Thus inter-particle pore for diffusion increased in response, which resulted in the decrease of membrane behavior. According to Sposito (1984), the hydration shell surrounding the cations in a DDL consists of about six water molecules for dilute solutions, but is reduced to about three water molecules for concentrated solutions. Consequently, bentonite cannot swell sufficiently, and the increase in inter-particle pores allows more solute to pass, thereby reducing the membrane behavior (Katsumi et al., 2008b).

To have a further research about the mechanism, standard swelling test were conducted by using sodium bentonite under different solutions with different conditions following ASTM D 5890-06, and the results were presented in Fig. 4.40(a)(b)(c). Consistent with the above findings as shown Fig. 4.40(a), it indicates that the free swelling volume of bentonite decreases as the KCl concentration increases (Jo et al., 2001; Gleason et al., 1997). According to Katsumi (2010), clayey soils such as bentonite provide smaller volumes for individual voids, so that the water cannot permeate as freely as it can in sandy oil due to the viscosity. In addition, DDL was also thought to contribute to the low hydraulic conductivity, since the existence of DDL can result in the liquid molecules are strongly attracted by the clay, which causes the reduction of space for liquid to permeate. Thus, as more DDL develops, lower levels of hydraulic conductivity are obtained. For the case of bentonite, Katsumi (2010) thought the adsorbed water layer by DDL and the swelling results in the extremely low hydraulic conductivity.

Figure 4.40(b) shows the free swelling of bentonite at different pH values and different concentrations. Consistent with Katsumi et al. (2008b), it was found that the free swelling volume decreased as the concentration of KCl increases. And under the same concentration condition, the free-swell volume increased as pH increased. For example, for concentrations of 10 mM and 100 mM, the free-swell volumes at pH = 12.0 were 28% and 25% greater than those at pH = 3.0, respectively. Jo et al. (2001) gave the plausible explanation that the decrease in swell volume in acid solution was due to dissolution of clay particles. As pH decreases, Al in the octahedral layers of the bentonite can dissolve by hydrolysis, resulting in the exchange of Al^{3+} for K^{+} and a decrease in the volume of bound water (Norrish and Quirk, 1954; Mathers et al., 1956; Grim, 1968). The destruction of the structure of bentonite also results in the decrease of the volume of bound water (Forster, 1953; Egloffstein, 1995).

Figure 4.40(c) shows the results of swelling test of bentonite and FC towards Ca, Na, Zn and Pb. According to the results, the Fukakusa clay almost no expands no matter the concentration of surrounding solution. For the case of bentonite, it was clear that the swelling volume under Na solution was higher than others, especially at elevated concentration. Such phenomenon was summarized as the influence of valence by Shackelford et al. (2000), and the similar trend that swelling volume decreased as valence of cation increased was also observed by Jo et al. (2001). For sodium bentonite, replacement of sodium in the exchange complex with other ions affects the thickness of the adsorbed layer, thus swelling volume of bentonite (James et al. 1997; Katsumi et al. 2008b). The higher valence cation showed the larger affect on the swelling capacity, which is consistent with the Gouy-Chapman and Stern-Gouy theories (Shackelford et al. 2000). Thus, the inter-particle pore increased as valence increased, which caused the decrease of membrane behavior that Na and K > Ca, Zn and Pb as shown in Fig. 4.39(e).

Among the divalent cations, membrane behavior towards Ca was higher than heavy metals Zn(II) and Pb(II) as Fig. 4.39(e), and in Fig. 4.40(c), the swelling volume of Ca was lower compared to heavy metals Zn(II) and Pb(II). Ruhl and Daniel (1997) studied the response of geosynthetic clay liners to permeation with various chemicals. The results showed that Ca was more aggressive than others, which was also proved by the boundary concentration in Fig. 4.33. Ca ion from dilute solutions can gradually exchange Na on the exchange complex, resulting in gradual compression of the adsorbed layer and consequent gradual decrease of membrane behavior (Ruhl and Daniel 1997; Di Emidio 2010).

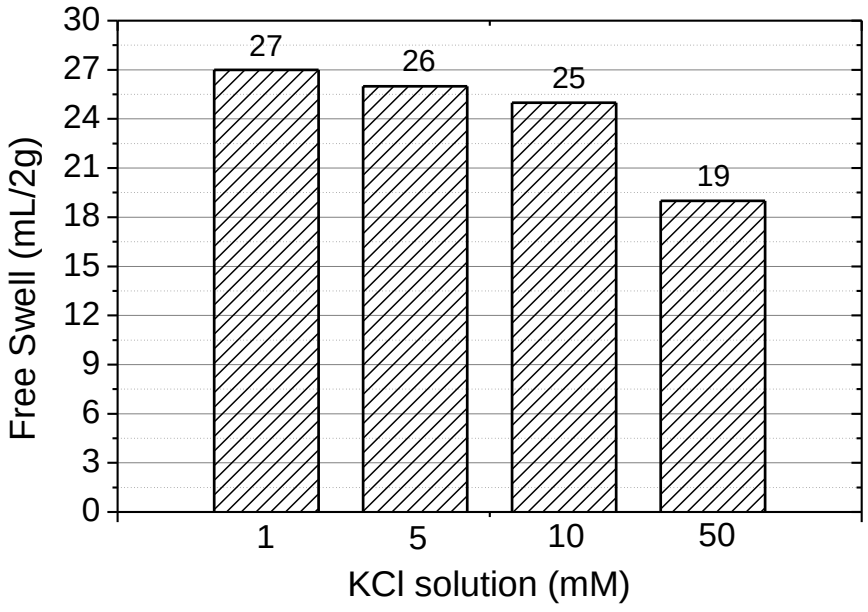

(a)

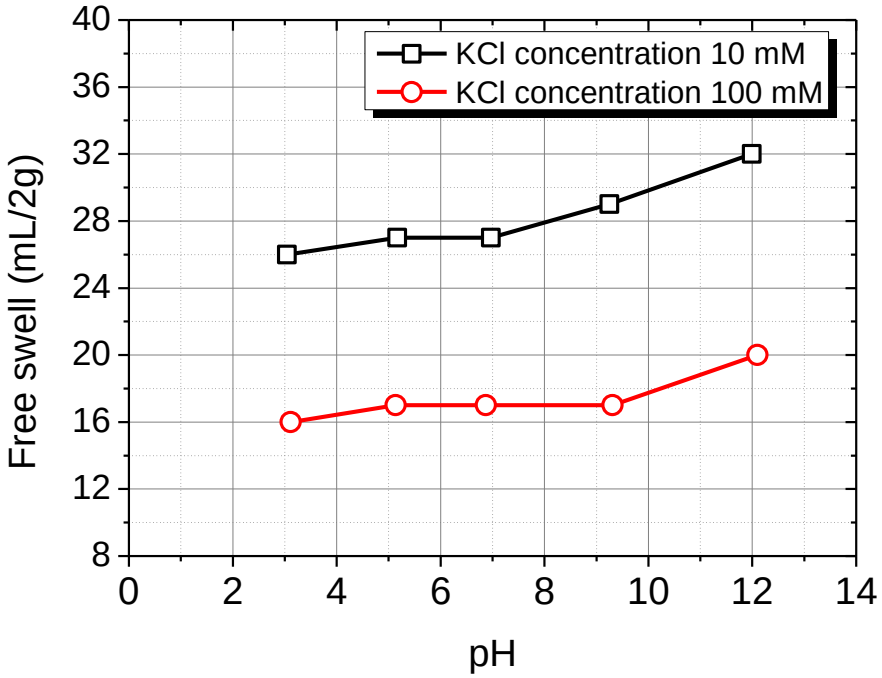

(b)

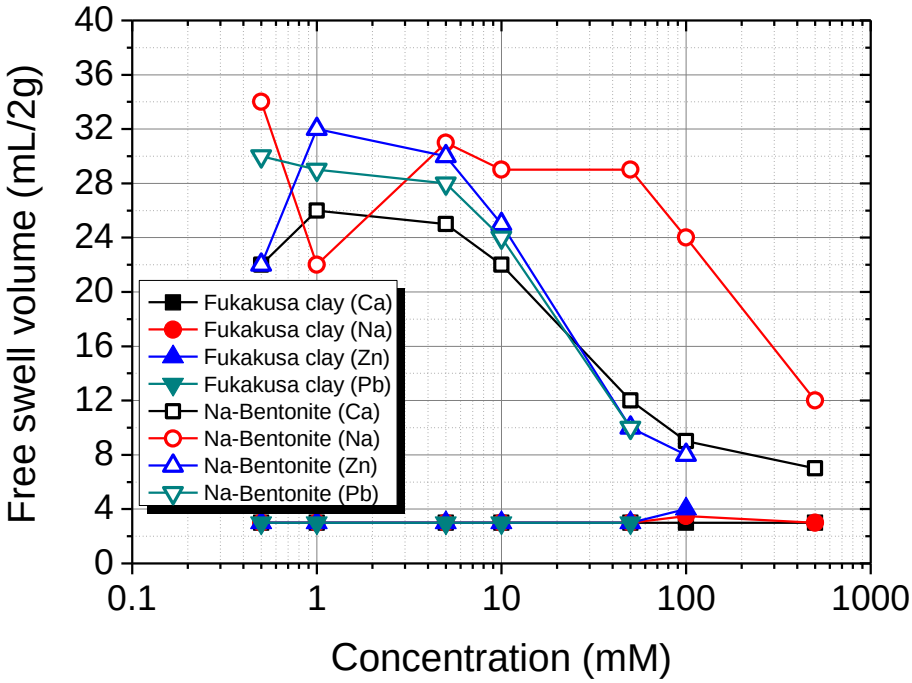

(c)

Fig. 4.40 Swelling test results of sodium bentonite: (a) Sodium bentonite towards KCl, (b) Sodium bentonite towards KCl with different pH, (c) Sodium bentonite towards Ca, Na, Zn and Pb solution

Di Emidio (2010) thought when two charged surfaces approach on another, their DDL are likely to overlap if the energetic of two surfaces favors attraction. Overlapping DDL are the normal conditions governing the behavior of clay-water systems, especially in the presence of bentonite. The region of overlapping DDL was always characterized by a relatively high concentration of cations because they are effectively restrained from diffusing to other regions (Di Emidio, 2010). In addition, continuous solute diffusion in Fig. 4.10 is also likely to be responsible for the time-dependent decrease in ΔP, as shown in Fig. 4.19. At the beginning of every stage for almost all the specimens, the concentration of KCl increases, resulting in a rapid increase in ΔP followed by a gradual reduction before reaching equilibrium. Such degrading effect of salts diffusion on chemico-osmotic pressure was also observed by Shackelford and Lee (2003). For example, when 10 mM KCl is introduced into the FC plus 20% bentonite system, the osmotic pressure reaches a peak chemico-osmotic pressure, ΔP_{peak}, of 16.8 kPa after about 1 day, but subsequently decreases to the steady value ΔP_e of 11.2 kPa. This phenomenon becomes more significant as the solute concentration increases, which should greatly reduce the ω and compress or shrink the double layers (Malusis and Shackelford, 2002b). Fig. 4.41 shows the ratio of ΔP_{peak} to the equilibrium ΔP_e (ΔP_{peak} / ΔP_e) as a function of KCl concentration for specimens with different bentonite content. As the solute concentration increases, the DDL becomes more compressed which will spent more time. It can also help to explain the time required for membrane behavior to equilibrate increase as the concentration difference increase as shown in Fig. 4.19. For the same solute concentration, the reduction in ω is largest for the specimen with the highest bentonite content. These observations confirm that in addition to being affected by the solute concentration, the DDL property is determined by the bentonite content.

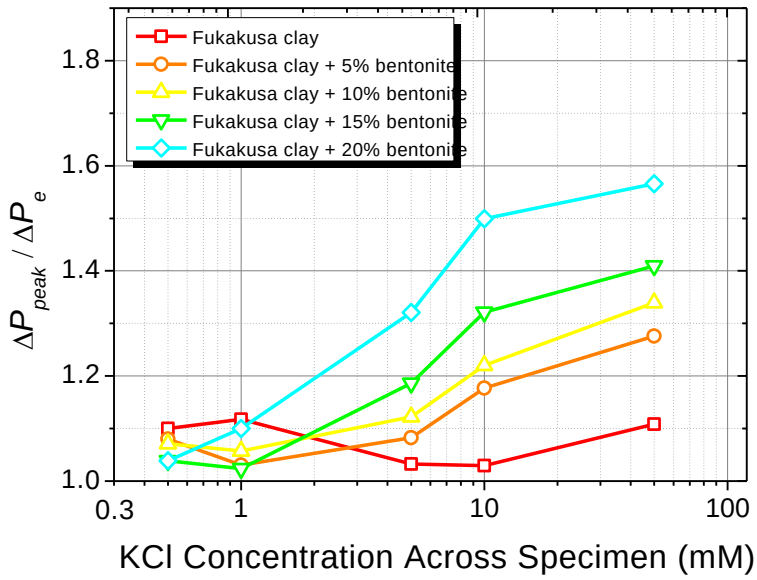

Fig. 4.41 Ratio of the peak chemico-osmotic pressure, ΔP_{peak}, to the chemico-osmotic pressure at the steady status, ΔP_e , as a function of KCl concentration

Another factor affecting the membrane behavior is the inter-particle pores. The membrane behaviors ω_{ave}, the sodium bentonite > clay-bentonite mixture > natural clay, and this order can be ascribed to the bentonite content (Benson and Trast, 1995). According to Benson and Trast (1995), the presence of more active clay minerals such as bentonite here generally corresponds to a decrease in the size of microscale pores, which control the solute transport inside soil. Consequently, it resulted in the decrease of membrane behavior ω_{ave} as bentonite decrease. Fig. 4.42 show Scanning Electron Microscope (SEM) (JSM-5510LV, JEOL, Japan) images of FC, FC plus 5%, 10%, 15%, and 20% bentonite, respectively following Vacuum-dry method. The FC‘s surface is full of tiny soil minerals and micropores, and the soil clusters lack effective cohesions as shown in Fig. 4.42(a). Bentonite plays a significant role in the adhesion of clay particles and remediates leaking. From a microstructure viewpoint, introducing bentonite causes FC to become denser, and the size of soil clusters almost two or three times bigger than that of FC, besides no micro pore was observed at the soil surface as shown in Fig 4.42(b)-(e). Hence, the lack of interparticle pores is another reason that the membrane behavior rapidly increases upon the addition of bentonite from 0 to 5%.

However, as the bentonite content increases from 5% to 20%, the change in the microstructure is rather limited, as shown in Fig 4.42(b)-(e). According to the values of ω under the same concentration conditions (Fig. 4.39a), ω follows the order of the bentonite content; FC plus 20% bentonite > FC plus 15% bentonite > FC plus 10% bentonite > FC plus 5% bentonite > FC. Thus, this phenomenon may be due to the effect of bentonite on the DDL because as the bentonite content increases, the clay–bentonite material becomes thicker and has a denser DDL, improving the membrane behavior performance.

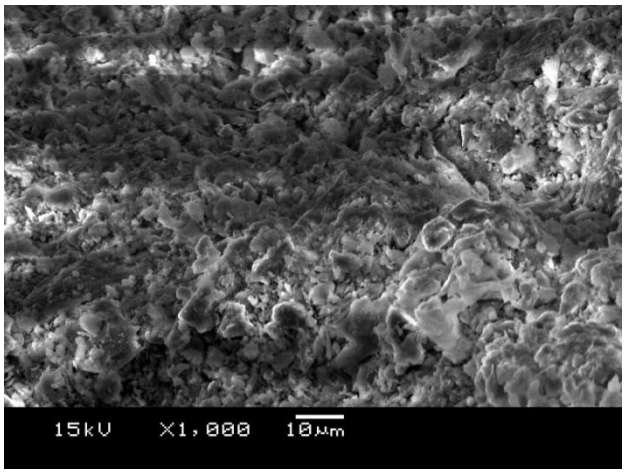

(a)

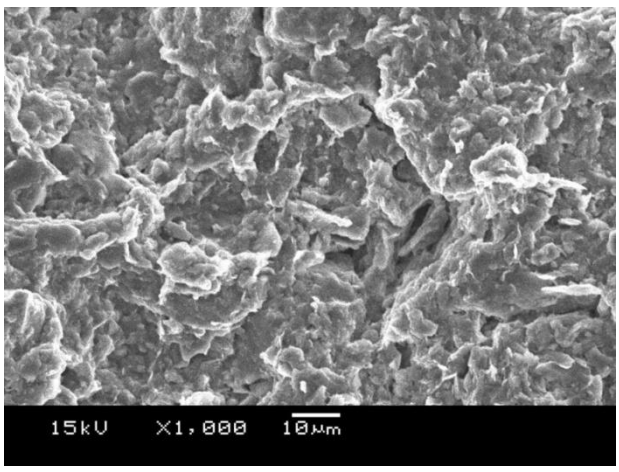

(b)

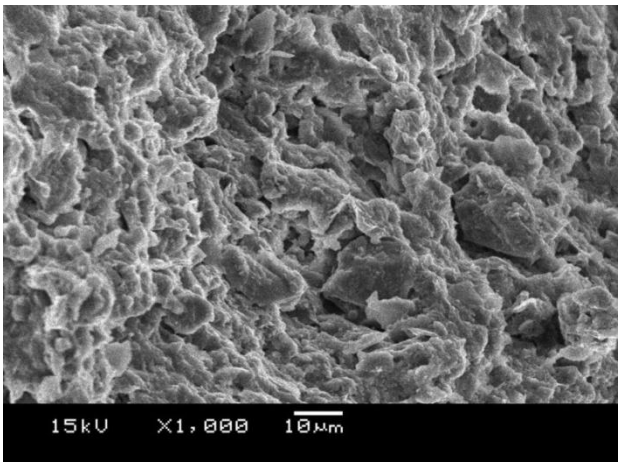

(c)

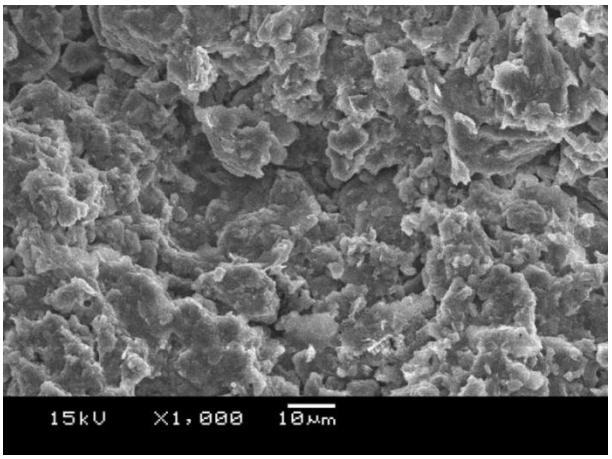

(d)

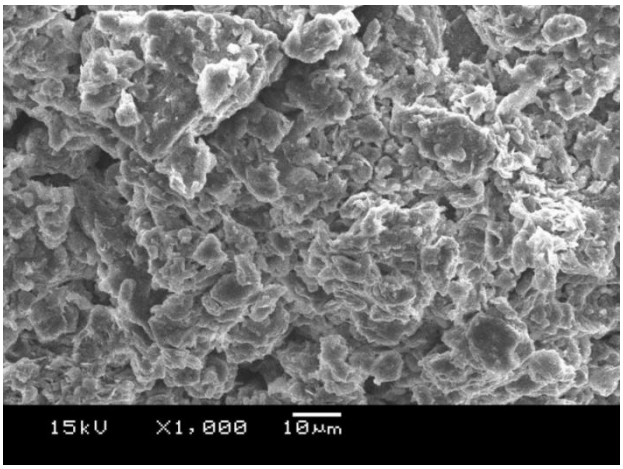

(e)

Fig. 4.42 SEM pictures of the five specimens. (a) FC; (b) FC plus 5% bentonite; (c) FC plus 10% Benton ite; (d) FC plus 15% bentonite; (e) FC plus 20% bentonite

Figure 4.43 (a)-(c) show scanning electron microscope images of the specimens after membrane tests at pH values of 4.0, 7.0, and 11.0, respectively. From the images, it is evident that the soil clusters became larger as pH increased. The average size of the soil clusters in alkaline condition was around 30 μm (Fig. 4.43c), about two to three times larger than the average size (5 to 10 μm) in acidic conditions (Fig. 4.43a). Some pores also were observed as the pH of the solution decreased to 4.0, while, in alkaline condition, the free iron ions and aluminum ions have the trend of combining with OH^- to form floccules, which are adsorptive and can block the permeable path (Crerar et al., 1981; Grathoff et al., 2007; Aspé et al., 2012). Hence, it can be inferred that the specimens became denser in the presence of alkaline solution, and the above considerations as well as the free swell shown in Fig. 4.40(b) provide a plausible explanation for the increase in membrane behaviors, ω, as pH increased.

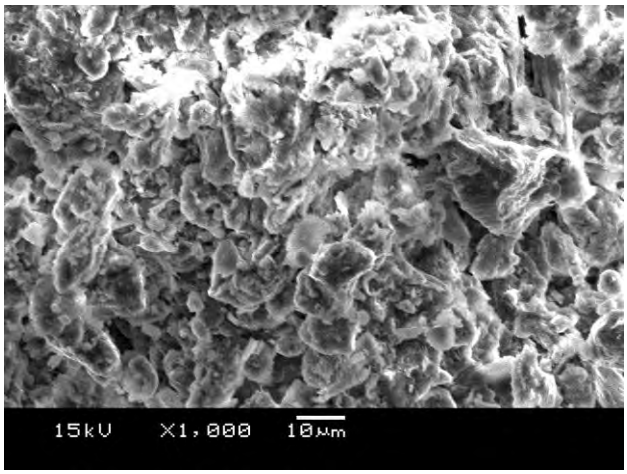

(a)

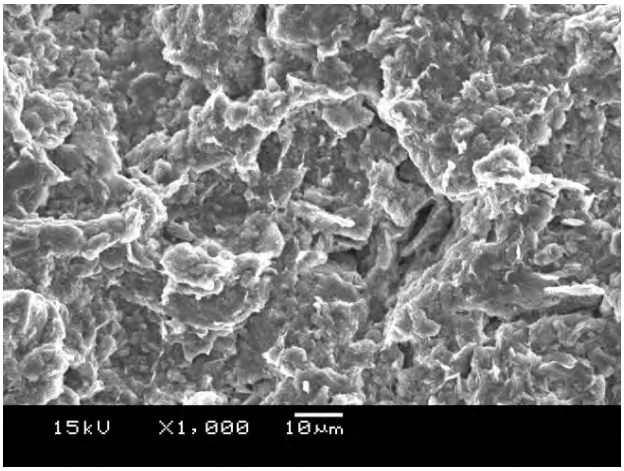

(b)

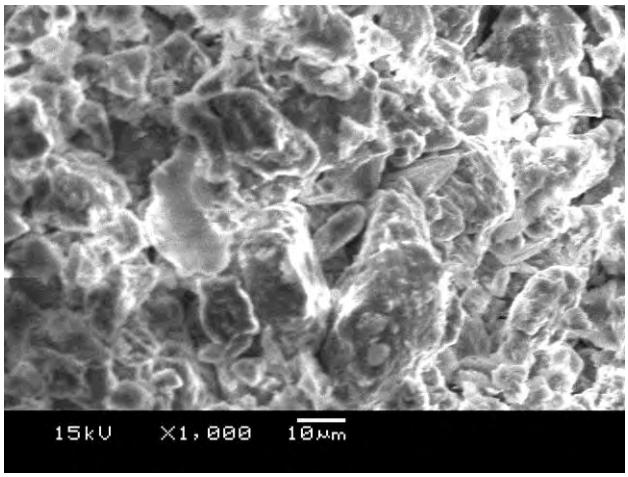

(c)

Fig. 4.43 SEM images of the three specimens at three different pH values: (a) pH = 4.0, (b) pH = 7.0, (c) pH = 11.0

According to Kooistra (1994), the pore with mean diameter > 100 μm can be distinguished macropores while the smaller pores which were considered as micropores. She showed that the micropores cannot be effectively compressed by compaction than the macroporosity. Richard et al. (2001) also pointed out that compaction can mainly reduces the volume of large pores for most soils and results the decrease of porosity, consequently affects the solution transport. Thus, it is rational to demonstrate the decrease of membrane behavior ω_{ave}, as the decrease of compactness from 100% to 80% as shown in Fig. 4.39(b).

Monnier et al. (1973) proposed another approach for porosity analysis that takes pore origin into account instead of just pore size. They considered pores within the soil to be of two types: (1) structural pores which result from tillage, traffic, weather and biological activity, and thus are affected by compaction, and (2) textural pores which result from the arrangement of the elementary soil particles. Textural pores are unaffected by compaction, which was also proved by Grimaldi

(1981). Since the existence of large amount of textural pores inside the specimens in this study which cannot be effectively compressed through compaction, it helps to explain the membrane behavior ω_{ave} cannot reach 1 in most cases, and not perfect compared to ~~"i~~deal" semipermeable membrane. The images of all three samples under different compactness were shown in Fig. 4.44 to have a further study about the change in the soil cluster packing. It is obvious that under 100% compactness, the soil clusters have very close cohesion with the assistance of bentonite, and no visible pores can be observed at the surface. And when the compactness decreased to 90%, some minor pore appeared with size around 2-3 μm. For the specimen with compaction degree 80%, some bigger pores appeared with diameter around 10-15μm. Such observation also helped to prove that the membrane behavior can be improved through the compaction method.

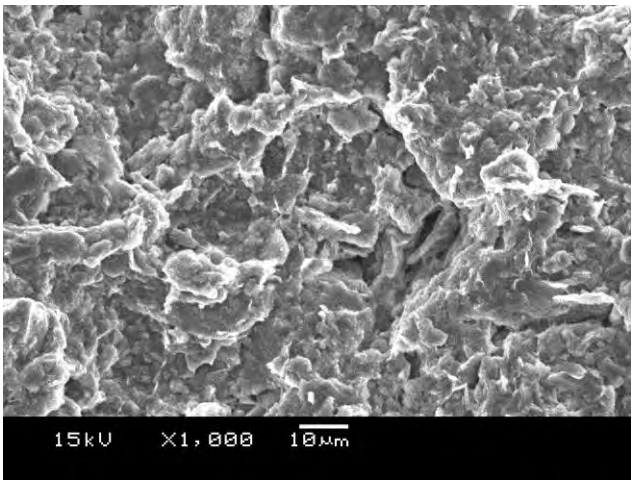

(a)

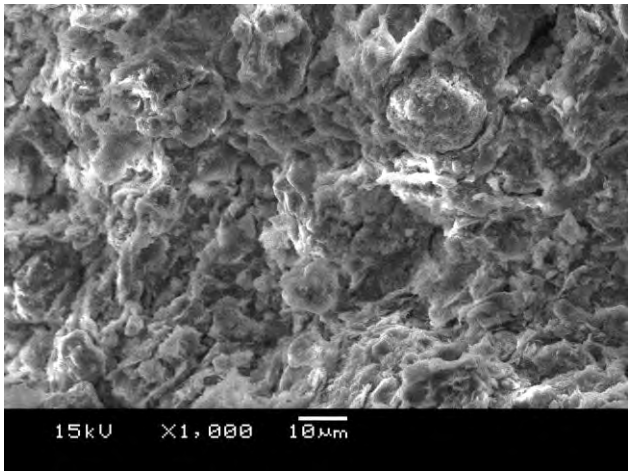

(b)

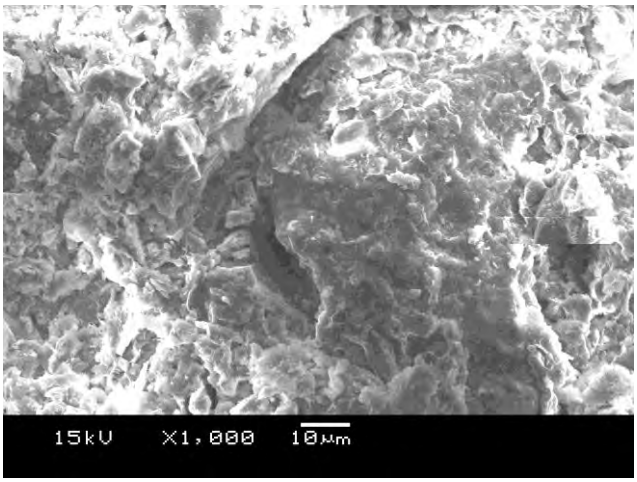

(c)

Fig. 4.44 SEM images of the three specimens at different compactness: (a) 100%, (b) 90%, (c) 80%

Figure 4.45(a)-(e) shows Scanning Electron Microscope images of specimens after membrane test towards different solutions. From the image, it‘s apparent that the size of soil clusters significantly differed, e.g. the average size of soil clusters under monovalent ions Na and K condition was almost 30 μm; And for the case of divalent ions Ca, Zn(II) and Pb(II) condition, the average size of soil clusters was less than 10 μm, e.g. the average size of soil clusters under Zn(II) condition was only 5-10 μm, and 10 μm for Pb(II). It indicated that divalent ions can cause greater shrink to the soil clusters, especially for heavy metals and some observable pores can be observed at the surface of the specimens under Ca, Zn(II) and Pb(II), which was the permeable path during the diffusion, which caused the decrease of membrane behavior. Therefore, it can be explained the relative position of average chemico-osmotic efficiency coefficient ω_{ave} that K > Na > Ca > Pb > Zn as shown in Fig. 4.39(e).

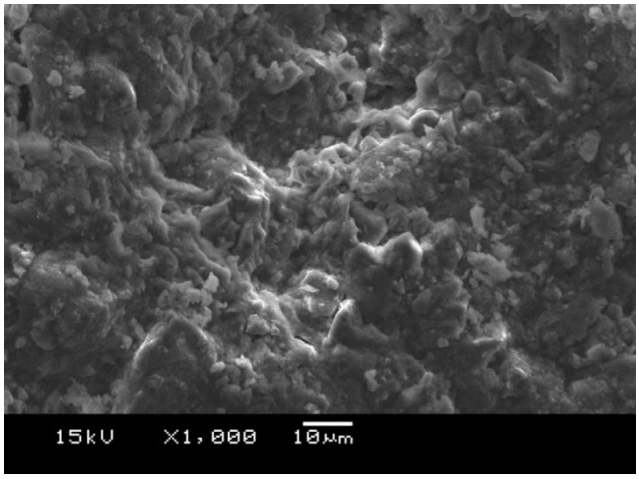

(a)

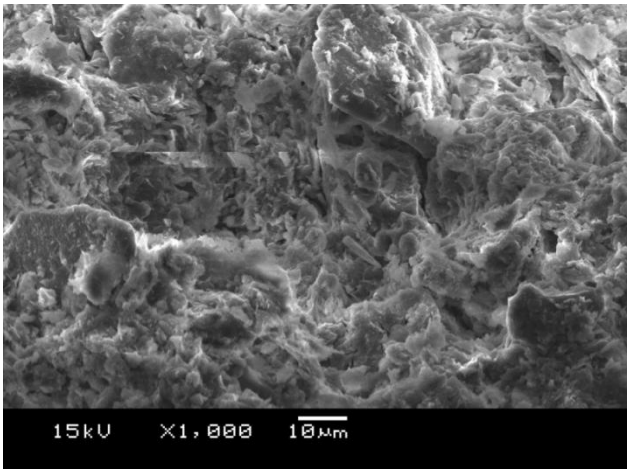

(b)

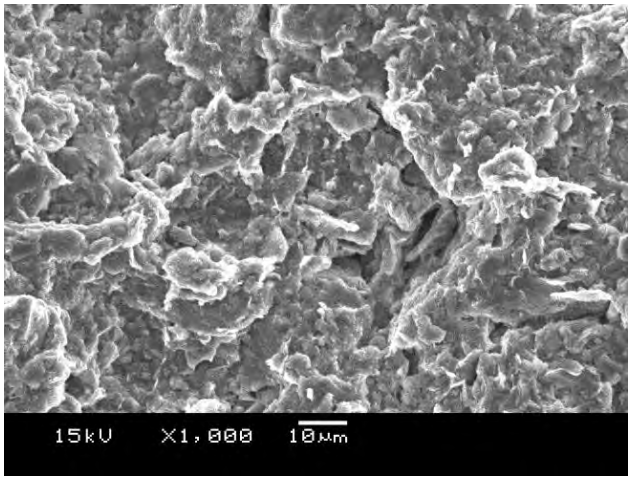

(c)

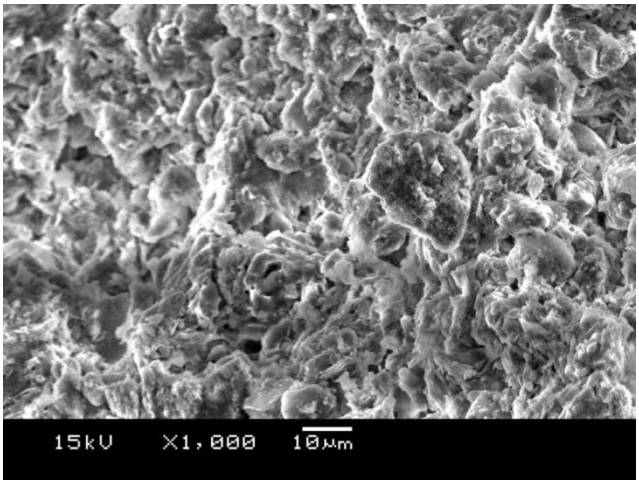

(d)

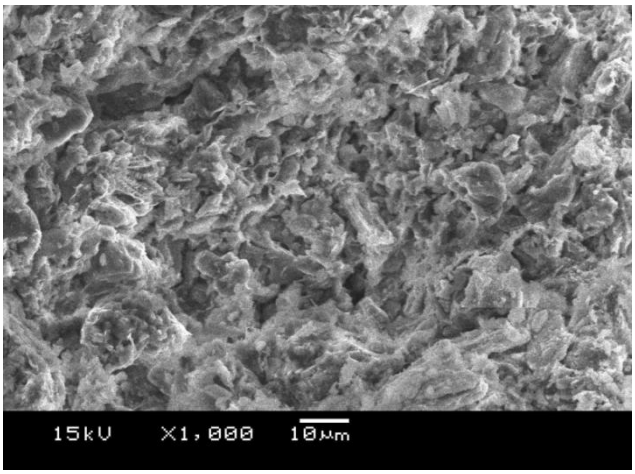

(e)

Fig. 4.45 SEM images of the specimens after membrane test: (a) Na, (b) Ca, (c) K, (d) Zn, (e) Pb

Based on the flushing data and the results of the standard test for the pH of soil, as shown in Table 4.1 and Fig. 4.9, Fukakusa clay exhibits an acidic nature. The pH of Fukakusa clay is around 3.0 – 3.2, which is significantly more acidic than normal clays, which generally have pH values greater than 7.0. We attempted to assess the abnormal characteristics of the Fukakusa clay using XRF (EDX-720, Shimadzu, Japan) and X-ray diffraction patterns (RAD-2B, Rigaku Corporation, Japan), and the results are shown in Table 4.2 and Fig. 4.46. Fig. 4.46 shows the X-ray diffraction patterns of the three samples after the membrane tests were conducted at three different pH conditions (4.0, 7.0, and 11.0). It was obvious that Fukakusa clay-bentonite composite materials contained abundant clay minerals, including montmorillonite ($2\theta = 6.42^o$, 8.94^o, 19.92^o, and 35.08^o), mica ($2\theta = 12.48^o$), quartz ($2\theta = 20.98^o$, 26.78^o, 36.68^o, 39.6^o, 40.38^o, 42.6^o, and 45.94^o), and feldspar ($2\theta = 22.12^o$ and 28.04^o). All of these clay minerals are aluminosilicate compounds ($xAl_2O_3 \cdot ySiO_2$ and $Fe_2O_3 \cdot xAl_2O_3 \cdot ySiO_2$), which contain high contents of Al and Fe, while also identified by the XRF results listed in Table 4.2. During flushing and the membrane tests, the aluminosilicate compounds likely released Fe and Al in the form of free ions, as shown in Eq. (4.10) and (4.11):

$$Fe_2O_3 \cdot xAl_2O_3 \cdot ySiO_2 \rightarrow 2Fe^{3+} + 2xAl^{3+} \quad (4.10)$$

$$xAl_2O_3 \cdot ySiO_2 \rightarrow 2xAl^{3+} \quad (4.11)$$

The free Fe and Al ions tend to bind with aqueous OH^- to form $Al(OH)_3$ and $Fe(OH)_3$ floccules (Crerar et al., 1981; Grathoff et al., 2007; Aspé et al., 2012), and the reactions can be written as:

$$Fe^{3+} + 3H_2O \leftrightarrow Fe(OH)_3\downarrow + 3H^+ \quad (4.12)$$

$$Al^{3+} + 3H_2O \leftrightarrow Al(OH)_3\downarrow + 3H^+ \quad (4.13)$$

The H^+ ions that are created in these reactions decrease the pH of the solution. Therefore, based

on Equations (4.10), (4.11), (4.12) and (4.13), we can describe the acidic nature of Fukakusa clay. However, it should be noted that Eqs (4.12) and (4.13) represent reversible reactions. Thus, flushing with distilled water can only dilute the H^+ concentration, not remove these ions completely. Thus, it is understandable that the pH of the outflow was always less than 7.0, even though, as shown in Fig. 4.9, the pH closely approached a value of 7.0 after almost 80 days of flushing before the membrane tests.

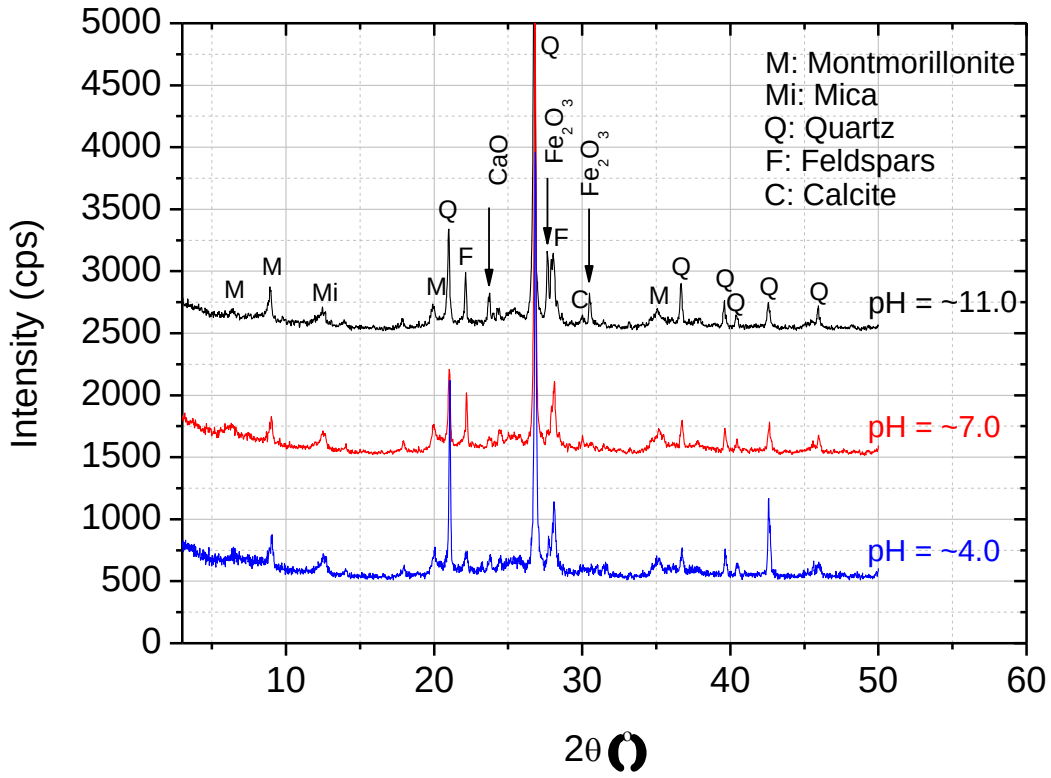

Fig. 4.46 X-ray diffraction patterns of the samples at different solution pH

Based on the XRD patterns, the characteristic peaks of calcite ($CaCO_3$) ($2\theta = 30.0^o$) and CaO ($2\theta = 23.68^o$) appeared in the alkaline condition. This information, combined with the XRF results in Table 4.2, proves the presence of these two substances. However, the two characteristic peaks of calcite and CaO disappeared in the acid condition, so the following two chemical reaction can be conjectured:

$$CaO + 2H^+ \rightarrow Ca^{2+} + H_2O \quad (4.14)$$

$$CaCO_3 + 2H^+ \rightarrow Ca^{2+} + H_2O + CO_2 \quad (4.15)$$

Figure 4.12(a) shows that these two equations can contribute to the buffer capacity of the

specimens to resist changes in pH in the acid solution. But the buffer capacity was very limited, which may have been due to the small amounts of calcite and CaO, which was demonstrated by the weak characteristic peaks in the XRD pattern. In addition, the characteristic peaks of Fe_2O_3 (2θ = 27.62° and 30.5°) were observed in the samples, as shown in the pictures of the tops of the specimens in Fig. 4.47. But, at the alkaline condition, the characteristic peaks of Fe_2O_3 no longer existed, so we can infer the following possible reactions:

$$Fe^{3+} + 3H_2O \leftrightarrow Fe(OH)_3\downarrow + 3H^+ \quad (4.16)$$

$$H^+ + OH^- \rightarrow H_2O \quad (4.17)$$

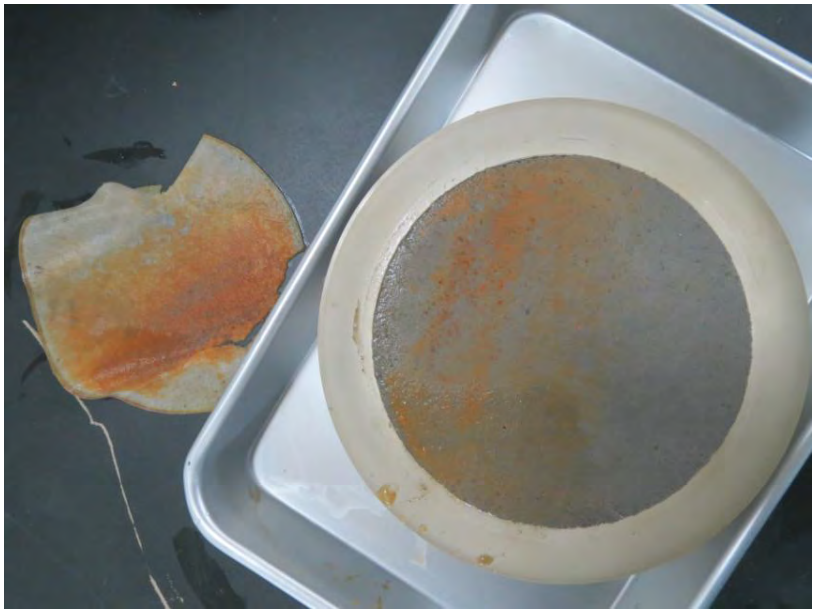

Fig. 4.47 Fe_2O_3 at the top side of specimens under alkaline condition after the membrane tests

Equation (4.16) is a reversible reaction, and, under alkaline conditions, the mass consumption of H^+ ions, as shown in Equation (4.17), caused Equation (4.16) to shift its equilibrium condition to the right, resulting in a significant increase in the production of $Fe(OH)_3$. Then, during the process of drying the samples, the following reaction occurred:

$$2Fe(OH)_3 \rightarrow 3H_2O + Fe_2O_3 \quad (4.18)$$

As a result of Equations (4.16), (4.17), and (4.18), this composite material possesses excellent buffer capacity to resist pH changes in an alkaline solution as shown in Fig. 4.12(b).

As shown in Fig. 4.39(e), for heavy metal ions Zn(II) and Pb(II), their average chemico-osmotic efficiency coefficient ω_{ave} were much lower compared to other ions. In contrast, during the membrane test, almost no diffusion of heavy metals occurred, which can be attributed to adsorption. For further studying the mechanism, X-ray diffraction was used to help analyze the specimen after

the membrane test as shown in Fig. 4.48. The characteristic peak 2θ = 6.42° represents the presence of Montmorillonite, and the weak intensity indicated the limit amount (5% by dry weight). Mica (2θ = 12.48 °), Illite (2θ = 8.96°, 17.92°, 19.68°, 23.72°), Quartz (2θ = 20.98°, 26.78°, 36.68°, 39.6°, 40.38°, 42.6° and 45.94°) and Feldspars (2θ = 28.04°) were also found.

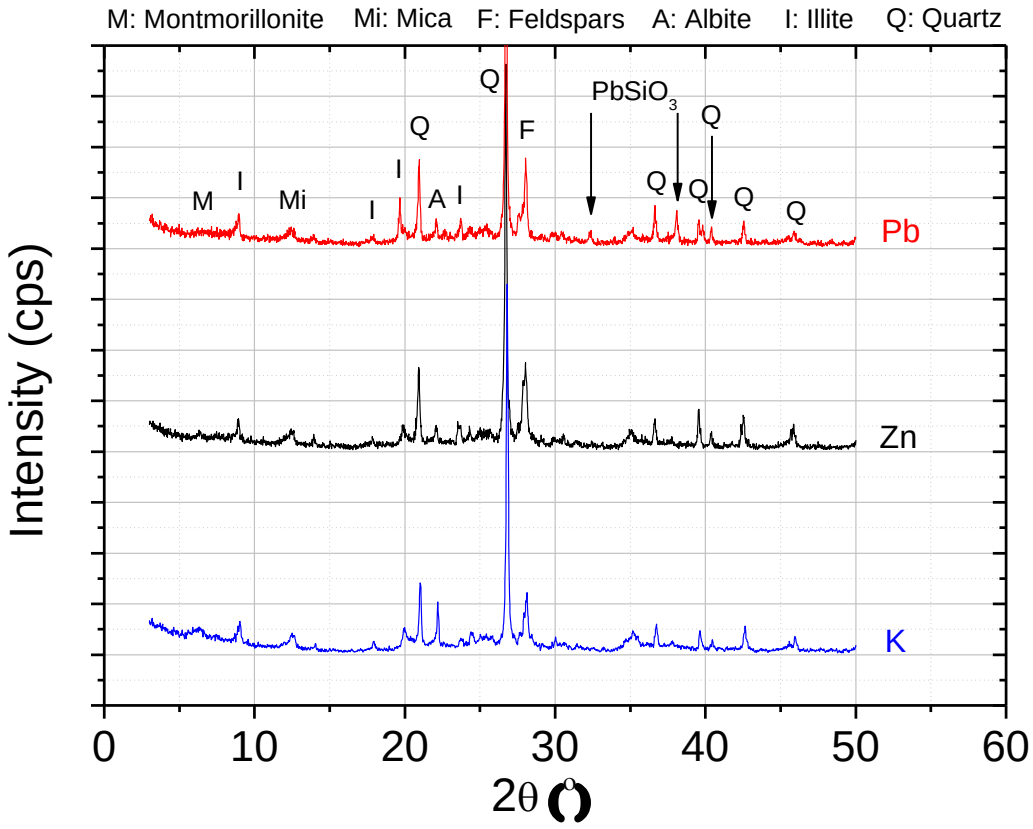

Fig. 4.48 X-ray diffraction patterns of the samples for heavy metals after membrane test

Based on XRD pattern, for specimen under Pb(II) condition, two characteristic peaks appeared at 2θ = 32.36° and 38.10°, which can be identified as $PbSiO_3$. Tang et al. (2010) thought quartz was likely to hydrolyze to form SiO_3^{2-} ion, thus it can help to explain the origin of $PbSiO_3$ as follows,

$$SiO_2 + H_2O \rightarrow SiO_3^{2-} + 2H^+ \quad (4.19)$$

$$SiO_3^{2-} + Pb^{2+} \rightarrow PbSiO_3\ (s)\downarrow \quad (4.20)$$

Since the generated $PbSiO_3$ in Eq. (4.20) was stable compound, it was rational to predict that this reaction ended until all Pb(II) be adsorbed or soil reached the maximum adsorption capacity, which was also proved by the top boundary concentration as shown in Fig. 4.17(d). Compared to that under K condition, the intensity of the characteristic peak represents albite at 2θ = 22.10° under Zn(II)

and Pb(II) condition were a little weak. Considering the pH condition around 5.0, the albite might to be expected to hydrolyze and to form quartz (SiO_2), and this can be also proved by the intensity of Quartz, which did not become weak after Eq. (4.19) and (4.20).

Since the pH condition at the top circulation during the membrane test, Pb(II) may be in the form of $Pb(OH)^+$ and the existence of lead hydroxide indicates the following precipitation reaction (Tang et al., 2009),

$$Pb^{2+} + H_2O \rightarrow Pb(OH)^+ + H^+ \quad (4.21)$$

$$Pb(OH)^+ + H_2O \rightarrow Pb(OH)_2\ (s)\downarrow + H^+ \quad (4.22)$$

Above Eq. (4.21) can be proved by Table 2, that the Pb(II) solution exhibited a acid nature. And Eq. (4.22) can help to explain the reason that pH value always decreased at the end of every stage in Fig. 4.18(d). Tang et al. (2012) refer the other possible reaction to help to explain the adsorption of Zn(II),

$$SiO_2 + 2H_2O \rightarrow SiO_4^{4-} + 4H^+ \quad (4.23)$$

$$SiO_4^{4-} + 2Zn^{2+} \rightarrow Zn_2SiO_4\ (s)\downarrow \quad (4.24)$$

Above Eq. (4.23) and (4.24) can be proved by the pH decrease at the end of every stage in Fig. 18(c).

4.5 Summary

In this chapter, a series of lab-scale experiments were conducted on locally available FC and bentonite amended FC composite materials. According to the results, the hydraulic conductivity of FC is 1.58×10^{-9} m/s, indicating that FC is not suitable for use as a compacted clay liner unless amended with bentonite. For bentonite amended clay, hydraulic conductivities are 1.07×10^{-9} m/s for FC plus 5% bentonite, 6.04×10^{-10} m/s for FC plus 10% bentonite, 2.74×10^{-10} m/s for FC plus 15% bentonite, and 8.23×10^{-11} m/s for FC plus 20% bentonite, which indicated that adding bentonite make natural FC suitable for use as a liner. According to the results of the specimens with different compactness, as compaction degree increased from 80% to 90% and 100%, the hydraulic conductivity decreased from 2.01×10^{-9} m/s to 1.49×10^{-9} m/s and 1.07×10^{-9} m/s.

Bentonite is an effective additive, and may greatly improve the membrane behavior of natural FC. When the bentonite concentration is low (C_{t0} = 0.5 mM), the values of ω for the bentonite amended clays are close to 1, suggesting an ideal membrane property. As C_{t0} increases to 5 mM, the membrane behaviors of the bentonite amended FCs are several times higher compared to FC; even at extremely high concentrations of 10 and 50 mM, bentonite amended FC still exhibits a membrane behavior of $\omega_0 > 0.20$ and $\omega_0 > 0.04$, respectively. Among the bentonite amended FCs, the membrane

behavior property typically follows the order of the bentonite content: FC plus 20% bentonite > FC plus 15% bentonite > FC plus 10% bentonite > FC plus 5% bentonite. The time required for the membrane behavior to equilibrate depends on the concentration: less than one day for a low concentration (0.5 mM), two or three days for medium concentrations (1 and 5 mM), and four or five days for high concentrations (10 and 50 mM).

pH is proved have a significant effect on the performance of the membranes, especially in alkaline conditions. When the pH of the solution was 11.0, the membrane coefficient, ω, was 1.2 - 1.3 times greater than the coefficient when the pH was 7.0 at lower concentration, and it was almost 2.5 times greater at the higher concentration. When the pH was 4.0, the membrane coefficient, ω, was 90% of the coefficient when the pH was 7.0 at lower concentration. The coefficient remained the same as the concentration increased. The similarity of the membranes‘ behaviors between pH values of 4.0 and 7.0 suggested the existence of a very slight erosion effect of the acid solution.

Compactness has proved have significant effect on membrane behavior. The membrane behavior of specimen with compactness of 100% was almost 30% higher than that with compactness of 80% under concentration difference of 5, 10 and 50 mM.

Solute type also proved great effect on membrane behaviors. And the average chemico-osmotic membrane coefficient ω_{ave} follows the order that K, Na > Ca > Pb, Zn. Ca ion is a active ion and hard to fix during the diffusion process. Although the low membrane behavior of heavy metal ions, almost no diffusion occurred during the membrane test, which can be attributed to the adsorption.

Additionally, at the beginning of every stage, introducing a higher concentration KCl solution causes a rapid increase in the chemico-osmotic pressure, which peaks at ΔP_{peak}, and then reaches an equilibrium pressure of ΔP_e, especially for specimens with different bentonite content. The difference between $\Delta P_{peak} - \Delta P_e$ increases as the solute concentration or bentonite content increases because the double layer is more compressed. The values of ω_0 based on the initial concentration and a perfect flushing boundary, are corrected to ω_{ave}. The values of ω_{ave} are slightly higher after accounting for the changes in the boundary concentrations due to solute diffusion, and in most cases, $\omega_{ave} - \omega_0 < 0.06$.

As the bentonite content increases from 0 to 5%, the membrane behavior rapidly increases, which is likely due to the decreased pore size and increased thickness of the DDL. Although increasing the bentonite content from 5% to 20% does not significantly change the pore size within the specimens, the membrane behavior slightly improves, suggesting that the DDL contributes more to the improvement of the membrane property. As the solution concentration increases, more exchange sites at the DDL are occupied by cations instead of water molecules, which strengthens the attractive forces while shrinking the DDL. Hence, the increased interparticle voids allow more solute molecules to pass, greatly reducing the membrane behavior.

Since there were large amounts of minerals in the clay, such as montmorillonite, mica, quartz, and feldspar, the Fukakusa clay-bentonite composite material releases free Al^{3+} and Fe^{3+} ions that can react in solution to form H^+, making the samples exhibit a more acidic nature.

The mechanisms that produced changes in membrane performance also were assessed and discussed using XRD patterns, free swelling volume, XRF results, SEM images, and camera images. At a pH value of 11.0, the samples exhibited better swelling performance, thus the soil clusters became larger than they were in the neutral condition, and the Fe^{3+} ions that released were likely to bind with OH^- to form floccules, which results in more narrow inter-particle space and blocks the permeable paths. Since there is a large amount of Fe in the Fukakusa clay-bentonite material, it also possessed strong buffer capacity in the alkaline solution. In contrast, at a pH value of 4.0, the soil clusters became smaller than they were in the neutral condition, and some clay minerals, such as CaO and calcite, were dissolved, which resulted in larger inter-particle spaces and permeable paths. The small amounts of CaO and calcite resulted in a very limited buffer capacity in the acid solution.

CHAPTER 5: SOLUTE TRANSPORT ANALYSIS AND PRACTICAL IMPLICATIONS

5.1 Solute transport analysis for diffusion considering membrane behavior

5.1.1 The model proposal

In geoenvironmental engineering field, the contaminant transport and fate was governed by three transport processes, including advection, diffusion and dispersion. For advection, it is also known as advective transport or convection, refers to the contaminant movement by flowing water in response to a hydraulic gradient (Sharma and Reddy, 2004). For example, when pore water containing chemicals flows under the action of a hydraulic gradient, there is a concurrent flow of chemical through the soil. This type of chemical transport is termed advection (Mitchell and Soga, 2005). The advection process is usually determined by several parameters, such as hydraulic gradient, hydraulic conductivity, porosity and effective porosity. From the macroscale level, the contaminant transport is defined by average water velocity in advection, however, when consider the dispersion process at the microscale level, the actual velocity of water may vary from point to point either lower or higher than the average velocity. The influence factors of dispersion include pore size, path length and friction in pores (Sharma and Reddy, 2004).

Differed from the above two process, diffusion refers to the movement of contaminants under a chemical concentration gradient (i.e., from an area of greater concentration toward an area of lower concentration). Diffusion can occur even when the fluid in not flowing or is lowing the direction opposite to contaminant movement and diffusion will cease only if there is no concentration gradient (Sharma and Reddy, 2004). In addition, owing to the existence of surface charges on soil particles, especially clays, there are nonuniform distributions of cations and anions within soil pores resulting from the attraction of cations to and repulsion of anions from the negatively charged particle surfaces. Because of the small pore sizes in fine-grained soils and the strong local electrical fields, clay layers exhibit membrane properties or membrane behavior. This means that the passage of certain ions and molecules through the clay may be restricted in part or in full at both microscopic and macroscopic levels (Mitchell and Soga, 2005).

The importance of the membrane behavior on the contaminant migration through mineral barriers is well known (Kemper & Rollins, 1966; Olsen, 1969; Greenberg et al., 1973; Fritz & Marine, 1983; Olsen et al., 1990; Mitchell, 1991, 1993; Shackelford, 1997; Malusis & Shackelford, 2002a, b). However, the experimental results obtained in above research have not always been thoroughly understood, particularly in terms of their theoretical implications. This can be a serious obstacle for their use in practical applications and/or for their extrapolation to any scales, conditions or boundaries that are different from those used in the laboratory investigations (Manassero and

Dominijanni, 2003).

To make the parameter about the membrane behavior better understood and for their use in practical applications, in this chapter, the theoretical numerical analysis of the osmotic effect or membrane behavior on solute transport was done consider the solute concentration and other experimental conditions.

The model used in this chapter was proposed by Manassero and Dominijanni, (2003), which tries to describe the mechanisms that govern osmotic phenomena in fine grained porous media, is based on non-equilibrium thermodynamics (Katchalsky & Curran, 1965), and take into account of all advection, diffusion and dispersion process. The membrane behavior on solute transport was also reflected by parameter chemico-osmotic efficiency coefficient ω, and the expressions of the molar flow of the solvent and solute can be written as following Eq. (5.1) and (5.2) (Manassero and Dominijanni, 2003):

$$J_v = \frac{k}{V_w \gamma}[\nabla(-P) - \omega RT\nabla(-c_s)] \tag{5.1}$$

$$J_s = (1-\omega)\{\frac{c_s k}{\gamma}[\nabla(-P) - \omega RT\nabla(-c_s)] + n\tau D_0 \nabla(-c_s)\} \tag{5.2}$$

Where J_v is the molar flow of the solvent and J_s is the solute flow rate; k is the hydraulic conductivity of the porous medium, V_w is the partial molar volume of the solvent (the volume occupied by a mole of the solvent in the solution), γ is the unit weight of the solution (equal to the unit weight of the solvent for practical purposes), P represents the hydraulic pressure, ω is chemico-osmotic efficiency coefficient which reflect the membrane behavior, R is the universal gas constant, T is the absolute temperature, c_s is the molar concentration of the solute; n is the effective or connected porosity of the soil skeleton, which represented by the interconnected voids related to the motion of pore fluids. D_0 is the diffusivity in free solution and τ is a tortuosity factor given by the squared ratio of the straight-line macro-scopic distance between two points along a solute molecule migration path, to the actual length of the same solute molecule migration path (Porter et al., 1960).

The mathematical model is considered to be an open system consisting of a solute and solvent flowing in the pores of a soil, and some assumptions are as follows (Manassero and Dominijanni, 2003)

(a) One-dimensional flow

(b) Solid skeleton and solvent incompressibility

(c) Isothermal conditions

(d) No electrical or electromagnetic gradients

(e) Electrically uncharged species or no chemical dissociation of the solute and bulk electro-neutrality

(f) Sufficiently diluted solution so that ideal solution relationships are valid, and the volume flow

rate of the solution is roughly equal to the volume flow rate of the solvent

(g) Complete saturation

(h) Applicability of the postulates of irreversible thermodynamics.

Considered the assumed rigid skeleton for the porous medium, incompressible solvent and the continuity of solvent flux, as well as the mass balance for the solute (Freeze and Cherry, 1979), the general differential equations that describe the evolution in space and time of the solute concentration and solution pressure can be obtained as follows (Manassero and Dominijanni, 2003),

$$\omega RT\frac{\partial^2 c_s}{\partial x^2}-\frac{\partial^2 P}{\partial x^2}=0 \tag{5.3}$$

$$R_d\frac{\partial c_s}{\partial t}=(1-\omega)\{[\tau D_0-\frac{k\omega RT}{\gamma n}c_s]\frac{\partial^2 c_s}{\partial x^2}-\frac{k}{\gamma n}\frac{\partial}{\partial x}(-\frac{\partial P}{\partial x}c_s)-\omega\frac{kRT}{\gamma n}(\frac{\partial c_s}{\partial x})^2\} \tag{5.4}$$

Consider that there is no hydraulic gradient applied during the membrane test, the above differential equation group can be solved and the solution was written as follows,

$$R_d\frac{\partial c_s}{\partial t}=(1-\omega)D^*\frac{\partial^2 c_s}{\partial x^2} \tag{5.5}$$

As shown in above Eq. (5.5), D^* also accounts for tortuosity in the soils and can be related to diffusivity in free solution D_0 as follows (Sharma and Reddy, 2004; Mitchell and Soga, 2005),

$$D^*=\tau D_0 \tag{5.6}$$

D^* can be determined by laboratory tests using the steady-state method, time-lag method and transient method as described by Rowe et al., (1988), Shackelford and Daniel, (1991) and Sharma and Lewis, (1994).

5.1.2 Initial input parameters

To have a further numerical analysis by using Eq. (5.5), the adopted boundary conditions and the main parameters of the mineral barrier are assumed and reported in Table 5.1 as follows.

As shown in above Table 5.1 and Table 5.2, the parameters solvent unit weight, hydraulic gradient, absolute temperature and chemico-osmotic efficiency coefficient are data measured in this study, while the values of effective diffusion coefficient and retardation factor are data recommended by Manassero and Dominijanni, (2003).

Table 5.1 Input parameters adopted for result analysis (Consider membrane behavior)

		Unit	Value
Parameters			
Solvent (water) unit weight	γ	kN/m^3	10
Hydraulic gradient	i_h		0
Effective diffusion coefficient	D^*	m^2/s	2.00×10^{-10}
Retardation factor	R_d		1
Barrier thickness	L	m	1
Absolute temperature	T	K	293
Chemico-osmotic efficiency coefficient	ω		Table 5.2
Boundary conditions			
Entrance boundary condition	$c_s(x = 0, t) = c_0$	M	0.0005, 0.001, 0.005, 0.01 and 0.05
Exit boundary condition	$\frac{\partial c_s}{\partial x}(x = L, t)$	M/m	0
Initial condition	$c_s(x, t = 0)$	M	0

Table 5.2 Input ω values for results analysis

ω	0.5 mM	1 mM	5 mM	10 mM	50 mM
Fukakusa Clay	0.85	0.35	0.12	0.07	0.02
FC+5% bentonite	0.99*	0.63	0.42	0.23	0.05
FC+10% bentonite	0.99*	0.66	0.39	0.24	0.05
FC+15% bentonite	0.99*	0.8	0.41	0.25	0.06
FC+20% bentonite	0.99*	0.59	0.43	0.26	0.07

* Since the original values are higher than 1, assumed ω at 0.99 for results analysis

5.1.3 Results

Based on Eq. (5.5), the breakthrough curves of specimens under different experimental conditions were obtained and shown in following Fig. 5.1 (a)-(e).

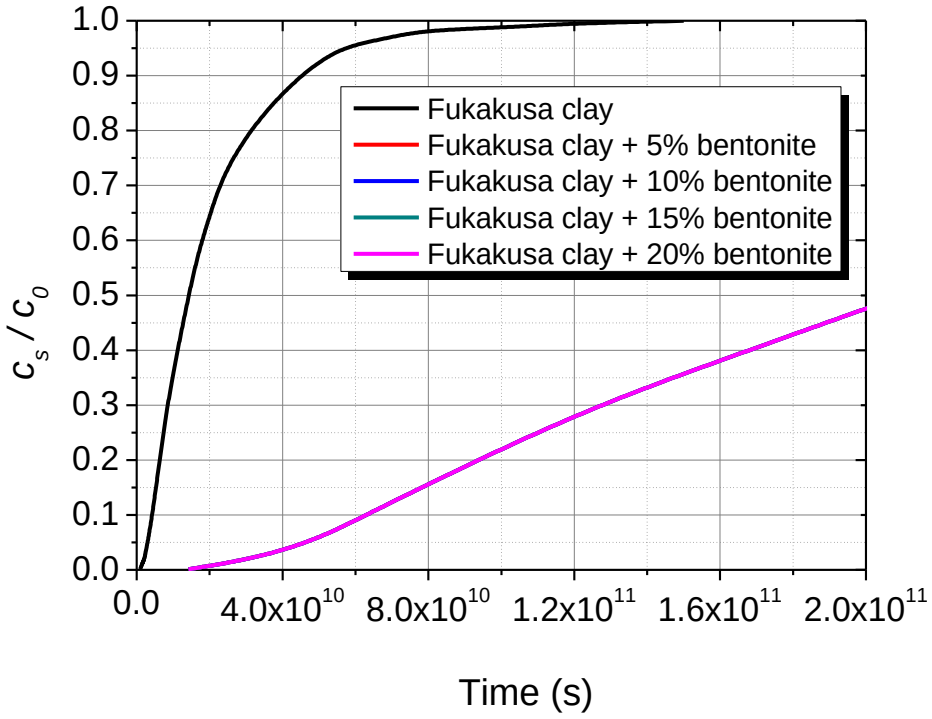
1.0
0.9
0.8
0.7
0.6
0.5
0.4
0.3
0.2
0.1
0.0
c_s / c_0
Fukakusa clay
Fukakusa clay + 5% bentonite
Fukakusa clay + 10% bentonite
Fukakusa clay + 15% bentonite
Fukakusa clay + 20% bentonite
0.0
4.0x10^10
8.0x10^10
1.2x10^11
1.6x10^11
2.0x10^11
Time (s)

(a)

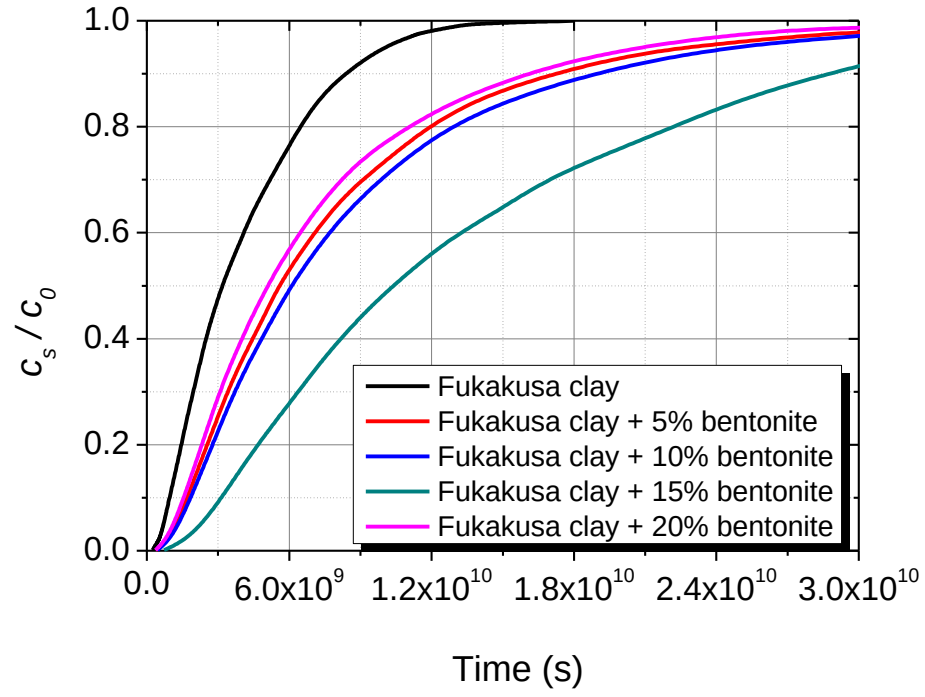
1.0
0.8
0.6
0.4
0.2
0.0
c_s / c_0
Fukakusa clay
Fukakusa clay + 5% bentonite
Fukakusa clay + 10% bentonite
Fukakusa clay + 15% bentonite
Fukakusa clay + 20% bentonite
0.0
6.0x10^9
1.2x10^10
1.8x10^10
2.4x10^10
3.0x10^10
Time (s)

(b)

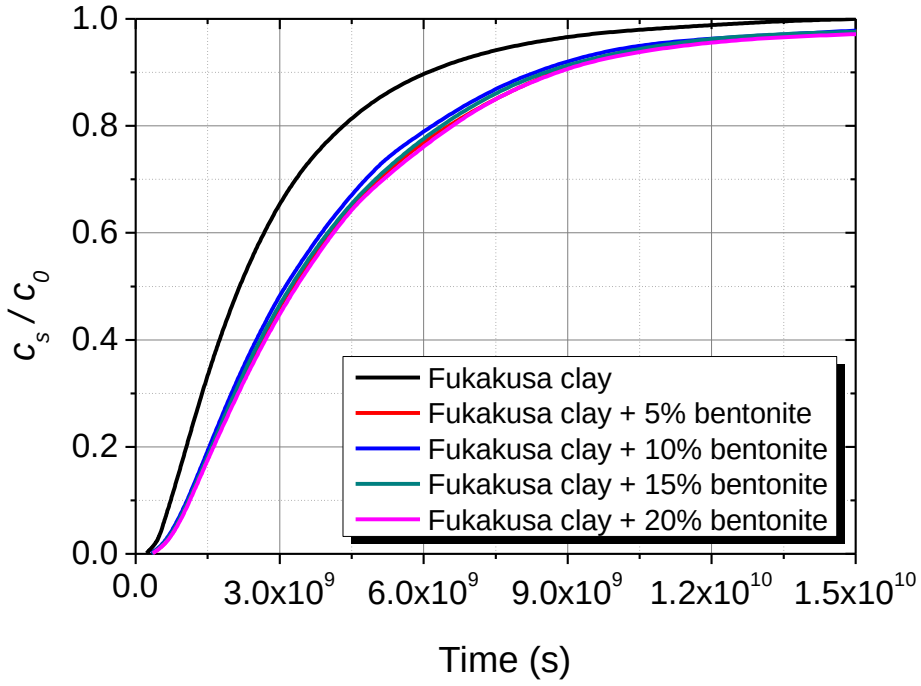
1.0
0.8
0.6
0.4
0.2
0.0
c_s / c_0
0.0
3.0x10^9
6.0x10^9
9.0x10^9
1.2x10^10
1.5x10^10
Time (s)
Fukakusa clay
Fukakusa clay + 5% bentonite
Fukakusa clay + 10% bentonite
Fukakusa clay + 15% bentonite
Fukakusa clay + 20% bentonite

(c)

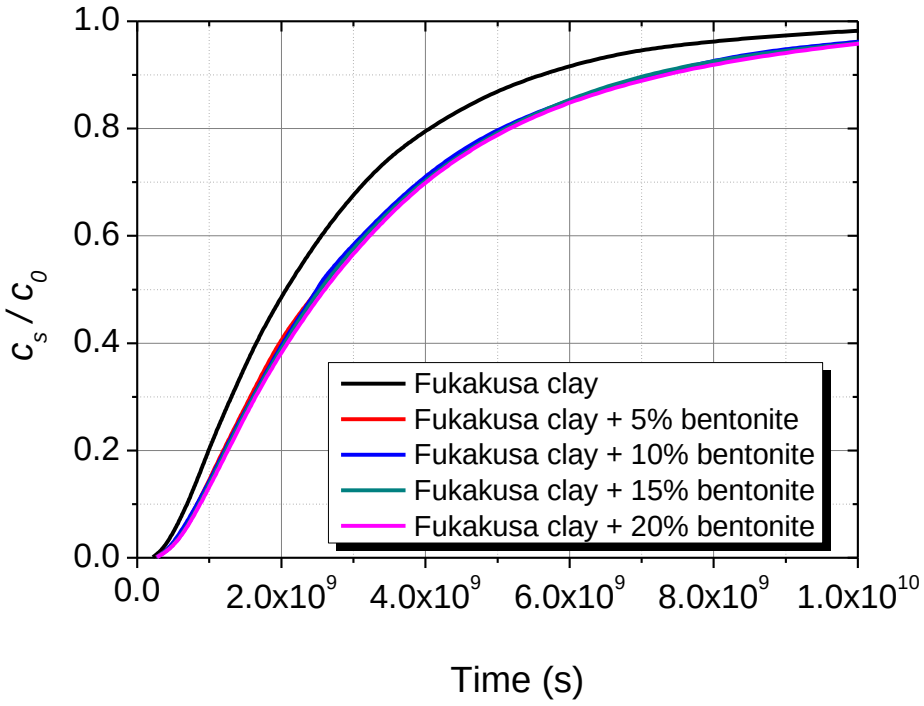
1.0
0.8
0.6
0.4
0.2
0.0
c_s / c_0
0.0
2.0x10^9
4.0x10^9
6.0x10^9
8.0x10^9
1.0x10^10
Time (s)
Fukakusa clay
Fukakusa clay + 5% bentonite
Fukakusa clay + 10% bentonite
Fukakusa clay + 15% bentonite
Fukakusa clay + 20% bentonite

(d)

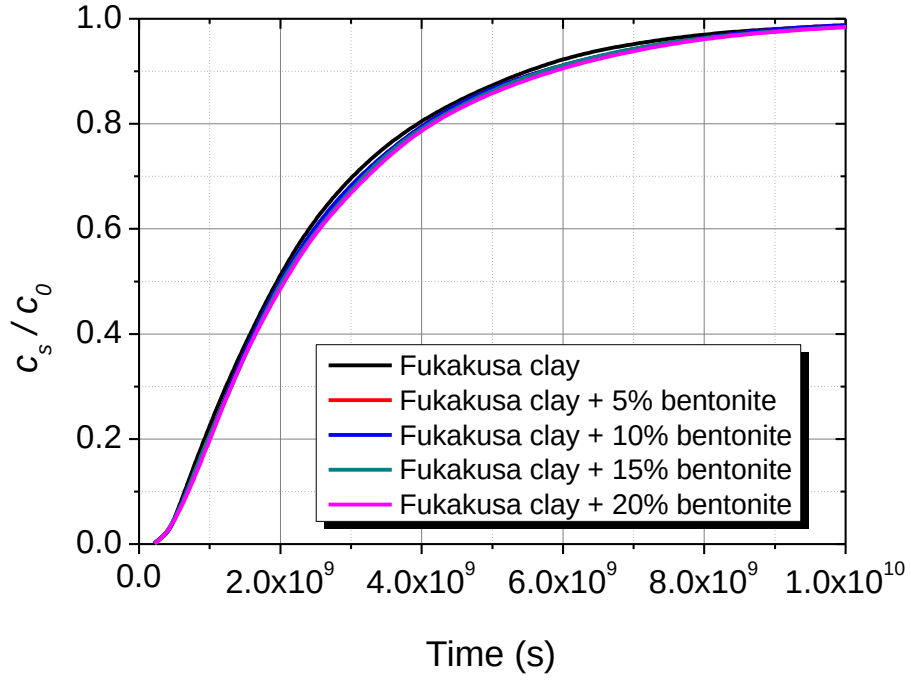

(e)

Fig. 5.1 Breakthrough curves for FC bentonite material: (a) 0.5 mM, (b) 1 mM, (c) 5 mM, (d) 10 mM, (e) 50 mM

5.2 Solute transport analysis for advection neglecting membrane behavior

5.2.1 The model proposal

The model used in this chapter was same as previous section 5.1, proposed by Manassero and Dominijanni, (2003), which take into account of all advection, diffusion and dispersion process as well as the membrane behavior. The expressions of the molar flow of the solvent and solute can be written as following Eq. (5.1) and (5.2) (Manassero and Dominijanni, 2003):

$$J_v = \frac{k}{V_w \gamma}[\nabla(-P) - \omega RT\nabla(-c_s)] \tag{5.1}$$

$$J_s = (1-\omega)\{\frac{c_s k}{\gamma}[\nabla(-P) - \omega RT\nabla(-c_s)] + n\tau D_0 \nabla(-c_s)\} \tag{5.2}$$

Where J_v is the molar flow of the solvent and J_s is the solute flow rate; k is the hydraulic conductivity of the porous medium, V_w is the partial molar volume of the solvent (the volume occupied by a mole of the solvent in the solution), γ is the unit weight of the solution (equal to the unit weight of the solvent for practical purposes), P represents the hydraulic pressure, ω is chemico-osmotic efficiency

coefficient which reflect the membrane behavior, R is the universal gas constant, T is the absolute temperature, c_s is the molar concentration of the solute; n is the effective or connected porosity of the soil skeleton, which represented by the interconnected voids related to the motion of pore fluids. D_0 is the diffusivity in free solution and τ is a tortuosity factor given by the squared ratio of the straight-line macro-scopic distance between two points along a solute molecule migration path, to the actual length of the same solute molecule migration path (Porter et al., 1960).

Considered the assumed rigid skeleton for the porous medium, incompressible solvent and the continuity of solvent flux, as well as the mass balance for the solute (Freeze and Cherry, 1979), the general differential equations that describe the evolution in space and time of the solute concentration and solution pressure can be obtained as follows (Manassero and Dominijanni, 2003),

$$\omega RT\frac{\partial^2 c_s}{\partial x^2}-\frac{\partial^2 P}{\partial x^2}=0 \tag{5.3}$$

$$R_d\frac{\partial c_s}{\partial t}=(1-\omega)\{[\tau D_0-\frac{k\omega RT}{\gamma n}c_s]\frac{\partial^2 c_s}{\partial x^2}-\frac{k}{\gamma n}\frac{\partial}{\partial x}(-\frac{\partial P}{\partial x}c_s)-\omega\frac{kRT}{\gamma n}(\frac{\partial c_s}{\partial x})^2\} \tag{5.4}$$

Assuming that there is no membrane behavior exist during the membrane test ($\omega = 0$), the above differential equation group can be solved and the solution was written as follows,

$$R_d\frac{\partial c_s}{\partial t}=\tau D_0\frac{\partial^2 c_s}{\partial x^2}-\frac{ki_h}{n}\frac{\partial c_s}{\partial x} \tag{5.7}$$

As shown in above Eq. (5.7), D^* also accounts for tortuosity in the soils and can be related to diffusivity in free solution D_0 as previous Eq. (5.6) (Sharma and Reddy, 2004; Mitchell and Soga, 2005),

$$D^*=\tau D_0 \tag{5.6}$$

5.2.2 Initial input parameters

To have a further numerical analysis by using Eq. (5.7), the adopted boundary conditions and the main parameters of the mineral barrier are assumed and reported in Table 5.3 as follows.

As shown in above Table 5.3 and Table 5.4, the parameters solvent unit weight, hydraulic gradient, absolute temperature and hydraulic conductivity are data measured in this study, while the porosity, values of effective diffusion coefficient and retardation factor are data recommended by Manassero and Dominijanni, (2003). The thickness of barrier was assumed as 1 m, consider the actual thickness of CCL applied in practice.

Table 5.3 Input parameters adopted for result analysis (Neglect membrane behavior)

		Unit	Value
Parameters			
Solvent (water) unit weight	γ	kN/m^3	10
Hydraulic gradient	i_h		1, 2, 5 and 10
Effective diffusion coefficient	D^*	m^2/s	2.00×10^{-10}
Retardation factor	R_d		1
Barrier thickness	L	m	1
Absolute temperature	T	K	293
Hydraulic conductivity	k	m/s	Table 5.4
Porosity	n		0.7
Boundary conditions			
Entrance boundary condition	$c_s(x = 0, t) = c_0$	M	0.005
Exit boundary condition	$\frac{\partial c_s}{\partial x}(x = L, t)$	M/m	0
Initial condition	$c_s(x, t = 0)$	M	0

Table 5.4 Input hydraulic conductivities for results analysis

	Hydraulic conductivity (m/s)
Fukakusa Clay	1.58×10^{-9}
FC+5% bentonite	1.07×10^{-9}
FC+10% bentonite	6.04×10^{-10}
FC+15% bentonite	2.74×10^{-10}
FC+20% bentonite	8.23×10^{-11}

5.2.3 Results

Based on Eq. (5.7), the breakthrough curves of specimens under different experimental conditions were obtained and shown in following Fig. 5.2 (a)-(d).

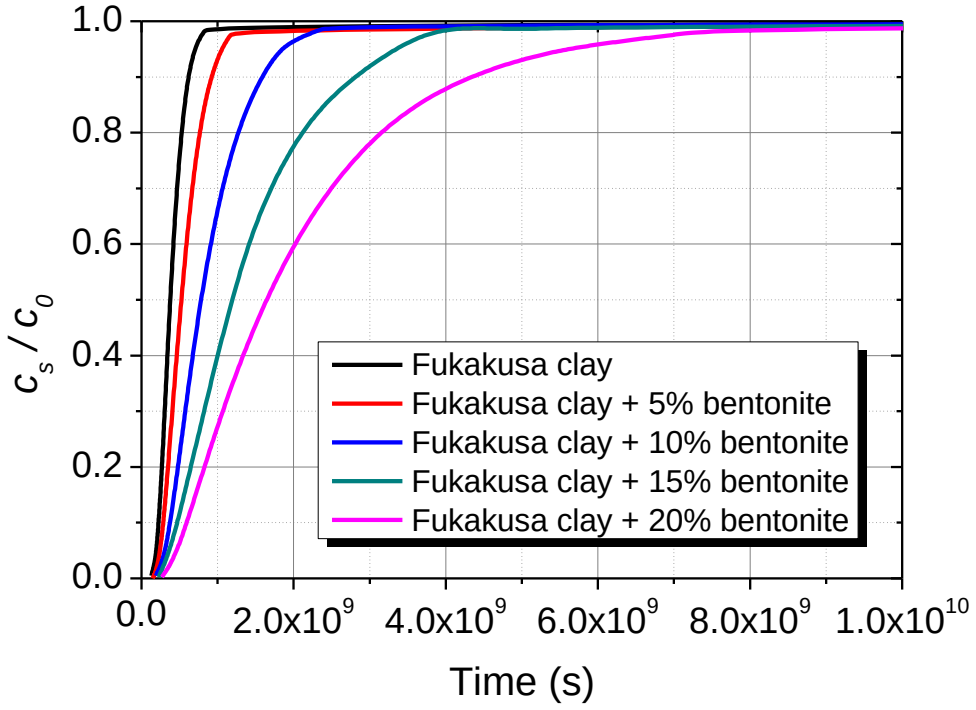
1.0
0.8
0.6
0.4
0.2
0.0
c_s / c_0
0.0
2.0x10^9
4.0x10^9
6.0x10^9
8.0x10^9
1.0x10^10
Time (s)
Fukakusa clay
Fukakusa clay + 5% bentonite
Fukakusa clay + 10% bentonite
Fukakusa clay + 15% bentonite
Fukakusa clay + 20% bentonite

(a)

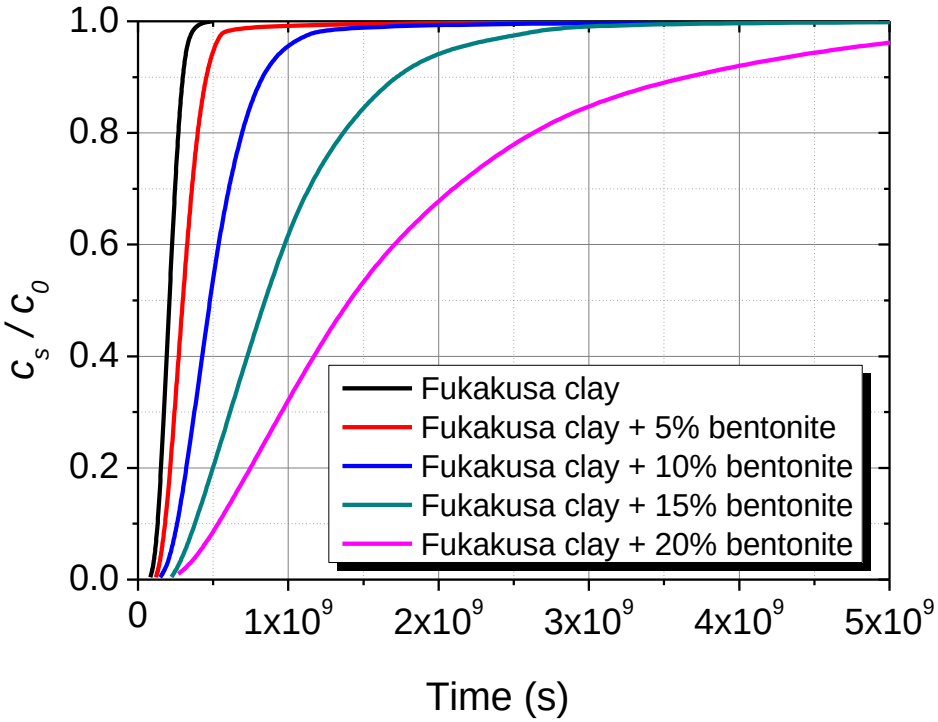
1.0
0.8
0.6
0.4
0.2
0.0
c_s / c_0
0
1x10^9
2x10^9
3x10^9
4x10^9
5x10^9
Time (s)
Fukakusa clay
Fukakusa clay + 5% bentonite
Fukakusa clay + 10% bentonite
Fukakusa clay + 15% bentonite
Fukakusa clay + 20% bentonite

(b)

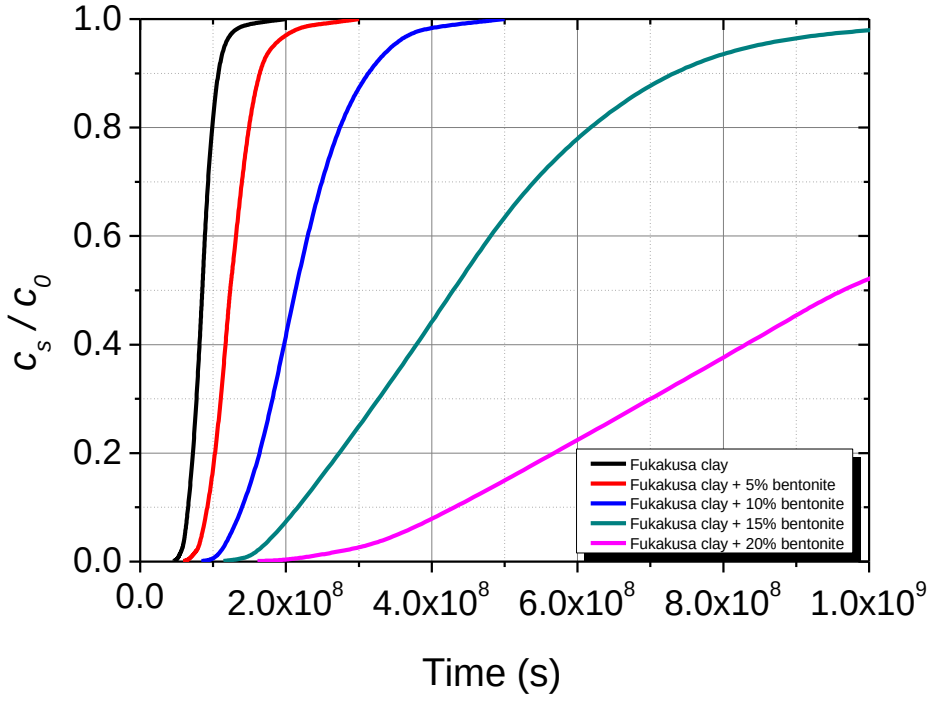

(c)

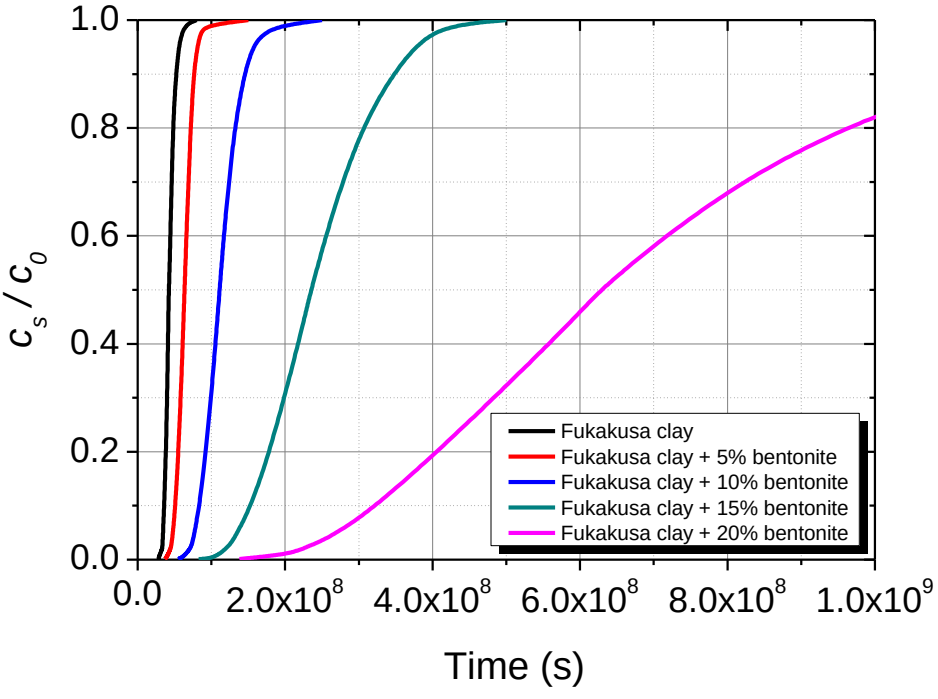

(d)

Fig. 5.2 Breakthrough curves for FC bentonite material under different gradient: (a) 1, (b) 2, (c) 5, (d) 10

5.3 Results discussions and prediction towards the service life of bottom liner

As the increase of life style and the development of industry and economy, more and more household waste and solid waste are produced in the past 30 years, especially in developing countries, such as China, Vietnam, Bangladesh, India etc. Limited by the economical status and the technology level, landfill is the predominant choice, and thus a large number of modern sanitary landfill sites are still urgently neededfor minimizing the negative environmental impact and the threaten to humans‘ health.

For the material of bottom liners system, GCL, geomembrane and other geotexile composite material has already proved most effective in cut off the migration of contaminant around the world. However, consider the expense and technology limit, pure CCL is still applied commonly especially in rural areas in those developing countries. Unlike geomembrane or some geotexile material which can serve for hundreds to thousands of years, the service life of CCL is always less than 100 years (Rowe and Hoor, 2009; Rowe and Islam, 2009). Compared to other materials, the barrier performance of CCL is more sensitive to external and environmental conditions, such as the solute concentration, solute type, the compactness, hydraulic gradient of leachate etc.

According to the laboratory-scale experiment conducted in Chapter 4 in this study, we can have a deeper understand the barrier performance of the CCL. According to the results, bentonite has proved an effective additive to improve the barrier performance through both hydraulic conductivity and membrane behavior to prevent the migration of contaminant. For membrane behavior of bottom liner, the bentonite content, leachate concentration, leachate pH, the compactness, thickness and composition of leachate were found to have significant effect on barrier performance. In addition, the mechanism of membrane behavior was discussed from macro and micro scale with assistance of XRF, XRD, SEM and method.

The achievement in this study is promising in application during the landfill site design process, especially designing the bottom liners system. As above Section 5.1 and 5.2 exhibited the method for result analysis, and based on the calculation results in Fig. 5.1, the service life of bottom liners system can be predicted as shown in following Table 5.5.

Table 5.5 Prediction of the service life of landfill liner (Consider the membrane behavior)

Bentonite content	Concentration	0.5 mM	1 mM	5 mM	10 mM	50 mM
0%	$t_{0.001}$ (year)	29.8	7.4	7.2	7.0	6.7
5%		450.0	12.7	11.1	8.3	6.9
10%		450.0	13.9	10.3	8.4	6.9
15%		450.0	23.0	10.8	8.6	7.0
20%		450.0	11.7	11.4	8.8	7.1
0%	$t_{0.02}$ (year)	66.0	15.8	13.6	12.9	12.2
5%		1015.0	28.2	20.7	15.6	12.6
10%		1015.0	30.1	19.6	15.8	12.6
15%		1015.0	52.0	20.3	16.0	12.7
20%		1015.0	25.1	21.2	16.2	12.8
0%	$t_{0.5}$ (year)	452.8	101.5	68.8	65.9	61.4
5%		6741.5	174.7	103.9	79.6	63.4
10%		6741.5	193.6	99.0	79.6	63.4
15%		6741.5	329.8	101.9	79.6	49.3
20%		6741.5	162.7	105.4	81.6	65.4
0%	t_1 (year)	3779.8	440.1	414.4	384.0	367.8
5%		48991.6	1407.9	770.5	533.4	374.2
10%		48991.6	1577.2	845.4	595.8	374.2
15%		48991.6	1642.6	868.8	613.9	378.0
20%		48991.6	1597.2	945.3	634.2	384.0

Note: $t_{0.001}$, the time period when ratio of c_s/c_0 reached 0.001; $t_{0.02}$, the time period when ratio of c_s/c_0 reached 0.02; $t_{0.5}$, the time period when ratio of c_s/c_0 reached 0.5; t_1, the time period when ratio of c_s/c_0 reached 1.

Table 5.6 Prediction of the service life of landfill liner (Neglect membrane behavior)

Bentonite content	Hydraulic gradient	1	2	5	10
0%	$t_{0.001}$ (year)	3.4	2.4	1.4	0.9
5%		4.0	3.0	1.9	1.2
10%		4.7	3.8	2.7	1.7
15%		5.4	4.8	3.6	2.6
20%		6.0	5.7	5.1	4.4
0%	$t_{0.02}$ (year)	5.2	3.4	1.8	1.0
5%		6.3	4.4	2.4	1.4
10%		6.1	6.1	3.7	2.3
15%		9.7	8.2	5.6	3.8
20%		11.2	10.5	8.9	7.1
0%	$t_{0.5}$ (year)	11.8	6.2	2.7	1.3
5%		16.3	9.3	3.9	2.0
10%		24.2	14.9	6.7	3.5
15%		36.5	25.7	13.7	7.5
20%		51.0	43.7	30.3	19.9
0%	t_1 (year)	31.5	11.1	4.5	1.9
5%		42.3	20.4	7.8	2.9
10%		87.2	43.7	12.6	6.2
15%		193.9	94.4	36.6	13.3
20%		270.6	244.6	124.7	59.9

Note: $t_{0.001}$, the time period when ratio of c_s/c_0 reached 0.001; $t_{0.02}$, the time period when ratio of c_s/c_0 reached 0.02; $t_{0.5}$, the time period when ratio of c_s/c_0 reached 0.5; t_1, the time period when ratio of c_s/c_0 reached 1.

Table 5.5 present the service life of bottom liners system under different external and environmental conditions, in which effect of membrane behavior was considered. To take an explanation to the role of membrane behavior in migration of contaminant, Table 5.6 presented the service life of bottom liners system according to the calculated results in Section 5.2, in which the effect of membrane behavior was neglected.

As shown in above Table 5.5 and Table 5.6, four parameters $t_{0.001}$, $t_{0.02}$, $t_{0.5}$ and t_1 were utilized to describe the breakthrough curve of specimen under different external conditions. $t_{0.001}$ is the time period when the ratio of c_s/c_0 reached 0.001, which represent the start of the diffusion. $t_{0.02}$ and $t_{0.5}$ are two special values and usually used in breakthrough curve analysis, when the ratio of c_s/c_0 reached 0.02 and 0.5. t_1 represent the concentration of the outflow equal to that of the inflow, the time period when ratio of c_s/c_0 reached 1.

t_1 represent the time spent when the barrier has been completely breakdown, while the surrounding soil and groundwater environment has already been polluted at that moment. Thus t_1 are usually used to analyze the performance of barrier in laboratory-scale experiment. $t_{0.001}$ is the time cost when the contaminant started to breakdown, and it is occurred at very early stage and can be used for forewarning of the diffusion of contaminant. Compared to above two parameters, $t_{0.02}$ and $t_{0.5}$ consider both the time spent and environmental impact, and can be regarded as balance criteria, and have been applied in many previous researches (Thomas and Swoboda, 1970; Czurda and Wagner, 1991; Chern and Chien, 2002; Murillo et al., 2004; Pan et al., 2005; Lange et al., 2010). To summarise the results listed in Table 5.5 and Table 5.6, Fig. 5.3 was drawn and showed as follows.

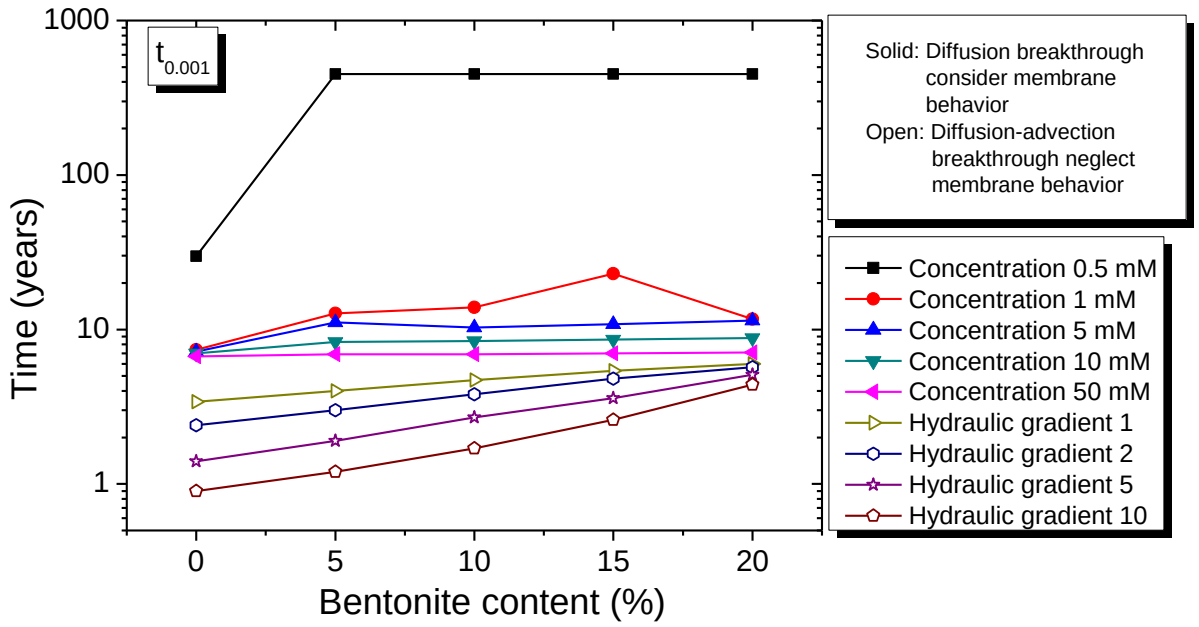

(a)

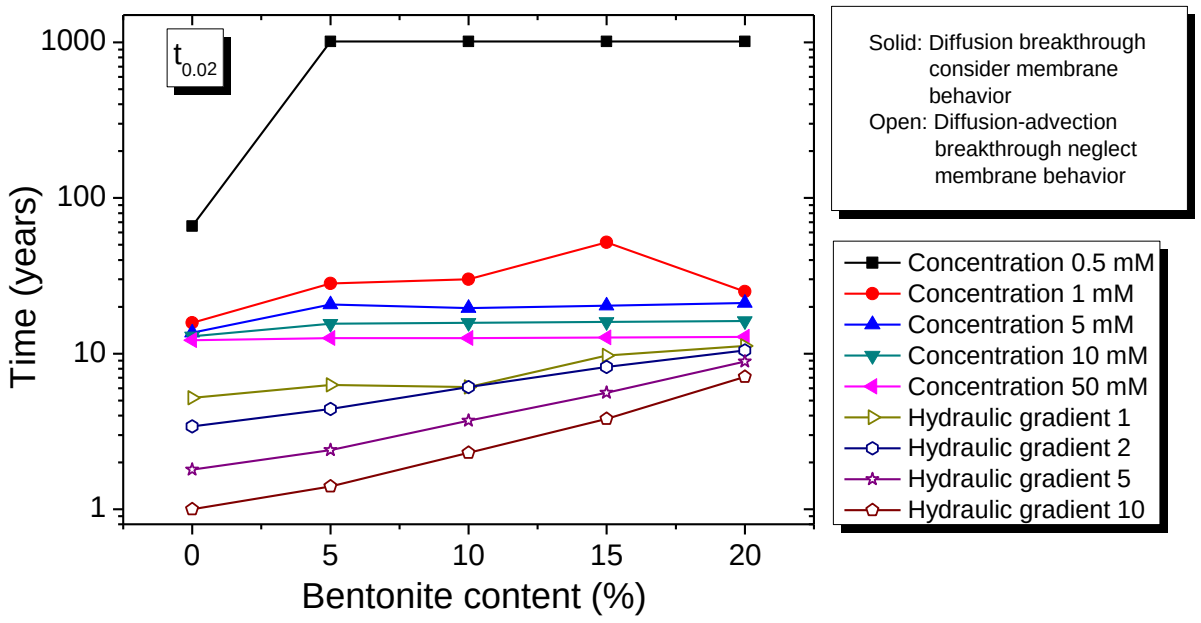
t0.02
Time (years)
Bentonite content (%)
Solid: Diffusion breakthrough consider membrane behavior
Open: Diffusion-advection breakthrough neglect membrane behavior
Concentration 0.5 mM
Concentration 1 mM
Concentration 5 mM
Concentration 10 mM
Concentration 50 mM
Hydraulic gradient 1
Hydraulic gradient 2
Hydraulic gradient 5
Hydraulic gradient 10

(b)

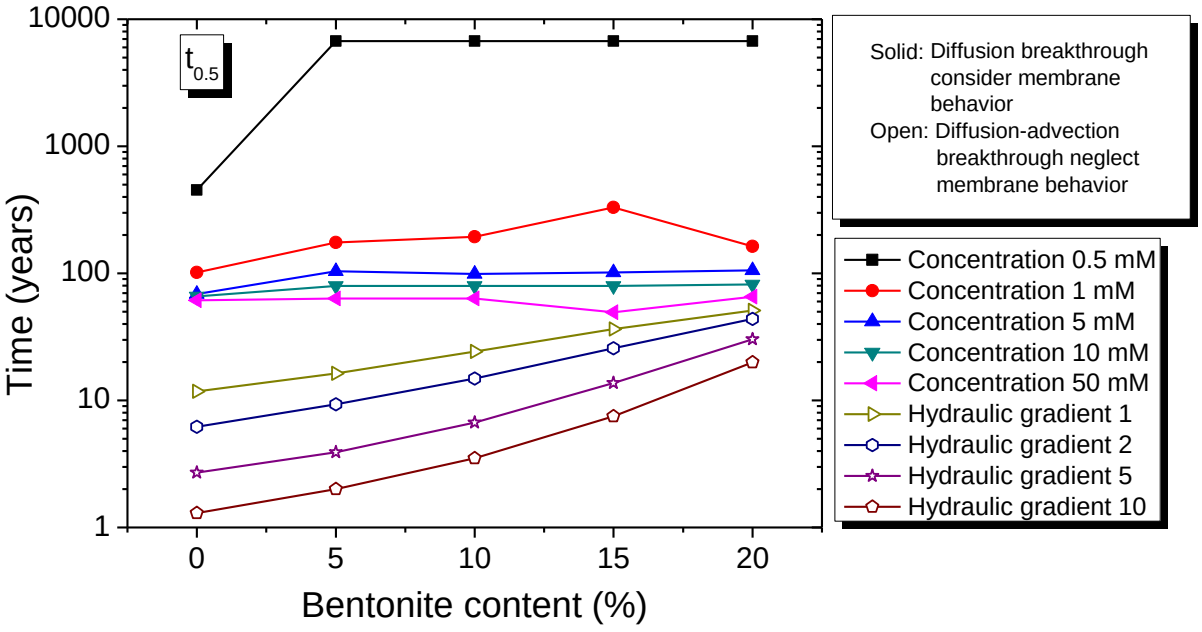
t0.5
Time (years)
Bentonite content (%)
Solid: Diffusion breakthrough consider membrane behavior
Open: Diffusion-advection breakthrough neglect membrane behavior
Concentration 0.5 mM
Concentration 1 mM
Concentration 5 mM
Concentration 10 mM
Concentration 50 mM
Hydraulic gradient 1
Hydraulic gradient 2
Hydraulic gradient 5
Hydraulic gradient 10

(c)

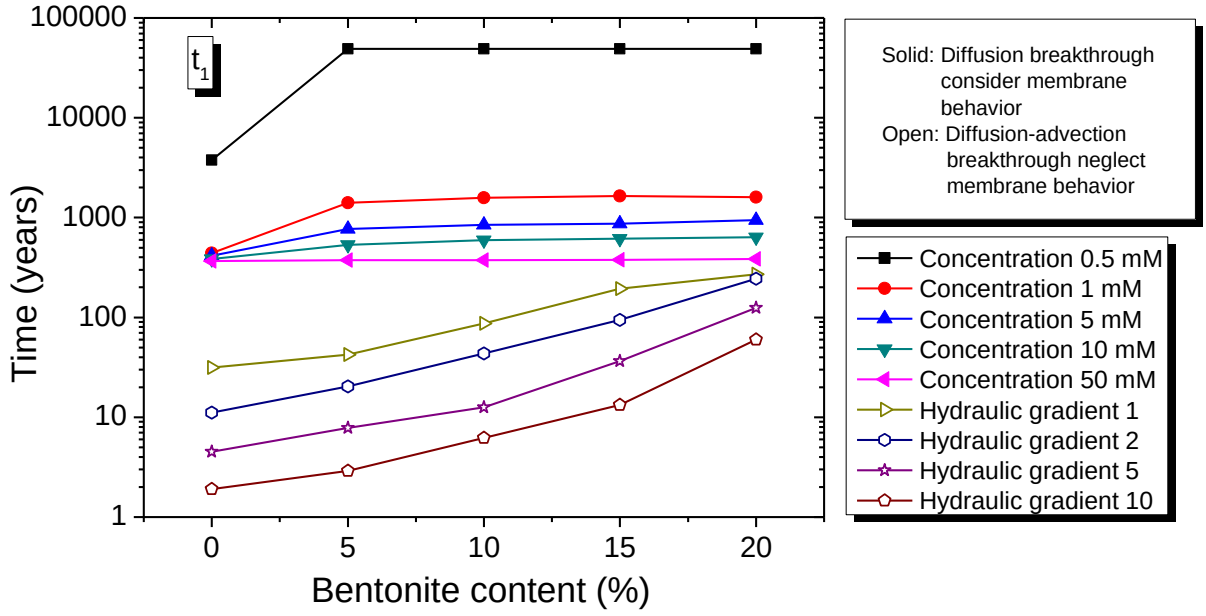

(d)

Fig. 5.3 Breakthrough time as function of bentonite content: (a) $t_{0.001}$, (b) $t_{0.02}$, (c) $t_{0.5}$ and (d) t_1

As shown in above Fig. 5.3(a)-(d), it is apparent that the barrier performance of liners which exhibited membrane property are much better than that without membrane behavior. The performance of liners are greatly improved when consider their membrane property, and the durations for breakthrough, $t_{0.001}$, $t_{0.02}$, $t_{0.5}$ and t_1 of liners increased 1.5-100 times. For diffusion-advection breakthrough curve neglect the membrane behavior, as the bentonite increase from 0 to 20%, the hydraulic conductivity k decreased, and resulted in the increase of the breakthrough time. Four parameters $t_{0.001}$, $t_{0.02}$, $t_{0.5}$ and t_1 all proved that as bentonite content increased, the barrier performance can be improved not matter the change of hydraulic gradient i.

For diffusion breakthrough curve consider the membrane behavior, as the bentonite increase from 0 to 20%, the membrane behavior change by two types. One is the great increase when bentonite content increased from 0 to 5%; while the other is the very limited increase when bentonite content increased from 5% to 20%. In addition, the membrane behavior was significantly affected by the concentration of inflow, as the concentration increased, the membrane behavior decreased, which leaded to the decrease of breakthrough time. However, when concentration reached 50 mM, the membrane behavior can be neglected.

Compare the results caculted when consider and neglect the membrane behavior, it is rational to expect that as the continual increase of bentonite content, the hydraulic conductivity will also decrease and then lead to the increase of breakthrough time continually. It can also be rational to believe that the as the continual increase of bentonite content higher than 5%, the improvement on membrane behavior will be very limited. To reach the optimum barrier performance, for soil-, sand-,

silt- and clay-bentonite composite material, at least 5% bentonite should be added. Based on the requirements or rules of different countries, extra bentonite is introduced to meet the requirement on hydraulic conductivity. Since the membrane behavior is significantly affected by the solute concentration, it is rational to neglect the membrane behavior when the concentration of leachate can be higher than 50 mM.

Considering the economical status of most developing countries, it is necessary to choose the most suitable design of bottom liner to reach a balance between efficiency and expense. Besides the design process, the achievement in this study can also apply in the environmental safety assessment. Chapter 4 studied the different factors on barrier performance through membrane behavior. Following the results, it is possible to make a prediction of the barrier performance of bottom liners system of landfill in practical condition in landfill.

CHAPTER 6: CONCLUSIONS AND FUTURE RESEARCH DIRECTIONS

6.1 Conclusions

The main results of this research are summarized as follows:

In chapter 3, lysimeter tests were conducted in six lysimeters to estimate the effect of height and H/W ratio on leachate generation and leaching behavior of C&D waste residue. The C&D waste was collected from an intermediate treatment facility located in Ibaraki Prefecture. To avoid the effect of particle size on test results, the C&D waste selected in this study had particles of < 5 mm.

The physical characteristics of C&D waste residue, such as particle density and hydraulic conductivity, closely resembled those of sand and ash. According to the leaching test results, the concentrations of each inorganic ion showed similar levels regardless of the particle size of the residue. The C&D waste showed strong alkalinity with pHs in the range of 11.7 to 12.2, and EC values in the small particles were found to be higher than those in the large particles. Such a decrease of pH and EC value as a function of particle size can be attributed to particle size of soluble content, since in most cases, soluble content exists in the form of powder or very small particle in nature.

In the lysimeter tests, the soluble constituent (Cl, Na, K, Ca) concentrations decreased with increasing L/S ratio. There were two types of decreasing shape; First is the relatively sharp decrease in concentrations of non-reactive constituents, shown in R1 and R2 which have a short width; second is the gradual decrease shown in R5 and R6. It is likely that it is caused by the preferential and sidewall flows which can easily occur in lysimeters with high H/W ratios. The highest concentrations of inorganic constituent always appeared in R2, rather than the longer R3 and R4, which suggests that the filtration water can completely flush inside of the lysimeters which have a height lower than 0.7 m. The concentration of salt leached out in R2 was lower than that from R1, which can also be attributed the height of the lysimeter; as the height of lysimeter increased, the waste particles at the bottom must bear a greater upper loading, resulting in the lower leaching behavior. The leaching behavior of heavy metal ions (Ba, Cu, Fe, Mg, Mo, Ni and Sr) clearly prove that although C&D waste is regarded as inert, under certain conditions (lower pH and microbial activity), the inherent heavy metals might be leached out, as their concentrations are higher than normal MSW leachate.

According to the results of COD, TN and TP, the values were a little lower compared to the leachate from MSW landfill due to several factors such as the composition of the waste. The general tendency of COD, TP and TN is decreased as L/S ratio, and can be explained as dilution effect due to the rainwater percolation. Nevertheless, for certain lysimeter, the decrease rate was different, the lysimeter with short height or low H/W ratio displayed more reduction within the same experimental durations. Since the COD value reflect the amount of the organic contaminant, which is abundant in elements such as C, N, P, S, which was the important composition of protein and the essential

nutrient for micro-organism and can be fixed during the leaching process, and to some extent, the change of COD, TN and TP partially reflected the microbial activity. The conclusion can be arrived that the lysimeter with lower H/W ratio or shorter height can promote the microbial activity and result in the acceleration of micro-organism in degradation of organic contaminant.

Based on the emission behavior of some soluble constituents, the microbial activity can have a significant effect on leaching behavior, the amount of SO_4^{2-} emission increased with L/S ratio, due to the active microbial activity, by which the sulfate salts originating from the gypsum in C&D waste were continually decomposed. Thus, the decomposition by microbial activity inside C&D waste has great effect on the leaching behavior, and should not be neglected in the research. The amount of NH_4^+ emission followed the order R1& R6 < R5 < R2 < R3& R4, which clearly indicated that shorter height, low H/W ratio or looser micro-structure inside the waste can provide more suitable conditions (density, upper loading, inter-particle cohesion, water content) and led to more active microbial activity.

In chapter 4, a series of lab-scale experiments were conducted on locally available FC and bentonite amended FC composite materials. According to the results, the hydraulic conductivity of FC is 1.58×10^{-9} m/s, indicating that FC is not suitable for use as a compacted clay liner unless amended with bentonite. For bentonite amended clay, hydraulic conductivities are 1.07×10^{-9} m/s for FC plus 5% bentonite, 6.04×10^{-10} m/s for FC plus 10% bentonite, 2.74×10^{-10} m/s for FC plus 15% bentonite, and 8.23×10^{-11} m/s for FC plus 20% bentonite, which indicated that adding bentonite make natural FC suitable for use as a liner. According to the results of the specimens with different compactness, as compaction degree increased from 80% to 90% and 100%, the hydraulic conductivity decreased from 2.01×10^{-9} m/s to 1.49×10^{-9} m/s and 1.07×10^{-9} m/s.

Bentonite is an effective additive, and may greatly improve the membrane behavior of natural FC. When the bentonite concentration is low (C_{t0} = 0.5 mM), the values of ω for the bentonite amended clays are close to 1, suggesting an ideal membrane property. As C_{t0} increases to 5 mM, the membrane behaviors of the bentonite amended FCs are several times higher compared to FC; even at extremely high concentrations of 10 and 50 mM, bentonite amended FC still exhibits a membrane behavior of $\omega_0 > 0.20$ and $\omega_0 > 0.04$, respectively. Among the bentonite amended FCs, the membrane behavior increase as the bentonite content increase.

pH is proved have a significant effect on the performance of the membranes, especially in alkaline conditions. When the pH of the solution was 11.0, the membrane coefficient, ω, was 1.2 - 1.3 times greater than the coefficient when the pH was 7.0 at lower concentration, and it was almost 2.5 times greater at the higher concentration. When the pH was 4.0, the membrane coefficient, ω, was 90% of the coefficient when the pH was 7.0 at lower concentration. The similarity of the membranes‘ behaviors between pH values of 4.0 and 7.0 suggested the existence of a very slight erosion effect of the acid solution.

Compactness has proved have significant effect on membrane behavior. The membrane behavior of specimen with compactness of 100% was almost 30% higher than that with compactness of 80%

under concentration difference of 5, 10 and 50 mM.

Solute type also proved great effect on membrane behaviors. And the average chemico-osmotic membrane coefficient ω_{ave} follows the order that K, Na > Ca > Pb, Zn. Ca ion is a active ion and hard to fix during the diffusion process. Although the low membrane behavior of heavy metal ions, almost no diffusion occurred during the membrane test, which can be attributed to the adsorption.

Additionally, at the beginning of every stage, introducing a higher concentration KCl solution causes a rapid increase in the chemico-osmotic pressure, which peaks at ΔP_{peak}, and then reaches an equilibrium pressure of ΔP_e, especially for specimens with different bentonite content. The difference between $\Delta P_{peak} - \Delta P_e$ increases as the solute concentration or bentonite content increases because the double layer is more compressed. The values of ω_0 based on the initial concentration and a perfect flushing boundary, are corrected to ω_{ave}. The values of ω_{ave} are slightly higher after accounting for the changes in the boundary concentrations due to solute diffusion, and in most cases, $\omega_{ave} - \omega_0 < 0.06$.

As the bentonite content increases from 0 to 5%, the membrane behavior rapidly increases, which is likely due to the decreased pore size and increased thickness of the DDL. Although increasing the bentonite content from 5% to 20% does not significantly change the pore size within the specimens, the membrane behavior slightly improves, suggesting that the DDL contributes more to the improvement of the membrane property. As the solution concentration increases, more exchange sites at the DDL are occupied by cations instead of water molecules, which strengthens the attractive forces while shrinking the DDL. Hence, the increased interparticle voids allow more solute molecules to pass, greatly reducing the membrane behavior.

Since there were large amounts of minerals in the clay, such as montmorillonite, mica, quartz, and feldspar, the Fukakusa clay-bentonite composite material releases free Al^{3+} and Fe^{3+} ions that can react in solution to form H^+, making the samples exhibit a more acidic nature.

The mechanisms that produced changes in membrane performance also were assessed and discussed using XRD patterns, free swelling volume, XRF results, SEM images, and camera images. At a pH value of 11.0, the samples exhibited better swelling performance, thus the soil clusters became larger than they were in the neutral condition, and the Fe^{3+} ions that released were likely to bind with OH^- to form floccules, which results in more narrow inter-particle space and blocks the permeable paths. Since there is a large amount of Fe in the Fukakusa clay-bentonite material, it also possessed strong buffer capacity in the alkaline solution. In contrast, at a pH value of 4.0, the soil clusters became smaller than they were in the neutral condition, and some clay minerals, such as CaO and calcite, were dissolved, which resulted in larger inter-particle spaces and permeable paths. The small amounts of CaO and calcite resulted in a very limited buffer capacity in the acid solution.

In chapter 5, the service life of landfill liners are predicted by using one solute transport model proposed by previous researcher. The input data are obtained based on the experiment results and calculation referred in chapter 4. Four parameters $t_{0.001}$, $t_{0.02}$, $t_{0.5}$ and t_1 were utilized to describe the breakthrough curve of specimens under different external conditions. $t_{0.001}$ is the time period when

the ratio of c_s/c_0 reached 0.001, which represent the start of the diffusion. Since $t_{0.001}$ is the time cost when the contaminant started to breakdown, and it is occurred at very early stage and can be used for forewarning of the diffusion of contaminant. $t_{0.02}$ and $t_{0.5}$ are two special values and usually used in breakthrough curve analysis, when the ratio of c_s/c_0 reached 0.02 and 0.5. $t_{0.02}$ and $t_{0.5}$ consider both the time spent and environmental impact, and can be regarded as balance criteria, and have been applied in many previous researches. t_1 represent the concentration of the outflow equal to that of the inflow, the time period when ratio of c_s/c_0 reached 1.

According to the calculation results, it is apparent that the barrier performance of liners which exhibited membrane property are much better than that without membrane behavior. The performance of liners are greatly improved when consider their membrane property, and the durations for breakthrough, $t_{0.001}$, $t_{0.02}$ $t_{0.5}$ and t_1 of liners increased 1.5-100 times. The solute concentration has a great effect on the barrier performance when consider the membrane behavior, by which the $t_{0.001}$, $t_{0.02}$ $t_{0.5}$ and t_1 decreased as the increase of concentration. It is also found that the $t_{0.001}$, $t_{0.02}$ $t_{0.5}$ and t_1 decreased as the increase of hydraulic gradient. Although different factors were found based on above two tables, the general trend is the same that the barrier performance is improved when bentonite content increase.

Considering the economical status of most developing countries, it is necessary to choose the most suitable design of bottom liner to reach a balance between efficiency and expense. Besides the design process, the achievement in this study can also apply in the environmental safety assessment. Chapter 4 studied the different factors on barrier performance through membrane behavior. Following the results, it is possible to make a prediction of the barrier performance of bottom liners system of landfill in practical condition in landfill.

6.2 Future research

In chapter 3, the C&D waste used in lysimeter test was only greatly homogenous samples (C&D waste residues with particle size < 5 mm), so the effect of preferential flows may be underestimated more than studies using the bigger size of waste. In addition, the particle size is a very important issue to affect other properties of material such as consolidation, hydraulic behavior, and so on. Therefore, a further study is necessary to estimate the effect of leaching behavior by the different particle size of wastes.

In chapter 5, the service life of landfill liners were predicted by using solute transport model. Although most of the input parameters were obtained from the experiment results measured in chapter 4, some parameters such as D and R were still based on previous literatures. To make the analysis results more reliable, in the future research, all parameters used should be measured through experiment. In addition, for the practical application of Fukakusa clay, the mechanical behavior should be considered.

The landfill leachate is always characterized with its high BOD and COD values which indicate

the active microorganism activity. The microorganism activity occurred inside or at the surface of landfill liners, and can greatly affect the composition and micro-structures of liner material. Thus the effect of microorganism activity should be also considered in the future research.

REFERENCES:

Ahn, W.Y., Kang, M.S., Yim, S.K., Choi, K.H., (2002). Advanced landfill leachate treatment using and integrated membrane process. *Desalination* 149, 109-114.

Allen, A., (2001). Containment Landfills: the myth of sustainability. *Engineering Geology* 60, 3-19.

Artiola-Fortuny, J., and Fuller, W.H., (1982). Humic substances in landfill leachates: I. Humic acid extraction and identification. *Journal of Environmental Quality* 11, 663-668.

Aspé, E., Roeckel, M., and Fernández, K., (2012). Use of biomass for the removal of heavy metals at low concentrations from freshwater for Chilean Atlantic salmon farms. *Aquacultural Engineering* 49, 1-9.

Aubertin, M., Busslere, B. and Chapuis, R.P., (1996). Hydraulic conductivity of homogenized tailings from hard rock mines. *Canadian Geotechnical Journal* 33, 470-482.

Baig, S., Coulomb, I., Courant, P., Liechti, P., (1999). Treatment of landfill leachates: Lapeyrouse and Satrod case studies. *Ozone: Science & Engineering* 21, 1–22.

Bashir, M.J.K., Aziz, H.A., Yusoff, M.S., Adlan, M.N., (2010). Application of response surface methodology (RSM) for optimization of ammoniacal nitrogen removal from semi-aerobic landfill leachate using ion exchange resin. *Desalination* 254, 154-161.

Barbour, S.L. and Fredlund, D.G., (1989). Mechanisms of osmotic flow and volume change in clay soils. *Canadian Geotechnical Journal* 26(4), 551-562.

Baun, D.L., Christensen, T.H., (2004). Speciation of heavy metals in landfill leachate: a review. *Waste Management & Research* 22, 3–23.

Benson, C.H., Trast, J.M., (1995). Hydraulic conductivity of thirteen compacted clays. *Clays and Clay Minerals* 43(6), 669-681.

Bianchini, G., Marrocchino, E., Tassinari, R., Vaccaro, C., (2005). Recycling of construction and demolition waste materials: a chemical-mineralogical appraisal. *Waste Management* 25, 149-159.

Boynton, S., and Daniel, D., (1985). Hydraulic conductivity tests on compacted clay. *Journal of Geotechnical and Geoenvironmental Engineering (ASCE)* 111(4), 465-478.

Brunner, P.H., Fellner, J., (2007). Setting priorities for waste management strategies in developing countries. *Waste Management & Research* 25 (3), 234–240.

Burnes, T.A., Blanchette, R.A., Farrell, R.L., (2000). Bacterial biodegradation of extractives and patterns of bordered pit membrane attack in pinc wood. *Appl. Environ. Microb.* 66(12), 5201-5205.

Canadian Water Quality Guidelines. (2004). Guidelines for Canadian drinking water quality. ⟨www.worldcat.org/identities/lccn-n82-136902⟩ (Jan. 27, 2012).

Castrillón, L., Fernández-Nava, Y., Ulmanu, M., Anger, I., Marañón E., (2010). Physico-chemical and biological treatment of MSW landfill leachate. *Waste Management* 30, 228-235.

Cervantes, F.J., Pavlostathis, S.G., Van Handeel, A.C., (2006). Advanced biological treatment processes for industrial wastewaters-principles and applications, first ed. IWA Publishing, UK.

CFR (Code of Federal Regulations), 40 CFR, Parts 258, (1994). *U.S. Government Printing Office*, Washington DC.

Chapuis, R.P., (2002). The 2000 R.M. Hardy Lecture: Full-scale hydraulic performance of soil–bentonite and compacted clay liners. *Canadian Geotechnical Journal* 39(2), 417-439.

Chern, J.M., Chien, Y.W., (2002). Adsorption of nitrophenol onto activated carbon: isotherms and breakthrough curves. *Water Research* 36, 647–655.

Chian, E.S.K., DeWalle, F.B., (1976). Sanitary landfill leachates and their treatment, *Journal of the Environmental Engineering Division (ASCE)*,411–431.

Chichester, D.L., and Landsberger, S., (1996). Determination of the leaching dynamics of metals from municipal solid waste incinerator fly ash using a column test. *Journal of the Air & Waste Management Association* 46, 643-649.

China Statistical Yearbook, (1991-2012). *National Bureau of Statistics of China*, http://www.stats.gov.cn/tjsj/ndsj/ (March. 21st, 2013).

Christensen, T.H., Kjeldsen, P., (1989). Basic biochemical processes in landfills. In: *Christensen, T.H., Cossu, R., Stegmann, R. (Ed.). Sanitary landfilling: Process, technology and environmental impact*, Chapter 2.1. Academic Press, London, 29-49.

Christensen, T.H., Kjeldsen, P., Albrechtsen, H.J., Heron, G., Nielsen, P.H., Bjerg, P.L., and Holm, P.E., (1994). Attenuation of landfill leachate pollutants in aquifers. *Critical Reviews in Environmental Science and Technology* 24(119).

Christensen, T.H., Kjeldsen, P., Bjerg, P.L., Jensen, D.L., Christensen, J.B., Baun, A., Albrechtsen, H.J., and Heron, G., (2001). Biogeochemistry of landfill leachate plumes. *Applied Geochemistry* 16, 659–718.

Chu, L.M., Cheung, K.C., and Wong, M.H., (1994). Variations in the chemical properties of landfill leachate. *Environmental Management* 18, 105–117.

Clark, C., Jambeck, J., and Townsend, T., (2006). A review of construction and demolition debris regulations in the U.S. *Crit. Rev. Environ. Sci. Technol.* 36, 141-186.

Clement, B., and Thomas, O., (1995). Application of ultra-violet spectrophotometry and gel permeation chromatography to the characterization of landfill leachates. *Environmental Technology* 16, 367–377.

Cosper, S.D., Hallenbeck, W.H., Brenniman, G.R., (1993). Construction and Demolition Waste. *Office of Solid Waste Management*. The University of Illinois at Chicago.

Crannell, B.S., Eighmy, T.T., Krzanowski, J.E., EusdenJr, J.D., Shaw, E.L., Francis, C.A., (2000). Heavy metal stabilization in municipal solid waste combustion bottom ash using soluble phosphate. *Waste Management* 20, 135-148.

Crerar, D.A., Means, J.L., Yuretich, R.F., Borcsik, M.P., Amster, J.L., Hastings, D.W., Knox, G.W., Lyon, K.E., Quiett, R.F., (1981). Hydrogeochemistry of the New Jersey Coastal Plain: 2.

Transport and deposition of iron, aluminum, dissolved organic matter, and selected trace elements in stream, ground- and estuary water. *Chemical Geology* 33, 23-44.

Czurda, K.A., and Wagner, J.F., (1991). Cation transport and retardation processes in view of the toxic waste deposition problem in clay rocks and clay liner encapsulation. *Engineering Geology* 30, 103-113.

Daniel, D.E., Anderson, D.C. and Boynton, S.S., (1985). Fixed-wall versus flexible-wall permeameters. In: *Johnson, A.I., Frobel, R.K., Cavalli, N.J., Pettersson, C.B. (Eds.), Hydraulic Barriers in Soil and Rock*. ASTM STP 874. ASTM, West Conshohoken, PA, 107–126.

Daniel, D.E., and Benson, C.H., (1990). Water content – density criteria for compacted soil liners. *Journal of Geotechnical Engineering (ASCE)* 116(GT12), 1811–1830.

Delage, P., Audiguier, M., Cui, Y.J., and Howat, M.D., (1996). Microstructure of a compacted silt. *Canadian Geotechnical Journal* 33, 150–158.

DEPA. (2005). Waste Statistics 2003. *Environmental Protection Agency.* [online]. http://www.mst.dk/homepage/default.asp?Sub=http://www.mst.dk/udgiv/Publications/2005/87-7614-585-9/html/default_eng.htm [Accessed 28 June 2006]

Di Emidio, G., (2010). Hydraulic and Chemico-osmotic performance of polymer treated clays. *PhD Diss., Ghent University*, Ghent, Belgium.

Dijkstra, J.J., van der Sloot, H.A., Comans, R.N.J., (2006). The leaching of major and trace elements from MSWI bottom ash as a function of pH and time. *Applied Geochemistry* 21, 335-351.

Dominijanni, A. and Manassero, M., (2012a). Modelling the swelling and osmotic properties of clay soils. Part I: The phenomenological approach. *International Journal of Engineering Science* 51, 32–50.

Dominijanni, A. and Manassero, M., (2012b). Modelling the swelling and osmotic properties of clay soils. Part II: The physical approach. *International Journal of Engineering Science* 51, 51–73.

EEA (European Environment Agency) (2002). Review of Selected Waste Streams: Sewage sludge, construction and demolition waste, waste oils, waste from coal-fired power plants and biodegradable municipal. *Technical Report* 69.

Egloffstein, T., (1995). Properties and test methods to assess bentonite used in geosynthetic clay liners. *Geosynthetic clay liners*, Balkema, Rotterdam, The Netherlands, 51-72.

Ehrig, H.J., (1983). Quality and quantity of sanitary landfill leachate. *Waste Management & Research* 1, 53–68.

Ehrig, H.J., (1988). Water and element balances of landfills. In: *Baccini, P. (ed.) The Landfill*, pp. 83–116. (Lecture Notes in Earth Sciences, Vol. 20). Springer Verlag, Berlin, Germany.

El-Fadel, M., Findikakis, A.N., Leckie, J.O., (1997). Environmental impacts of solid waste landfilling. *Journal of Environmental Management* 50, 1-25.

Environment Agency (2002). *National Waste Production Survey*. http://www.defra.gov.uk/environment/statistics/index.htm.

Environment Agency, (2007). Guidance for the Treatment of Landfill Leachate. Integrated Pollution

Prevention and Control (IPPC), Sector Guidance Note IPPC S5.03, February 2007.

Eurostat, (2010). Europe in Figures – Eurostat Yearbook 2010. *Statistical Books*. Eurostat, Belgium.

Evans, J.C., Shackelford, C.D., Yeo, S.S. and Henning, J., (2008). Membrane behavior of soil-bentonite slurry-trench cutoff walls. *Soil & Sediment Contamination* 17, 316-322.

Fatta, D., Papadopoulos, A., Avramikos, E., Sgourou, E., Moustakas, K., Kourmoussis, F., Mentzis, A., Loizidou, M., (2003). Generation and management of construction and demolition waste in Greece—an existing challenge. *Resources, Conservation and Recycling* 40, 81-91.

Forster, M.D., (1953). Geochemical studies of clay minerals III. The determination of free silica and free alumina in montmorillonites. *Geochimica et Cosmochimical Acta*, London 3, 143-154.

Freeze, R.A., Cherry, J.A. (1979). *Groundwater*. Prentice-Hall, Englewood Cliffs, N.J, p. 604.

Freyssinet, Ph., Piantone, P., Azaroual, M., Itard, Y., Clozel-Leloup, B., Guyonnet, D., Baubron, J.C., (2002). Chemical changes and leachate mass balance of municipal solid waste bottom ash submitted to weathering. *Waste Management* 22(1) 159-172.

Fritz, S.J. and Marine, I.W., (1983). Experimental support for a predictive osmotic model of clay membranes. *Geochimica et Cosmochimica Acta* 47(8), 1515-1522.

Fritz, S.J., (1986). Ideality of clay membranes in Osmotic processes: A review. *Clays and Clay Minerals* 34(2), 214-223.

Gleason, M.H., Daniel, D.E., and Eykholt, G.R. (1997). Calcium and sodium bentonite for hydraulic containment applications. *Journal of Geotechnical and Geoenvironmental Engineering (ASCE)* 123(5), 438-445.

Gordon, M.E., Huebner, P.M., and Mitchell, G.R., (1990), Regulation, Construction and Performance of Clay-Lined Landfills in Wisconsin. *Waste Containment Systems* Geotechnical Special Publication 26, 14-29.

Grathoff, G.H., Baham, J.E., Easterly, H.R., Gassman, P., Hugo, R.C., (2007). Mixed-valent Fe films (schwimmeisem) on the surface of reduced ephemeral pools. *Clays and Clay Minerals* 55(6), 635-643.

Grathwohl, P., (1998). Diffusion in Natural Porous Media, Contaminant Transport, Sorption/Desorption and Dissolution Kinetics. *Kluwer Academic Publishing*, Norwell, MA, USA.

Greenberg, J.A., Mitchell, J.K. and Witherspoon, P.A., (1973). Coupled salt and water flows in a groundwater basin. *Journal of Geophysical Research* 78(27), 6341-6353.

Grim, R., (1968). *Clay mineralogy*, 2nd Ed. McGraw-Hill, New York.

Grimaldi, M., (1981). Modifications structurales d‘un materiau limoneux soumis a un compactage dynamique. *Science du Sol* 3, 269-284.

Groenevelt, P.H. and Elrick, D.E., (1976). Coupling phenomena in saturated homo-ionic montmorillonite: II. Theoretical. *Soil Science Society of America Journal* 40(6), 820-823.

Guyonnet, D., Bodénan, F., Brons-Laot, G., Burnol, A., Chateau, L., Crest, M., Méhu, J., Moszkowicz, P., and Piantone, P., (2008). Multiple-scale dynamic leaching of a municipal solid

waste incineration ash. *Waste Management* 28 (10), 1963-1976.

Hanashima, M., and Furuichi, T., (2000). Landfill sites in Japan 2000, *The Landfill System Technologies Research Association of Japan (Ed)*, The Journal of Waste Management Press.

Hanshaw, B.B. and Coplen, T.B., (1973). Ultrafiltration by a compacted clay membrane-II. Sodium ion exclusion at various ionic strengths. *Geochimica et Cosmochimica Acta* 37(10), 2311-2327.

Harsem, J., (1983). Identification of organic compounds in leachate from a waste tip, *Water Research* 17, 699–705.

Heister, K., (2005). Coupled transport in clayey materials with emphasis on induced electrokinetic phenomena. *Ph.D. thesis, Utrecht University*, Utrecht.

Henken-Mellies, W.U., and Schweizer, A., (2011). Long-term performance of landfill covers-results of lysimeter test fields in Bavaria (Germany). *Waste Management & Research* 29(1), 59-68.

Henning, J., Evans, J.C. and Shackelford, C.D., (2006). Membrane behavior of two backfills from field-constructed soil-bentonite cutoff walls. *Journal of Geotechnical and Geoenvironmental Engineering (ASCE)* 132(10), 243-249.

Hong, S.M., Candelone, J.P., Patterson, C.C., and Boutron, C.F., (1994). Greenland ice evidence of hemispheric lead pollution twomillennia ago by Greek and Roman civilizations. *Science* 265,1841–1843.

Indian Standard. (1991). Drinking water—Specification (first revision). *Indian Standard 10500*, New Delhi, India.

Jambeck, J.R., Townsend, T.G., and Solo-Gabriele, H., (2006). Leaching of chromate copper arsenate (CCA)-treated wood in a simulated monofill and its potential impacts to landfill leachate. *Journal of Hazardous Materials* A135, 21-31.

Jambeck, J.R., Townsend, T.G., and Solo-Gabriele, H.M., (2008). Landfill disposal of CCA-treated wood with construction and demolition (C&D) debris: arsenic, chromium, and copper concentrations in leachate. *Environ. Sci. Technol.* 42, 5740-5745.

Jang, Y., and Townsend, T., (2003). Effect of waste depth on leachate quality from laboratory construction and demolition debris landfills. *Environ. Eng. Sci.*, 20, 183-196.

Jørgensen, M., and Kjeldsen, P., (1995). Composition of leachate from old landfills (Kildestyrkevurdering af gamle lossepladser). Projects about soil and groundwater from The Danish Environmental Protection Agency, 16. Danish Environmental Protection Agency, Copenhagen, Denmark.

Jo, H.Y., Katsumi, T., Benson, C.H. and Edil, T.B., (2001). Hydraulic conductivity and swelling of nonprehydrated GCLs permeated with single-species salt solutions. *Journal of Geotechnical and Geoenvironmental Engineering (ASCE)* 127(7), 557-567.

Johannessen, L.M., (1999). Guidance note on recuperation of landfill gas from municipal solid waste landfills. *Working Paper Series* 4, World Bank, USA.

Johansen, O.J., & Carlson, D.A., (1976). Characterization of sanitary landfill leachates. *Water Research* 10, 1129–1134.

Kalbe, U., Berger, W., Eckardt, J., and Simon, F.G., (2008). Evaluation of leaching and extraction procedures for soil and waste. *Waste Management* 28, 1027-1038.

Kamon, M., (1999). Appropriate structural code for waste disposal site. *J. Waste Management Research* 10(2), 147-155. (In Japanese)

Kamon, M. and Katsumi T., (2001). Clay liners for waste landfill. *Clay Science for Engineering*. Rotterdam, Balkema, 29-45.

Kang, J.B., Shackelford, C.D., (2009). Clay membrane testing using a flexible-wall cell under closed-system boundary conditions. *Applied Clay Science* 44, 43-58.

Kang, J.B. and Shackelford, C.D., (2010). Membrane behavior of compacted clay liners. *Journal of Geotechnical and Geoenvironmental Engineering (ASCE)* 136, 1368-1382.

Kang, J.B., Shackelford, C.D., (2011). Consolidation enhanced membrane behavior of a geosynthetic clay liner. *Geotextiles and Geomembranes* 29, 544-556.

Katchalsky, A., and Curran, P.F., (1965). *Nonequilibrium thermodynamics in biophysics*, Harvard University Press, Cambridge, MA.

Katsumi, T., Ishimori, H., Ogawa, A., Yoshikawa, K., Hanamoto, K. and Fukagawa, R., (2007). Hydraulic conductivity of nonprehydrated geosynthetic clay liners permeated with inorganic solutions and waste leachates. *Soil and Foundations (JGS)* 47(1), 79-96.

Katsumi, T., Ishimori, H., Ogawa, A., Maruyama, S. and Fukagawa, R., (2008a). Effects of water content distribution on hydraulic conductivity of prehydrated FCLs against calcium chloride solutions. *Soil and Foundations* 48(3), 407-417.

Katsumi, T., Ishimori, H., Onikata, M. and Fukagawa, R., (2008b). Long-term barrier performance of modified bentonite materials against sodium and calcium permeant solutions. *Geotextiles and Geomembranes* 26, 14-30.

Katsumi, T. (2010). *Geosynthetic Clay Liners for Waste Containment Facilities* (Chapter: Hydraulic conductivity of geosynthetic clay liners), number 4.

Keijzer, T.J.S., Kleingeld, P.J. and Loch, J.P.G., (1997). Chemical osmosis in compacted clayey material and the prediction of water transport. *Geoenvironmental engineering, contaminated ground: Fate of pollutants and remediation, R.N. Yong and H.R. Thomas, eds.* Thomas Telford, London, 199-204.

Kemper, W.D., and Quirk, J.P., (1972). Ion mobilities and electric charge of external clay surfaces inferred from potential differences and osmotic flow. *Proceedings of Soil Science Society of America* 36(3) 426-433.

Kemper, W.D. and Rollins, J.B., (1966). Osmotic efficiency coefficients across compacted clays. *Proceedings of Soil Science Society of America* 30(5), 529-534.

Khattabi, H., Aleya, L., Mania, J., (2002). Changes in the quality of landfill leachates from recent and aged municipal solid waste. *Waste Management & Research* 8, 357–364.

Kim, H.J., Endo, K., and Yamada, M., (2010). Review on the method of lab-scale experiment to improve stabilization of landfilled waste. *Proceedings of Japan Society of Material Cycles and*

Waste Management 21th Annual Conference, Kanazawa, Japan

Kim, H.J., Endo, K., Tang, Q., Katsumi, T., and Yamada, M., (2011). Leaching behaviors of inorganics in construction and demolition waste residues by the different height/width ratios of columns. *Proceedings of the 9th JGS symposium on Environmental Geotechnics*, Kyoto, Japan, 367-372.

Kim, H., Jang, Y.C., and Townsend, T., (2011). The behavior and long-term fate of metals in simulated landfill bioreactors under aerobic and anaerobic conditions. *Journal of Hazardous Materials* 194, 369-377.

Kjeldsen, P., Barlaz, M.A., Rooker, A.P., Baun, A., Ledin, A., Christensen, T.H., (2002). Present and long-term composition of MSW landfill leachate: a review. *Critical Reviews in Environmental Science and Technology* 32 (4), 297–336.

Kjeldsen, P., and Christophersen, M., (2001). Composition of leachate from old landfills in Denmark. *Waste Management & Research* 19, 249–256.

Kooistra, M.J., (1994). Effects of compaction on soil microstructure. In: *Soil Compaction in Crop Production (eds B.D. Soane & C. van Ouwerkerk)*, Elsevier, Amsterdam, 91-111.

Kostova, I., (2006). Leachate from sanitary landfills-origin, characteristics, treatment. University of Architecture, Civil Engineering and Geodesy, –Iskar's Summer School"-Borovetz, 26-29 July.

Krug, M.N. and Ham, R.K., (1997). Analysis of long-term leachate characteristics. In: *Christensen, T.H., Cossu, R., & Stegmann, R. (eds), Proceedings of Sardinia 1997, Sixth International Landfill Symposium*, Margherita di Pula, Cagliari, Italy, 13–17 October 1997, 117-131S. CISA, Cagliari, Italy.

Kulikowska, D., and Klimiuk, E., (2008). The effect of landfill age on municipal leachate composition. *Bioresource Technology* 99, 5981–5985.

Kylefors, K., Andreas, L., and Lagerkvist, A., (2003). A comparison of small-scale, poilt-scale and large-scale tests for predicting leaching behavior of landfilled wastes. *Waste Management* 23, 45-59.

Laner, D., Crest, M., Scharff, H., Morris, J.W.F., and Barlaz, M.A., (2012). A review of approaches for the long-term management of municipal solid waste landfills. *Waste Management* 32, 498–512.

Lange, K., Rowe, R.K., and Jamieson, H., (2010). The potential role of geosynthetic clay liners in mine water treatment systems. *Geotextiles and Geomembranes* 28, 199-205.

Li, Z.Z., Tang, Q., Katsumi, T., Tang, X.W., Inui, T. and Imaizumi, S., (2010). Leaf char: An alternative adsorbent for Cr(III). *Desalination* 264, 70–77.

Lundgren, T. A., (1981). Some bentonite sealants in soil mixed blankets. *Proceedings, 10th International Conference on Soil Mechanics and Foundation Engineering*, Stockholm, 2, 349-354.

Malusis, M.A., Shackelford, C.D., Olsen, H.W., (2001). A laboratory apparatus to measure chemico-osmotic efficiency coefficients for clay soils. *Geotechnical Testing Journal* 24(3),

229-242.

Malusis, M.A. and Shackelford, C.D., (2002a). Coupling effects during steady-state solute diffusion through a semipermeable clay membrane. *Environmental Science and Technology* 36(6), 1312-1319.

Malusis, M.A. and Shackelford, C.D., (2002b). Chemico-osmotic efficiency of a geosynthetic clay liner. *Journal of Geotechnical and Geoenvironmental Engineering (ASCE)* 128(2), 97-106.

Malusis, M.A., Shackelford, C.D. and Olsen, H.W., (2003). Flow and transport through clay membrane barriers. *Engineering Geology* 70, 235-248.

Malusis, M.A. and Shackelford, C.D., (2004). Predicting solute flux through a clay membrane barrier. *Journal of Geotechnical and Geoenvironmental Engineering (ASCE)* 130(5), 477-487.

Manassero, M., Van Impe, W.F., and Bouazza, A. (1997). Waste disposal and containment. *Environmental Geotechnics, M. Kamon (Ed.)*, Balkema, 1425-1474.

Manassero, M. and Dominijanni, A., (2003). Modelling the osmosis effect on solute migration through porous media. *Geotechnique* 53(5), 481-492.

Marine, I.W. and Fritz S.J., (1981). Osmotic model to explain anomalous hydraulic heads. *Water Resources Research* 17(1), 73-82.

Mathers, A.C., Weed, S.B., Coleman, N.T., (1956). The effect of acid and heat treatment on montmorillonids. *Nat. Acad. Sci. Publ.* 395, 403-413.

Matsufuji, Y., Hirata, O., Tanaka, A., Yanase, R., and Suzuki, S., (2007). Biodegradation process and mass balance of different landfill types using large scale simulator - Quality control of experimental method with lysimeter-. *Proceedings Sardinia 2007, Eleventh International Waste Management and Landfill Symposium*, Cagliari, Italy

Mckelvey, J.G., and Milne, I.H., (1962). The flow of salt solutions through compacted clay. *Clays and clay minerals* 9, 248-259.

Mesri, G., and Olson, R.E., (1971). Mechanisms controlling the permeability of clays. *Clay and Clay Minerals* 19, 151-158.

Metten, U., (1966). Desalination by reverse osmosis. *M.I.T. Press*, Cambridge, MA.

Ministry of the Environment, Japan. (2010). Environmental statistics. http://www.env.go.jp/doc/toukei/contents/index.html.

Mitchell, J.K., Hooper, D.R., and Campanella, R.G., (1965). Permeability of compacted clays. *Journal of the Soil Mechanics and Foundations Division (ASCE)* 91(SM4), 41–65.

Mitchell, J. K. (1976). *Fundamentals of soil behavior*. John Wiley & Sons, New York.

Mitchell, J. K. (1991). Conduction phenomena: from theory to geotechnical practice. *Geotechnique* 41(3), 299–340.

Mitchell, J.K., (1993). *Fundamentals of Soil Behavior*. 2nd Ed., Wiley, New York.

Mitchell, J.K., and Soga, K., (2005). *Fundamentals of Soil Behavior*. 3rd Ed., Wiley, New York.

Miyawaki, K., Tanaka, N., and Matsuto, T., (1995). Study of environmental conditions on sulfate reduction in leachate from incinerator ash. *Material Cycles and Waste Management Research*

6(3), 95-104.

Monnier, G., Fies, J.C., and Stengel, P., (1973). Une methode de mesure de la densite apparente de petits agglomerats terreux: application a l'analyse de la porosite du sol. *Annales Agronomiques* 24, 533-545.

Monteiro, V.E.D., Melo, M.C., Juca, J.F.T., (2002). Biological degradation analysis in muribeca solid waste landfill associated with local climate. Recife, Brazil, *Proceedings of the Fourth International Congress on Environmental Geotechnics*, vol. 2, Balkema, Rio Janeiro, 799-803.

Montero, J.A., (2011). Reduction and utilization of fine residue generated from mixed construction and demolition waste sorting facilities. *Division of Solid Waste, Resources and Geo-environmental Engineering*, 1-6.

Mulder, M., (1991). Basic Principles of Membrane Technology. *Kluwer Academic Publishers*, Dordrecht, The Netherlands, pp. 363.

Murillo, R., Garcıa, T., Aylon, E., Callen, M.S., Navarro, M.V., Lopez, J.M., Mastral, A.M., (2004). Adsorption of phenanthrene on activated carbons: Breakthrough curve modeling. *Carbon* 42, 2009–2017.

Norrish, K., and Quirk, J., (1954). Crystalline swelling of montmorillonite, use of electrolytes to control swelling. *Nature* 173, 255-257.

Nunes, K.R.A., Mahler, C.F., Valle, R., Neves, C., (2007). Evaluation of investments in recycling centres for construction and demolition wastes in Brazilian municipalities. *Waste Management* 27(11), 1531-1540.

Olsen, H.W., (1969). Simultaneous fluxes of liquid and charge in saturated kaolinite. *Soil Science Society of America Proceedings* 33(3), 338-344.

Olsen, H.W., (1972). Liquid movement through kaolinite under hydraulic, electric, and osmotic gradients. *AAPG Bulletin* 56(10), 2022–2028.

Olsen, H.W., Yearsley, E.N. and Nelson, K.R., (1990). Chemicoosmosis versus diffusion-osmosis. *Transportation Research Record 1288*, Trasportation Research Board, Washington D.C., 15–22.

Osako, M., Kim, Y.J., Sakai, S., (2004). Leaching of brominated flame retardants in leachate from landfills in Japan. *Chemosphere* 57, 1571–1579.

Palmisano, A.C. and Barlaz, M.A., (Eds.) (1996). *Microbiology of Solid Waste*. CRC Press, Florida, USA.

Pan, B.C., Meng, F.W., Chen, X.Q., Pan, B.J., Li, X.T., Zhang, W.M., Zhang, X., Chen, J.L., Zhang, Q.X., Sun, Y., (2005). Application of an effective method in predicting breakthrough curves of fixed-bed adsorption onto resin adsorbent. *Journal of Hazardous Materials* B124, 74–80.

Poon, C.S., (2007). Management of construction and demolition waste. Editorial / *Waste Management* 27, 159-160.

Porter, L. K., Kemper, W. D., Jackson, R. D. & Steward, B. A., (1960). Chloride diffusion in soils as influenced by moisture content. *Soil Science Society of America Proceedings* 24(6), 460–463.

Prapaharan, S., White, D.M., and Altschaeffl, A.G., (1991). Fabric of field- and

laboratory-compacted clay. *Journal of Geotechnical Engineering (ASCE)* 117(GT12), 1934–1940.

Productivity Commission, (2006). Waste Management – Productivity Commission Inquiry Report. *Commonwealth of Australia*, Canberra, p. 562.

Rafizul, I.M., Howlader, M.K., and Alamgir, M., (2012). Construction and evaluation of simulated pilot scale landfill lysimeter in Bangladesh. *Waste Management* 32, 2068–2079.

Rao, A., Jha, K.N., Misra, S., (2007). Use of aggregates from recycled construction and demolition waste in concrete. *Resources, Conservation and Recycling* 50, 71-81.

Renou, S., Givaudan, J.G., Poulain, S., Dirassouyan, F., Moulin, P., (2008). Landfill leachate treatment: Review and opportunity. *Journal of Hazardous Materials* 150, 468-493.

Richard, G., Cousin, I., Sillon, J.F., Bruand, A., Guerif, J., (2001). Effect of compaction on the porosity of a silty soil: influence on unsaturated hydraulic properties. *European Journal of Soil Science* 52, 49-58.

Ritcey, G.M., (1989). Tailings managements, problems and solutions in the mining industry. *Elsevier*, Masterdam.

Robinson, H.D., (1995). The Technical Aspects of Controlled Waste Management. A Review of The composition of Leachates from Domestic Wastes in Landfill Sites. Report for the UK Department of the Environment. *Waste Science and Research*, CWM/072/95. Aspinwall & Company, Ltd, London, UK.

Roussat, N., Mehu, J., Abdelghafour, M., Brula, P., (2008). Leaching behavior of hazardous demolition waste. *Waste Management* 28, 2032-2040.

Rowe, R.K., Caers, C.J., and Barone, F., (1988). Laboratory determination of diffusion and distribution coefficients of contaminants using undisturbed clayey soils. *Canadian Geotechnical Journal* 25, 108-118.

Rowe, R. K., and Hoor, A., (2009). Predicted temperatures and service lives of secondary geomembrane landfill liners. *Geosynthetics International* 16(2), 71-82.

Rowe, R. K., and Islam, M.Z., (2009). Impact of landfill liner time–temperature history on the service life of HDPE geomembranes. *Waste Management* 29, 2689–2699.

Ruhl, J. L. and Daniel, D. E. (1997). Geosynthetic clay liners permeated with chemical solutions and leachates. *Journal of Geotechnical and Geoenvironmental Engineering (ASCE)* 123(4), 369–381.

Sakai, S., Urano, S., Takatsuki, H., (2000). Leaching behavior of PCBs and PCDDs/DFs from some waste materials. *Waste Management* 20, 241-247.

Salati, S., Scaglia, B., Di Gregorio, A., Carrera, A., Adani F., (2013). The use of the dynamic respiration index to predict the potential MSW-leachate impacts after short term mechanical biological treatment. *Bioresource Technology* 128, 351-358.

Sällfors, G., Öberg-Högsta, A.L., (2002). Determination of hydraulic conductivity of sand-bentonite mixtures for engineering purposes. *Geotechnical & Geological Engineering* 20, 65-80.

Sarsby, R., (2000). *Environmental Geotechnics*. Thomas Telford.

Shackelford, C.D. and Daniel, D.E., (1991). Diffusion in saturated soil: II. Results for compacted clay. *Journal of Geotechnical Engineering (ASCE)*, 117 (3), 485-506.

Shackelford, C.D., (1997). Modelling and analysis in environmental geotechnics: an overview of practical applications. *Proc. 2nd Int. Cong. Environmental Geotechnics*, Osaka, 1375–1404, Balkema: Rotterdam.

Shackelford, C.D., Benson, C.H., Katsumi, T., Edil, T.B., and Lin, L., (2000). Evaluating the hydraulic conductivity of GCLs permeated with non-standard liquids. *Geotextiles & Geomembranes* 18(2-4), 133-161.

Shackelford, C.D., and Lee, J.M., (2003). The destructive role of diffusion on clay membrane behavior. *Clays and Clay Minerals* 51(2), 187-197.

Shackelford, C.D., Malusis, M.A. and Olsen, H.W., (2003). Clay membrane behavior for geoenvironmental containment. In: *Culligan, P.J., Einstein, H.H., Whittle, A.J. (Eds.), Soil and Rock America Conference 2003*, vol. 1. Verlag Glückauf GMBH, Essen, Germany, 767–774.

Shackelford, C.D., (2011). Membrane behavior in geosynthetic clay liners. *Geo-Frontiers 2011*, Dallas, TX, March 13-16, 2011, (CD-ROM). ASCE, Reston, VA, 1961-1970.

Shackelford, C.D., (2012). Membrane behavior of engineered clay barriers for geoenvironmental containment: State of the art. *GeoCongress 2012-State of the Art and Practice in Geotechnical Engineering*, R.D. Hryciw, A. Athanasopoulos-Zekkos, and N. Yesiller, Eds., Geotechnical Special Publication 225, Oakland, CA, March 25-29, ASCE, Reston, VA, 3419-3428.

Shackelford, C.D., (2013). Membrane behavior in engineered bentonite-based containment barriers: State of the art. *Coupled Phenomena in Environmental Geotehnics*, Manassero et al, Eds., Taylor & Francis Group, London.

Sharma, H.D., and Lewis, S.P., (1994). *Waste containment systems, waste stabilization, and landfills: design and evaluation*. Wiley, New York.

Sharma, H.D., and Reddy, K.R., (2004). *Geoenvironmental Engineering: Site Remediation, Waste Containment, and Emerging Waste Management Technologies*. John Wiley & Sons, NJ (2004).

Shelley, T. and Daniel, D., (1993). Effect of gravel on hydraulic conductivity of compacted soil liners. *Journal of Geotechnical and Geoenvironmental Engineering (ASCE)* 119(1), 54-68.

Silva, A.C., Dezotti, M., Sant'Anna, Jr.G.L., (2004). Treatment and detoxification of a sanitary landfill leachate. *Chemosphere* 55, 207-214.

Spiegler, K.S. and Kedem, O., (1966). Thermodynamics of hyperfiltration (reverse osmosis): criteria for efficient membranes. *Desalination* 1, 311-326.

Sposito, G., (1984). *The surface chemistry of soils*. Oxford University Press, New York.

Staverman, A.J., (1952). Non-equilibrium thermodynamics of membrane processes. *Transactions of the Faraday Society* 48(2), 176-185.

Stessel, R.I. and Murphy, R.J., (1992). A lysimeter study of the aerobic landfill concept. *Waste Management & Research* 10, 485-503.

Tanaka, N., Tojo, Y., Matsuto, T., (2005). Past, present, and future of MSW landfills in Japan. *Journal of Material Cycles and Waste Management* 7 (2), 104–111.

Tang, Q., Tang, X.W., Li, Z.Z., Chen, Y.M., Kou, N.Y., Sun, Z.F., (2009). Adsorption and desorption behavior of Pb(II) on a natural kaolin: equilibrium, kinetic and thermodynamic studies. *Journal of Chemical Technology and Biotechnology* 84, 1371–1380.

Tang, Q., Tang, X.W., Hu, M.M., Li, Z.Z., Chen, Y.M., Lou, P., (2010). Removal of Cd(II) from aqueous solution with activated Firmiana Simplex Leaf: Behaviors and affecting factors. *Journal of Hazardous Materials* 179, 95–103.

Tang, Q., Tang, X.W., Li, Z.Z., Wang, Y., Hu, M.M., Zhang, X.J., Chen, Y.M., (2012). Zn(II) Removal with Activated Firmiana Simplex Leaf: Kinetics and Equilibrium Studies. *Journal of Environmental Engineering (ASCE)* 138(2), 190–199.

Tang, Q., Katsumi, T., Inui, T., and Li, Z.Z., (2013a). Membrane behavior of bentonite amended compacted clay. *Soils and Foundations (JGS)*, under review.

Tang, Q., Katsumi, T., Inui, T. and Li, Z.Z., (2013b). Effect of mixing ratio on membrane behavior of clay-bentonite composite material. *New Frontiers in Chinese and Japanese geotechnique, Proceedings of the Fifth China-Japan Geotechnical Symposium*, April. 18-19, Chengdu, China, 494-498.

Tang, Q., Katsumi, T., Inui, T., Takai, A., and Li, Z.Z., (2014). Influence of compaction degree on membrane behavior of clay-bentonite material. *Proceedings of Geo-congress 2014 (ASCE)*, Atlanta, Georgia, U.S.A., under review.

Tchobanoglous, G., Kreith, F., (2002). *Handbook of solid waste management*. McGraw-Hill publishers, New York, USA.

Thomas, G.W., and Swobada, A.R., (1970). Anion exclusion effects on chloride movement in soils. *Soil science* 110(3), 163-166.

Tinoco, I., Sauer, K. and Wang, J.C., (1995). *Physical chemistry*, Prentice-Hall, Upper Saddle River, N.J.

Townsend, T.G., Miller, W.L., Lee, H.J., Earle, J.F.K., (1996). Acceleration of landfill stabilization using leachate recycling. *Journal of Environmental Engineering (ASCE)* 122, 263-268.

Trankler, J., Visvanathan, C., Kuruparan, P., Tubtimthai, O., (2005). Influence of tropical seasonal variations on landfill leachate characteristics—Results from lysimeter studies. *Waste Management* 25, 1013–1020.

Tuwiner, S.B., (1962). *Diffusion and Membrane Technology*. Reinhold Publishing Corporation, New York, pp. 421.

USEPA, (2009). Municipal Solid Waste Generation, Recycling, and Disposal in the *United States Detailed Tables and Figures for 2008*. United States Environmental Protection Agency, Washington, DC.

USEPA, (2010). Municipal Solid Waste Generation, Recycling, and Disposal in the *United States: Facts and Figures for 2010*. United States Environmental Protection Agency, Washington, DC.

USEPA, (2011). US EPA Drinking Water Standards and Health Advisories. *EPA 820-R-11-002*. Washington, DC: U.S. Environmental Protection Agency.

Van, O.E., Hale, A.H., Mody, F.K. and Roy, S., (1996). Transport in shales and the design of improved water-based shale drilling fluids. *SPEDC* 11(3), 137-146.

Van der Sloot, H.A., Van Zomeren, A., Rietra, R.P., Hoede, D., and Scharff, H., (2001). Integration of lab-scale testing, lysimeter studies and pilot scale monitoring of a predominantly inorganic waste landfill to reach sustainable landfill conditions. In: Christensen, Th., Cossu, R., Stegmann, R. (Eds.), SARDINIA-2001, S. *Margherita di Pula*, Cagliari (Italy), 1, 254–264.

Van Gerven, T., Geysen, D., Stoffels, L., Jaspers, M., Wauters, G., Vandecasteele, C., (2005). Management of incinerator residues in Flanders (Belgium) and in neighbouring countries. A comparison. *Waste Management* 25, 75–87.

Van Impe, P.O., (2002). Consolidation, contaminant transport and chemico-osmotic effects in liner materials. A theoretical and experimental study. *Doctor thesis*.

Vanapalli, S.K., Fredlund, D.G., and Pufahl, D.E., (1999). The influence of soil structure and stress history on the soil-water characteristics of a compacted till. *Géotechnique* 49(2), 143–159.

Vicente-ferreira, L., Amaral, L., Agostinho, I., and Santana, F., (2007). Reactor geometry interference with the kinetics of the biological process. *Proceedings Sardinia 2007, Eleventh International Waste Management and Landfill Symposium*, Cagliari, Italy.

Voegelin, A., Barmettlert, K., and Kretzschmar, R., (2003). Heavy metal release from contaminated soils: comparison of column leaching and batch extraction results. *Journal of Environmental Quality* 32, 865-875.

Wall, D.K., Zeiss, C., (1995). Municipal landfill biodegradation and settlement. *Journal of Environmental Engineering (ASCE)* 121, 214-223.

Welander, U., Henryson, T., Welander, T., (1997). Nitrification of landfill leachate using suspended-carrier biofilm technology, *Water Research* 31, 2351–2355.

WEPA, Water Environment Partnership in Asia, (2011). State of water: Japan. www.wepa-db.net/policies/state/japan/japan.htm

Westlake, K., (1995). *Landfill waste pollution and control*. Albion Publishing, Chichester, UK.

Watabe, Y., Leroueil, S., and Le Bihan, J.P., (2000). Influence of compaction conditions on pore-size distribution and saturated hydraulic conductivity of a glacial till. *Canadian Geotechnical Journal* 37, 1184–1194.

Williams, P.T., (1998). *Waste Treatment and Disposal*. John Wiley & Sons, Chichester, UK, Chapter 5, pp. 223-240.

World Health Organization (WHO), (2006). Guidelines for drinking-water quality: Incorporating first addendum. Vol.1, Recommendations, World Health Organization, Geneva.

Yaroshchuk, A.E., (1995). Osmosis and reverse osmosis in fine-charged diaphragms and membranes. *Advances in Colloid and Interface Science* 60, 1-93.

Yanase, R., Hirata, O., Matsuhuji, Y., and Hanashima, M., (2009). Behavior of mercury from used

batteries in landfills over 20 years. *Material Cycles and Waste Management Research* 20(1) 12-23.

Yeo, S.S., Shackelford, C.D., and Evans, J.C., (2005). Membrane Behavior of Model Soil–Bentonite Backfills. *Journal of Geotechnical and Geoenvironmental Engineering (ASCE)* 131(4), 418-429.

Yong, R.N., Pusch, R. and Nakano, M., (2010). *Containment of High-level Radioactive and Hazardous Solid Wastes with Clay Barriers*. Spon Press, Taylor & Francis, London and New York.

Zehnder, J.A.B., (1988). *Biology of Anaerobic Microorganisms*. Wiley Series in Ecological and Applied Microbiology, USA.

Zhang, H.Y., (2002). Redox effect on heavy metal mobility and dydraulic conductivity of clay liners at landfill sites. *Ph.D Diss. Kyoto University*, Japan